Alternative solvents in separation processes

Marina Manic

Dissertation presented to obtain the Ph.D degree in Sustainable Chemistry

Caparica, May, 2012

Acknowledgments

Summary

The work presented in this thesis aims at the development of novel environmentally sustainable separation processes, namely deacidification of soybean oil, purification of an antibiotic, and extraction of high-value compounds from vegetable materials by replacing volatile organic solvents with environmentally benign alternatives, such as polyethylene glycols (PEGs), ionic liquids (ILs), supercritical carbon dioxide ($scCO_2$) or ethyl lactate.

The extraction of linoleic acid from soybean oil was carried out using PEGs with various molar masses and the ILs (AMMOENG100 and [C_4mim][DCA]). As it is presented in Chapter II, liquid-liquid phase equilibrium was measured for binary (PEG/IL + soybean oil) and ternary (PEG/IL + soybean oil + linoleic acid) mixtures. The influence of temperature, initial acid content of the oil and solvent to oil ratio on distribution coefficients and separation factors were studied.

Liquid-liquid extraction of erythromycin from aqueous solution using a hydrophobic IL as a solvent, and its recovery from the IL using $scCO_2$ are presented in Chapter III. Phase equilibria of binary mixtures (ILs + erythromycin) was studied in a wide range of temperatures, at atmospheric pressure. Additionally, single- and multi-stage extraction of erythromycin from aqueous solutions by [C_4mpyr][NTf$_2$] was studied as a function of pH and feed to solvent volume ratio. The influence of pressure, temperature and presence of water on recovery of erythromycin from [C_4mpyr][NTf$_2$] by $scCO_2$ was further studied.

The solubility of CO_2 in the studied ILs as a function of pressure and temperature was measured as well, which significantly contributed to evaluate the importance of explicitly including association in the modelling of such systems. (Chapter IV).

Chapter V encloses data on solubility of caffeine, vanillic acid, ferulic acid, caffeic acid and thymol in both dry and water-saturated ethyl lactate, as a function of temperature, at atmospheric pressure. Additionally, accelerated solvent extraction of caffeine from either entire or ground green coffee beans is presented for the first time. Extraction yield and caffeine recovery when using ethyl lactate were compared with those obtained by ethyl acetate or ethanol. The undesirable extraction of active principles, such as coffee oil and phenolic compounds, was further analysed.

The results presented in this thesis comprise information on successful utilization of those environmentally benign extraction solvents.

Keywords: Solubility, Extraction, Green solvents, High-value solutes.

Resumo

O trabalho apresentado nesta tese visa o desenvolvimento de novos processos de separação, tais como desacidificação de óleo de soja, purificação de um antibiótico, e extração de compostos de alto valor a partir de materiais vegetais, substituindo solventes orgânicos voláteis por alternativas que são ambientalmente sustentáveis: polietilenoglicóis (PEGs), líquidos iónicos (ILs), dióxido de carbono supercrítico ($scCO_2$) ou lactato de etilo.

A extração de ácido linoleico do óleo de soja foi realizada usando polietilenoglicóis de várias massas molares e os líquidos iónicos (AMMOENG100 e [C_4mim][DCA]). Tal como apresentado no Capítulo II, o equilíbrio líquido-líquido foi medido para misturas binárias (PEG/IL + óleo de soja) e para misturas ternárias (PEG/IL + óleo de soja + ácido linoleico). Foi estudada a influência da temperatura, do teor de ácido inicial no óleo e da proporção entre solvente e óleo sobre o coeficiente de distribuição e fator de separação.

A extração da eritromicina inicialmente em solução aquosa usando um líquido iónico hidrofóbico como solvente de extração, e sua posterior recuperação utilizando dióxido de carbono supercrítico são apresentadas no Capítulo III. O equilíbrio de misturas binárias (ILs + eritromicina) foi estudado numa ampla gama de temperaturas, à pressão atmosférica. Adicionalmente, a extração de eritromicina em solução aquosa, numa etapa única e em etapas múltiplas com [C_4mpyr][NTf_2], foi estudada em função do pH e da proporção entre as duas fases líquidas, assim como a influência da temperatura, pressão e teor de água na recuperação de eritromicina dissolvida em [C_4mpyr][NTf_2] usando $scCO_2$.

A solubilidade do CO_2 nos líquidos iónicos estudados foi medida em função da pressão e da temperatura. Os dados de solubilidade experimentalmente obtidos contribuíram significativamente para avaliar a importância de incluir explicitamente um termo de associação para descrever tais sistemas a partir de modelos termodinâmicos (Capítulo IV).

O Capítulo V inclui os dados da solubilidade de cafeína, ácido vanílico, ácido ferúlico, ácido cafeico e timol, tanto em lactato de etilo seco como em lactato de etilo saturado de água, medidos em função da temperatura, à pressão atmosférica. Além disso, é apresentada pela primeira vez a potencial utilização do lactato de etilo como um solvente "verde" na extração da cafeína a partir de grãos inteiros ou triturados de café verde. O rendimento de extração e a recuperação de cafeína, utilizando lactato de etilo, foram comparados com dados obtidos no caso de utilização do acetato de etilo ou do etanol. Foi ainda analisada a extração indesejável de princípios ativos, tais como o óleo de café e os compostos fenólicos.

Os resultados apresentados nesta tese incluem informações sobre a utilização bem sucedida desses solventes de extração ambientalmente favoráveis.

Termos chave: Solubilidade, Extração, Solvente "verde", Compostos de alto valor.

Table of contents

Table of figures

Table of tables

Abbreviations and acronyms

VOCs	volatile organic compounds
GHGs	greenhouse gases
EPA	Environmental Protection Agency
REACH	Registration, Evaluation, Authorisation and restriction of Chemicals
LCA	life cycle assessment
ESA	energy separation agent
MSA	mass separation agent
CO_2	carbon dioxide
$scCO_2$	supercritical carbon dioxide
IL	ionic liquid
PILs	phosphonium based ionic liquids
AMMOENG100	Cocos alkyl pentaethoxi methyl ammonium methylsulfate
PEG	polyethylene glycol
EC_{50}	median lethal dose
FDA	Food and Drug Administration
GRAS	Generally Recognized as Safe
PTC	phase-transfer catalyst
ABS	aqueous biphasic system
FFA	free fatty acid
SCF	supercritical fluid
ASE	accelerated solvent extraction
DSC	differential scanning calorimetry
HPLC	high-performance liquid chromatography
GC	gas chromatography
UV-Vis	ultraviolet-visible
NMR	nuclear magnetic resonance
MeOH	methanol
LA	linoleic acid
FAMEs	fatty acid methyl esters
FC	Folin-Ciocalteau reagent
NOL	neutral oil loss
TPC	total phenolic compounds
LLE	liquid-liquid equilibrium
SLE	solid-liquid equilibrium
EoS	equation of state
PR	Peng-Robinson
SRK	Soave-Redlich-Kwong
MKP	Mathias-Klotz-Prausnitz mixing rule

CPA	Cubic Plus Association
soft-SAFT	Soft Statistical Associating Fluid Theory
PC-SAFT	Perturbed-Chain Statistical Associating Fluid Theory
COSMOtherm	Quantum chemistry calculations of solvation thermodynamics
UNIQUAC	UNIversal QUAsiChemical
UNIFAC	UNIversal Functional Activity Coefficient
AAD	absolute average deviations

IL's cations

$[C_n mim]^+$	1-alkyl-3-methylimidazolium
$[C_n mpyr]^+$	1-alkyl-1-methylpyrrolidinium
$[N_{x\,y\,z\,w}]^+$	tetraalkylammonium
$[P_{x\,y\,z\,w}]^+$	tetraalkylphosphonium

IL's anions

$[BF_4]^-$	tetrafluoroborate
$[PF_6]^-$	hexafluorophosphate
$[Cl]^-$	chloride
$[Br]^-$	bromide
$[DCA]^-$	dicyanamide
$[NO_3]^-$	nitrate
$[EtSO_4]^-$	ethylsulfate
$[OTf]^-$	trifluoromethanesulfonate
$[NTf_2]^-$	bis(trifluoromethylsulfonyl)imide

Chapter I

Introduction

1.1 Environmental concerns

In last decades became very clear that human activities have influenced environment, exposing it to many hazardous impacts and thus, endanger the human society itself. Volatile organic compounds (VOCs), greenhouse gasses (GHGs), organic and inorganic species in the waste, all associated with industrial processes, leaks and spills, waste disposal and incineration, product use and application, lead to contamination of air, land, water and have a huge impact on global changes (climate change, ozone depletion, land surface change). Climate change refers manly to global warming and additional changes as a result of rising temperatures. Global warming has been provoked by uncontrolled realising of greenhouse gasses such as carbon dioxide (CO_2), methane (CH_4), nitrogen oxides (NO_x) and fluorinated gases (HFCs, PFCs and SF_6). Some GHGs (carbon dioxide and water vapour) occur naturally and help to regulate temperature on the Earth, trapping some of the outgoing energy in the atmosphere. However, human activities have been added other gases to the natural mix, leading to global warming. In addition to act as greenhouse gases, CO_2, SO_2 and NO_x contribute to acid rain which has negative impact on plants, animals and materials. It has been shown [1] that power plants were the largest emitters of GHGs in 2010, followed by petroleum refineries and mines. It was also shown that 95 % of the total emission was CO_2, 4 % was methane and all other gases contributed by only 1 %. As a result, the average temperature could increase up to 4 ^{o}C by 2100 if emission reminds uncontrolled [2]. Additionally, changes in ocean circulation, rising sea levels (flooding and erosion of coastal areas), changes in precipitation or wind might occur. Also, it can have negative influence on ecosystems, as well as on some of the benefits that ecosystems provide to society. They have already been affected by pollution, overharvesting and development. These are the reasons why society needs to act in environmental protection, promoting safer renewable materials and process design in order to reduce material waste and chemical contamination.

1.2 Sustainable approach

The awareness of health and environment hazards results as an idea of green chemistry which was presented in 1991 by Paul T. Anastas in a special program of the US Environmental Protection Agency (EPA). The main goal was to introduce sustainable development in chemistry and chemical technology, not only by industry, but also through government and academia. As it was reported by the World Commission on Environment and Development [3]: "*Sustainable development meets the needs of the present without compromising the ability of future generations to meet their own needs*". The concept of sustainable chemistry became important in the US and Europe, especially evident by governmental and scientific activities which have been occurred in the last decades. The annual US Presidential Green Chemistry Challenge Awards were established in 1995. The Green Chemistry Institute was founded in 1997 in order to facilitate contact between industrial corporations, governmental agencies and research

institutes from different countries. In the same year, the first conference on green chemistry was held in Washington. The first books and journals related to the subject appeared at the end of 90's: "Green Chemistry: Theory and Practice" [4] written by Anastas and Warner was published in 1998 and the scientific journal Green Chemistry was founded by the Royal Society of Chemistry in 1999. The European Community regulation (REACH – Registration, Evaluation, Authorisation and restriction of Chemicals) [5], in force since 2007, is mandatory on chemicals produced in the quatities over 1 t/year and their safety use. REACH was introduced to ensure human and environmental safety, with a goal of achieving the sustainable development.

The strategy of green chemistry and engineering is to minimize environmental hazards by the safer design of chemical products and their manufacture. The main goal of green chemistry is to reduce or eliminate the use and generation of hazardous substances. Green engineering is commercialization and use of products and processes while minimizing pollution and the risk to human health and environment. The development of this approach has been improved by introducing 12 principles of green chemistry and 12 principles of green engineering, and metrics which guide the design towards sustainability. These metrics can be assembled as: material efficiency (atom economy [6], E-factor [7], reaction mass efficiency and mass productivity [8]), energy efficiency and toxicity which are usually used to evaluate individual chemicals, chemical reactions or one-step processes. The 12 principles of green chemistry and the life cycle assessment (LCA) are the most commonly used tools for evaluating the product's life cycle.

According to Anastas and Warner [4], the 12 principles of green chemistry for design of safer chemicals and processes are:

1. Prevention - it is better to prevent waste than to treat or clean up waste after it has been created.
2. Atom economy – synthetic methods should be designed to maximize the incorporation of all materials used in the process into the final product.
3. Less hazardous chemical synthesis – wherever practicable, synthetic methods should be designed to use and generate substances that possess little or no toxicity to human health and the environment.
4. Designing safer chemicals – Chemical products should be designed to affect their desired function while minimizing their toxicity.
5. Safer solvent and auxiliaries – the use of auxiliary substances (e.g., solvents, separation agents, etc.) should be made unnecessary whenever possible and innocuous when used.
6. Design for energy efficiency – energy requirements of chemical processes should be recognized for their environmental and economic impacts and should be minimized. If possible, synthetic methods should be conducted at ambient temperature and pressure.
7. Use of renewable feedstocks – a raw material or feedstock should be renewable rather than depleting whenever technically and economically practicable.

8. Reduced derivatives – unnecessary derivatization (use of blocking groups, protection/ deprotection, temporary modification of physical/ chemical processes) should be minimized or avoided if possible, because such steps require additional reagents and can generate waste.

9. Catalysis – catalytic reagents (as selective as possible) are superior to stoichiometric reagents.

10. Design for degradation – chemical products should be designed so that at the end of their function they break down into innocuous degradation products and do not persist in the environment.

11. Real-time analysis for pollution prevention – analytical methodologies need to be further developed to allow for real-time, in-process monitoring and control prior to the formation of hazardous substances.

12. Inherently safer chemistry for accident prevention – substances and the form of a substance used in a chemical process should be chosen to minimize the potential for chemical accident, including releases, explosions and fires.

The 12 principles of green engineering [9], are the tool for scientist and engineers to design new materials, product, processes which are benign to human health and environment. These are:

1. Designers need to strive to ensure that all materials and energy inputs and outputs are as inherently nonhazardous as possible.

2. It is better to prevent waste than to treat or clean up waste after it is formed.

3. Separation and purification operations should be designed to minimize energy consumption and materials use.

4. Products, processes and systems should be designed to maximize mass, energy, space and time efficiency.

5. Products, processes and systems should be "output pulled" rather than "input pushed" through the use of energy and materials.

6. Embedded entropy and complexity must be viewed as an investment when making design choices on recycle, reuse or beneficial disposition.

7. Targeted durability, not immortality, should be a design goal.

8. Design for unnecessary capacity or capability (e.g., "one size fits all") solutions should be considered a design flaw.

9. Material diversity in multicomponent products should be minimized to promote disassembly and value retention.

10. Design of products, processes and systems must include integration and interconnectivity with available energy and materials flows.

11. Products, processes and systems should be designed for performance in a commercial "afterlife".

12. Material and energy inputs should be renewable rather than depleting.

Life cycle assessment (LCA) [10, 11] is a comprehensible set of certain metrics used to evaluate all stages along the life cycle of a product. The LCA procedure is outlined in the International Standards Organization protocol, ISO 14040. It identifies and quantifies energy and material usage end environmental releases in order to assess the impact of these uses on the environment and defined required improvements. Four different stages of LCA could be recognized: (i) goal definition and scoping; (ii) an inventory of materials, energy inputs, wastes and emissions through entire production process (row material extraction, pre-production, production, use, recycling and disposal); (iii) a statement of the environmental impact of each element from the inventory stage is required; (iv) a strategy for reducing the overall impact of the process by suggesting particular steps for improvement. The LCA incorporates material efficiency, energy efficiency and toxicity consideration, as well as concerns to product degradation and various environmental impacts. It is a useful tool for evaluating already existing products or processes and compares these with existing alternatives, or to design new safer products and processes.

Over the decades, organic chemicals has been plentifully manufactured from petroleum feedstock, requiring high energetic and economical consumption [12]. Their excessive use (4 × 10^6 tons / year in Europe and a comparable amount in USA), with an estimated cost of 6 billion € / year is a major concern for chemical industry [13]. The strategy of green chemistry has been recognized as crucial for both social and economic growth. Thus, industrial processes have faced many economical, technical and regulatory barriers [14], being challenged to achieve environmental and economic stability. The reduction of hazards is emphasized by careful selection of feedstock and reagents, use of alternative solvents and synthesis pathways, as well as use of renewable energy. Petroleum non-renewable sources should be replaced by biomass, the only sustainable alternative when possible, as a source of carbon for our material and chemical needs. Natural feedstocks show economical advantage, as a financially stable starting material, as well as safety and environmental benefits reflected through the final naturally derived product. For example, production of adipic acid was transformed to sustainable process such as a catalytic synthesis from renewable feedstock [15]. Large amount of adipic acid are used for manufacturing of nylon 66, polyurethanes, lubricants and plasticizers. Traditionally, adipic acid is produced from petroleum-derived benzene as a starting material, where a nitric acid oxidation occurs in the last step of the process, generating nitrous oxide as a by-product. Recently, chemists from State University of Michigan [15] developed the Draths-Frost synthesis of adipic acid using natural row material, glucose. Glucose is converted to *cis,cis*-muconic acid by an enzyme from genetically modified bacteria, which is furthermore hydrogenated to adipic acid. This synthesis eliminates the use of benzene (carcinogenic compound) and the formation of nitrous oxide (greenhouse gas), meeting sustainability requirements.

The production of biodiesel oil is a promising possibility and their combustion is more preferable than combustion of fossil fuels from depleting limited sources. A bio-refinery could convert biomass and postconsumer waste to both fuel and fine chemicals [16, 17]. Sustainability has

been recognized in using of renewable starting material for biodiesel production, their combustion does not generate sulphur compounds in the atmosphere, and also it might reduce waste generation if it is additionally produced from postconsumer waste (e.g. oils used in restaurants). Chemical synthesis methodologies should be catalytic rather than stoichiometric. The catalytic synthesis can reduce or even eliminate volatile organic compounds from the process, getting the environmental advantage over stoichiometric reaction. However, energy consumption can be increased by the catalyst recovery step. The BHC Company improved the manufacturing of ibuprofen [18], where three catalytic steps replaced the previous technology with six stoichiometric steps. Anhydrous hydrogen fluoride, which is used as both a catalyst and a solvent, is recovered with over 99 % efficiency when process is finished. Additionally, the reaction selectivity is improved and waste generating decreased.

Separation processes have been recognized as a critical for environmental remediation and protection. They can be applied for industrial or domestic waste treatment in order to minimize the quantity of potentially toxic and hazardous materials released to the environment. Also, separations allow recovery, recycle or reuse of high-value materials. As catalytic reactions are favourable in order to meet sustainable requests, separation processes can play important role in recovery of catalyst at the end of chemical process, giving an opportunity of its reuse. Furthermore, minimization of waste is an additional advantage. Separation processes, such as extraction and purification, can be used as sustainable if traditional organic solvents are replaced by alternative solvents. Brief introduction of separation processes and their application in green processing will be further discussed in the section 1.3.

The enormous hazard to the environment are organic solvents due to their extensive use in a variety of processes including synthesis, separation, extraction, purification, dilution, coating, cleaning and many others. They play the key role in mass and heat transfer of many processes and furthermore improve reactions' velocity, selectivity and rates. Many commercial organic solvents are volatile, flammable, corrosive, toxic and environmentally persistent. Volatile organic compounds (VOCs) are usually applied due to a benefit of their easily removal or evaporation from the system. They are released to environment from industrial processes by leaks and spills, waste disposal and incineration, product use and application, having a detrimental effect on human health and environment. For example, in the USA, the extraction of numerous natural products and vegetable oils has been performed using hexane, a hazardous air pollutant, where more than 20 million kg of hexane are released into the atmosphere each year, according to the EPA Toxic Release Inventory [19]. Thus, the development and implementation of greener alternatives are mandatory. When possible, the elimination of solvent is the greenest alternative. Although solvent-free process has been recognized as a solution for achieving sustainability goals, it may have poor heat and mass transfer or high viscosity, and therefore it could lead to excessive use of energy or less pure product. Some processes cannot be run in a solvent-free environment. "Solvent substitution" idea was promoted in 90's as an environmentally friendly approach and way to reduce the amount of hazardous waste. Thus, the

replacement of VOCs with benign alternatives (benign non-volatile organic solvents, supercritical fluids, water-based processes, ionic liquids and fluorinated systems) stands for a pollution prevention goal.

1.3 Separation processes

Separation processes are used to remove a single component from a mixture or separate solutions of different components into products that diverge in composition. The mechanisms for separation use a physical and/ or a chemical property difference as a driving force for a separation, through energy or mass separation agent. Separation processes are applied for three main functions: purification, concentration and fractionation. Purification is separation of desired and undesired species from the mixture. Concentration process obtains a higher concentration of a desired component which is initially in diluted mixture. Fractionation is separation of feed stream of few components into relatively pure streams of each component. Moreover, separation processes can be characterized as equilibrium and rate processes.

The equilibrium processes are designed using thermodynamic equilibrium relationships between phases, normally performed as countercurrent cascade processes. The main processes from this group are distillation, extraction and leaching. Distillation utilizes vapour pressure as a separation mechanism, while extraction and leaching are based on partitioning between phases. The degree of change in composition between the phases is an important factor for using this mechanism.

The rate processes are based on the rate of mass transfer of a component from one phase into another due to a gradient in a chemical/ physical property. Concentration gradient is the most common in processes, while pressure, temperature, electric fields and gravity gradients could occur. The mass transfer based processes are absorption, desorption, adsorption, ion-exchange and membrane separations. Absorption, desorption (stripping) and adsorption use the partitioning between phases as the separation mechanism. Ion-exchange process is based on chemical reaction equilibrium since the species removed from solution are replaced by the species from the solid resin. Membrane separations are based on differences in permeability due to molecular size and shape, and chemical selectivity for the membrane material between components in a feed mixture.

Both, the equilibrium and rate processes utilize separating agents. An energy separation agent (ESA) usually provokes a formation of an additional phase. Heat is the most common ESA, while gravitational, electric and magnetic fields are used rarely. A mass separation agent (MSA) can facilitate formation of a second phase or modify the existing phase equilibrium, changing a solute distribution between phases. The solute must have higher affinity for the MSA in order to be transfer from the mixture to the MSA phase. The use of a MSA requires two steps: the solute separation from the mixture and the recovery of MSA in order to recycle it in the process. Thus,

the fact that no additional material is added into the system gives an advantage to ESA. On the other hand, the processes with ESA require high energy consumption when heat is employed, which should be considered before giving an advantage to ESA over MSA.

The environmental and economical importance of separation processes have been recognized in many different processes. Large quantities of waste generated by both industry and domestic use must be remediated, recycled or limited. It is important to recover and recycle useful materials, as well as to isolate hazardous materials from effluent or waste streams. Chemical separation processes have been already used in biotechnology, metals recovery and purification, chemical processing plants and feedstock and microelectronics.

Schügerl [20, 21] has shown that various separation processes can be used to isolate a potentially valuable material in downstream processing. The efficiency of the established methodologies to separate, concentrate and recover alcohols, organic acids, antibiotics and proteins has been demonstrated. Membrane-based processes play a critical role in separation/ purification of biotechnological products [22, 23]. In the last two decades membranes have been developed due to the requirements of the biotechnology industry. Furthermore, membrane filtration is an interesting approach for process intensification in catalysis, due to its immense potential of catalyst recovery and recycling [24]. Other separation techniques, such as ion-exchange resins and biphasic systems, have been proposed for the same purpose by Barbaro and Liguori [25] and Afonso et al. [26], respectively. Metal ions isolation from waste streams has been widely studied applying techniques mentioned above [27, 28], as well as solvent extraction in which alternative media has been used instead [29, 30].

Solvent extraction technique that facilitates isolation of valuable materials from the process is used in most chemical application, due to its energy efficiency. It is promising towards sustainability, since the volatile organic compounds, commonly used in recovery step, can be replaced by benign, non-volatile solvents.

1.4 Alternative solvents in separation processes

It is well known that volatile organic solvents have been widely used in various industrial processes. They have caused environmental and health problems in the last few decades and thus, their use have been limited. Benzene and chloroform were removed from general use, due to their toxic and carcinogenic characteristics, while aromatic hydrocarbons were partially removed. The use of ozone depleting compounds (e.g. chlorofluorocarbons, bromofluorocarbons and 1,1,1-trichloroethane) and carbon tetrachloride as solvents, refrigerants and fire extinguisher have been excluded. For example, extremely hazardous carbon tetrachloride, initially used in dry cleaning, became outlawed and it was substituted by perchloroethane, an uncertain alternative (suspected carcinogen). Dichloromethane, the ideal extraction solvent in the decaffeination of coffee after replacing chloroform and benzene, was

substituted by alternatives such as $scCO_2$, water or ethyl acetate, as it turned to be carcinogenic. Therefore, VOCs incompatibility with the aims of green chemistry leads to alternative solvents for their replacement.

Alternative solvents such as water, carbon dioxide, ionic liquids and fluorinated systems are the most studied ones. Some alcohols (e.g. ethanol, glicerol), poliethylen glycols and ethyl lactate also became potential replacement for chlorinated, aromatic and volatile solvents. Alternative solvents should be as harmless as possible, easily recovered and recycled. They should have advantages over commonly used VOCs in order to replace them in existing processes.

In this thesis, several alternative solvents and their advantages over VOCs in various separation processes will be discussed. Deacidification of edible, soybean oil was performed by both polyethylene glycols and ionic liquids (Chapter II). Ionic liquids and supercritical carbon dioxide ($scCO_2$) were employed in two-step recovery of an antibiotic (Chapter III), while ethyl lactate was studied as a potential extraction media of antioxidants from solid matrix (Chapter V).

1.4.1   Polyethylene glycols

Polyethylene glycols (PEGs, $HO(CH_2CH_2O)_nH$) are an important group of ethylene oxide polymers. PEGs are available in a range of molecular weights from 200 to tens of thousands. The numerical name of PEGs (e.g., PEG-400) indicates the average molecular weight, although they are not monodisperse polymers. At ambient temperature, the polymer could be liquid or solid, depending on its molecular weight. The polymer is a colourless viscous liquid, miscible with water in all proportions at molecular weight lower than 600. When molecular weight crosses 800, it turns to be waxy, white solid which is highly soluble in water. Liquid PEGs have low vapour pressure and low flammability. They are stable to acid, base, high oxidation systems, $NaBH_4$ reduction systems and high temperature [31-33]. They are biodegradable [34, 35], biocompatible. The PEGs' toxicity (LD_{50} = 17-76 gkg^{-1}, orally, rat/rabbit/guinea pig) and ecotoxicity are extremely low [36]. Moreover, it has been shown that biodegradability decreases with increasing molecular weight of PEGs [35].

PEGs have been approved by the U.S. Food and Drug Agency (FDA) as a GRAS (Generally Recognized as Safe) compounds [37]. Enormous worldwide manufacture reaches millions of tons of PEGs per year. Therefore, PEGs became abundant and cheap material which can be further used in production of pharmaceuticals, cosmetics, lubricants and surfactants. PEGs have been found application in biotechnology and medicine [38, 39]. Besides, using PEG as a co-solvent improves the solubility of organic molecules in water, due to decrease of the aqueous solution polarity [19]. It also can be used as phase-transfer catalyst (PTC) since the polyethylene oxide chains are capable to form complexes with metal cations. Thus, there is a potential application of PEGs as a solvent and PTC in organic synthesis [40-43].

Although PEG is water soluble, the PEG aqueous solutions may display phase separations under controlled condition, forming polymer-reach and polymer-poor phases. This is due to the hydrophobic methylene groups and hydrophilic ether groups combined along the polymer chains, and alcohol-end groups. The aqueous biphasic system (ABS), discovered by Albertsson, has been used in bio-separation for almost fifty years [19]. PEGs and their aqueous solutions have been widely used in green separation chemistry [30, 44-49]. Solvent extraction of metal ions has been studied by Rogers et al. [47]. Among others, the partitioning behaviour of strontium and cesium in aqueous biphasic system was presented [30]. The same group has scrutinized the recovery of food colouring dyes, testing aqueous biphasic systems utility to remove textile dyes and other industrial and natural pigments from industrial plant wastes [45]. Furthermore, successful separation of anti-HIV monoclonal antibodies from tobacco crude extract was achieved using ABS and reported by Platis and Labrou [48], while aqueous two phase system containing PEG6000 was employed in separation of amino acids [49]. Deacidification of soybean oil by low molecular weight PEGs has been studied, indicating that PEGs can be feasible alternative to generally used organic solvents [50].

Liquid-liquid extraction of free fatty acids (FFAs) from edible oil using PEGs will be discussed in Chapter II of this thesis.

1.4.2   Ionic liquids

Ionic liquids (ILs) stand for a new class of chemicals although they have been known since 1914, when the physical properties of ethylammonium nitrate were reported by Walden [51]. The discovery of a new class of liquids did not get any significant attention at the time. Few attempts to apply new liquids in electrochemistry were patented in 1940s and 1970s. Although, the very first class of ILs had serious limitation, such as moisture and air sensitivity, this was the pioneer work in the field of ILs. The titles as: "*Air and water stable 1-ethyl-3-methylimidazolium based ionic liquids*" [52] and "*New, stable, ambient-temperature molten salts*" [53] appeared in 1992, and called attention to narrow scientific community. However, ILs became promising chemicals in the late 1990s, when their use in green and industrial chemistry was recognized by Seddon: "*... all the indications are that room-temperature ionic liquids are the basis of a new industrial technology. They are truly designer solvents: either the cation or anion can be changed [...] in order to optimise such phenomena as the relative solubilities of the reactants and products, the reaction kinetics, the liquid range of the solvent, the intrinsic catalytic behaviour of the media, and air-stability of the system. For the first time, it is possible to design a solvent to optimise a reaction (with control over both yield and selectivity), rather than to let the solvent dictate the course of the reaction [...] it will never be the same again!*" [13].

Ionic liquids are most commonly defined as materials that are composed of cations and anions, which melt below the conventional temperature of 100 ^{o}C, even though this temperature does not have any chemical or physical significance. The low melting points of ILs are a result of

combining bulky asymmetric organic cations and significantly smaller anions, due to lower lattice energy. Although novel chemical structures appear extremely fast, most of ILs are based on imidazolium, ammonium, phosphonium, sulfonium, pyridinium and pyrrolidinium cation. The commonly used anions can be divided in two groups: fluorinated anions such as hexafluorophosphate ($[PF_6]^-$), tetrafluoroborate ($[BF_4]^-$), trifluoroacetate ($[CF_3CO_2]^-$), trifluoromethanesulfonate ($[OTf]^-$), and bis(trifluoromethylsulfonyl)imide ($[NTf_2]^-$); and non-fluorinated anions: tetrachloroaluminate ($[AlCl_4]^-$), nitrate ($[NO_3]^-$), acetate ($[CH_3CO_2]^-$), methanesulfonate ($[CH_3SO_3]^-$), chloride ($[Cl]^-$), bromide ($[Br]^-$). Dialkylimidazolium cation coupled with fluorinated anions are the most studied ionic liquids up to date, which can be fairly disappointment due to an estimated 10^{18} possible low melting point salts. The anions $[PF_6]^-$ and $[BF_4]^-$ may decompose when heated in the presence of water forming HF [54], while trifluoromethane sulfonate anions are a firm replacement since C-F bond is inert to hydrolysis. The undeniable potential of ionic liquids is based on their vast chemical diversity regarding both cation and anion. Their physical and chemical properties are highly tuneable, defined by combination of cation and anion, size, geometry and charge distribution.

In the literature, ionic liquids have been described as green solvents, non-volatile, non-flammable, chemically and thermally stable, highly polar, capable to dissolve many different chemicals, recyclable *ect*. None of these characteristics can be applied to all ILs in general. The vapour pressures of ionic liquids are extremely low and thus, their non-volatility is the major reason to classify those as green solvents. However, Earle et al. [55] showed that some ILs can be distilled at 200-300 ^{o}C and under high vacuum (0.05 mbar), yet they still remind non-volatile at ambient condition. The solvent properties of ILs are fairly defined by hydrogen-bond donor and/ or acceptor capacity and charge distribution. Low symmetry of cation and/ or anion leads to wide liquid window, and reduce density and conductivity of ILs. Hydrophobicity, thermal stability and viscosity are also dependent on chemical structure, on longer alkyl substituent in particular. H-bonding and van der Waals interaction that occur in the species strongly influence viscosity, which are generally higher than that of other solvents [56]. The existence of polar and non-polar domains explains the powerful solvent property of ILs for both polar and non-polar species. They are capable to dissolve various materials such as salts, fats, proteins, amino acids, DNA, sugars, inks, plastics, crude oil *ect* [57]. Understanding structure-property relationship plays a key role in selection of an appropriate ionic liquid for a particular application.

Despite the fact that ILs are known over decades, there is still lack of knowledge on toxicity and ecotoxicity, environmental persistence and sustainable synthetic pathways. Such information regarding ILs is required in order to might consider them "green" solvents. Recently, the potential toxicological effect of ILs on various model organisms has been intensively studied [58, 59]. In general, these studies demonstrated a higher toxicity of ILs with the increase of alkyl chain length in cation, while anion contribute to toxic effect of ILs still remind uncertain. Wells and Coombe [60] showed that ILs can demonstrate either moderate or highly toxic effect on model organism. The ecotoxicity of less toxic ILs were comparable to those provoked by

toluene or xylene, while the most toxic ILs were even more ecotoxic than organic solvents such as methanol, phenol and acetonitrile. Consequently, there are main concerns related to biodegradability and environmental persistence of ILs. The outstanding work, presented by Abrusci et al. [61] demonstrated efficient biodegradation of common ILs by *Sphingomonas paucimobilis* bacterium. Even so, the design of biocompatible ionic liquids, novel formulation that incorporates amino acids [62, 63], cholinium [64, 65], fructose [66], glucose [67], and non-nutritive sweeteners [68] has been proposed. Toxicity, ecotoxicity and biodegradability are finely tuneable characteristics, which depend on composition and syntheses methods of ILs. A solvent free, microwave assisted method [69] and neutralization are greener synthetic routs than alkylation and methatesis. Novel synthetic methods are continuously being developed, promising the design of safer ILs with required properties. Nevertheless, ability to recycle ILs is an important issue for both economical and environmental suitability. Several studies regarding recycle and reuse of ionic liquids has been reported. Supercritical carbon dioxide extraction is a promising technique for this purpose due to specific phase behaviour of the systems, which will be further discussed in Chapter IV.

Opportunity to design task specific ionic liquids, able to control thermodynamics, kinetic and reaction outcomes, allows rapid advance in various application. ILs have been used in chemical reaction, both as a solvent [70] and a catalyst [71]; in electrochemistry [72], for batteries [73] and fuel cell [74]; in nanotechnology [75, 76]; as stationary phases for chromatography [77, 78]; in separation technologies [79-81]; and biotechnology [82, 83]. ILs' accessibility and thus their lower costs have been achieved by their commercialization (MERC, BASF, IoLiTec, Cytec, Sigma-Aldrich), introducing them into several industrial processes [84]. The very first industrial application of ionic liquids was achieved by BASF (BASIL[®] - Biphasic Acid Scavening utilizing Ionic Liquids) in 2003 [85]. The original process was improved replacing triethylamine by 1-methylimidazole, which purpose is to eliminate the acid that was formed in the reaction, forming a discreet phase of an ionic liquid, 1-methylimidazolium chloride. The reaction is an outstanding example of ILs industrial application due to a multi-ton scale production. The remarkable examples of ILs application in large-scale processes are BASF (Cellulose dissolution and aluminium plating), Institut Français du Pétrole (Difasol), Degusa (paint additives), Pionics (lithium batteries) and G24i (solar cells). The Central Glass Co., Ltd., Japan is the first company to produce pharmaceuticals intermediates using ionic liquids technology [84].

Ionic liquids have found application as an alternative replacement to VOCs in liquid-liquid extraction and in supported membranes processes towards more efficient and eco-friendly separation methods. The separation of azeotropic mixtures has been fairly challenging task since their separation by simple distillation is basically impossible. Potential of ILs use for this purpose has been widely studied and reviewed by Pereiro et al. [79]. Extraction of metal ions [86, 87] and biomolecules [88-91], gas separation [92, 93], deacidification of oils [50] and desulfurization of fuels [94] testify ILs' potential use in separation processes.

Two different approaches towards ILs application in liquid-liquid separation, deacidification of soybean oil and purification of erythromycin, will be further discussed in Chapter II and Chapter III of this thesis, respectively.

1.4.3   Supercritical carbon dioxide

A supercritical fluid (SCF) is defined as a compound which is above its critical temperature and pressure. The critical point represents the highest temperature and pressure at which the compound exists as a liquid and vapour in equilibrium. Rising the temperature and pressure, the liquid becomes less dense according to thermal expansion and the gas becomes denser due to its compressibility. At the critical point, the liquid and vapour phase become indistinguishable since the densities become equal and thus, a supercritical fluid is obtained. Consequently, the physical properties of SCFs are in-between those of a liquid and a gas. The densities of SCFs are similar to those of a liquid, while they are characterized by gas like viscosities. Although the properties of a compound vary as the temperature and pressure change, their significant changes are observed near critical point. As the critical point is approached, the compressibility of the fluid becomes very large, turning to be infinite at the critical point, while both, speed of sound and surface tension between phases go to zero. Fluctuation in density is due to large compressibility and thermal oscillation. As SCFs have no surface tension and express high diffusion rates. Supercritical fluids application shows significant potential due to their improved heat and mass transfer, solvent properties adjustment by varying temperature and pressure, and easy solvent removal and recycling.

Any solvent can be used as a supercritical fluid, while its potential application is determined by critical properties, salvation power, toxicity and cost. Several solvents (see Table 1) have been studied as SCF solvents. For example, the Born-Haber process for ammonia synthesis and the synthesis of low-density polyethene were the most known supercritical processes at the beginning of 1980s. Although some of these have acceptable critical properties, their applications are limited due to toxicity issue. Carbon dioxide and water are the most studied SCFs regarding their safe and nontoxic nature. However, the critical temperature just above ambient (31.1 ^{o}C) and relatively low critical pressure (73.8 bar) of carbon dioxide is obvious advantage over supercritical water (T_c = 374.2 ^{o}C and P_c = 220.5 bar). Furthermore, high pressure water is corrosive which represent another limitation for its utilization.

In particular, nontoxic, inexpensive, non-flammable, abundant and generally recognized as a safe, carbon dioxide, in its supercritical fluid state ($scCO_2$) demonstrates interesting and unique solvent properties. It is characterized by densities similar to those of liquid and the rapid mass transfer due to its low viscosity. Even if carbon dioxide is non-polar, the charge distribution of molecule results in very high quadrupole moment, which is responsible for its unusual solvating behaviour [95]. Moreover, density and polarity of $scCO_2$ become highly tuneable near critical point by slightly alters in temperature and pressure, creating versatile and selective solvent. The

solvent power limitations can be overcome by using small quantities of co-solvent and thus extend the range of $scCO_2$ solvating strength. Although, CO_2 is chemically inert under most conditions, it cannot be used in certain reaction due to its interaction with good nucleophiles (amines). Considering partial negative charges on oxygen atoms and partial positive charge on carbon, carbon dioxide can act as either weak Lewis acid or Lewis base. Additionally, $scCO_2$ is fully miscible with other gasses (i.e. H_2, O_2) and hence expected to be suitable reaction media for hydrogenation, oxidation and hydroformylation [96]. Considering the fact that it is a greenhouse gas, it is important to use it with no negative effect on the environment. The large quantities of high purity CO_2 are easily obtained as a by-product of biomass fermentation or ammonia manufacturing. The source of carbon dioxide as well as level of energy consumption due to its compression should be considered, when the $scCO_2$ potential to perform in various sustainable processes is evaluated.

Table 1.1 Critical properties of some SCFs

Fluid	T_c (^oC)	P_c (MPa)	Remarks
Carbon dioxide	31.1	7.38	
Ammonia	132.4	11.29	Toxic
Water	374.1	22.1	High T_c, corrosive
Ethane	32.5	4.91	Flammable
Propane	96.8	4.26	Flammable
Cyclohexane	279.9	4.03	High T_c
Methanol	240.0	7.95	High T_c
Ethanol	243.1	6.39	High T_c
Isopropanol	235.6	5.37	High T_c
Acetone	235.0	4.76	High T_c

The unique solvent characteristics and facile separation of product due to simple depressurization have involved $scCO_2$ in different reaction and separation processes. Although chemical reactions in $scCO_2$ have been intensively studied [97], only few researcher groups have been focused on continuous process [96, 98, 99]. There have been two successful industrial hydrogenation processes in $scCO_2$, namely: 1) the synthesis of vitamins by Hoffman la Roche [100] and 2) the hydrogenation of isophorone by Thomas Swan & Co Ltd [101]. Additionally, scCO2 application in chemical processes is promising due to opportunity to join reaction and separation into a single process, which has been recently analysing by Han and Poliakoff [102]. ScCO$_2$ technology has been successfully used in nanotechnology, since synthesized nanostructure materials do not usually require additional purification or drying.

Moreover, their exact particle size and morphology can be easily achieved by using supercritical CO_2 [103, 104].

On the other hand, production of highly pure materials is assured due to absence of the solvent residues, which is particularly important in the pharmaceutical, cosmetics, food and electronic industries. Supercritical CO_2 extraction of natural products from solid plant matrices has been widely studied [105, 106], yet hundreds industrial applications have been established. However, very few of them have shown outstanding achievement. The supercritical decaffeination process has been known since the 1980s. The caffeine is selectively extracted from green coffee beans into the $scCO_2$. Additionally, it is recovered from the high pressure CO_2 in water wash column at reduced pressure rather than by realising the pressure, ensuring lower energy consumption. Another exceptional example is the Diamond process, developed by the Centre d'Energie Atomique and the French company Sabate [107]. Utilization of $scCO_2$ in cork stoppers treatment allows complete remove of trichloroanisol, the contaminant produced by fungi and responsible for the infamous cork taint taste of wine. Recently, an enhanced process with equivalent application has been developed and patented [108]. Furthermore, supercritical CO_2 extraction has been suggested as a deacidification method for vegetable oils [109-111].

High solubility of $scCO_2$ in ILs, whereas ILs are basically non soluble in CO_2, observed by Blanchard et al. [112], is the pioneer work in developing novel biphasic systems for either reaction or separation processes. Such a phase behaviour allow $scCO_2$ to extract a wide range of organic compounds from IL-phase with no cross-contaminations, while on the other hand facilitate recovery and reuse of catalyst and ILs in chemical reactions [98, 113-115]. Extraction of organic compounds (methanol [116], solid inorganic salts [117], aromatic and aliphatic solutes [118]) and bio molecules [90]) from ionic liquids by $scCO_2$ have been effectively performed. Relatively high recovery rates point towards successful utilization of ILs-$scCO_2$ separation media.

IL-$scCO_2$ biphasic system will be further discussed in Chapter III and Chapter IV of this thesis, wherein recovery of erythromycin from various ILs by supercritical carbon dioxide was performed (Chapter III) and ILs-CO_2 phase behaviour was studied (Chapter IV).

1.4.4   Ethyl lactate

Ethyl lactate ($C_5H_{10}O_3$), also known as lactic acid ethyl ester, is the main member of the lactate esters family. It can be either in levo (S) or dextro (R) forms, yet the S-enantiomer is obtained easierwhen produced from natural sources. Ethyl lactate can be easily derived from renewable resources [119], through a reversible reaction between lactic acid and ethanol, where water is a only by-product [120]. The reaction and separation are incorporated into a single unit, increasing the ethyl lactate yield and purity. Moreover, various approaches on process

intensification have been proposed in order to provide high quality ethyl lactate and decrease its cost [121].

Ethyl lactate has been intensively studied due to its suitable characteristics. It is clear, colourless liquid which can be found in trace in some natural products such as fruits, wine, and chicken. The detailed studies revealed that it does not show any potential environmental and health risk. Indeed, utilization of ethyl lactate as food additive is approved by FDA (US Food and Drug Agency), since it is fully biodegradable and has favourable toxicological properties [122, 123]. Clary et al. [122] demonstrated that toxicity of ethyl lactate are negligible ($LD_{50} > 2000$ $mgkg^{-1}$, orally, rat). Additionally, it is a high boiling polar solvent with low vapour pressure and surface tension, while its relatively low viscosity is important for both heat and mass transfer. It is noncorrosive, non-ozone depleting and easy to recycle. The molecular structure, particularly the position of the hydroxyl and carbonyl groups, allows formation of intra- and intermolecular interactions through hydrogen bonds formation. Aparicio et al. [124] demonstrated its proton donor/ acceptor nature, since ethyl lactate molecules form clusters between themselves.

Excellent solvent properties over a wide range of solutes that ethyl lactate offers, as well as its suitable physicochemical characteristics provide its potential application as a green solvent in chemical reactions and separations, coating industry, pharmaceutical preparation and as a food additive. Ethyl lactate has been used as a solvent for several synthetic processes, either aril aldimines synthesis [125] or stereo-selective synthesis [126, 127]. As reported by Bennett et al. [125], an efficient, green synthesis was developed, since ethyl lactate was used as an alternative to commonly employed toxic solvents. The pure product was obtained and no additional purification procedure was needed. Substitution of the hazardous air pollutants (butan-2-one, tetrahydrofurane and toluene) by ethyl lactate in magnetic tape coating was reported by Nikles et al. [128]. Moreover, ethyl lactate can successfully remove copper from contaminated soils [129] and it can be used as an emulsifying/ dispersing media for biologically active compounds in pharmaceutical industry [130].

Solubility of various compounds in ethyl lactate, as essential information for its application in separation processes has been studied [131-136]. There are several examples in the literature wherein ethyl lactate was used as an extraction solvent: a gas anti-solvent process was proposed by Tombokan et al. [131] in order to obtain high purity sclareol from Clary sage. Ethyl lactate was used for sclareol extraction, while its precipitation from the solvent was achieved by CO_2; Hernandéz et al. [132] reported recovery of squalene from olive oil deodorized distillates using ethyl lactate; the potential application of ethyl lactate for selective separation of tocopherol from olive oil was proposed by Vicente et al. [133]; few studies pointed out ethyl lactates' capability to extract carotenoids from various sorces, either lycopene recovery from tomato [137, 138], or lutein and *β*-carotene extraction from corn and carrots [137]. Accelerated solvent extraction of caffeine from green coffee beans, as well as ethyl lactate extraction ability over both ethanol and ethyl acetate has been recently studied by our group.

Ethyl lactate potential for extraction processes will be further discussed in Chapter V of this thesis. Solubility of high-value compounds with antioxidants characteristics in ethyl lactate will be reported. Moreover, decaffeination of green coffee beans using ethyl lactate will be discussed.

1.5 References

[1] U.S. Envitonmental Protection Agency, http://www.epa.gov/climatechange/.

[2] N.E. Hultman, D.M. Hassenzahl, S. Rayner, Climate risk, Annual Review of Environment and Resources, 35 (2010) 283-303.

[3] World Commision on Environment and Development, Our common future, in, New York, 1987.

[4] P.T. Anastas, J.C. Warner, Green chemistry: Theory and practice, Oxford University Press, 2000.

[5] REACH – Registration, Evaluation, Authorisation and restriction of Chemicals, http://ec.europa.eu/enterprise/sectors/chemicals/reach/.

[6] B. Trost, The atom economy--a search for synthetic efficiency, Science, 254 (1991) 1471-1477.

[7] R.A. Sheldon, Atom efficiency and catalysis in organic synthesis, Pure and Applide Chemistry, 72 (2000) 1233-1246.

[8] D.J.C. Constable, A.D. Curzons, V.L. Cunningham, Metrics to 'green' chemistry-which are the best?, Green Chemistry, 4 (2002) 521-527.

[9] P.T. Anastas, J.B. Zimmerman, Peer reviewed: Design through the 12 principles of green engineering, Environmental Science & Technology, 37 (2003) 94A-101A.

[10] M. Herrchen, W. Klein, Use of the life-cycle assessment (LCA) toolbox for an environmental evaluation of production processes, Pure and Applide Chemistry, 72 (2000) 1247-1252.

[11] J.A. Fava, Life-cycle assessment: A new way of thinking, Environmental Toxicology and Chemistry, 13 (1994) 853-854.

[12] H.-J. Arpe, Industrial organic chemistry, Wiley-VCH, Weinheim, 2010.

[13] K.R. Seddon, Ionic Liquids for Clean Technology, Journal of Chemical Technology & Biotechnology, 68 (1997) 351-356.

[14] J.C. Warner, A.S. Cannon, K.M. Dye, Green chemistry, Environ. Impact Assess. Rev, 24 (2004) 775-799.

[15] W. Niu, K.M. Draths, J.W. Frost, Benzene-free synthesis of adipic acid, Biotechnology Progress, 18 (2002) 201-211.

[16] J. H. Clark, F. E. I. Deswarte, T. J. Farmer, The integration of green chemistry into future biorefineries, Biofuels, Bioproducts and Biorefining, 3 (2009) 72-90.

[17] A. Corma, S. Iborra, A. Velty, Chemical routes for the transformation of biomass into chemicals, Chemical Reviews, 107 (2007) 2411-2502.

[18] Greener synthesis of ibuprofen, Chemistry Innovation, http://www.chemistryinnovation.co.uk/stroadmap/roadmap.asp-id=172.htm.

[19] F.M. Kerton, Alternative solvents for green chemistry, Royal Society of Chemistry, Cambridge, UK, 2009.

[20] S. Karl, Integrated processing of biotechnology products, Biotechnology Advances, 18 (2000) 581-599.

[21] K. Schügerl, J. Hubbuch, Integrated bioprocesses, Current Opinion in Microbiology, 8 (2005) 294-300.

[22] R. van Reis, A. Zydney, Bioprocess membrane technology, Journal of Membrane Science, 297 (2007) 16-50.

[23] A. Saxena, B.P. Tripathi, M. Kumar, V.K. Shahi, Membrane-based techniques for the separation and purification of proteins: An overview, Advances in Colloid and Interface Science, 145 (2009) 1-22.

[24] M. Janssen, C. Muller, D. Vogt, Recent advances in the recycling of homogeneous catalysts using membrane separation, Green Chemistry, 13 (2011).

[25] P. Barbaro, F. Liguori, Ion exchange resins: Catalyst recovery and recycle, Chemical Reviews, 109 (2008) 515-529.

[26] C.A.M. Afonso, L.C. Branco, N.R. Candeias, P.M.P. Gois, N.M.T. Lourenco, N.M.M. Mateus, J.N. Rosa, Efficient catalyst reuse by simple dissolution in non-conventional media, Chemical Communications, (2007) 2669-2679.

[27] G. Borbély, E. Nagy, Removal of zinc and nickel ions by complexation–membrane filtration process from industrial wastewater, Desalination, 240 (2009) 218-226.

[28] L. Zeng, C. Yong Cheng, A literature review of the recovery of molybdenum and vanadium from spent hydrodesulphurisation catalysts: Part II: Separation and purification, Hydrometallurgy, 98 (2009) 10-20.

[29] A.P. Abbott, G. Frisch, J. Hartley, K.S. Ryder, Processing of metals and metal oxides using ionic liquids, Green Chemistry, 13 (2011) 471-481.

[30] R.D. Rogers, C.B. Bauer, A.H. Bond, Novel polyethylene glycol-based aqueous biphasic systems for the extraction of strontium and cesium, Separation Science and Technology, 30 (1995) 1203-1217.

[31] J. Chen, S.K. Spear, J.G. Huddleston, J.D. Holbrey, R.D. Rogers, Application of polyethylene glycol-based aqueous biphasic reactive extraction to the catalytic oxidation of cyclic olefins, Journal of Chromatography B, 807 (2004) 145-149.

[32] A. Haimov, R. Neumann, Polyethylene glycol as a non-ionic liquid solvent for polyoxometalate catalyzed aerobic oxidation, Chemical Communications, (2002) 876-877.

[33] J.R. Blanton, Selective reduction of aldehydes using polyethylene glycol-sodium borohydride derivatives as phase transfer reagents, Synthesis Communication, 27 (1997) 2093-2102.

[34] D.J. Heldebrant, H.N. Witt, S.M. Walsh, T. Ellis, J. Rauscher, P.G. Jessop, Liquid polymers as solvents for catalytic reductions, Green Chemistry, 8 (2006) 807-815.

[35] G.K. Watson, N. Jones, The biodegradation of polyethylene glycols by sewage bacteria, Water Research, 11 (1977) 95-100.

[36] K. Verschueren, Handbook of environmental data on organic chemicals (4th Edition), in, John Wiley & Sons, 2001.

[37] D.A. Herold, K. Keil, D.E. Bruns, Oxidation of polyethylene glycols by alcohol dehydrogenase, Biochemical Pharmacology, 38 (1989) 73-76.

[38] J.M. Harris, Poly (ethylene glycol) chemistry: Biotechnical & biomedical applications, Plenum Press, New York, 1992.

[39] A. Sousa-Herves, R. Riguera, E. Fernandez-Megia, PEG-dendritic block copolymers for biomedical applications, New Journal of Chemistry, 36 (2012) 205-210.

[40] G.E. Totten, N.A. Clinton, Poly(ethylene glycol) and derivatives as phase transfer catalysts, Journal of Macromolecular Science, Part C: Polymer Reviews, 38 (1998) 77-142.

[41] B. Sauvagnat, F. Lamaty, R. Lazaro, J. Martinez, Polyethylene glycol (PEG) as polymeric support and phase-transfer catalyst in the soluble polymer liquid phase synthesis of α-amino esters, Tetrahedron Letters, 39 (1998) 821-824.

[42] G.D. Yadav, B.G. Motirale, Microwave-irradiated synthesis of nitrophen using PEG 400 as phase transfer catalyst and solvent, Organic Process Research & Development, 13 (2009) 341-348.

[43] J. Chen, S.K. Spear, J.G. Huddleston, R.D. Rogers, Polyethylene glycol and solutions of polyethylene glycol as green reaction media, Green Chemistry, 7 (2005) 64-82.

[44] J.G. Huddleston, H.D. Willauer, S.T. Griffin, R.D. Rogers, Aqueous polymeric solutions as environmentally benign liquid/liquid extraction media, Industrial & Engineering Chemistry Research, 38 (1999) 2523-2539.

[45] J.G. Huddleston, H.D. Willauer, K.R. Boaz, R.D. Rogers, Separation and recovery of food coloring dyes using aqueous biphasic extraction chromatographic resins, Journal of Chromatography B: Biomedical Sciences and Applications, 711 (1998) 237-244.

[46] R.D. Rogers, H.D. Willauer, S.T. Griffin, J.G. Huddleston, Partitioning of small organic molecules in aqueous biphasic systems, Journal of Chromatography B: Biomedical Sciences and Applications, 711 (1998) 255-263.

[47] R.D. Rogers, A.H. Bond, C.B. Bauer, J. Zhang, S.T. Griffin, Metal ion separations in polyethylene glycol-based aqueous biphasic systems: correlation of partitioning behavior with available thermodynamic hydration data, Journal of Chromatography B: Biomedical Sciences and Applications, 680 (1996) 221-229.

[48] D. Platis, N.E. Labrou, Application of a PEG/salt aqueous two-phase partition system for the recovery of monoclonal antibodies from unclarified transgenic tobacco extract, Biotechnology Journal, 4 (2009) 1320-1327.

[49] A. Salabat, M.H. Abnosi, A. Motahari, Investigation of amino acid partitioning in aqueous two-phase systems containing polyethylene glycol and inorganic salts, Journal of Chemical & Engineering Data, 53 (2008) 2018-2021.

[50] M.S. Manic, V. Najdanovic-Visak, M.N. da Ponte, Z.P. Visak, Extraction of free fatty acids from soybean oil using ionic liquids or poly(ethyleneglycol)s, AIChE Journal, 57 (2011) 1344-1355.

[51] P. Walden, Ueber die Molekulargrösse und elektrische Leitfähigkeit einiger geschmolzenen salze, Bull. Acad. Impér. Sci. St. Pétersbourg, 8 (1914) 405-422.

[52] J.S. Wilkes, M.J. Zaworotko, Air and water stable 1-ethyl-3-methylimidazolium based ionic liquids, J. Chem. Soc. Chem. Commun., (1992) 965-967.

[53] E.I. Cooper, E.J.M. O'Sullivane, New, stable, ambient-temperature molten salts, in: R.J. Gale, G. Blomgren, H. Kojima (Eds.) Eighth International Molten Salts Symposium, The Electrochemical Society, Inc., Pennington, New Jersey, 1992, pp. 386-396.

[54] M.G. Freire, C.M.S.S. Neves, I.M. Marrucho, J.o.A.P. Coutinho, A.M. Fernandes, Hydrolysis of tetrafluoroborate and hexafluorophosphate counter ions in imidazolium-based ionic liquids, The Journal of Physical Chemistry A, 114 (2009) 3744-3749.

[55] M.J. Earle, J.M.S.S. Esperanca, M.A. Gilea, J.N. Canongia Lopes, L.P.N. Rebelo, J.W. Magee, K.R. Seddon, J.A. Widegren, The distillation and volatility of ionic liquids, Nature, 439 (2006) 831-834.

[56] F. Endres, S. Zein El Abedin, Air and water stable ionic liquids in physical chemistry, Physical Chemistry Chemical Physics, 8 (2006) 2101-2116.

[57] R. Renner, Ionic liquids: An industrial cleanup solution, Environmental Science & Technology, 35 (2001) 410A-413A.

[58] T.P. Thuy Pham, C.-W. Cho, Y.-S. Yun, Environmental fate and toxicity of ionic liquids: A review, Water Research, 44 (2010) 352-372.

[59] M. Petkovic, K.R. Seddon, L.P.N. Rebelo, C. Silva Pereira, Ionic liquids: a pathway to environmental acceptability, Chemical Society Reviews, 40 (2011) 1383-1403.

[60] A.S. Wells, V.T. Coombe, On the freshwater ecotoxicity and biodegradation properties of some common ionic liquids, Organic Process Research & Development, 10 (2006) 794-798.

[61] C. Abrusci, J. Palomar, J.L. Pablos, F. Rodriguez, F. Catalina, Efficient biodegradation of common ionic liquids by Sphingomonas paucimobilis bacterium, Green Chemistry, 13 (2011) 709-717.

[62] W. Bao, Z. Wang, Y. Li, Synthesis of chiral ionic liquids from natural amino acids, The Journal of Organic Chemistry, 68 (2002) 591-593.

[63] K. Fukumoto, M. Yoshizawa, H. Ohno, Room temperature ionic liquids from 20 natural amino acids, Journal of the American Chemical Society, 127 (2005) 2398-2399.

[64] Y. Fukaya, Y. Iizuka, K. Sekikawa, H. Ohno, Bio ionic liquids: room temperature ionic liquids composed wholly of biomaterials, Green Chemistry, 9 (2007) 1155-1157.

[65] M. Petkovic, J.L. Ferguson, H.Q.N. Gunaratne, R. Ferreira, M.C. Leitao, K.R. Seddon, L.P.N. Rebelo, C.S. Pereira, Novel biocompatible cholinium-based ionic liquids-toxicity and biodegradability, Green Chemistry, 12 (2010) 643-649.

[66] S.T. Handy, M. Okello, G. Dickenson, Solvents from biorenewable sources: Ionic liquids based on fructose, Organic Letters, 5 (2003) 2513-2515.

[67] L. Poletti, C. Chiappe, L. Lay, D. Pieraccini, L. Polito, G. Russo, Glucose-derived ionic liquids: exploring low-cost sources for novel chiral solvents, Green Chemistry, 9 (2007) 337-341.

[68] E.B. Carter, S.L. Culver, P.A. Fox, R.D. Goode, I. Ntai, M.D. Tickell, R.K. Traylor, N.W. Hoffman, J.J.H. Davis, Sweet success: ionic liquids derived from non-nutritive sweeteners, Chemical Communications, (2004) 630-631.

[69] R.S. Varma, V.V. Namboodiri, An expeditious solvent-free route to ionic liquids using microwaves, Chemical Communications, (2001) 643-644.

[70] J.D. Holbrey, K.R. Seddon, Ionic liquids, Clean Technologies and Environmental Policy, 1 (1999) 223-236.

[71] A.C. Cole, J.L. Jensen, I. Ntai, K.L.T. Tran, K.J. Weaver, D.C. Forbes, J.H. Davis, Novel brønsted acidic ionic liquids and their use as dual solvent−catalysts, Journal of the American Chemical Society, 124 (2002) 5962-5963.

[72] H. Ohno, Electrochemical Aspects of Ionic Liquids 2nd ed., John Wiley & Sons, Inc., 2011.

[73] H. Sakaebe, H. Matsumoto, K. Tatsumi, Application of room temperature ionic liquids to Li batteries, Electrochimica Acta, 53 (2007) 1048-1054.

[74] M. Armand, F. Endres, D.R. MacFarlane, H. Ohno, B. Scrosati, Ionic-liquid materials for the electrochemical challenges of the future, Nature Matererials, 8 (2009) 621-629.

[75] F. Endres, M. Bukowski, R. Hempelmann, H. Natter, Electrodeposition of nanocrystalline metals and alloys from ionic liquids, Angewandte Chemie International Edition, 42 (2003) 3428-3430.

[76] E. Redel, M. Walter, R. Thomann, C. Vollmer, L. Hussein, H. Scherer, M. Krüger, C. Janiak, Synthesis, stabilization, functionalization and, DFT calculations of gold nanoparticles in fluorous phases (PTFE and ionic liquids), Chemistry – A European Journal, 15 (2009) 10047-10059.

[77] C.F. Poole, S.K. Poole, Ionic liquid stationary phases for gas chromatography, Journal of Separation Science, 34 (2011) 888-900.

[78] A. Berthod, M.J. Ruiz-Ángel, S. Carda-Broch, Ionic liquids in separation techniques, Journal of Chromatography A, 1184 (2008) 6-18.

[79] A.B. Pereiro, J.M.M. Araújo, J.M.S.S. Esperança, I.M. Marrucho, L.P.N. Rebelo, Ionic liquids in separations of azeotropic systems – A review, The Journal of Chemical Thermodynamics, 46 (2012) 2-28.

[80] P.S. Kulkarni, L.A. Neves, I.M. Coelhoso, C.A.M. Afonso, J.G. Crespo, Supported ionic liquid membranes for removal of dioxins from high-temperature vapor streams, Environmental Science & Technology, 46 (2011) 462-468.

[81] L.J. Lozano, C. Godínez, A.P. de los Ríos, F.J. Hernández-Fernández, S. Sánchez-Segado, F.J. Alguacil, Recent advances in supported ionic liquid membrane technology, Journal of Membrane Science, 376 (2011) 1-14.

[82] R. Ferraz, L.C. Branco, C. Prudêncio, J.P. Noronha, Ž. Petrovski, Ionic liquids as active pharmaceutical ingredients, ChemMedChem, 6 (2011) 975-985.

[83] P. Domínguez de María, Z. Maugeri, Ionic liquids in biotransformations: from proof-of-concept to emerging deep-eutectic-solvents, Current Opinion in Chemical Biology, 15 (2011) 220-225.

[84] N.V. Plechkova, K.R. Seddon, Applications of ionic liquids in the chemical industry, Chemical Society Reviews, 37 (2008) 123-150.

[85] M. Maase, K. Massonne, Biphasic acid scavenging utilizing ionic liquids: The first commercial process with ionic liquids, in: R.D. Rogers, K.R. Seddon (Eds.) Ionic Liquids IIIB: Fundamentals, Progress, Challenges, and Opportunities - Transformations and Processes, American Chemical Society, Washington D.C., 2005, pp. 126-132.

[86] N. Papaiconomou, J.-M. Lee, J. Salminen, M. von Stosch, J.M. Prausnitz, Selective extraction of copper, mercury, silver, and palladium ions from water using hydrophobic ionic liquids, Industrial & Engineering Chemistry Research, 47 (2007) 5080-5086.

[87] Y. Baba, F. Kubota, N. Kamiya, M. Goto, Recent advances in extraction and separation of rare-Earth metals using ionic liquids, Journal of Chemical Engineering of Japan, 44 (2011) 679-685.

[88] S.G. Cull, J.D. Holbrey, V. Vargas-Mora, K.R. Seddon, G.J. Lye, Room-temperature ionic liquids as replacements for organic solvents in multiphase bioprocess operations, Biotechnology and Bioengineering, 69 (2000) 227-233.

[89] M.G. Freire, C.L.S. Louros, L.P.N. Rebelo, J.A.P. Coutinho, Aqueous biphasic systems composed of a water-stable ionic liquid + carbohydrates and their applications, Green Chemistry, 13 (2011) 1536-1545.

[90] M.S. Manic, M.N. da Ponte, V. Najdanovic-Visak, Recovery of erythromycin from aqueous solutions with an ionic liquid and high-pressure carbon dioxide, Chemical Engineering Journal, 171 (2011) 904-911.

[91] J. Wang, Y. Pei, Y. Zhao, Z. Hu, Recovery of amino acids by imidazolium based ionic liquids from aqueous media, Green Chemistry, 7 (2005) 196-202.

[92] P. Scovazzo, D. Havard, M. McShea, S. Mixon, D. Morgan, Long-term, continuous mixed-gas dry fed CO_2/CH_4 and CO_2/N_2 separation performance and selectivities for room temperature ionic liquid membranes, Journal of Membrane Science, 327 (2009) 41-48.

[93] M. Hasib-ur-Rahman, M. Siaj, F. Larachi, Ionic liquids for CO_2 capture—Development and progress, Chemical Engineering and Processing: Process Intensification, 49 (2010) 313-322.

[94] P. Wasserscheid, A. Jess, Deep desulfurization of oil refinery streams by extraction with ionic liquids, Green Chemistry, 6 (2004) 316-322.

[95] J.F. Kauffman, Quadrupolar solvent effects on solvation and reactivity of solutes dissolved in supercritical CO_2, The Journal of Physical Chemistry A, 105 (2001) 3433-3442.

[96] J.R. Hyde, P. Licence, D. Carter, M. Poliakoff, Continuous catalytic reactions in supercritical fluids, Applied Catalysis A: General, 222 (2001) 119-131.

[97] E.J. Beckman, Supercritical and near-critical CO_2 in green chemical synthesis and processing, The Journal of Supercritical Fluids, 28 (2004) 121-191.

[98] D.J. Cole-Hamilton, Asymmetric catalytic synthesis of organic compounds using metal complexes in supercritical fluids, Advanced Synthesis & Catalysis, 348 (2006) 1341-1351.

[99] C. Wiles, P. Watts, Continuous flow reactors: a perspective, Green Chemistry, 14 (2012) 38-54.

[100] L. Devetta, P. Canu, A. Bertucco, K. Steiner, Modelling of a trickle-bed reactor for a catalytic hydrogenation in supercritical CO_2, Chemical Engineering Science, 52 (1997) 4163-4169.

[101] P. Licence, J. Ke, M. Sokolova, S.K. Ross, M. Poliakoff, Chemical reactions in supercritical carbon dioxide: from laboratory to commercial plant, Green Chemistry, 5 (2003) 99-104.

[102] X. Han, M. Poliakoff, Continuous reactions in supercritical carbon dioxide: problems, solutions and possible ways forward, Chemical Society Reviews, 41 (2012) 1428-1436.

[103] D. Sanli, S. Bozbag, C. Erkey, Synthesis of nanostructured materials using supercritical CO2: Part I. Physical transformations, Journal of Materials Science, 47 (2012) 2995-3025.

[104] S. Bozbag, D. Sanli, C. Erkey, Synthesis of nanostructured materials using supercritical CO2: Part II. Chemical transformations, Journal of Materials Science, 47 (2012) 3469-3492.

[105] G. Brunner, Gas extraction. An introduction to fundamentals of supercritical fluids and the application to separation processes, Springer, New York, 1994.

[106] H. Sovová, R.P. Stateva, Supercritical fluid extraction from vegetable materials, Reviews in Chemical Engineering, 27 (2011) 79-156.

[107] G. Lumia, C. Perre, J.-M. Aracil, Method for treating and extracting cork organic compounds with a dense fluid under pressure, in, 1999.

[108] M. Nunes da Ponte, J.A. Da Silva Lopes, V. Najdanovic-Visak, M.S. Manic, A.C. Cardoso Mesquita, R.P. Moreira da Silva, I.M. Sollarri Allegro, Method for direct treatment of cork stoppers, using supercritical fluids, in, 2010.

[109] M. Gonçalves, A. Vasconcelos, E. Gomes de Azevedo, H. Chaves das Neves, M. Nunes da Ponte, On the application of supercritical fluid extraction to the deacidification of olive oils, Journal of the American Oil Chemists' Society, 68 (1991) 474-480.

[110] P. Zacchi, S.C. Bastida, P. Jaeger, M.J. Cocero, R. Eggers, Countercurrent de-acidification of vegetable oils using supercritical CO2: Holdup and RTD experiments, The Journal of Supercritical Fluids, 45 (2008) 238-244.

[111] L. Lai, K. Soheili, W. Artz, Deacidification of soybean oil using membrane processing and subcritical carbon dioxide, Journal of the American Oil Chemists' Society, 85 (2008) 189-196.

[112] L.A. Blanchard, D. Hancu, E.J. Beckman, J.F. Brennecke, Green processing using ionic liquids and CO2, Nature, 399 (1999) 28-29.

[113] F. Jutz, J.-M. Andanson, A. Baiker, Ionic liquids and dense carbon dioxide: A beneficial biphasic system for catalysis, Chemical Reviews, 111 (2010) 322-353.

[114] L.C. Branco, A. Serbanovic, M. Nunes da Ponte, C.A.M. Afonso, Clean osmium-catalyzed asymmetric dihydroxylation of olefins in ionic liquids and supercritical CO2 product recovery, Chemical Communications, (2005) 107-109.

[115] A. Serbanovic, L.C. Branco, M. Nunes da Ponte, C.A.M. Afonso, Osmium catalyzed asymmetric dihydroxylation of methyl trans-cinnamate in ionic liquids, followed by supercritical CO2 product recovery, Journal of Organometallic Chemistry, 690 (2005) 3600-3608.

[116] A.M. Scurto, S.N.V.K. Aki, J.F. Brennecke, CO2 as a separation switch for ionic liquid/organic mixtures, Journal of the American Chemical Society, 124 (2002) 10276-10277.

[117] E.M. Saurer, S.N.V.K. Aki, J.F. Brennecke, Removal of ammonium bromide, ammonium chloride, and zinc acetate from ionic liquid/organic mixtures using carbon dioxide, Green Chemistry, 8 (2006) 141-143.

[118] L.A. Blanchard, J.F. Brennecke, Recovery of organic products from ionic liquids using supercritical carbon dioxide, Industrial and Engineering Chemistry Research, 40 (2001) 287-292.

[119] K.-i. Ago, S. Hasegawa, M. Azuma, K. Takahashi, Lactic acid extraction and enzymatic esterification for the ethyl lactate production from rice, Separation Science and Technology, 46 (2011) 1931-1935.

[120] N. Asthana, A. Kolah, D.T. Vu, C.T. Lira, D.J. Miller, A continuous reactive separation process for ethyl lactate formation, Organic Process Research & Development, 9 (2005) 599-607.

[121] C.S.M. Pereira, V.M.T.M. Silva, A.E. Rodrigues, Ethyl lactate as a solvent: Properties, applications and production processes - a review, Green Chemistry, 13 (2011) 2658-2671.

[122] J.J. Clary, V.J. Feron, J.A. van Velthuijsen, Safety assessment of lactate esters, Regulatory Toxicology and Pharmacology, 27 (1998) 88-97.

[123] C.T. Bowmer, R.N. Hooftman, A.O. Hanstveit, P.W.M. Venderbosch, N. van der Hoeven, The ecotoxicity and the biodegradability of lactic acid, alkyl lactate esters and lactate salts, Chemosphere, 37 (1998) 1317-1333.

[124] S. Aparicio, S. Halajian, R. Alcalde, B. García, J.M. Leal, Liquid structure of ethyl lactate, pure and water mixed, as seen by dielectric spectroscopy, solvatochromic and thermophysical studies, Chemical Physics Letters, 454 (2008) 49-55.

[125] J.S. Bennett, K.L. Charles, M.R. Miner, C.F. Heuberger, E.J. Spina, M.F. Bartels, T. Foreman, Ethyl lactate as a tunable solvent for the synthesis of aryl aldimines, Green Chemistry, 11 (2009) 166-168.

[126] B. Srinivas, R. Sridhar, K.R. Rao, Stereoselective total synthesis of (+)-varitriol, Tetrahedron, 66 (2010) 8527-8535.

[127] G. Sabitha, A.S. Rao, J.S. Yadav, Stereoselective synthesis of (−)-synparvolide B, Tetrahedron: Asymmetry, 22 (2011) 866-871.

[128] S.M. Nikles, M. Piao, A.M. Lane, D.E. Nikles, Ethyl lactate: a green solvent for magnetic tape coating, Green Chemistry, 3 (2001) 109-113.

[129] H. Guo, W. Wang, Y. Sun, H. Li, F. Ai, L. Xie, X. Wang, Ethyl lactate enhances ethylenediaminedisuccinic acid solution removal of copper from contaminated soils, Journal of Hazardous Materials, 174 (2010) 59-63.

[130] J. Muse, H.A. Colvin, Use of ethyl lactate as an excipient for pharmaceutical composition, in, 2005.

[131] X.C. Tombokan, R.M. Aguda, D.A. Danehower, P.K. Kilpatrick, R.G. Carbonell, Three-component phase behavior of the sclareol–ethyl lactate–carbon dioxide system for GAS applications, The Journal of Supercritical Fluids, 45 (2008) 146-155.

[132] E.J. Hernández, P. Luna, R.P. Stateva, V. Najdanovic-Visak, G. Reglero, T. Fornari, Liquid−liquid phase transition of mixtures comprising squalene, olive oil, and ethyl lactate: Application to recover squalene from oil deodorizer distillates, Journal of Chemical & Engineering Data, 56 (2011) 2148-2152.

[133] G. Vicente, A. Paiva, T. Fornari, V. Najdanovic-Visak, Liquid–liquid equilibria for separation of tocopherol from olive oil using ethyl lactate, Chemical Engineering Journal, 172 (2011) 879-884.

[134] M.S. Manic, D. Villanueva, T. Fornari, A.J. Queimada, E.A. Macedo, V. Najdanovic–Visak, Solubility of high-value compounds in ethyl lactate: Measurements and modeling, The Journal of Chemical Thermodynamics, 48 (2012) 93-100.

[135] M.E. Zakrzewska, M.S. Manic, E.A. Macedo, V. Najdanovic-Visak, Liquid–liquid equilibria of mixtures with ethyl lactate and various hydrocarbons, Fluid Phase Equilibria, 320 (2012) 38-42.

[136] H. Kaemmerer, S.K. Tulashie, H. Lorenz, A. Seidel-Morgenstern, Solid−liquid phase equilibria of n-methylephedrine enantiomers in two chiral solvents, Journal of Chemical & Engineering Data, 55 (2009) 1131-1136.

[137] B.K. Ishida, M.H. Chapman, Carotenoid extraction from plants using a novel, environmentally friendly solvent, Journal of Agricultural and Food Chemistry, 57 (2009) 1051-1059.

[138] I.F. Strati, V. Oreopoulou, Effect of extraction parameters on the carotenoid recovery from tomato waste, International Journal of Food Science & Technology, 46 (2011) 23-29.

Chapter II

Extraction of free fatty acids from soybean oil using ionic liquids or polyethylene glycols

Introduction

The presence of free fatty acids (FFAs) in vegetable oils is undesirable for both biodiesel and food oil productions.   The most common way to produce biodiesel is through the transesterification of vegetable oils with an alcohol, yielding fatty acid alkyl esters and glycerol [1]. Commercial processes use alkaline catalysts, NaOH or KOH, which are relatively inexpensive. However, vegetable oils contain considerable quantity of FFAs that react with the alkaline catalyst to form soap, reducing the ester yield. In respect to fat containing food, the presence of FFAs is associated to an undesirable rancid flavour. The deacidification process determines the quality of oil, having, thus, a major economic impact on oil production. The removal of FFAs from crude oils represents the most important stage in their refining cycle.

Conventional methods for FFA removal present various limitations. A typical chemical deacidification may lead to an excessive loss of neutral oil with high FFA content as well as to production of low commercial value soap stock. Physical deacidification methods, although suitable for high FFA content oils, require pretreatments that are performed under very harsh conditions - high temperatures and high vacuum. The latter cause thermal polymerization and decomposition of high value oil constituents. According to Leibovitz et al. [2], chemical deacidification of crude corn oil with FFA content between 8.4% and 14% resulted in neutral oil loss of 15-25 %, while for physical refining the loss of neutral oil varied between 11 % and 20 %.

These drawbacks associated with the conventional deacidification processes may be overcome by new approaches and their combination with current technologies. Bhosle and Subramanian [3] have reviewed alternative deacidification technologies reported in the literature, such as biological deacidification, solvent extraction, reesterification, supercritical fluid extraction, and membrane processing. Fixation of FFAs on an anion exchange resin was also proposed [4]. The authors succeed to efficiently reduce FFA content of synthetic oil. However, in the case of viscous oils, an organic solvent is necessary to use for dilution of the system. This implies subsequent recovery of free fatty acids from an organic phase. Nevertheless, these new approaches are possibly more environmentally acceptable and may reduce energy consumptions and oil losses.

The most studied extraction solvents for deacidification are short–chain alcohols. Mierelles and co-workers [5-10] have intensively studied the distribution coefficients of free fatty acids between oil- and alcohol-rich phases. Independently of temperature or chemical structures of vegetable oil, selected short chain alcohols and FFA studied, the distribution coefficients of FFA have relatively low values (close to 1), indicating similar solubility of FFA in both oil-rich and solvent-rich phases. Presence of water in alcohols lowers losses of neutral oils, but leads to slightly inferior FFA distribution coefficients compared with the case when dry alcohols were used [11, 12]. Moreover, the solubility of triglycerides (vegetable oils) increases proportionally to their FFA contents, thus leading to the loss of neutral oils.

The aim of this work was to explore the possibility of using alternative solvents for vegetable oil deacidification studies, using room temperature ionic liquids (ILs) and polyethylene glycols (PEGs). ILs have appeared as alternative extraction solvents, reaction media and catalysts [13, 14] because of their practically null-volatility [15], non-flammability [16], comparative thermal stability [17], and versatile solubility towards both polar and non-polar solutes [18]. Combining different cations and anions, a variety of ionic liquids can be obtained with desired ("task specific") solvent properties [19]. The incorporation of specific functional groups enhances solubility with specific solutes, such as polar substrates or catalysts [20], or leads to unexpected anti-solvent/co-solvent effects [21]. Therefore, ILs offer wide potential in industrial applications [22]. Ionic liquids [C$_4$mim][DCA] and Cocos alkyl pentaethoxi methyl ammonium methylsulfate (AMMOENG100) were chosen due to their extremely low miscibility with soybean oil, complete miscibility with FFA studied, and low viscosity and cost.

Liquid PEGs are also non-volatile, exhibit a very low toxicity (low enough for PEG to be approved as a food additive for humans) and biodegradability [23]. Moreover, PEGs and their aqueous solutions have already been widely used as sustainable medium for chemical reactions and liquid-liquid extractions (see Refs. [24, 25] and as well as references therein). In respect to solvent ability, PEGs form hydrogen bonds, because they are both proton donors and proton acceptors [26], but posses as well an aliphatic back bone that can provide van der Waals interactions.

In this work, liquid-liquid equilibrium (LLE) measurements on mixtures of soybean oil and several extraction solvents were used to evaluate the feasibility of FFA extraction. Two ILs were used: [C$_4$mim][DCA] and Cocos aklyl pentaethoxi methyl ammonium methylsulfate (AMMOENG100). Poly(ethyleneglycol)s of average molar mass of 200, 400, 2000, and 4000 were also used. Linoleic acid was chosen as a model FFA. The effects of: concentration, temperature, polymer molar mass, water content, and solvent to oil ratio were scrutinized. The experimental LLE results were correlated using a model based on the Peng-Robinson cubic equation of state and Mathias-Klotz-Prausnitz mixing rule – the PR-MKP model, which showed very good results for all the studied systems.

Materials

Refined soybean oil, anhydrous methanol (99.8 %) and linoleic acid (99.5 %, GC) were obtained from Sigma Aldrich, whereas diethyl ether and ethanol were purchased from Panreac. Analytical grade poly(ethyleneglycol)s with molar mass, in g/mol, of 200 (PEG200), 400 (PEG400), 2000 (PEG2000), and 4000 (PEG4000) were supplied by Fluka. ILs, [bmim][DCA] and AMMOENG100 were purchased from IoLiTec and Solvent Innovation, respectively. Chemical structures of solvents used for extraction of FFAs from soybean oil are shown in figure 2.1.
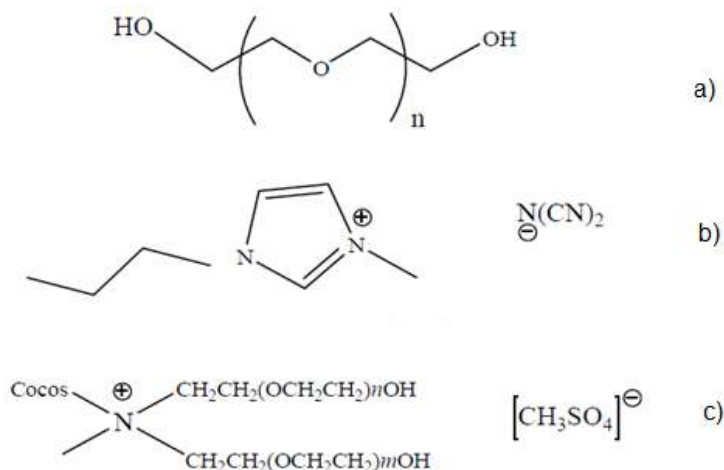
Figure 2.1 Structures of extraction solvents used in this study: a) PEGs, b) [C₄mim][DCA], and c) AMMOENG100.

The fatty acid methyl esters used in GC analysis, namely methyl heptanoate, methyl palmitoleate, methyl palmitate, methyl linoleate, methyl oleate, and methyl stearate, were purchased from MERC and used without further purification. Water was distilled and deionized using a Milli-Q water filtration system from Millipore.

To reduce the water content and volatile compounds to negligible values, vacuum (0.1 Pa) and moderate temperature (60 °C) were applied to the ILs samples for at least 3 days immediately prior to their use.

Experimental procedure

To determine the fatty acid methyl esters composition of soybean oil, deacidification followed by transesterification were performed, according to a procedure in the literature [27]. Products of transesterified soybean oil were analyzed in a VARIAN CHROMPACK CP-3800 gas chromatograph equipped with a 30 m x 0.32 mm i.d. fused silica capillary column, coated with a 0.25 μm thickness film of 5 % phenyl groups dissolved in dimethylpolysiloxane polymer, from Chrompack Company. The column temperature program started at 50 °C for 1 minute and went up to 185 °C, with the heating rate of 20 °C/min. The temperature was kept at 185 °C for 2 min and then increased up to 250°C, with the heating rate of 0.8 °C/min. Volumes of injected samples were 0.5 μL. The carrier gas, helium, was delivered at 0.7 bar. The injector temperature and flame ionization detection temperature were 250°C and 300 °C, respectively. Methyl heptanoate in hexane was used as standard for GC analysis. Retention times in minutes were: methyl heptanoate 5.0; methyl palmitoleate 15.50; methyl palmitate 16.16; methyl linoleate 22.21; methyl oleate 22.5; and methyl stearate 23.71.

Model fatty systems were prepared by addition of known quantities of linoleic acid to refined soybean oil. All liquid solutions were gravimetrically prepared to an estimated uncertainty of 0.02 %.

Cloud points were determined by the cloud-point titration method in a temperature-controlled equilibrium cell, with a magnetic stirrer inside. Each soybean oil + linoleic acid mixture of known composition was titrated by the solvent, methanol or PEGs or ionic liquid, at constant temperature, with continuous stirring. The transition point is taken as the appearance/ disappearance of turbidity in the solution, and it is defined as a cloud point. The liquid phase occupied almost the whole volume of the cell, to avoid corrections to composition due to vaporization. All experiments were performed at least twice. The temperature was controlled within ± 0.1 K and monitored by a calibrated mercury thermometer.

Liquid-liquid extractions were performed according to the following procedure: the model soybean oil mixtures containing from 2.62 to 17.3 mass % linoleic acids were mixed with the extraction solvent either PEG200, PEG400, PEG2000, PEG4000, $[C_4mim][DCA]$, or AMMOENG100 in the ratios 1:1, 1:2 and 2:1 mass ratio at temperatures 298.2 K, 323.2 K and 343.2 K. Before commencing the work, the time taken to reach equilibrium was estimated by sampling the phases every 5 min until a few consecutive samples produced essentially the same result of the analysis. It was determined that 30 min were sufficient to reach equilibrium. After stirring, the mixtures were centrifuged and left still for at least 60 minutes at the given temperature, to allow a complete phase separation. Using a Hamilton syringe, the two liquid phases (oil- and solvent-rich) were carefully drawn to other vials and prepared for further analysis of the FFA content.

The concentrations of FFAs were determined by titration under dry nitrogen atmosphere. Approximately 2 g of sample were weighed and then 25 mL of (ethyl ether: ethyl alcohol 2:1 (v:v)) mixture as well as two drops of phenolphthalein solution were added. These mixtures were titrated with 0.05 mol/L KOH in ethanol solution until solutions changes their colour from transparent to light pink. In the case of experiments involving PEGs as extraction solvents, samples of both extract (PEG-rich) and raffinate (oil-rich) phases were titrated directly. Since ILs are compounds composed of ions, the determination of FFAs concentration is not possible by alkali titration. In these experiments, only oil-rich phases washed with water (to remove traces of IL) and dried over Na_2SO_4 were analyzed for the FFA content. Afterwards, the FFA content of the related IL-rich phase was calculated as a difference.

For those mixtures where concentrations of linoleic acid were measured for both phases in equilibrium, the cloud-point data were used to determine tie-lines. The cloud-point compositions were fitted by a linear equation in the ternary diagram at a certain temperature. The interception in the ternary diagram of the cloud-point line for each phase, with the line corresponding to the measured concentration of linoleic acid in the same phase, gave the equilibrium composition for that phase, including the concentration of the other two components (oil and solvent). As the

overall composition of the mixture is known, the procedure could be validated by checking whether the tie-line connecting the equilibrium compositions thus determined passed through the point in the ternary diagram representing the overall composition. In all cases, the maximum deviations were below ± 0.001 mass fraction of linoleic acid.

Results

The determined composition of the soybean oil used in this study is shown in table 2.1, allowing estimation of an average molecular mass of 866.5 g/mol. The main constituents of the soybean triglycerides are tri-esters of linoleic, oleic and palmitic acid. Even though the oil is a mixture of various triglycerides, we considered it as a single component linoleic acid tri-ester (glyceryl trilinoleate). The concentration of FFAs in the refined oil is 0.14 mass %.

Table 2.1 Fatty acid composition of refined soybean oil used in this study

Fatty acid	mass %
Linoleic acid (C18:2)	59
Oleic acid (C18:1)	20
Palmitic acid (C16:0)	16
Stearic acid (C18:0)	2
Palmitoleic acid (C16:1)	2
Others	1

It should be noted that AMMOENG100 is an unknown isomer mixture where (m + n) varies from 4 to 14 while the cocos alkyl chain is a variable mixture of several fatty acid chains.

Table 2.2 presents the obtained cloud-point liquid-liquid equilibrium data for the pseudo-binary (extraction solvent + (soybean oil + linoleic acid)) systems using the following extraction solvents: PEG200, PEG400, PEG2000, PEG4000, AMMOENG100, [C_4mim][DCA] and methanol. The latter was chosen for comparison. Data in table 2.2 show large immiscibility gaps with very steep binodal lines. This is also illustrated in figure 2.2 for (oil + methanol), (oil + PEGs), and (oil + ILs) systems.

Table 2.2 Cloud point data for [extraction solvent (sol) + soybean oil (oil) + linoleic acid (LA)] systems presented in mass fraction (w_{sol}) and moll fraction (x_{sol}) of extraction solvent in the oil-rich and solvent-rich phase

Solvent	w_{LA} initial	T= 298 K		T= 323 K		T= 343 K		T= 298 K		T= 323 K		T= 343 K	
		oil rich w_{sol}	sol. rich w_{sol}	oil rich w_{sol}	sol. rich w_{sol}	oil rich w_{sol}	sol. rich w_{sol}	oil rich x_{sol}	sol. rich x_{sol}	oil rich x_{sol}	sol. rich x_{sol}	oil rich x_{sol}	sol. rich x_{sol}
PEG200	0.0014	0.0055	0.9991	0.0068	0.9991	0.0075	0.9991	0.0233	0.9998	0.0287	0.9998	0.0316	0.9998
	0.0572	0.0061	0.9990	0.0123	0.9990	0.0189	0.9990	0.0232	0.9997	0.0460	0.9997	0.0694	0.9997
	0.1554	0.0064	0.9989	0.0220	0.9989	0.0369	0.9989	0.0206	0.9997	0.0685	0.9997	0.1113	0.9997
PEG400	0.0014	0.0031	0.9989	0.0048	0.9989	0.0077	0.9989	0.0067	0.9995	0.0205	0.9995	0.0165	0.9997
	0.0572	0.0047	0.9988	0.0089	0.9988	0.0135	0.9988	0.0091	0.9994	0.0336	0.9994	0.0258	0.9997
	0.1554	0.0056	0.9987	0.0142	0.9987	0.0275	0.9987	0.0091	0.9992	0.0450	0.9992	0.0442	0.9996
PEG2000	0.0014	a	a	0.0004	0.9984	0.0009	0.9984	a	a	0.0017	0.9963	0.0004	0.9963
	0.0572	a	a	0.0009	0.9983	0.0012	0.9983	a	a	0.0035	0.9956	0.0005	0.9956
	0.1554	a	a	0.0014	0.9981	0.0017	0.9981	a	a	0.0046	0.9941	0.0006	0.9941
PEG4000	0.0014	a	a	a	a	0.0007	0.9987	a	a	a	a	0.0002	0.9940
	0.0572	a	a	a	a	0.0008	0.9986	a	a	a	a	0.0002	0.9928
	0.1554	a	a	a	a	0.0016	0.9983	a	a	a	a	0.0003	0.9899
AMMOENG100	0.0014	0.0028	0.9872	0.0052	0.9802	0.0060	0.9862	b	b	b	b	b	b
	0.0572	0.0040	0.9864	0.0056	0.9786	0.0081	0.9859	b	b	b	b	b	b
	0.1554	0.0082	0.9837	0.0087	0.9767	0.0093	0.9840	b	b	b	b	b	b
[C$_4$mim][DCA]	0.0014	0.0012	0.9987	0.0012	0.9987	0.0012	0.9987	0.0050	0.9997	0.0052	0.9997	0.0050	0.9997
	0.0572	0.0011	0.9986	0.0011	0.9982	0.0011	0.9982	0.0041	0.9996	0.0042	0.9995	0.0041	0.9995
	0.1554	0.0016	0.9984	0.0016	0.9983	0.0016	0.9983	0.0051	0.9995	0.0052	0.9995	0.0051	0.9995
MeOH	0.0014	0.0493	0.9963	0.0739	0.9929	0.0989	0.9885	0.5830	0.9999	0.6827	0.9997	0.7474	0.9996
	0.0565	0.0712	0.9966	0.1008	0.9940	0.1328	0.9889	0.6497	0.9999	0.7306	0.9998	0.7874	0.9995
	0.1551	0.1126	0.9967	0.1408	0.9943	0.1755	0.9896	0.7216	0.9998	0.7700	0.9997	0.8130	0.9995

$w_{LA, init.}$ corresponds to the initial mass fraction of linoleic acid in soybean oil.

[a] PEG is solid in given temperature.

[b] Molar mass cannot be calculated since AMMOENG100 is an unknown isomer mixture.
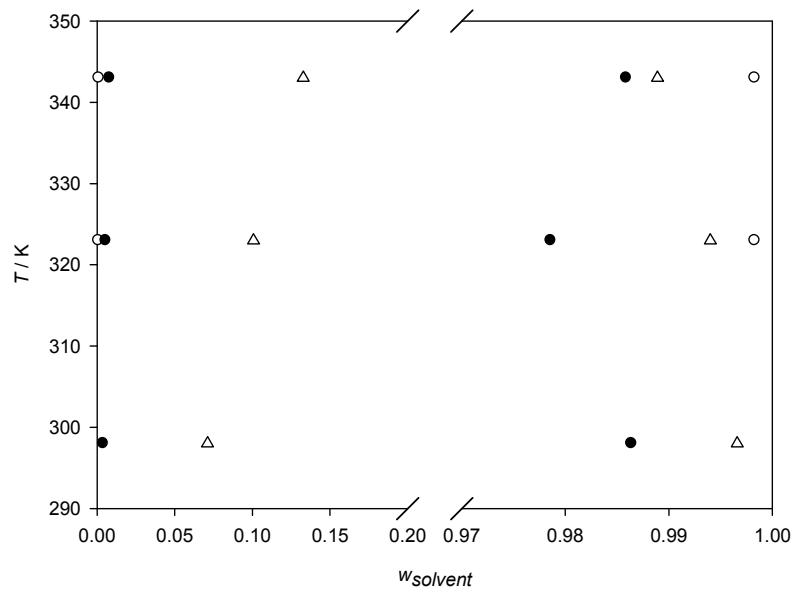
Figure 2.2 Temperature – mass fraction diagrams at atmospheric pressure of the preudo-binary [extraction solvent + (soybean oil + linoleic acid)] mixtures. Extraction solvent stands for either PEG2000 (empty cycles) or AMMOENG100 (filled cycles) or methanol (empty triangles). The initial composition of the (soybean oil + linoleic acid) mixture in mass fraction of LA is 0.0572.
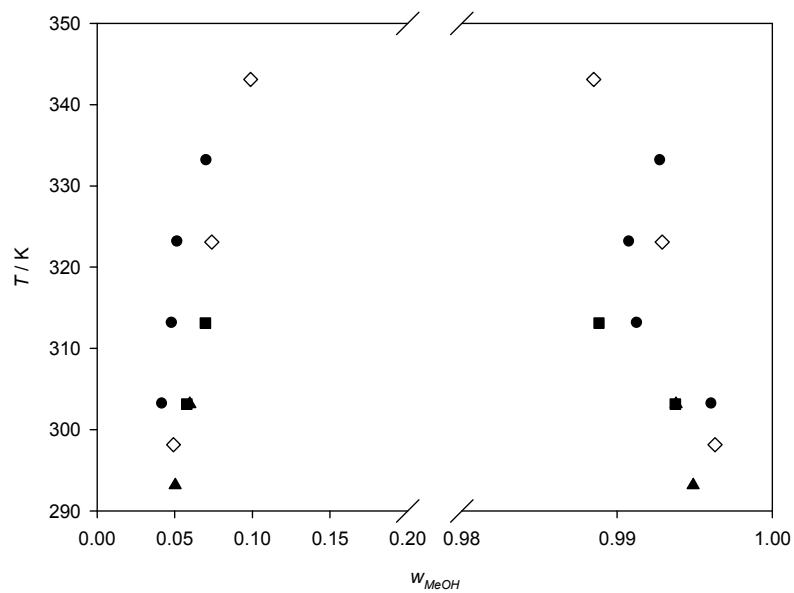
Figure 2.3 Temperature – mass fraction phase diagram of the (methanol + sunflower oil) mixture taken from Mohsen-Nia et al. (filled squares), (methanol + canola oil) mixture taken from Batista et al. (filled triangles), (methanol + Jatropha curcas L. oil) taken from Liu et al. (filled cycles) and (methanol + soybean oil) mixture-data from this work (empty diamonds).

Although the mutual solubility of (soybean oil + methanol) mixture was reported in the literature [28], it was not possible to quantitatively compare results as they are given solely in graphical form. However, the same data for the similar systems (sunflower oil + methanol), (canola oil + methanol), and (Jatropha curcas L. oil + methanol) have been reported by Mohsen-Nia and Khodayari [29], Batista et al. [5], and Liu et al. [30], respectively. Figure 2.3 shows the comparison of our results for (soybean oil + methanol) with the results for the aforementioned systems. It can be observed that the mutual solubilities in the studied systems are relatively similar, independently of the vegetable oil involved. In fact, this could be expected as the triglyceride compositions of soybean, sunflower, canola and Jatropha curcas L. oils are very much alike. All the studied solvents exhibited complete solubility with free fatty (linoleic) acid in the studied range of temperature.

Ternary LLE data for all the studied (linoleic acid + soybean oil + extraction solvent) systems as function of temperature, initial linoleic acid content of oil ($w_{LA,init.}$) and oil to solvent ratio (L) are given in table 2.3. The compositions of both solvent-rich and oil-rich phase – the tie-lines – are presented. Furthermore, table 2.4 reveals the distribution of the linoleic acid between soybean oil and solvents – ILs and PEGs containing 10 mass % of water, as a function of initial linoleic acid content, at 298.2 K.

Calculations

The tie-line compositions can be used to calculate partition coefficients, according to the relation:

$$K_i = \frac{w_i^{solvent\ phase}}{w_i^{oil\ phase}} \tag{2.1}$$

where $w_i^{solvetn\ phase}$ and $w_i^{oil\ phase}$ are mass fractions of component i (i = linoleic acid or soybean oil) in the solvent-rich and the oil-rich phase, respectively. The separation factor α of linoleic acid and soybean oil is given as the ratio of their partition coefficients:

$$\alpha = \frac{K_{linoleic\ acid}}{K_{soybean\ oil}} = \frac{w_{LA}^{solvent\ phase}}{w_{oil}^{solvent\ phase}} \cdot \frac{w_{oil}^{oil\ phase}}{w_{LA}^{oil\ phase}} \tag{2.2}$$

where $w_{LA}^{solvent\ phase}$, $w_{LA}^{oil\ phase}$, $w_{oil}^{solvent\ phase}$ and $w_{oil}^{oil\ phase}$ are the mass fractions of linoleic acid (LA) and soybean oil (oil) in the respective phases. Table 2.3 includes the calculated values of the distribution coefficients and separation factors according to equations 2.1 and 2.2 as well as the corresponding values of neutral oil loss (NOL) for the given temperature expressed as:

$$NOL = \frac{w_{oil}^{solvent\ phase}}{L} \cdot 100 \tag{2.3}$$

where $w_{oil}^{\ solvent\ phase}$ and L are mass fraction of oil in solvent-rich phase and mass ratio of soybean oil and solvent used, respectively. It presents a percentage of oil taken by solvent rich phase.

Discussion

Considering the oil with the lowest acid content studied (0.0014 mass fraction of linoleic acid) it can be concluded from table 2.2 that the relative affinity of soybean oil to the various solvents follows the order methanol > PEG200 > PEG400 > AMMOENG100 > [C$_4$mim][DCA] > PEG2000 > PEG4000. This order stands for both mass and mole fractions [in the case of AMMOENG100, mole fraction cannot be calculated, because the exact molar mass is not available due to its undefined cation alkyl chain structure (Private communication with *Solvent Innovation*)]. Although, methanol has the highest polarity of all the studied solvents it is the most soluble in nonpolar soybean oil. The long-chain PEGs are the least soluble while the studied ionic liquids, though being ionic compounds, are in the middle. Obviously, polarity does not count much and the presence of higher polymer chain lengths has not improved the van der Waals interactions with the corresponding aliphatic chains in triglycerides.

The increase of the acid content in the soybean oil increases its mutual solubility with the studied extraction solvents as presented in table 2.2. This effect is more pronounced in the case of methanol. On the contrary, in the case of higher molar mass PEGs and ionic liquids, the mutual solubility does not change significantly with oil´s acidity.

It is interesting that the temperature – composition phase diagram of the (AMMOENG100 + soybean oil) system shows an hour-glass shape, which shrinks as the acid content increases. Eventually, this would lead to the formation of both Upper Critical Solution Temperature and Lower Critical Solution Temperature if oil with high enough acid content were used.

Table 2.2 and figure 2.2 show that the mutual solubility of soybean oil with each of the studied alternative solvents, except AMMOENG100, is considerably lower than that with methanol thus making them very promising media to carry out deacidification with lower losses of vegetable oil. As it can be observed from table 2.2, solubility of soybean oil ($w_{LA,init.}$=0.0014) in solvent phase at 343 K are 0.09, 0.11, 1.98, 0.13, and 0.71 %, for PEG200, PEG400, AMMOENG100, [C$_4$mim][DCA], and methanol, respectively. On the other hand, the studied solvents are completely miscible with free fatty (linoleic) acid. It was shown in the literature [31] that, at a given temperature, the mutual solubility of triglycerides increases with an increase of the alcohol carbon chain length. The aforementioned facts apparently indicate that the alternative solvents proposed here show better potentials for the deacidification purposes than short-chain alcohols which are considered as the best solvents in this respect.

Relatively low solubilities of ionic liquids and PEGs solvents in oil phase ($w_{sol}^{oil\,rich}$) were observed, ranging from 0.09 to 0.93 mass % depending on solvent and conditions. Eventual removal of these solvents from oil should be addressed in future studies.
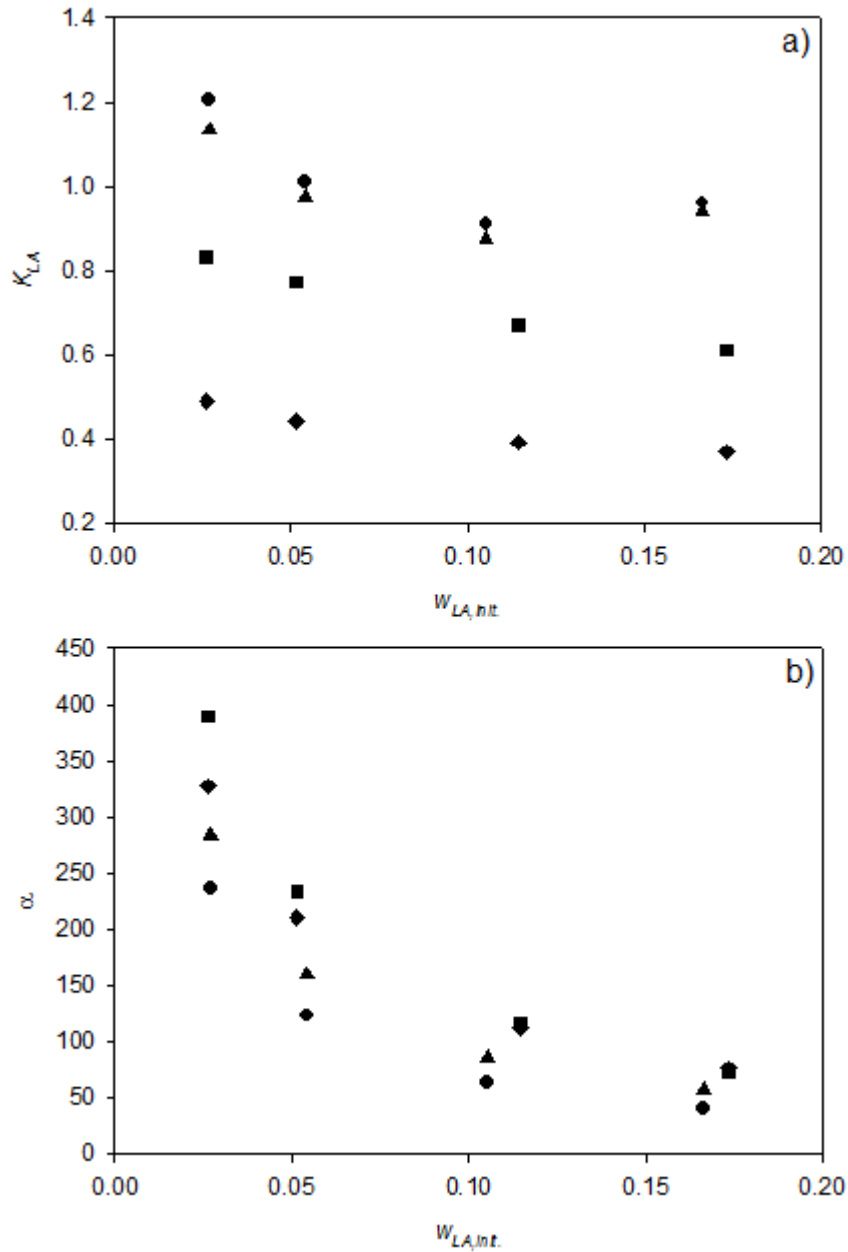
Figure 2.4 The influence of initial acid content of soybean oil on distribution of linoleic acid between phases (a) and on separation factor (b), using PEG200 (diamonds), PEG400 (squares), PEG2000 (triangles), and PEG4000 (cycles) for mass ratio of soybean oil and solvent (*L*) 1:1 at 298.2 K.

Table 2.3 Ternary liquid-liquid equilibrium data for (soybean oil (oil) + linoleic acid (LA) + extraction solvent (sol)) systems as function of temperature, initial linoleic acid mass fraction ($w_{LA,init.}$) and oil to solvent mass ratio (L)

Solvent	L	wLA init	overall composition			oil phase			solvent phase			KLA	Koil	α	NOL
			wsol	woil	wLA	wsol	woil	wLA	wsol	woil	wLA				
							T = 298 K								
	0.815	0.0263	0.5508	0.4374	0.0118	0.0060	0.9778	0.0163	0.9905	0.0015	0.0080	0.4922	0.0015	324.4	0.1840
	0.999	0.0515	0.5001	0.4741	0.0257	0.0060	0.9585	0.0355	0.9823	0.0020	0.0157	0.4428	0.0021	211.4	1.5716
	1.001	0.1145	0.4998	0.4429	0.0573	0.0062	0.9111	0.0827	0.9643	0.0032	0.0325	0.3936	0.0035	113.7	0.3197
	1.001	0.1733	0.4998	0.4135	0.0867	0.0063	0.8658	0.1279	0.9484	0.0042	0.0474	0.3711	0.0048	77.1	0.4195
	1.671	0.0265	0.3744	0.6091	0.0165	0.0060	0.9735	0.0205	0.9878	0.0017	0.0105	0.5121	0.0017	301.5	0.1017
	0.553	0.0263	0.6439	0.3468	0.0093	0.0060	0.9799	0.0141	0.9921	0.0014	0.0065	0.4609	0.0014	326.9	0.2532
PEG 200							T = 323 K								
	1.835	0.0264	0.3527	0.6302	0.0171	0.0087	0.9711	0.0202	0.9878	0.0017	0.0105	0.5198	0.0017	305.2	0.0093
	0.823	0.0238	0.5486	0.4407	0.0107	0.0082	0.9765	0.0153	0.9905	0.0015	0.0080	0.5228	0.0015	344.1	0.1820
	0.543	0.0265	0.6480	0.3427	0.0093	0.0080	0.9792	0.0129	0.9916	0.0014	0.0070	0.5447	0.0014	376.8	0.2578
							T = 343 K								
	1.835	0.0264	0.3527	0.6302	0.0171	0.0119	0.9684	0.0198	0.9868	0.0017	0.0115	0.5822	0.0018	327.4	0.0926
	0.818	0.0264	0.5501	0.4381	0.0119	0.0112	0.9725	0.0163	0.9905	0.0015	0.0080	0.4907	0.0015	321.7	0.1834
	0.553	0.0265	0.6440	0.3466	0.0094	0.0105	0.9768	0.0127	0.9911	0.0014	0.0075	0.5928	0.0015	399.5	0.2530
							T = 298 K								
	0.815	0.0263	0.5511	0.4372	0.0118	0.0033	0.9837	0.0130	0.9870	0.0021	0.0108	0.8343	0.0022	386.5	0.2577
	0.973	0.0515	0.5070	0.4677	0.0254	0.0036	0.9679	0.0286	0.9747	0.0032	0.0221	0.7757	0.0033	235.3	0.3415
	0.999	0.1145	0.5002	0.4425	0.0572	0.0042	0.9273	0.0685	0.9486	0.0054	0.0460	0.6713	0.0059	114.3	0.5405
	0.997	0.1733	0.5008	0.4127	0.0865	0.0048	0.8868	0.1084	0.9263	0.0074	0.0663	0.6123	0.0083	73.7	0.7422
PEG 400	1.839	0.0265	0.3522	0.6307	0.0171	0.0034	0.9783	0.0183	0.9807	0.0027	0.0166	0.9069	0.0027	332.7	0.1468
	0.576	0.0263	0.6346	0.3558	0.0096	0.0033	0.9862	0.0105	0.9889	0.0020	0.0091	0.8662	0.0020	436.3	0.3472
							T = 323 K								
	1.840	0.0264	0.3521	0.6308	0.0171	0.0058	0.9769	0.0174	0.9813	0.0026	0.0161	0.9277	0.0027	346.0	0.1413
	0.818	0.0238	0.5502	0.4391	0.0107	0.0054	0.9830	0.0116	0.9869	0.0021	0.0109	0.9436	0.0022	434.9	0.2567
	0.539	0.0265	0.6496	0.3411	0.0093	0.0053	0.9853	0.0094	0.9889	0.0020	0.0091	0.9676	0.0020	487.0	0.3711

K_{LA} and K_{oil} correspond to distribution coefficients of linoleic acid and soybean oil, respectively. $α$ stands for separation factor, while NOL is neutral oil loss.

Table 2.3 Continuation

Solvent	L	wLA init	overall composition			oil phase			solvent phase			KLA	Koil	α	NOL
			wsol	woil	wLA	wsol	woil	wLA	wsol	woil	wLA				
						T = 343 K									
PEG400	1.853	0.0264	0.3505	0.6323	0.0172	0.0099	0.9731	0.0170	0.9802	0.0027	0.0171	1.0086	0.0028	361.6	0.1457
	0.821	0.0264	0.5493	0.4388	0.0119	0.0093	0.9788	0.0120	0.9857	0.0022	0.0121	1.0122	0.0023	442.0	0.2680
	0.546	0.0265	0.6468	0.3439	0.0093	0.0090	0.9813	0.0098	0.9882	0.0020	0.0097	0.9995	0.0021	485.7	0.3663
						T = 343 K									
PEG 2000	1.001	0.0271	0.4999	0.4866	0.0136	0.0010	0.9863	0.0127	0.9817	0.0039	0.0144	1.1344	0.0040	285.3	0.3896
	0.999	0.0542	0.5003	0.4726	0.0271	0.0010	0.9716	0.0274	0.9674	0.0059	0.0267	0.9750	0.0061	160.3	0.5906
	1.002	0.1053	0.4994	0.4479	0.0527	0.0012	0.9427	0.0562	0.9412	0.0095	0.0493	0.8774	0.0101	86.6	0.9481
	1.026	0.1665	0.4935	0.4221	0.0843	0.0013	0.9119	0.0868	0.9034	0.0148	0.0818	0.9433	0.0162	58.1	1.4425
						T = 343 K									
PEG 4000	1.060	0.0271	0.4853	0.5007	0.0139	0.0004	0.9869	0.0127	0.9797	0.0050	0.0153	1.2023	0.0051	235.7	0.4717
	1.005	0.0542	0.4988	0.4740	0.0271	0.0005	0.9725	0.0270	0.9647	0.0080	0.0273	1.0103	0.0082	123.2	0.7960
	1.003	0.1053	0.4994	0.4479	0.0527	0.0007	0.9441	0.0552	0.9362	0.0136	0.0502	0.9099	0.0144	63.2	1.3559
	1.013	0.1665	0.4968	0.4194	0.0838	0.0010	0.9136	0.0855	0.8965	0.0214	0.0821	0.9608	0.0234	41.1	2.1100
						T = 298 K									
	0.833	0.0263	0.5456	0.4425	0.0119	0.0012	0.9845	0.0144	0.9884	0.0017	0.0099	0.6907	0.0018	393.2	0.2041
	1.007	0.0515	0.4983	0.4759	0.0258	0.0012	0.9673	0.0315	0.9777	0.0022	0.0201	0.6402	0.0022	284.8	0.2185
	1.001	0.1145	0.4997	0.4430	0.0573	0.0014	0.9239	0.0748	0.9572	0.0030	0.0398	0.5324	0.0033	162.3	0.3000
	0.989	0.1733	0.5027	0.4111	0.0862	0.0015	0.8812	0.1173	0.9409	0.0037	0.0554	0.4725	0.0042	112.3	0.3471
[C₄mim][DCA]	1.732	0.0265	0.3661	0.6172	0.0168	0.0012	0.9783	0.0205	0.9880	0.0017	0.0103	0.5026	0.0018	281.6	0.0982
	0.554	0.0263	0.6435	0.3471	0.0094	0.0011	0.9867	0.0122	0.9906	0.0016	0.0078	0.6429	0.0017	387.3	0.2889
						T = 323 K									
	1.829	0.0264	0.3535	0.6295	0.0171	0.0012	0.9796	0.0192	0.9786	0.0082	0.0132	0.6855	0.0084	81.7	0.4483
	0.848	0.0238	0.5411	0.4480	0.0109	0.0012	0.9853	0.0135	0.9854	0.0059	0.0087	0.6471	0.0060	108.1	0.6958
	0.562	0.0265	0.6402	0.3503	0.0095	0.0011	0.9869	0.0120	0.9863	0.0056	0.0081	0.6820	0.0057	120.4	0.9964

K_{LA} and K_{oil} correspond to distribution coefficients of linoleic acid and soybean oil, respectively. α stands for separation factor, while *NOL* is natural oil loss.

Table 2.3 Continuation

Solvent	L	wLA init	overall composition			oil phase			solvent phase			KLA	Koil	α	NOL
			wsol	woil	wLA	wsol	woil	wLA	wsol	woil	wLA				
						T = 343 K									
[C₄mim][DCA]	1.802	0.0264	0.3569	0.6261	0.0170	0.0012	0.9807	0.0182	0.9760	0.0091	0.0149	0.8206	0.0093	88.2	0.5050
	0.841	0.0264	0.5432	0.4447	0.0120	0.0012	0.9851	0.0138	0.9825	0.0069	0.0106	0.7705	0.0070	110.5	0.8205
	0.557	0.0265	0.6423	0.3482	0.0095	0.0011	0.9871	0.0118	0.9862	0.0056	0.0082	0.6914	0.0057	122.0	1.0054
						T = 298 K									
	1.012	0.0263	0.4970	0.4898	0.0132	0.0026	0.9943	0.0031	0.9632	0.0134	0.0234	7.5881	0.0134	564.5	1.3240
	1.002	0.0515	0.4994	0.4748	0.0258	0.0027	0.9908	0.0065	0.9411	0.0139	0.0451	6.9314	0.0140	494.6	1.3872
	0.998	0.1145	0.5005	0.4423	0.0572	0.0031	0.9802	0.0167	0.8873	0.0151	0.0976	5.8442	0.0155	378.3	1.5030
	0.998	0.1733	0.5004	0.4131	0.0866	0.0036	0.9668	0.0296	0.8403	0.0162	0.1434	4.8454	0.0168	288.4	1.6232
	1.839	0.0265	0.3522	0.6307	0.0171	0.0026	0.9925	0.0049	0.9466	0.0138	0.0396	8.0900	0.0139	583.7	0.7504
AMMOENG100	0.542	0.0263	0.6486	0.3421	0.0092	0.0025	0.9961	0.0014	0.9734	0.0131	0.0135	9.6154	0.0132	729.6	2.4170
						T = 323 K									
	1.835	0.0264	0.3527	0.6302	0.0171	0.0050	0.9893	0.0057	0.9423	0.0197	0.0380	6.6626	0.0199	334.3	1.0736
	0.841	0.0238	0.5432	0.4460	0.0109	0.0049	0.9925	0.0026	0.9624	0.0198	0.0178	6.8582	0.0199	344.0	2.3543
	0.559	0.0265	0.6416	0.3490	0.0095	0.0049	0.9931	0.0020	0.9665	0.0198	0.0137	6.8298	0.0199	342.5	3.5420
						T = 343 K									
	1.822	0.0264	0.3544	0.6286	0.0171	0.0065	0.9873	0.0062	0.9452	0.0180	0.0368	5.9397	0.0182	326.2	0.9879
	0.839	0.0264	0.5438	0.4442	0.0120	0.0064	0.9909	0.0027	0.9643	0.0158	0.0199	7.5035	0.0159	471.2	1.8832
	0.560	0.0265	0.6411	0.3494	0.0095	0.0064	0.9915	0.0021	0.9714	0.0150	0.0136	6.4899	0.0151	429.9	2.6786

K_{LA} and K_{oil} correspond to distribution coefficients of linoleic acid and soybean oil, respectively. *α* stands for separation factor, while *NOL* is natural oil loss.

Considering the values of K and α given in table 2.3, it can be observed that the efficiency of the extraction – deacidification was, to some extent, influenced by temperature in the studied range. It indicates that increasing the temperature enhanced K_{LA}. On the other hand the distribution coefficient of linoleic acid decreases with increasing the initial linoleic acid content – figure 2.4, which can be attributed to the enhancement of the oil-solvent mutual solubility at higher temperatures. In the case of higher molar mass PEGs (PEG2000 and PEG4000), it appears that there is a minimum of the initial value of the w_{LA} – approximately 0.10. However, there are not enough data points to prove this trend.

Also, it is clear that using the higher molar mass PEGs resulted in the enhanced distribution of linoleic acid between the phases. Conversely, the influence of molar mass on the separation factor α is not that straightforward. For the soybean oil with the initial mass fractions smaller than 0.1, the separation factor decreased in the order: PEG400 > PEG200 > PEG2000 > PEG4000. Deacidification of the oils with higher acid concentration ($w_{LA,init.} > 0.10$) gave similar value of separation factor whether PEG200 or PEG400 were used, while PEG2000 demonstrated a higher separation factor in comparison to PEG4000.

Considerably high distribution coefficients of linoleic acid between oil-rich and solvent-rich phase were obtained for AMMOENG100, ranging from approximately 5 to 8. To the best of our knowledge, these present the highest values ever reported in literature in the case of deacidification of oils by solvent extraction. The great affinity between linoleic acid and AMMOENG100 may be explained by the fact that AMMOENG100 ionic liquid originates from fatty acids – the Cocos alkyl chain in AMMOENG100 is a mixture having approximately 50 mass % of lauric acid alkyl chain (Private communication with *Solvent Innovation*). Somewhat smaller values were obtained using [C$_4$mim][DCA], as presented in figure 2.5. As expected, K_{LA} and α decreased as initial acid content of oil increased.

When compared with the most studied extraction solvents, short chain alcohols, PEGs and ionic liquids showed favourable values of neutral oil loss (*NOL*) which present another important parameter for the extraction process design decisions. On average, the *NOL* in this study is 0.10 %, having the highest value of 3.51 % for AMMOENG100 at 323.2 K (table 2.3). The typical *NOL* when using short chain alcohols is 5 % [32].
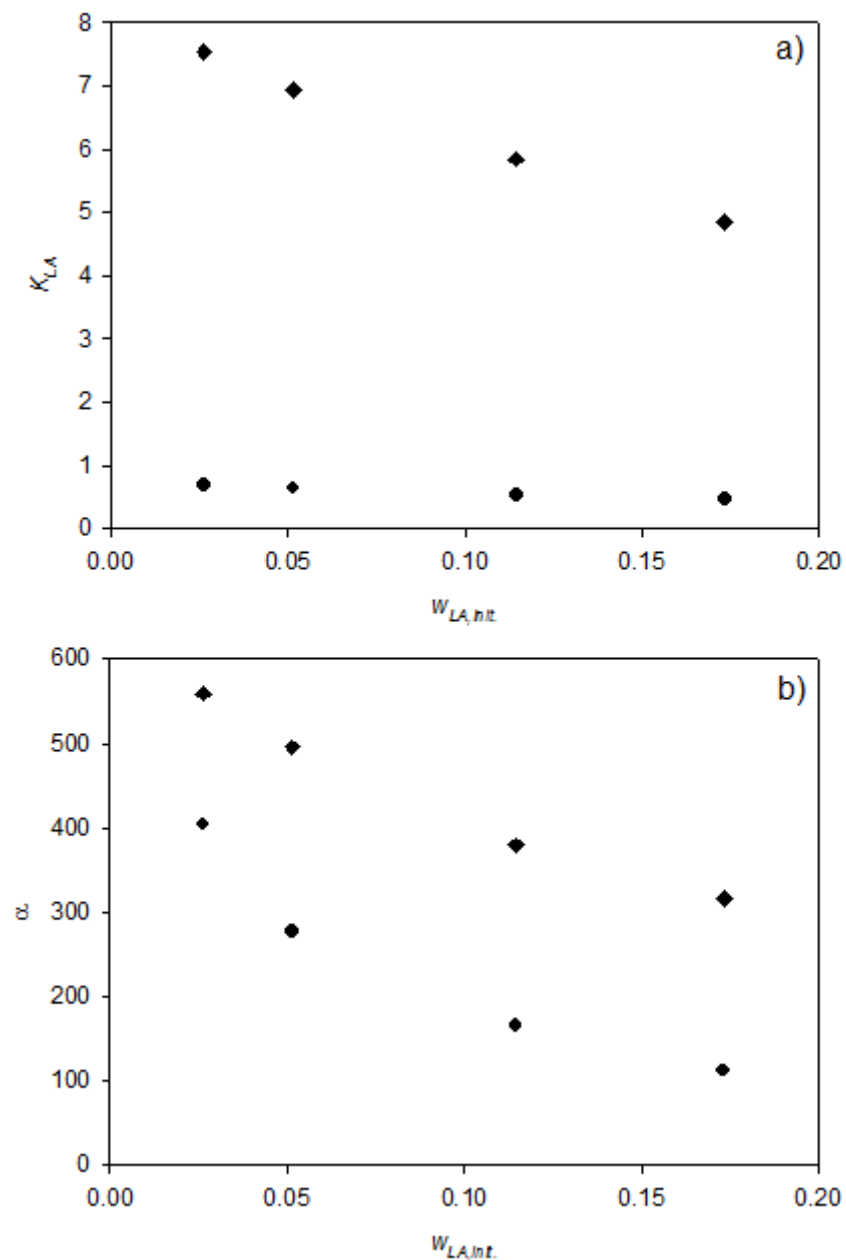
Figure 2.5 The influence of initial acid content of soybean oil on distribution of LA between phases (a) and on separation factor (b), using [C$_4$mim][DCA] (cycles) and AMMOENG100 (diamonds) for mass ratio of soybean oil and solvent (*L*) 1:1 at 298.2 K.

In this work, the influence of water addition to the extraction solvents was investigated as well. Table 2.4 presents the distribution of linoleic acid between the two phases at 298.2 K, as a function of initial mass fraction of linoleic acid, when the solvent having 10 mass % of water is used.

Table 2.4 Linoleic acid distribution between soybean oil and solvent containing 10 mass % of water phases as a function of initial linoleic acid content at 298.2 K.

Solvent	$w_{LA,init}$	Overall composition				Oil-rich phase	Solvent-rich phase	K_{LA}
		w_{solv}	w_{oil}	w_{LA}	w_{water}	w_{LA}	w_{LA}	
PEG200 + 10%H2O	0.0262	0.4553	0.4861	0.0131	0.0455	0.0114	0.0017	0.1474
	0.0514	0.4511	0.4779	0.0259	0.0451	0.0231	0.0028	0.1197
	0.1145	0.4574	0.4400	0.0569	0.0457	0.0513	0.0056	0.1090
	0.1731	0.4559	0.4122	0.0863	0.0456	0.0791	0.0072	0.0914
PEG400 + 10%H2O	0.0262	0.4615	0.4790	0.0129	0.0466	0.0098	0.0030	0.3089
	0.0514	0.4557	0.4727	0.0256	0.0460	0.0204	0.0053	0.2582
	0.1145	0.4545	0.4424	0.0572	0.0459	0.0468	0.0104	0.2233
	0.1733	0.4543	0.4132	0.0866	0.0459	0.0721	0.0145	0.2014
PEG2000 + 10%H2O	0.0298	0.4482	0.4854	0.0149	0.0515	0.0093	0.0057	0.6109
	0.0571	0.4492	0.4712	0.0286	0.0510	0.0182	0.0104	0.5722
	0.1075	0.4480	0.4459	0.0537	0.0524	0.0349	0.0189	0.5409
	0.1527	0.4480	0.4251	0.0766	0.0504	0.0502	0.0265	0.5272
PEG4000 + 10%H2O	0.0298	0.4501	0.4849	0.0149	0.0502	0.0089	0.0060	0.6787
	0.0571	0.4474	0.4725	0.0286	0.0515	0.0177	0.0109	0.6145
	0.1075	0.4504	0.4449	0.0536	0.0511	0.0333	0.0203	0.6112
	0.1527	0.4485	0.4243	0.0765	0.0507	0.0488	0.0277	0.5672
[C$_4$mim][DCA] + 10%H2O	0.0261	0.4450	0.4964	0.0133	0.0453	0.0111	0.0022	0.2016
	0.0514	0.4540	0.4741	0.0257	0.0462	0.0220	0.0037	0.1681
	0.1145	0.4568	0.4399	0.0569	0.0464	0.0497	0.0071	0.1433
	0.1731	0.4537	0.4136	0.0866	0.0461	0.0777	0.0089	0.1145
AMMOENG100 + 10%H2O	0.0262	0.4450	0.4863	0.0131	0.0456	0.0015	0.0116	7.8980
	0.0515	0.4536	0.4752	0.0258	0.0454	0.0036	0.0222	6.2388
	0.1144	0.4544	0.4429	0.0572	0.0455	0.0099	0.0474	4.7828
	0.1732	0.4529	0.4148	0.0869	0.0454	0.0177	0.0692	3.9207

The oil to solvent mass ratio is 1:1.

The distribution coefficient of linoleic acid decreases with increasing the initial acid content. As in the case of the pure solvents, water containing PEGs show the same influence of molar mass on K_{LA}. However, higher distribution coefficients were obtained using aqueous higher molar mass PEGs. It is possible to compare the results when 10 % water containing solvents were used with pure solvents (table 2.3). The presence of water in studied extraction solvents demonstrated unfavourable influence on related distribution coefficients. The effect was also observed in the case of short-chain alcohols by Rodrigues and Meirelles [31].

Modelling

Experimental liquid-liquid equilibria (LLE) results of the studied ternary mixtures were correlated using the Peng-Robinson equation of state [33] coupled with the Mathias-Klotz-Prausnitz (MKP) mixing rule [34]. The PR-MKP model is presented by following set of equations:

$$p = \frac{RT}{V-b} - \frac{a(T)}{V^2+2bV-b^2} \tag{2.4}$$

$$a_i(T) = 0.45724 \frac{R^2 T_c^2}{P_c} \left[1 + (0.37464 + 1.54226\omega - 0.266992\omega^2)(1 - \sqrt{T_r})\right]^2 \tag{2.5}$$

$$b_i = 0.0778 \frac{RT_c}{P_c} \tag{2.6}$$

$$a = \sum_{i=1}^{N}\sum_{j=1}^{N} x_i x_j \sqrt{a_i a_j}(1 - k_{ij}) + \sum_{i=1}^{N} x_i \left[\sum_{j=1}^{N} x_j \left(\sqrt{a_i a_j}\lambda_{ij}\right)^{1/3}\right]^3 \tag{2.7}$$

$$b = \sum_{i=1}^{N}\sum_{j=1}^{N} x_i x_j b_{ij} \tag{2.8}$$

$$b_{ij} = \frac{b_i+b_j}{2}\left(1 - l_{ij}\right) \tag{2.9}$$

where P is the pressure, T is the temperature, V is the molar volume, R is the universal gas constant, a is the energy parameter and b is the co-volume parameter, while a_i and b_i are the pure component parameters.

The correlations were carried out using the program PE 2000 developed by Pfohl et al [35].

Normal boiling points, critical temperatures, and acentric factors of the pure components are presented in table 2.5. In this respect, a few clarifications should be given. Ionic liquid AMOENG100 does not have a completely defined structure, due to two reasons: (i) the total number (m + n) of ethylene-oxide units in the cation varies from 4 to 14 (figure 2.1); (ii) since this ionic liquid originates from fatty acids the Cocos alkyl chain is a variable mixture of several fatty acid alkyl chains, with that of the lauric acid having the major presence (50 %). Consequently, we calculated critical parameters and acentric factors for three cases of AMOENG100, having distinct total number of ethylene-oxide units (m + n = 4, 6, 8). However, to simplify the calculations it was assumed that the Cocos alkyl chain is represented only by lauric acid. After such assumptions, the critical parameters and acentric factor for AMOENG100 were obtained applying the modified Lydersen-Joback-Reid method given by Valderrama and Robles [36-38]. For the ionic liquid [C₄mim][DCA], these values were taken directly from literature [36]. In the case of PEG200, PEG400, soybean oil and fatty acids the boiling point, critical temperature and pressure were calculated using the method of Gani and co-workers [39, 40] as in the case of other substances of high molecular masses [41, 42]. For soybean oil – a mixture of triglycerides – a pseudo-component had to be introduced to simplify the calculation of critical parameters. According to table 2.1, we have chosen linoleic acid tri-methyl ester (C18:2) to represent the mixture. For fatty acids, linoleic acid was chosen as a major one. The acentric

factor for PEG200 was obtained using the Lee-Kesler equation [43], while for PEG400 the method of Gani had to be applied, because otherwise the optimization could not converge. For PEG2000 and PEG4000, we assumed critical temperature and pressure that were suggested as universal for all polymers [44], T_c = 1800 K and P_c = 1 MPa. The boiling point of these polymers was estimated using the usual ratio of $T_b/T_c \approx 0.7$ for hydrogen bonding substances. In respect to acentric factor, it was accepted to be zero because this assumption gave very good correlations, which was not the case when the higher values were tried – see table 2.5.

Table 2.5 Normal boiling points, critical temperatures and acentric factors of the components of the studied mixtures

	T_b / K	T_c / K	P_c / MPa	ω
AMOENG100-1 (m+n = 4, Mw = 561)	1275.1	1549.4	11.30	1.1109
AMOENG100-2 (m+n = 6, Mw = 649)	1411.4	1754.7	9.72	0.7482
AMOENG100-3 (m+n = 8, Mw = 737)	1547.8	1997.6	8.53	0.3768
[bmim][DCA]	783	1035.8	24.4	0.8419
PEG 200	565.5	726.6	2.43	1.1467
PEG 400	685.7	839.4	1.02	0.9844
PEG 2000	1260	1800	10	0 [c]
PEG 4000	1260	1800	10	0 [c]
Linoleic acid tri-methyl ester (C18:2) [a]	826.8	958.8	0.344	0.4461
Linoleic acid (C18:2) [b]	626.8	798.4	1.29	0.7749

[a] This ester was taken as a pseudo-component that represents a complex mixture of esters that constitute the deacidified soybean oil used in this study – see Table 1.

[b] This acid was taken as a major one that influences the acid number of the studied soybean oil.

[c] Higher values of the acentric factor (0.5, 2.0 and 2.5) have not given better correlation results.

The obtained binary interaction parameters and average absolute deviations of the calculations are given in table 2.6. It can be concluded that the PR-MKP model correlated very well the presented experimental LLE ternary data, in the temperature range of 298.15-343.15 K. This conclusion stands even more if one takes into consideration that the studied systems are quite complex consisting of components that (i) posses versatile solvent properties (ionic liquids [45]), (ii) provide strong hydrogen bonds both as proton donors and proton acceptors (PEG200 and PEG400 – see ref. [25]), (iii) allow van der Waals interactions due to long aliphatic chains (FFAs), and (iv) are real polymers for which the calculation of critical parameters and acentric factors is still open to discussion [46-48]. Even more, some of the components are mixtures themselves and had to be represented by a pseudo-component (see above). Consequently, the fact that the mixtures could not be well represented by using only a simple, quadratic mixing rule indicates the presence of diverse, specific interactions – thus, the values of the MKP mixing rule interaction parameter λ_{ij} are quite different from zero, in most of the studied cases. However, it has to be mentioned that the PR-MKP model did not exhibit fine correlation abilities

when using temperature independent parameters, showing the maximum absolute deviations between 0.02 and 0.03.

Table 2.6 Binary interaction parameters of the PR-MKP model and average absolute deviations of the compositions in the solvent-rich (δ') and the oil-rich phase (δ'') for the ternary systems free fatty acid(1) + soybean oil(2) + solvent(3)

T / K	k_{12} l_{12} λ_{12}	k_{13} l_{13} λ_{13}	k_{23} l_{23} λ_{23}	$\delta' \times 10^4$	$\delta'' \times 10^4$
Fatty acid (1) + Soybean oil (2) + AMOENG100-1 (3)
298.15	-0.0807 0.0959 0.0956	0.0483 0.0451 0.0426	0.0834 -0.2006 0.4249	29.0	59.6
323.15	-0.4619 0.0405 0.0274	0.0336 0.0235 0.0112	-0.0098 0.0042 0.0099	50.6	82.9
343.15	-0.2237 0.4034 0.3313	-0.1202 0.0792 0.1439	-0.1552 -0.2308 0.7208	2.39	67.9
Fatty acid (1) + Soybean oil (2) + AMOENG100-2 (3)
298.15	0.2521 0.3251 -0.0842	0.0649 0.0483 0.0030	0.0309 0.2283 0.2260	8.59	5.58
323.15	0.4695 0.3644 -0.2838	-0.0810 -0.0860 -0.1691	0.0951 0.2884 0.2988	3.53	0.18
343.15	-0.1435 0.4819 0.3551	-0.1403 0.0730 0.1384	-0.0569 -0.2436 0.6299	2.68	77.9
T / K	k12 l12 λ12	k13 l13 λ13	k23 l23 λ23	$\delta' \times 104$	$\delta'' \times 104$
Fatty acid (1) + Soybean oil (2) + AMOENG100-3 (3)
298.15	0.0942 0.3310 -0.1199	-0.0490 0.0674 0.0520	0.2036 0.2634 0.2191	6.56	4.10
323.15	-0.0050 0.0716 0.0030	0.0692 0.0315 0.0148	-0.0354 0.0454 0.0188	0.59	0.13
343.15	0.0141 0.1141 0.0801	0.1197 0.0574 -0.0082	-0.0230 0.0544 0.0369	3.30	2.65
Fatty acid (1) + Soybean oil (2) + [C$_4$mim][DCA] (3)
298.15	-0.1548 0.0532 0.0130	0.0404 0.0508 -0.0515	-0.3466 0.0694 0.0078	3.25	6.12
323.15	0.0480 0.0727 0.0488	0.0022 -0.0049 0.0123	-0.1901 0.1703 0.0041	0.75	10.56
343.15	-0.1917 0.2234 -0.3019	0.3803 0.4503 -0.0155	-0.3665 0.0861 -0.2249	0.92	3.91

Table 2.6 Continuation

T / K	k_{12} l_{12} λ_{12}	k_{13} l_{13} λ_{13}	k_{23} l_{23} λ_{23}	$\delta' \times 10^4$	$\delta'' \times 10^4$
	Fatty acid (1) + Soybean oil (2) + PEG200 (3)				
298.15	-0.0422 0.0093 0.0185	0.0129 -0.0153 0.0146	-0.0684 0.1734 -0.0015	4.44	6.54
323.15	-0.0356 0.0314 0.1199	0.0106 -0.0152 0.0394	-0.0595 0.1458 0.0260	6.63	2.25
343.15	-0.0437 -0.3431 -0.0001	-0.2708 -0.1265 0.6616	-0.1356 0.0484 0.1184	4.14	3.61
	Fatty acid (1) + Soybean oil (2) + PEG400 (3)				
298.15	-0.4027 -0.0684 0.0622	-0.0232 -0.0043 0.0182	-0.0326 0.1939 0.0114	6.99	8.06
323.15	-0.5866 0.2253 -0.4559	-0.0933 0.1184 -0.2419	0.3245 0.4788 0.1655	2.68	1.24
343.15	0.1199 0.1105 0.1105	0.0954 -0.0305 -0.0364	-0.1435 0.0661 -0.0536	0.94	1.04
	Fatty acid (1) + Soybean oil (2) + PEG2000 (3)				
343.15	0.0419 0.0416 0.0321	0.1099 -0.0004 -0.0910	-0.1390 -0.1895 -0.1648	16.4	36.1
	Fatty acid (1) + Soybean oil (2) + PEG4000 (3)				
343.15	-0.0309 0.0890 0.1391	0.1219 0.1067 0.0106	0.1135 0.0157 -0.2182	5.03	19.3

Conclusions

PEGs (M_w = 200, 400, 2000, and 4000 g/mol) and ILs, AMMOENG100 and [C$_4$mim][DCA], were tested as the alternative solvents for the deacidification of soybean oil. Liquid-liquid phase equilibrium experimental data of the binary and ternary mixtures (PEG + soybean oil), (IL + soybean oil), (PEG + soybean oil + linoleic acid) and (IL + soybean oil + linoleic acid) were obtained. All the studied solvents exhibited complete miscibility with free fatty (linoleic) acid and a very low solubility in soybean oil. Thus, they appeared as promising media for the deacidification, causing lower losses of neutral oil. The highest values of linoleic acid distribution coefficient were obtained when ionic liquid AMMOENG100 was employed as extraction solvent. The partition coefficient of linoleic acid between oil-rich and solvent-rich phases is enhanced by increasing temperature and molar mass of PEG. On the other hand, the distribution of linoleic acid decreases as initial linoleic acid content increases (figure 2.6). A model based on the Peng-Robinson cubic equation of state coupled with the Mathias-Klotz-Prausnitz mixing rule

showed good results in the correlation of the experimental results for the ternary studied mixtures.
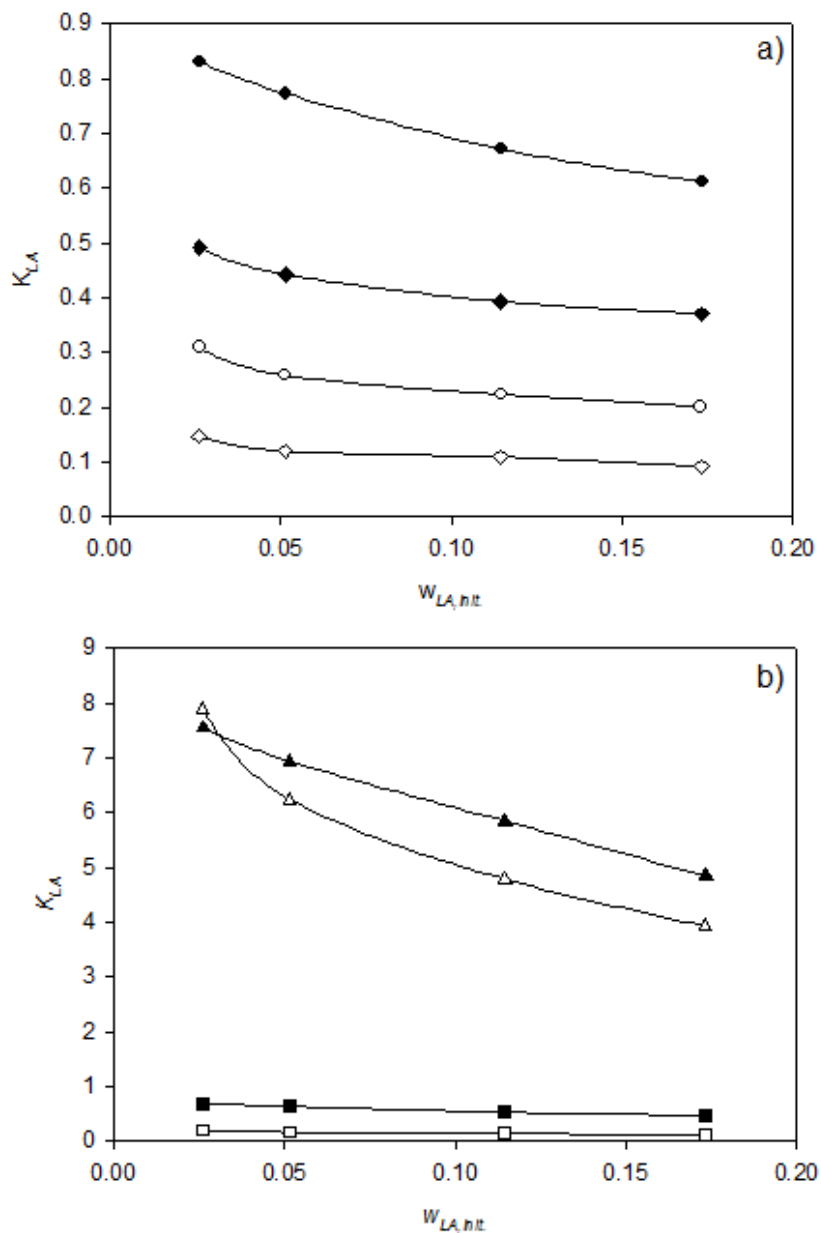
Figure 2.6 Comparison of partition coefficient as a function of initial linoleic acid content using oil to solvent ratio 1:1 at 298.2 K for: a) pure PEG200 (filled diamonds), 0.9 mass fraction PEG200 + 0.1 mass fraction water (empty diamonds), pure PEG400 (filled cycles) and 0.9 mass fraction PEG400 + 0.1 mass fraction water (empty cycles); b) pure [C$_4$mim][DCA] (filled squares), 0.9 mass fraction [C$_4$mim][DCA] + 0.1 mass fraction water (empty squares), pure AMMOENG100 (filled triangles) and 0.9 mass fraction AMMOENG100 + 0.1 mass fraction water (empty triangles).

References

[1] D. Ayhan, Comparison of transesterification methods for production of biodiesel from vegetable oils and fats, Energy Conversion and Management, 49 (2008) 125-130.

[2] Z. Leibovitz, C. Ruckenstein, Our experiences in processing maize (corn) germ oil, Journal of the American Oil Chemists' Society, 60 (1983) 395-399.

[3] B.M. Bhosle, R. Subramanian, New approaches in deacidification of edible oils——a review, Journal of Food Engineering, 69 (2005) 481-494.

[4] V. Eychenne, Z. Mouloungui, Deacidification of a synthetic oil with an anion exchange resin, Journal of the American Oil Chemists' Society, 75 (1998) 1437-1440.

[5] E. Batista, S. Monnerat, K. Kato, L. Stragevitch, A.J.A. Meirelles, Liquid−liquid equilibrium for systems of canola oil, oleic acid, and short-chain alcohols, Journal of Chemical & Engineering Data, 44 (1999) 1360-1364.

[6] C.B. Gonçalves, E. Batista, A.J.A. Meirelles, Liquid−liquid equilibrium data for the system corn oil + oleic acid + ethanol + water at 298.15 K, Journal of Chemical & Engineering Data, 47 (2002) 416-420.

[7] C.B. Gonçalves, A.J.A. Meirelles, Liquid–liquid equilibrium data for the system palm oil + fatty acids + ethanol + water at 318.2K, Fluid Phase Equilibria, 221 (2004) 139-150.

[8] C.E.C. Rodrigues, R. Antoniassi, A.J.A. Meirelles, Equilibrium data for the system rice bran oil + fatty acids + ethanol + water at 298.2 K, Journal of Chemical & Engineering Data, 48 (2003) 367-373.

[9] C.E.C. Rodrigues, A. Filipini, A.J.A. Meirelles, Phase equilibrium for systems composed by high unsaturated vegetable oils + linoleic acid + ethanol + water at 298.2 K, Journal of Chemical & Engineering Data, 51 (2005) 15-21.

[10] C.E.C. Rodrigues, E.C.D. Peixoto, A.J.A. Meirelles, Phase equilibrium for systems composed by refined soybean oil + commercial linoleic acid + ethanol + water, at 323.2 K, Fluid Phase Equilibria, 261 (2007) 122-128.

[11] K. Shah, T. Venkatesan, Aqueous isopropyl alcohol for extraction of free fatty acids from oils, Journal of the American Oil Chemists' Society, 66 (1989) 783-787.

[12] S. Turkay, H. Civelekoglu, Deacidification of sulfur olive oil. I. Single-stage liquid-liquid extraction of miscella with ethyl alcohol, Journal of the American Oil Chemists' Society, 68 (1991) 83-86.

[13] R.D. Rogers, K.R. Seddon, Ionic liquids--Solvents of the future?, Science, 302 (2003) 792-793.

[14] G. Charles M, New developments in catalysis using ionic liquids, Applied Catalysis A: General, 222 (2001) 101-117.

[15] M.J. Earle, J.M.S.S. Esperanca, M.A. Gilea, J.N. Canongia Lopes, L.P.N. Rebelo, J.W. Magee, K.R. Seddon, J.A. Widegren, The distillation and volatility of ionic liquids, Nature, 439 (2006) 831-834.

[16] M. Smiglak, W.M. Reichert, J.D. Holbrey, J.S. Wilkes, L. Sun, J.S. Thrasher, K. Kirichenko, S. Singh, A.R. Katritzky, R.D. Rogers, Combustible ionic liquids by design: Is laboratory safety another ionic liquid myth?, Chemical Communications, (2006) 2554-2556.

[17] K.J. Baranyai, G.B. Deacon, D.R. MacFarlane, J.M. Pringle, J.L. Scott, Thermal degradation of ionic liquids at elevated temperatures, Australian Journal of Chemistry, 57 (2004) 145-147.

[18] J.L. Anderson, J. Ding, T. Welton, D.W. Armstrong, Characterizing ionic liquids on the basis of multiple solvation interactions, Journal of the American Chemical Society, 124 (2002) 14247-14254.

[19] J.J. H. Davis, Task-specific ionic liquids, Chemistry Letters, 33 (2004) 1072-1077.

[20] L.C. Branco, J.N. Rosa, J.J. Moura Ramos, C.A.M. Afonso, Preparation and characterization of new room temperature ionic liquids, Chemistry – A European Journal, 8 (2002) 3671-3677.

[21] V. Najdanovic-Visak, A. Rodriguez, Z.P. Visak, J.N. Rosa, C.A.M. Afonso, M. Nunes da Ponte, L.P.N. Rebelo, Co-solvent effects in LLE of 1-hydroxyethyl-3-methylimidazolium based ionic liquids + 2-propanol + dichloromethane or 1,2-dichloroethane, Fluid Phase Equilibria, 254 (2007) 35-41.

[22] N.V. Plechkova, K.R. Seddon, Applications of ionic liquids in the chemical industry, Chemical Society Reviews, 37 (2008) 123-150.

[23] D.J. Heldebrant, H.N. Witt, S.M. Walsh, T. Ellis, J. Rauscher, P.G. Jessop, Liquid polymers as solvents for catalytic reductions, Green Chemistry, 8 (2006) 807-815.

[24] J. Chen, S.K. Spear, J.G. Huddleston, R.D. Rogers, Polyethylene glycol and solutions of polyethylene glycol as green reaction media, Green Chemistry, 7 (2005) 64-82.

[25] J.G. Huddleston, H.D. Willauer, S.T. Griffin, R.D. Rogers, Aqueous polymeric solutions as environmentally benign liquid/liquid extraction media, Industrial & Engineering Chemistry Research, 38 (1999) 2523-2539.

[26] I. Kim, M.D. Jang, Y.K. Ryu, E.H. Cho, Y.K. Lee, J.H. Park, Dipolarity, hydrogen-bond basicity and hydrogen-bond acidity of aqueous poly(ethylene glycol) solutions, Anal Sci, 18 (2002) 1357-1360.

[27] M.-H. Chuang, G. Brunner, Concentration of minor components in crude palm oil, The Journal of Supercritical Fluids, 37 (2006) 151-156.

[28] D. Boocock, S. Konar, H. Sidi, Phase diagrams for oil/methanol/ether mixtures, Journal of the American Oil Chemists' Society, 73 (1996) 1247-1251.

[29] M. Mohsen-Nia, A. Khodayari, De-acidification of sunflower oil by solvent extraction: (Liquid + liquid) equilibrium data at T = (303.15 and 313.15) K, The Journal of Chemical Thermodynamics, 40 (2008) 1325-1329.

[30] Y. Liu, H. Lu, C. Liu, B. Liang, Solubility measurement for the reaction systems in pre-esterification of high acid value Jatropha curcas L. oil, Journal of Chemical & Engineering Data, 54 (2008) 1421-1425.

[31] C.E.C. Rodrigues, A.J.A. Meirelles, Extraction of free fatty acids from peanut oil and avocado seed oil: Liquid−liquid equilibrium data at 298.2 K, Journal of Chemical & Engineering Data, 53 (2008) 1698-1704.

[32] C. Pina, A. Meirelles, Deacidification of corn oil by solvent extraction in a perforated rotating disc column, Journal of the American Oil Chemists' Society, 77 (2000) 553-559.

[33] D.-Y. Peng, D.B. Robinson, A new two-constant equation of state, Industrial & Engineering Chemistry Fundamentals, 15 (1976) 59-64.

[34] P.M. Mathias, H.C. Klotz, J.M. Prausnitz, Equation-of-State mixing rules for multicomponent mixtures: the problem of invariance, Fluid Phase Equilibria, 67 (1991) 31-44.

[35] O. Pfohl, S. Petkov, G. Brunner, Usage of PE - A program to calculate phase equilibria, Herbert Utz Verlag, München, 1998.

[36] J.O. Valderrama, P.A. Robles, Critical properties, normal boiling temperatures, and acentric factors of fifty ionic liquids, Industrial & Engineering Chemistry Research, 46 (2007) 1338-1344.

[37] J.O. Valderrama, W.W. Sanga, J.A. Lazzus, Critical properties, normal boiling temperature, and acentric factor of another 200 ionic liquids, Industrial & Engineering Chemistry Research, 47 (2008) 1318-1330.

[38] J.O. Valderrama, R.E. Rojas, Critical properties of ionic liquids. Revisited, Industrial & Engineering Chemistry Research, 48 (2009) 6890-6900.

[39] L. Constantinou, R. Gani, New group contribution method for estimating properties of pure compounds, AIChE Journal, 40 (1994) 1697-1710.

[40] L. Constantinou, R. Gani, J.P. O'Connell, Estimation of the acentric factor and the liquid molar volume at 298 K using a new group contribution method, Fluid Phase Equilibria, 103 (1995) 11-22.

[41] O.M. S. Glisic, A. Orlovic, D. Skala, Vapor–liquid equilibria of triglycerides–methanol mixtures and their influence on the biodiesel synthesis under supercritical conditions of methanol, Journal of the Serbian Chemical Society, 72 (2007) 13-27.

[42] M.E. Araújo, M.A.A. Meireles, Improving phase equilibrium calculation with the Peng–Robinson EOS for fats and oils related compounds/supercritical CO2 systems, Fluid Phase Equilibria, 169 (2000) 49-64.

[43] R.C. Reid, J.M. Prausnitz, B.E. Poling, The properties of gases and liquids, McGraw-Hill, New York, 1987.

[44] H. Orbey, C.P. Bokis, C.-C. Chen, Polymer−solvent vapor−liquid equilibrium: Equations of state versus activity coefficient models, Industrial & Engineering Chemistry Research, 37 (1998) 1567-1573.

[45] L. Crowhurst, P.R. Mawdsley, J.M. Perez-Arlandis, P.A. Salter, T. Welton, Solvent-solute interactions in ionic liquids, Physical Chemistry Chemical Physics, 5 (2003) 2790-2794.

[46] N. Orbey, S.I. Sandler, Vapor-liquid equilibrium of polymer solutions using a cubic equation of state, AIChE Journal, 40 (1994) 1203-1209.

[47] H. Orbey, C.-C. Chen, C.P. Bokis, An extension of cubic equations of state to vapor-liquid equilibria in polymer-solvent mixtures, Fluid Phase Equilibria, 145 (1998) 169-192.

[48] V. Louli, D. Tassios, Vapor–liquid equilibrium in polymer–solvent systems with a cubic equation of state, Fluid Phase Equilibria, 168 (2000) 165-182.

Chapter III

Purification of erythromycin using ionic liquids and high-pressure carbon dioxide

Introduction

Erythromycin, a broad-spectrum polypeptide (macroliolide) antibiotic, is industrially produced by aerobic fermentation, yielding low concentrations aqueous solutions. The fermentation process that produces commercial grade erythromycin is not entirely selective. It results in the production of small quantities of erythromycin B and C, in addition to erythromycin A, which is the major component. According to Tessier et al. [1], the purification costs related to recovery of antibiotics from fermentation broths can vary from 20 to 50% of the total production cost. There are various alternative separation methods suggested in literature [2], such as adsorption, crystallization and membrane-based techniques, but solvent extraction is the most used method. Due to favorable partition of erythromycin between organic and aqueous phases, butyl acetate is considered as the most suitable extraction solvent. Despite the fact that butyl acetate is biodegradable and exhibits relatively low toxicity [3], it has a relatively high boiling point (approximately 400 K), making subsequent evaporation energetically costly.

Room temperature ionic liquids (ILs) have emerged in recent years as alternative extraction solvents [4], due to their practically null-volatility, non-flammability, comparative thermal stability, and versatile solubility towards both polar and non-polar solutes. Combining different cations and anions, a variety of ionic liquids can be obtained with desired ("task specific") solvent properties, making them very attractive as extraction media in various processes. As an example, a range of ionic liquids with varying cation classes and with a range of anions types was employed for liquid-liquid extraction of dibenzothiophene from dodecane [5]. Similarly, a mixture containing limonene and linalool was successfully separated using 1-ethyl-3-methylimidazolium ethylsulfate ($[C_2mim][EtSO_4]$) [6], while ethyl tert-butil ether was recovered from its mixture with ethanol using 1-butil-3-methylimidazolium trifluoromethanesulfonate ($[C_4mim][OTf]$) solvent [7]. Recently, the reactive extraction of cycloolefins from their mixtures with cyclohexane, by chemical complexation with silver ions in ionic liquid solutions was reported [8].

Few studies have been undertaken to explore ability of ILs to extract biomolecules, with or without addition of inorganic salts [9-12]. Recovery of amino acids by imidazolium based ionic liquids from aqueous solutions was studied by Wang et al. [11]. It was concluded that the structure of ions in ionic liquids can be designed to meet the needs of a practical extraction process for amino acids. Cull et al. [13] have shown that 1-methyl-3-butylimidazolium hexafluorophosphate ($[C_4mim][PF_6]$) ionic liquid can be successfully used in place of conventional solvents for the extraction of erythromycin A from an aqueous solution. Partitioning of semi-synthetic antibiotics amoxicillin and ampicillin between water and ionic liquid 1-methyl-3-octylimidazolium tetrafluoroborate ($[C_8mim][BF_4]$ has been reported [14]. Also, the separation of tetracycline antibiotic in an aqueous two-phase system, consisting of a hydrophilic ionic liquid and NaH_2PO_4 was proposed recently [15]. Jiang et al. [16] employed terminal modified polyethylene glycol (PEG) as the phase-forming polymer to construct aqueous two-phase. After

the phase equilibrium, 95.8 % penicillin could be extracted into imidazole-terminal PEG-rich phase efficiently.

Yet, one of the main difficulties often encountered when using an ionic liquid as extraction solvents is its recovery from the products once the process is finished. It is well known that mixtures of supercritical carbon dioxide (scCO$_2$) with an ionic liquid show gas-liquid equilibrium behaviour, whereby carbon dioxide can dissolve significantly into the IL-rich liquid phase, but no ionic liquid dissolves in the gas phase [17]. Since ionic liquids do not dissolve in carbon dioxide and depressurization completely removes carbon dioxide from the ionic liquid phase, it is possible to recover pure products without any ionic liquid contamination and with minimal pollution. Based on this principle, researchers have successfully separated organic compounds from ionic liquids [18-21]. Extraction of high boiling point organics such as naphthalene and dibenzothiophene from ionic liquids by supercritical carbon dioxide was successfully performed [22]. Data from literature on erythromycin solubility in high-pressure carbon dioxide [23] suggest that it is possible to recover erythromycin.
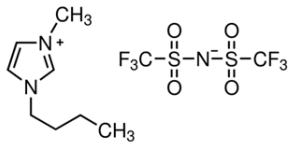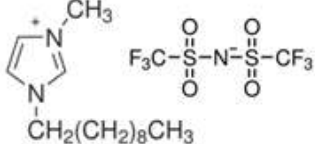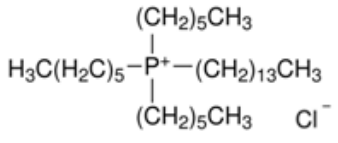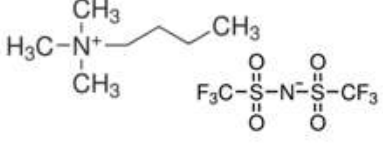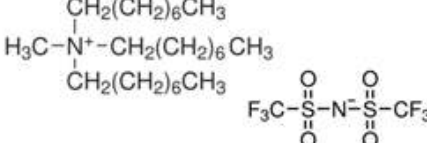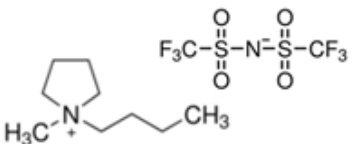
The aim of this work was to explore a possibility to recover erythromycin from aqueous solutions, using two steps: first, extraction of erythromycin from an aqueous solution using a hydrophobic ionic liquid and as a next step, supercritical CO$_2$ extraction of erythromycin from ionic liquid. Thus, the solubility of erythromycin in ionic liquids, as an essential parameter for the design of its eventual extraction process was studied as well.

In this work we performed studies on: (i) solubility of erythromycin in various ionic liquids, namely [C$_4$mim][NTf$_2$], [C$_{10}$mim][NTf$_2$], [P$_{6\ 6\ 6\ 14}$][Cl], [N$_{4\ 1\ 1\ 1}$][NTf$_2$], [N$_{1\ 8\ 8\ 8}$][NTf$_2$], and [C$_4$mpyr][NTf$_2$] as a function of temperature; (ii) supercritical carbon dioxide extraction of erythromycin from those ILs; and (iii) extraction of erythromycin from aqueous solution using the selected ionic liquid, as a function of pH and volume ratio of the ionic liquid to aqueous erythromycin solution, followed by high-pressure carbon dioxide extraction of erythromycin, as a function of pressure and temperature.

Materials

Erythromycin from *Streptomyces erythreus* (96.2 mass % purity) was supplied by Calbiochem while carbon dioxide (99.98 mass % purity) was purchased from Air Liquide. Water was distilled and deionised using a Milli-Q water filtration system from Millipore. All buffer components were ACS reagent grade or better and were obtained from Sigma-Aldrich. All ionic liquids were purchased from IoliTec and their full names, abbreviations, chemical structures and purity are presented in Table 3.1. In order to reduce the water content and volatile compounds to negligible values, vacuum at moderate temperature (333 K) was applied to the IL samples for several days, always immediately prior to their use. The water content after drying included in Table 3.1 was determined by Karl-Fischer Coulometric titration (Metrohm 831 KF Coulometer).

Table 3.1 Ionic liquids used in this study

Chemical Name	Abbreviation	Structure	Purity / mass %	Water content after the drying/ ppm
1-Butyl-3-methylimidazolium bis(trifluoromethylsulfonyl)imide	[C$_4$mim][NTf$_2$]		>98	60
1-Decyl-3-methylimidazolium bis(trifluoromethylsulfonyl)imide	[C$_{10}$mim][NTf$_2$]		>98	95
Trihexyltetradecylphophonium chloride	[P$_{6\,6\,6\,14}$][Cl]		>95	120
Butyltrimethylammonium bis(trifluoromethylsulfonyl)imide	[N$_{4\,1\,1\,1}$][NTf$_2$]		>99	155
Methyltrioctylammonium bis(trifluoromethylsulfonyl)imide	[N$_{1\,8\,8\,8}$][NTf$_2$]		>99	100
1-Butyl-1-methylpyrrolidinium bis(trifluoromethylsulfonyl)imide	[C$_4$mpyr][NTf$_2$]		>99	142

Molecular structure of erythromycin is presented in figure 3.1.
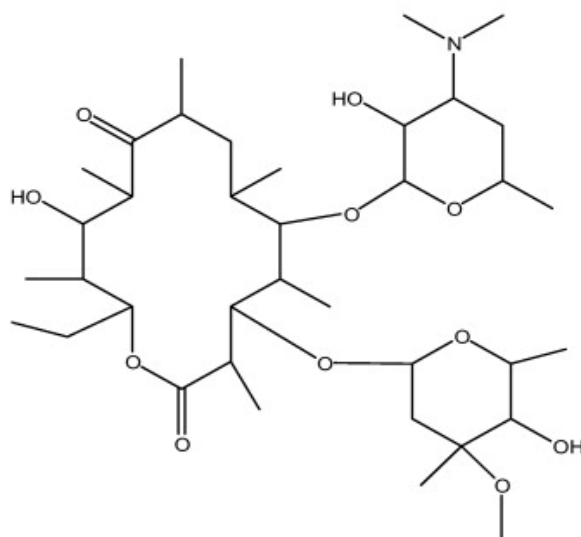
Figure 3.1 Chemical structure of erythromycin.

3.1 Solubility of erythromycin in ionic liquids

Experimental procedure

(Solid + liquid) and (liquid + liquid) phase equilibrium measurements were carried out using a visual dynamic method [24, 25]. Mixtures of the erythromycin and ionic liquid were gravimetrically prepared using a Kern 770 balance with a precision of ± 0.0001 g. The sample was heated very slowly (at a rate less than 5 $K \cdot h^{-1}$) with continuous stirring inside a Pyrex glass cell placed in a thermostatic bath equipped by temperature controller unit (Hart Scientific, model 2100) and immersion cooler. The temperature was measured by a calibrated mercury thermometer with accuracy of ± 0.1 K.

Since the rate of formation of liquid droplets is faster than that of crystal nuclei, the formation of a second liquid phase happens soon after the mixture enters the LLE region, while nucleation occurs only after the mixture is subcooled (typically 5 K to 10 K) below the thermodynamic dissolution temperature [26]. Therefore, the temperature at which the solid phase or one of the two liquid phases disappeared was taken as a cloud point. The average reproducibility of temperature and compositions (mole fractions of erythromycin in ionic liquid) was ± 0.5 K and 0.001, respectively. Triplicates of each measurement were performed in order to obtain reliable solubility data.

Calculations

The solubility of solid *i* in a solvent may be expressed by the equation [27]:

$$-\ln x_i = \frac{\Delta_{fus}H_i(T_{tp})}{R}\left(\frac{1}{T}-\frac{1}{T_{tp,i}}\right) - \frac{\Delta_{fus}C_{p,i}}{R}\left(\ln\frac{T}{T_{tp,i}}+\frac{T_{tp,i}}{T}-1\right) + \ln\gamma_i \tag{3.1}$$

where x_i, γ_i, $\Delta_{fus}H_i(T_{tp})$, $\Delta_{fus}C_{p,i}$, $T_{tp,i}$, *R* and *T* stand for mole fraction of the solute *i*, its activity coefficient, the enthalpy of fusion at the triple-point temperature, the difference in heat capacity between the liquid and solid solute at the triple-point temperature, the triple-point of the solute, universal gas constant, and equilibrium temperature, respectively. It is possible to make two assumptions which introduce only a slight error [27]. First, the difference between the triple-point temperature and a normal melting temperature is usually small, and therefore the distinction in the enthalpies of fusion at these two temperatures is often negligible. Second, the first term in equation 3.1 is the dominant one, and the terms which include ΔCp have a tendency to cancel each other. Consequently, the equation 3.1 can be modified and applied to the (erythromycin + ionic liquid) mixture in the following form:

$$-\ln x_{ery} = \frac{\Delta_{fus}H_{ery}}{R}\left(\frac{1}{T}-\frac{1}{T_{fus,ery}}\right) + \ln\gamma_{ery} \tag{3.2}$$

where x_{ery}, $T_{fus,ery}$, and $\Delta_{fus}H_{ery}$ are equilibrium mole fraction of erythromycin, its normal melting temperature and the enthalpy of fusion at the melting temperature, respectively. This equation was used to calculate activity coefficients of erythromycin from (solid + liquid) equilibrium data. In the case of an ideal solution, the activity coefficient is equal to unity and equation 3.2 can be written as:

$$-\ln x_{ery}^{ideal} = \frac{\Delta_{fus}H_{ery}}{R}\left(\frac{1}{T}-\frac{1}{T_{fus,ery}}\right) \tag{3.3}$$

The temperature dependence of erythromycin mole fraction in neat ionic liquid was also correlated by the semi-empirical equation introduced by Grant et al. [28]:

$$ln x_{ery} = \frac{A}{T} + B + C \cdot \ln T \tag{3.4}$$

where *A*, *B* and *C* are equation constants, while x_{ery} and *T* stand for mole fraction of erythromycin and temperature, respectively. This equation assumes that the apparent molar enthalpy of solution is a linear function of temperature ($\Delta H^* = a + b \cdot T$). If the coefficient *b* is assumed to be negligible, meaning that ΔH^* is independent of temperature, equation 3.4 becomes the van´t Hoff equation. On the other hand, if *a* is neglected it implies that $\Delta H_{ery} = T \cdot \Delta C_{p,ery}$ thus transforming equation 3.4 to the Hilderbrand equation.

Results and discussion

Table 3.2 and figure 3.2 present the solubility of erythromycin in various ionic liquids, at different temperatures, and at atmospheric pressure. To the best of our knowledge, there are no published data of the solubility of erythromycin in ionic liquids to compare with. The solubility of erythromycin is moderately enhanced by temperature rise. It should be noted that in the case of (erythromycin + [N$_{1\,8\,8\,8}$][NTf$_2$]) both (liquid + liquid) (LLE) and (solid + liquid) equilibria (SLE) were observed, intercepting at 310.2 K, as presented in figure 3.3. For the other systems, solely (solid + liquid) equilibrium was observed within the studied range of temperature. In respect to the SLE, the relative affinity of erythromycin to the studied ionic liquids follows the order [N$_{1\,8\,8\,8}$][NTf2] > [P$_{6\,6\,6\,14}$][Cl] > [C$_{10}$mim][NTf$_2$] > [N$_{4\,1\,1\,1}$][NTf$_2$] > [C$_4$mim][NTf$_2$] > [C$_4$mpyr][NTf$_2$].

Longer alkyl chains of both immidazolium and ammonium based ionic liquids led to higher solubility of the studied antibiotic. A very important result is that the observed solubilities of erythromycin in ionic liquids are considerably higher than in common organic solvents. According to Wang et al. [29], the solubility of erythromycin in mole fraction, in methanol, acetone, chloroform and ethanol is 0.0179, 0.0217, 0.0088 and 0.0254, respectively.

The enthalpy of fusion and the melting temperature of erythromycin was previously determined by Miroshnyk et al. [30], $\Delta_{fus}H_{ery}$ = 41.3 J·g^{-1}; $T_{fus,ery}$ = 465.2 K. According to equation 3.2, the calculation of the activity coefficients of erythromycin in ionic liquids is straightforward from the related solubility data - these calculated values are included in table 3.2.

In general, $\gamma > 1$ indicates a tendency toward phase separation or clustering in the solution, meaning that the attraction forces between like-molecules are superior to unlike-molecules. Conversely, $\gamma < 1$ indicates a tendency toward compound formation or ordering between the two unlike-molecule components. In the cases of [C$_4$mim][NTf$_2$], [C$_{10}$mim][NTf$_2$], [N$_{4\,1\,1\,1}$][NTf$_2$] and [C$_4$mpyr][NTf$_2$], the activity coefficients are both smaller and larger than unity. This suggests that the nature of interactions between erythromycin and the aforementioned ionic liquids changes depending on temperature and composition. On the other hand, activity coefficients of erythromycin in [P$_{6\,6\,6\,14}$][Cl] and [N$_{1\,8\,8\,8}$][NTf$_2$] are always less than unity, thus indicating the presence of specific attraction forces between erythromycin and the ionic liquid. Observed activity coefficient values for erythromycin in [C$_4$mpyr][NTf$_2$] were from 0.43 to 4.29 in temperature range from 284.4 K to 354.2 K. There are strong attraction bonds between unlike molecules at lower temperature. As the temperature increase, these specific bonds get weaker and eventually disappear (activity coefficient is close to 1) and a solution behaves as ideal one. With further increase of temperature, the attraction forces between like-molecules gets superior showing a tendency towards a phase separation.

Table 3.2 Solubility of erythromycin (ery) in various ionic liquids, at atmospheric pressure. Symbols w, x and γ stand for mass fraction, mole fraction and activity coefficient, respectively. Data points correspond to solid-liquid boundary if not stated otherwise

T / K	w_{ery}	x_{ery}	γ_{ery}	T / K	w_{ery}	x_{ery}	γ_{ery}
[C_4mim][NTf$_2$]				[$N_{1\,8\,8\,8}$][NTf$_2$]			
285.1	0.032	0.030	0.24	solid-liquid			
291.9	0.044	0.032	0.30	310.2	0.108	0.097	0.21
296.9	0.048	0.035	0.34	320.3	0.110	0.099	0.29
302.1	0.056	0.037	0.39	332.4	0.113	0.101	0.43
305.0	0.056	0.038	0.43	345.8	0.115	0.103	0.65
307.7	0.059	0.038	0.48	358.0	0.118	0.106	0.90
313.5	0.064	0.040	0.56	liquid-liquid			
319.2	0.071	0.042	0.66	294.1	0.013	0.012	–
333.9	0.082	0.044	1.04	302.4	0.017	0.015	–
348.2	0.086	0.047	1.53	309.1	0.023	0.020	–
[C_{10}mim][NTf$_2$]				313.7	0.026	0.023	–
288.2	0.099	0.070	0.12	324.5	0.035	0.031	–
305.4	0.102	0.072	0.23	326	0.04	0.036	–
321.4	0.103	0.073	0.41	328.5	0.052	0.046	–
356.2	0.105	0.074	1.23	329	0.058	0.052	–
[$P_{6\,6\,6\,14}$][Cl]				328.4	0.077	0.069	–
298.0	0.358	0.085	0.14	325.5	0.085	0.076	–
306.1	0.367	0.088	0.19	319.7	0.094	0.084	–
327.6	0.379	0.092	0.40	312.9	0.104	0.093	–
357.2	0.391	0.097	0.96	[C_4mpyr][NTf$_2$]			
[$N_{4\,1\,1\,1}$][NTf$_2$]				284.4	0.029	0.016	0.43
296.8	0.093	0.053	0.22	299.4	0.030	0.017	0.77
312.5	0.095	0.054	0.40	318.2	0.032	0.018	1.49
336.1	0.097	0.055	0.90	335.4	0.033	0.019	2.54
354.5	0.099	0.056	1.55	354.2	0.034	0.020	4.29
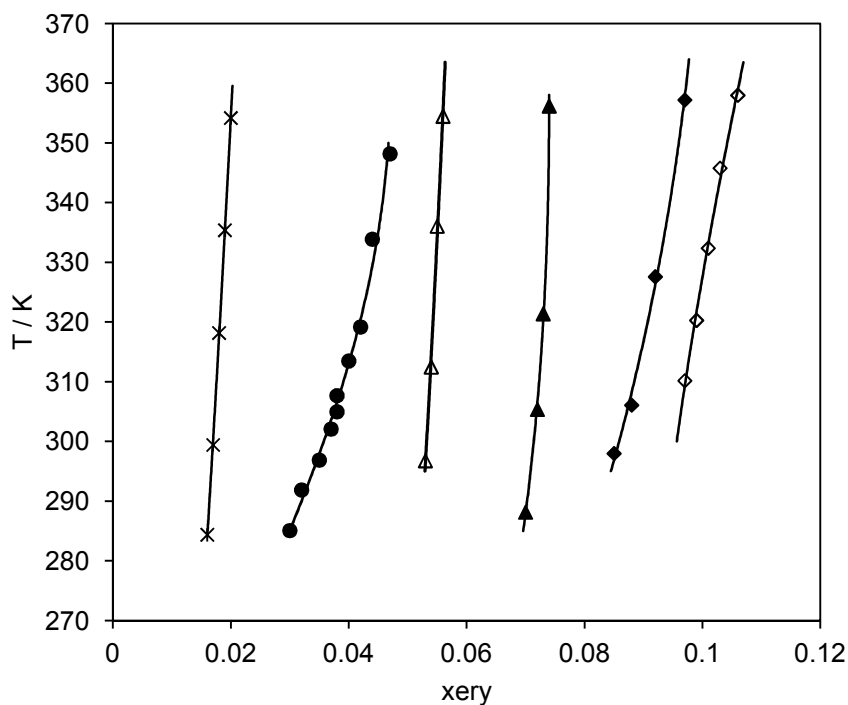
Figure 3.2 Experimental and correlated (solid + liquid) equilibria of the (erythromycin + ionic liquid) system. Ionic liquid stands for either [C$_4$mim][NTf$_2$] (filled circles) or [C$_{10}$mim][NTf$_2$] (filled triangles) or [P$_{6\,6\,6\,14}$][Cl] (filled diamonds) or [N$_{4\,1\,1\,1}$][NTf$_2$] (empty triangles) or [C$_4$mpyr][NTf$_2$] (stars) or [N$_{1\,8\,8\,8}$][NTf2] (empty diamonds). Lines present correlation by modified semi-empirical equation, Grant equation 3.4.
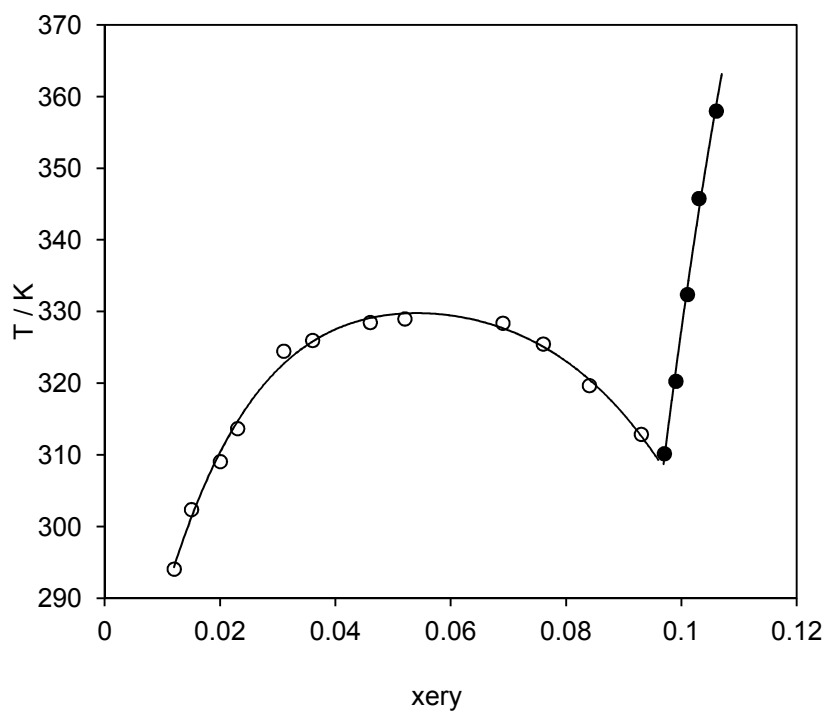
Figure 3.3 Experimental (solid + liquid) (filled circles) and (liquid + liquid) (empty circles) equilibrium of the (erythromycin + [N$_{1\,8\,8\,8}$][NTf$_2$]) system

Since the activity coefficients are influenced by both temperature and mole fraction, for comparison of the deviation from an ideal solution behaviour for various solvents, it is more convenient to construct ($-$ln x_{ery}) as a function of $1/T$ (figure 3.4). Straight dashed line corresponds to the ideal solution – activity coefficient $\gamma = 1$. On the other hand areas above and below this line present regions of $\gamma > 1$ and $\gamma < 1$, respectively. At lower temperatures, solubilities higher than ideal ones were observed, hence suggesting enhanced attraction forces between erythromycin and the studied ionic liquids. Increasing alkyl chain length of both immidazolium and ammonium based ionic liquids led to the enhancement of solubility and to higher deviation from the ideal behaviour.

The temperature dependence of solubility of erythromycin in ionic liquids was correlated by equation 3.4. It was considered that the equation constant C in equation 3.4 is zero. The solubility curves are shown in figure 3.2, while the model parameters and the root mean-square deviations are listed in table 3.3. The relative standard deviations among all of data do not exceed 0.12 %, which indicates that the equation 3.4 is suitable to correlate the solubility data.
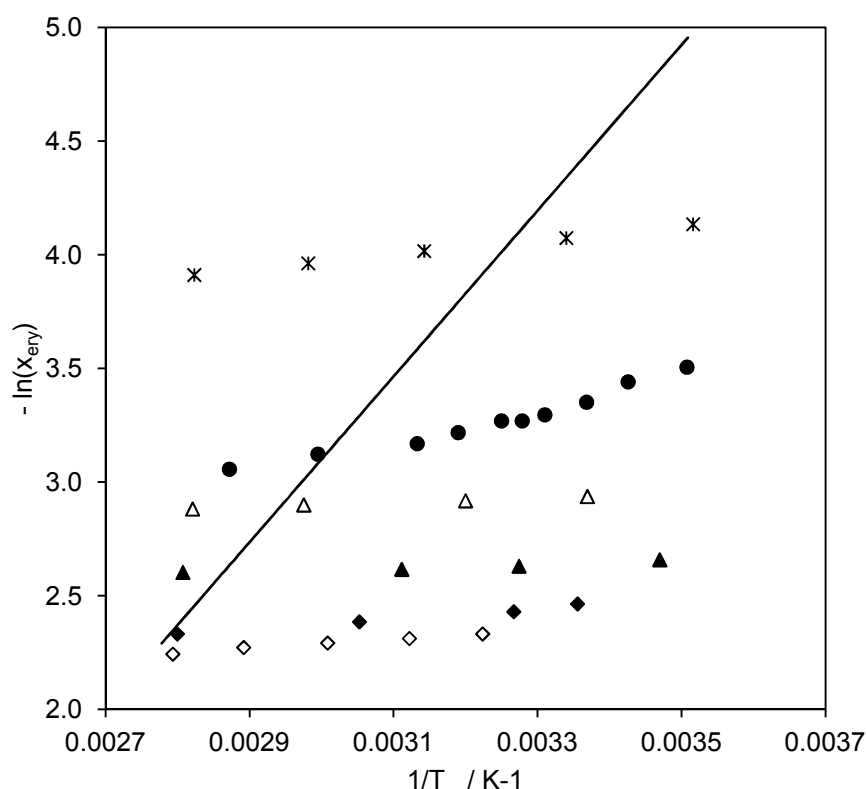
Figure 3.4 Experimental and ideal solubility of erythromycin in ionic liquids, namely [C$_4$mim][NTf$_2$] (filled circles), [C$_{10}$mim][NTf$_2$] (filled triangles), [P$_{6,6,6,14}$][Cl] (filled diamonds), [N$_{4,1,1,1}$][NTf$_2$] (empty triangles), [Pyrr$_{4,1}$][NTf$_2$] (stars), and [N$_{1,8,8,8}$][NTf$_2$] (empty diamonds). Straight line corresponds to the ideal solution (activity coefficient $\gamma = 1$) calculated from equation 3.3, while areas above and below this line present region of $\gamma > 1$ and $\gamma < 1$, respectively.

3.2 Supercritical carbon dioxide extraction of erythromycin from ionic liquids

Experimental procedure

Supercritical carbon dioxide ($scCO_2$) extraction of erythromycin from ionic liquids ($[C_4mim][NTf_2]$, $[C_{10}mim][NTf_2]$, $[P_{6\,6\,6\,14}][Cl]$, $[N_{4\,1\,1\,1}][NTf_2]$, $[N_{1\,8\,8\,8}][NTf_2]$, and $[C_4mpyr][NTf_2]$) was performed at 313.2 K and 20 MPa. The apparatus used for this purpose is presented in figure 3.5. It consists of manual pump, thermostated water bath, a stainless steel high-pressure cell with 25 mL internal volume, magnetic stirrer and cold trap. The measurement uncertainties for temperature and pressure are ±0.5 K and ±1 bar, respectively. According to the solubility data presented in the previous section (3.1), mixtures of the ionic liquids and erythromycin were prepared in glass vial at room temperature, with stirring applied for few minutes in order to achieve solubilisation. Then the mixture was placed into the high-pressure cell with magnetic stirrer and immersed into the termostated water bath. Carbon dioxide was first passed slowly through the cell in order to remove air, and then continuously added until the desired pressure was reached. After stirring for 1 h, the extraction was carried out keeping the internal pressure constant. The outgoing CO_2 was decompressed to atmospheric pressure and the dissolved erythromycin was precipitated in a cold trap. For all experimental runs, the flow rate of $scCO_2$ was approximately 1.7 g min^{-1}, while the initial mass of erythromycin in the ionic liquid samples placed into the cell was 0.05 g. The cold trap and corresponding lines were washed with 30 mL acetone and their contents were collected in separate vials. Subsequently, acetone was evaporated until a constant mass was achieved. The amount of precipitate was calculated from the difference in masses.

In order to verify the presence of ionic liquid in our collected extracts (erythromycin) after $scCO_2$ extraction, elemental and ^{19}F NMR analysis were performed. Elemental analyses were performed using a CHNS instrument model Flash EA 1112 (Thermo Finnigan-CE Instrument). The ^{19}F NMR and ^{13}C NMR spectroscopic analyses were performed on a BRUKER ARX 400 NMR spectrometer.

Results and discussion

Figure 3.6 present yields of the supercritical carbon dioxide extraction of erythromycin from various ionic liquids, namely $[C_4mim][NTf_2]$, $[C_{10}mim][NTf_2]$, $[N_{4\,1\,1\,1}][NTf_2]$, and $[C_4mpyr][NTf_2]$, performed at 313.2 K and 20 MPa, where the yield of erythromycin extract (g extracted erythromycin / g erythromycin in initial feed) is plotted versus the solvent to feed ratio through the cell, Q (mol CO_2 / mol erythromycin in initial feed).
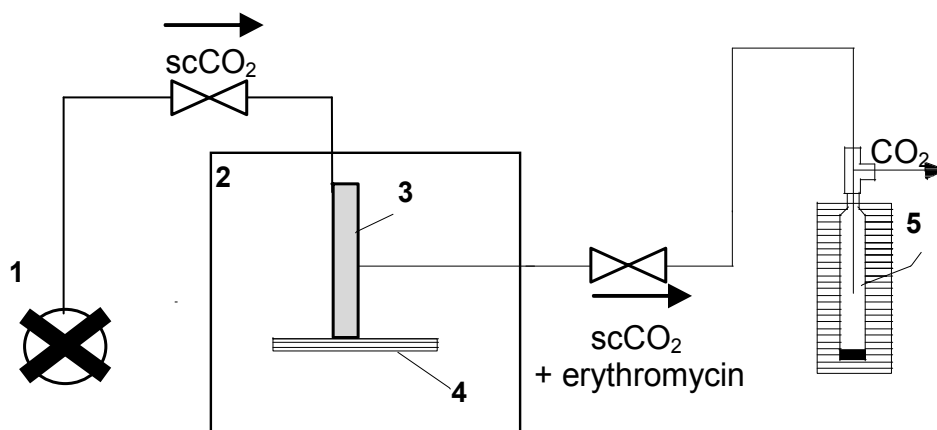
Figure 3.5 Scheme of high-pressure apparatus: manual pump (1), thermostated water bath (2),
a stainless steel high-pressure cell (3), magnetic stirrer (4) and cold trap (5)
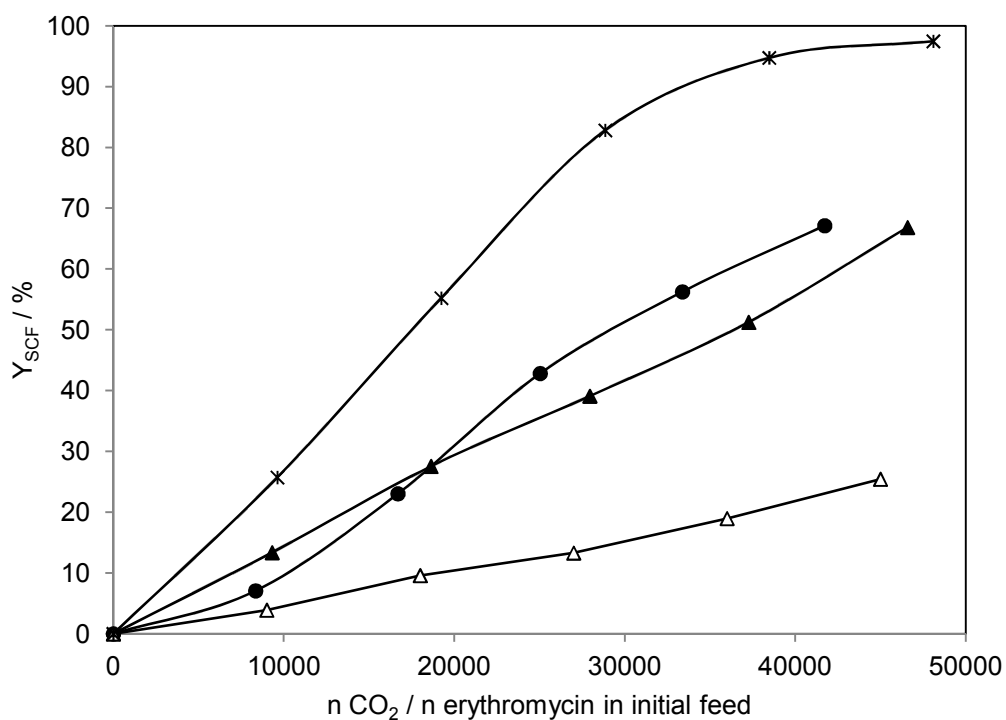
Figure 3.6 Dependence of the supercritical CO_2 extraction yield on the specific amount of the
solvent (Q) where filled circles, filled triangles, empty triangles and stars stand for $[C_4mim][NTf_2]$,
$[C_{10}mim][NTf_2]$, $[N_{4\ 1\ 1\ 1}][NTf_2]$, and $[C_4mpyr][NTf_2]$, respectively.

The highest extraction yield of erythromycin was achieved when its recovery was performed from [C$_4$mpyr][NTf$_2$], reaching 97.4 %. The extractions employing imidazolium based ionic liquids, either [C$_4$mim][NTf$_2$] or [C$_{10}$mim][NTf$_2$], attained comparable extraction yields, 67.1 % and 66.8 %, respectively, while only 25.4 % of erythromycin was extracted from [N$_{4\ 1\ 1\ 1}$][NTf$_2$] using scCO$_2$. However, interactions between erythromycin and ionic liquids, previously discussed in Section 3.1, are the dominant factor in controlling extraction yield. In the case of [C$_4$mpyr][NTf$_2$], the activity coefficient is larger than unity for the operational temperature (313.2 K), indicating a tendency toward phase separation and therefore, facilitating extraction of erythromycin. In all other cases, the attraction forces between unlike-molecules are stronger, limiting the extraction yields of erythromycin. Nonetheless, the mixture of erythromycin and corresponding ionic liquid were collected when supercritical CO$_2$ extraction was carried out from [P$_{6\ 6\ 6\ 14}$][Cl] and [N$_{1\ 8\ 8\ 8}$][NTf$_2$]. Thus, it was not possible to determine extraction yields and illustrate the results in figure 3.6.

Although, ionic liquids are usually scarcely soluble in supercritical CO$_2$, surprisingly high amount of ionic liquid was observed when supercritical CO$_2$ extraction of erythromycin was performed from either [P$_{6\ 6\ 6\ 14}$][Cl] or [N$_{1\ 8\ 8\ 8}$][NTf$_2$]. Besides, few cases on high solubility of ionic liquids in high-pressure CO$_2$ have been reported in the literature. Hutchings et al. [31] for instance, evidenced high solubility of the ionic liquid trihehyltetradecylphosphonium chloride in dense pure carbon dioxide. On the other hand, Wu et al. [32] have shown that the presence of co-solvents can considerably increase the solubility of ionic liquids that are practically insoluble in pure carbon dioxide.
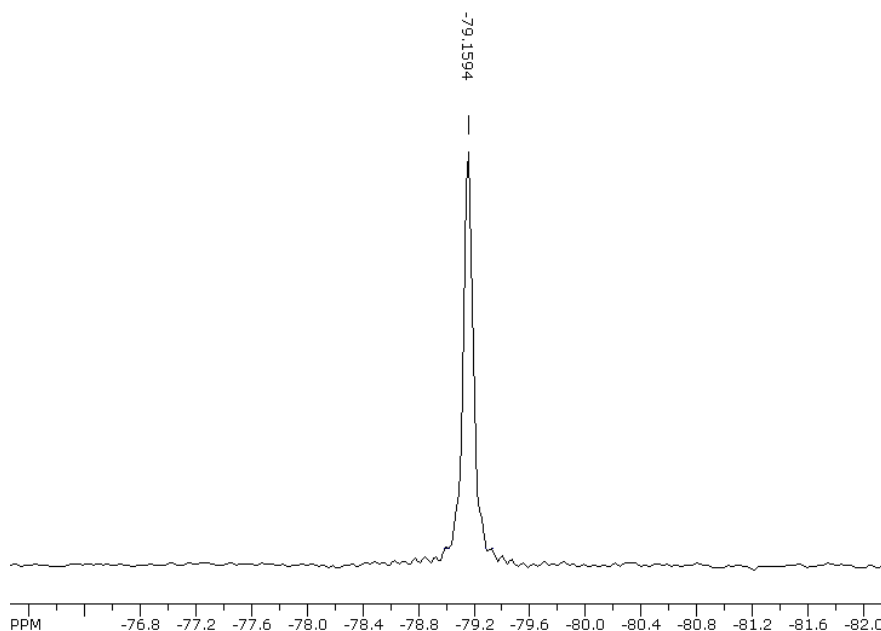
Figure 3.7 ^{19}F NMR spectra of either extracted sample from [C$_4$mim][NTf$_2$] or [C$_{10}$mim][NTf$_2$] or [N$_{4\ 1\ 1\ 1}$][NTf$_2$] or [C$_4$mpyr][NTf$_2$] ionic liquid.

This prompted us to determine the concentration of ionic liquids in our collected extracts.^{19}F NMR clearly show the presence of corresponding ionic liquid in each extract, while elemental analysis allowed determination of ILs' concentration in the collected samples. ^{19}F NMR spectrum presented in figure 3.7, had the same shape for each sample, where the chemical shift at – 79 ppm corresponds to CF_3-group of anion, confirming the presence of ionic liquids in all erythromycin extracts. Moreover, elemental analyses showed that the highest concentration of 10.9 mass % was observed in erythromycin's sample extracted from [C_{10}mim][NTf_2], followed by [$N_{4\ 1\ 1}$][NTf_2] (7.23 %), [C_4mim][NTf_2] (1.96 %), while no ionic liquid was detected when extraction was carried out from [C_4mpyr][NTf_2]. Obviously, the concentration of corresponding ionic liquid in the collected sample decreases as interactions between erythromycin and ionic liquid become weaker (see figure 3.4).

3.3 Two-steps recovery of erythromycin from aqueous solution using [C_4mpyr][NTf_2] and high-pressure carbon dioxide

Considering previous results, the ionic liquid 1-butyl-1-methylpyrrolidinium bis(trifluoromethylsulfonyl)imide, [C_4mpyr][NTf_2], was chosen for recovery of erythromycin from aqueous solution, while couple of additional studies were required: (i) mutual solubility of [C_4mpyr][NTf_2] and water; (ii) liquid-liquid extraction of erythromycin from aqueous solution using [C_4mpyr][NTf_2], as a function of pH and volume ratio of the ionic liquid to aqueous erythromycin solution; and (iii) high-pressure carbon dioxide extraction of erythromycin from [C_4mpyr][NTf_2], as a function of pressure and temperature.

Experimental procedure

For solubility measurements, liquid solutions were gravimetrically prepared (w/w ratio)using a Kern 770 balance (precision of ± 0.0001 g), while for extraction experiment, liquid solutions were prepared based on w/v ratio. A glass beaker of 2 L was used as a thermostat bath with water as thermostatic fluid. Temperatures were monitored using a calibrated mercury thermometer, having an accuracy of ± 0.1 K.

Mutual solubility of ([C_4mpyr][NTf_2] + water) was studied by the visual cloud-point titration method, based on the appearance of solution turbidity. The experiments were carried out in a temperature controlled equilibrium cell, immersed in the thermostat bath equipped by temperature controller unit. Firstly, the temperature of the bath was setup to a certain value by temperature controller unit and some time was allowed to reach a constant temperature which was verified by calibrated mercury thermometer. Then, known amounts of each pure component were titrated by the other one, at constant temperature, with continuous stirring. The titration point is taken as the appearance/ disappearance of turbidity in the solution and it is

defined as a cloud-point. After the turbidity was observed, final mixture was also weighted in order to calculate the composition.

Extraction of erythromycin from aqueous solution using [C_4mpyr][NTf_2], and the corresponding partition coefficients of erythromycin between aqueous and ionic liquid phases, was determined as a function of the aqueous phase pH. The latter were measured using a Crison Basic20 pH meter, with precision to within ± 0.01. The temperature was controlled at 303 K using the aforementioned water bath. Samples (2 mL) of aqueous solutions over the pH range 4-12, each containing erythromycin in concentration 264 µgmL^{-1} (C^0), were contacted with a different volume of [C_4mpyr][NTf_2] in glass vials. After vigorous stirring, solutions were centrifuged and left still, to allow a complete phase separation. Using a Hamilton syringe, the aqueous phases were carefully drawn to other vials and prepared for further analyses of erythromycin concentrations (C^{aq}). The erythromycin concentrations in ionic liquid (C^{IL}) phases were calculated by mass balance. Before commencing the work, the time taken to reach equilibrium was estimated by sampling the aqueous phase every 5 min until few consecutive samples produced essentially the same result of the analysis. It was determined that 15 min were sufficient to reach equilibrium.

Spectrophotometry (Beckman Coulter DU 800 spectrophotometer) was used to determined erythromycin concentrations in the aqueous phases (C^{aq}). A brownish-yellow colour is produced when sulphuric acid reacts with erythromycin, having a maximum absorption pick at 480 nm. Erythromycin concentrations were determined according to the method of Ford et al. [33]. The calibration curves were generated for each studied pH. All experiments were performed at least twice. The average is the result given.

The apparatus used for high-pressure carbon dioxide extraction of erythromycin, as well as experimental procedure were previously described in details (see Section 3.2).

Additionally, elemental and ^{19}F NMR analysis were performed in order to verify the presence of ionic liquid in collected erythromycin extracts after scCO$_2$ extraction. ^{13}C NMR was employed to confirm the stability of erythromycin. Elemental analyses were performed using a CHNS instrument model Flash EA 1112 (Thermo Finnigan-CE Instrument). The ^{19}F NMR and ^{13}C NMR spectroscopic analyses were performed on a BRUKER ARX 400 NMR spectrometer.

Results and discussion

Table 3.3 gives mutual solubility data for ([C_4mpyr][NTf_2] + water), at different temperatures and at atmospheric pressure. The ([C_4mpyr][NTf_2] + water) mixtures exhibits a wide immiscibility gap with very steep binodal lines.

Table 3.3 Mutual solubility of [C$_4$mpyr][NTf$_2$] (IL) and water (wat) at atmospheric pressure. Symbols w and x stand for mass and mole fraction, respectively

Water-rich phase				Ionic liquid-rich phase		
T / K	w_{IL}	x_{IL}		T / K	w_{wat}	x_{wat}
299.9	0.0068	0.0003		285.9	0.0089	0.1743
311.5	0.0077	0.0003		291.8	0.0106	0.2014
326.1	0.0092	0.0004		297.4	0.013	0.2360
337.6	0.0105	0.0005		306.3	0.0149	0.2625

Freire et al. [34] measured the solubility of water in [C$_4$mpyr][NTf$_2$] from 288 K to 318 K, using a sampling phase method followed by water content determination by Karl-Fischer titration. Figure 3.8 shows comparison with our data. Good agreement is observed at lower temperatures while at higher temperatures reported values are approximately 9 % higher than those represented in this work. As to the solubility of [C$_4$mpyr][NTf$_2$] in water, the single literature data point in the literature [35] is in close agreement with our results.
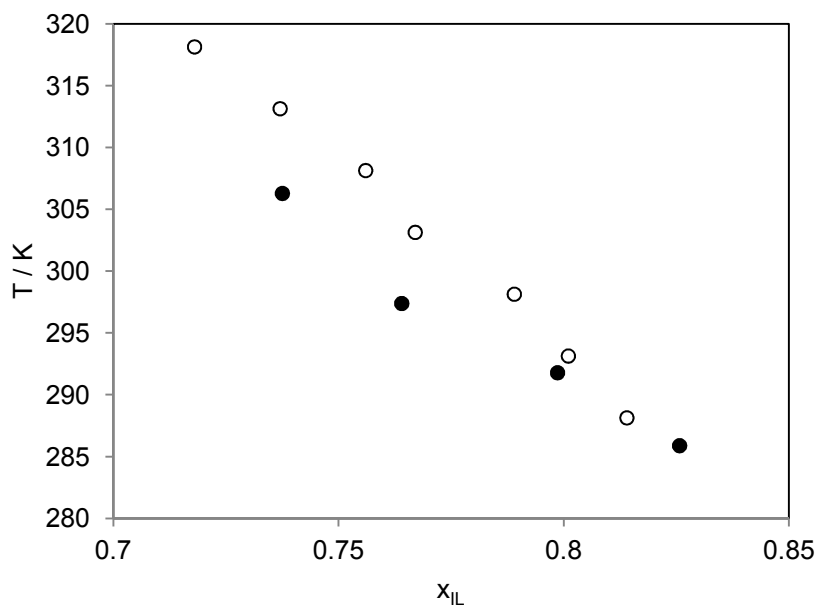
Figure 3.8 Comparison with literature data on solubility of water in [C$_4$mpyr][NTf$_2$]. Filled and empty circles stand for data from this work and Ref. [34], respectively.

Liquid-liquid extraction data as a function of pH are given in table 3.4 and figure 3.9. The erythromycin concentration in both IL-rich (C^{IL}) and water-rich phase (C^{aq}) – the tie-lines – are

presented along with the partition coefficients ($K_{ery} = C^{IL}/C^{aq}$) and extraction yields ($Y = m_{ery}^{extracted}/m_{ery}^{initial}$). As expected, figure 3.9 reveals that both K_{ery} and Y are strongly counter dependent on pH – as the pH values decreased these parameters rapidly increased. Erythromycin is a weak base containing one basic tertiary amine group (see figure 3.1) capable to undertake a protonation and therefore existing in cationic form in an acid medium. These results may indicate that the extraction is governed by the electrostatic interactions between the cationic form of the erythromycin and the anion of the ionic liquid. Wang et al. [11] observed a similar trend in the case of amino acid recovery from aqueous media by immidazolium based ionic liquids. Soto et al. [14] have also remarked that cationic forms of ampicillin and amoxicillin antibiotics favoured the extraction process by ionic liquids. Figure 3.9b clearly shows that the extraction yield of almost 100 % gently decreases in the range of pH < pKa (for erythromycin 8.8), where the ratio of cationic to molecular forms of erythromycin is higher than unity. On the other hand, a sharp decrease of extraction yield was observed when the majority of the antibiotic is in its molecular form (pH > pKa). On the contrary, when molecular solvents such as ethyl hexanol are used [36], the partition coefficient of erythromycin between organic and aqueous phase is higher at conditions where erythromycin exists mostly in its molecular form.

Table 3.4 Partition coefficients (K_{ery}) and yields (Y) of erythromycin extraction from aqueous solution by the ionic liquid [C_4mpyr][NTf$_2$], as a function of pH, at 303 K. The initial concentration of the antibiotic in water was 264 µgmL^{-1}, while the volume ratio of ionic liquid to the aqueous phase was 1:1. Extraction time was fixed to 15 min

pH	C^{aq} / µgmL^{-1}	C^{IL} / µgmL^{-1}	K_{ery}	Y / %
3.9	0	264	-	100.0
5.9	1	263	263.0	99.6
8.0	2	262	131.0	99.2
9.1	6	258	43.0	97.7
10.0	10	254	25.4	96.2
11.1	30	234	7.8	88.6
12.1	98	166	1.7	62.9

The partition coefficient decreased only from 43 to 38.2, while consequently, extraction yield diminished from 97.7 % to 90.5 % as the volume ratio of ionic liquid to antibiotic aqueous solution changed from 1 to 0.25, at fixed pH 9, as presented in table 3.5. These results suggest that it is possible to carry on an extraction with reasonable yields, using lower volumes of the ionic liquid solvent.
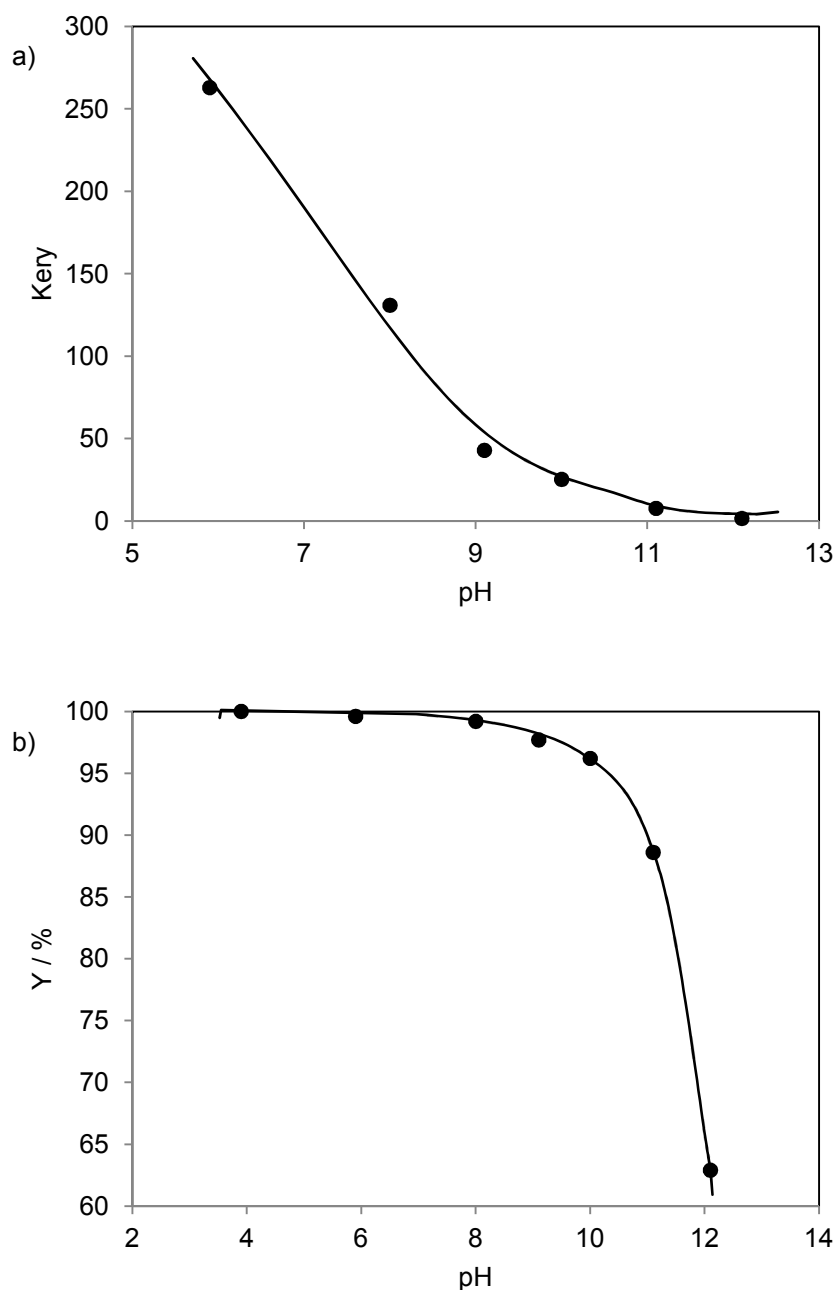
Figure 3.9 Partition coefficient of erythromycin between ionic liquid-rich and water-rich phase (a) and extraction yield (b) as a function of pH. Experimental conditions: initial concentration of erythromycin in aqueous solution C^0=264 µgmL^{-1}, volume ratio of ionic liquid to aqueous erythromycin solution, L =1:1, and extraction time, t=15 min.

The maximum observed concentration of erythromycin in the ionic liquid-rich phase was 956 µgmL^{-1} (see table 3.5) which is far lower than the solubility (0.018 mol fraction or approximately 30,000 µgmL^{-1}) of erythromycin in [C$_4$mpyr][NTf$_2$]. This prompted us to study a multistage extraction.

Table 3.5 The influence of volume ratio of ionic liquid solvent to erythromycin aqueous solution ($V^{IL}:V^{aq}$) on partition coefficient and extraction yield, at 303K. The initial concentration of antibiotic in water was 268 µgmL^{-1}, while the pH of the erythromycin solution was fixed at 9. Extraction time was fixed to 15 min.

$V^{IL}:V^{aq}$	C^{aq} / µgmL-1	C^{IL} / µgmL^{-1}	K_{ery}	Y / %
0.25	25	956	38.2	90.5
0.5	12	504	42.0	95.5
1.0	6	258	43.0	97.7
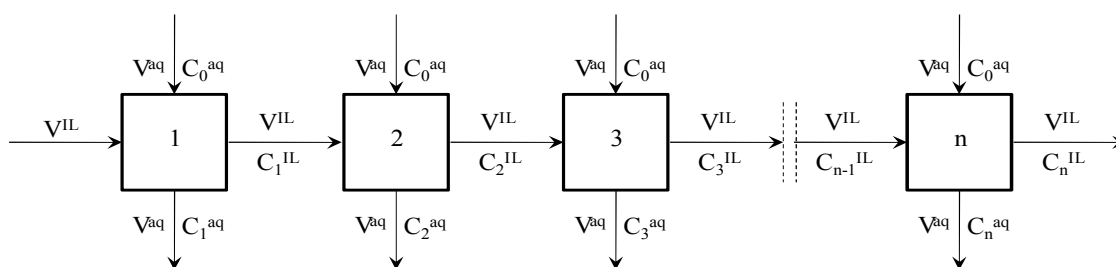
Figure 3.10 Scheme of the multistage extraction performed at ambient conditions with fixed pH 7.2. V^{IL} and V^{aq} stand for the volumes of [C$_4$mpyr][NTf$_2$] solvent and erythromycin aqueous solution, respectively. C^0, C_n^{IL} and C_n^{aq} stand for erythromycin concentration in initial aqueous solution, in the extract (IL phase) and the raffinate (aqueous phase), respectively. *i* is a number of extraction stages.

In this process, after the first extraction cycle, the same ionic liquid phase was brought into contact with a fresh antibiotic aqueous solution, with this procedure being repeated several times, as presented in figure 3.10. It should be noted that, contrary to common multistage extraction, when fresh solvent is added after each stage, in this work the same sample of the extract phase (IL phase) is contacted with the fresh initial erythromycin mixture, enriching the IL's erythromycin content. Taking in to account that: (i) the volumes of ionic liquid and fresh initial erythromycin solution are the same for each extraction stage; and (ii) the volume loss of ionic liquid is negligible, the following mass balance is:

$$C_n^{IL} = \frac{V^{aq}}{V^{IL}} \cdot \left(nC^0 - \sum_{i=1}^{n} C_i^{aq} \right) \tag{3.5}$$

where V^{aq} and V^{IL} denote volumes of ionic liquid [C$_4$mpyr][NTf$_2$] solvent and erythromycin aqueous solution, respectively. C^0 and C_i^{aq} stand for erythromycin concentration in initial and raffinate aqueous solution, respectively, while n represents the number of extraction stages. Eq. 3.5 permits the calculation of C_i^{IL} and of the corresponding extraction yield for each stage. These values are included in table 3.6.

Table 3.6 Ten-stage extraction of erythromycin using [C$_4$mpyr][NTf$_2$] at pH 7.2 and at 303 K, in accordance with the protocol presented in figure 3.10. The initial concentration of erythromycin (C^0) was 268 µgmL^{-1}, the total volume of the ionic liquid (V^{IL}) was 2 mL, while for each stage 8 mL of the fresh erythromycin solution (V^{aq}) was added

i	C^{aq} / µgmL-1	C^{IL} / µgmL^{-1}	Y / %
1	5.0	1052	98.1
2	13.2	2071	95.1
3	19.2	3067	92.9
4	28.9	4023	89.2
5	36.7	4948	86.3
6	49.2	5823	81.7
7	55.9	6672	79.2
8	63.0	7492	76.5
9	70.7	8281	73.6
10	87.9	9001	67.2

Table 3.7 Partition coefficients of erythromycin between various organic and water phase – data from the literature

Extraction solvent	C^0 / µgmL^{-1}	$V^{solvent}:V^{aq}$	T / K	pH	K_{ery}	Refs.
Butyl acetate	960	0.2	296	10.7	47	[36]
2-Ethyl hexanol	616	0.2	296	10.7	188	[36]
n-Octanol	616	0.2	296	10.7	162	[36]
2-Octanol	616	0.2	296	10.7	170	[36]
Acetonitrile/NaCl	7000	1	298	7	52	[37]
				9	290	
				11	350	
Acetonitrile	not stated	1.5	263	4	0.3	[38]
				7	2.2	
				10	2.9	
Butyl acetate	500	1	298	6	3	[13]
				7	7	
				8	12	
				9	21	
				10	3	
Decanol	500	1	298	7	0.2	[39]
				10	13	

In total, 80 mL (8 mL × 10 stages) of the initial erythromycin solution was treated with solely 2 mL of the ionic liquid solvent, resulting in an erythromycin content of 9001 µgmL^{-1}, and with the overall yield of 84 %. This suggests that, on the contrary to the traditional extraction, where abundant quantities of organic solvents are employed, the process with ionic liquid used forty times less solvent.

Results on erythromycin extraction from aqueous solution using various solvents already published in literature are presented in table 3.7. In general, partition coefficients were enhanced as the pH values increased. In strong acidic and alkaline solutions, erythromycin A undergoes degradation, forming products that are antibacterially inactive [40]. In the range of pH from 7 to 9, erythromycin A is the most stable, and therefore, although superior partition coefficients were observed outside this range, they are not relevant. The highest values of partition coefficients were reported for salt-induced phase separation process using acetonitrile/ NaCl solvent [37], having values 52 and 290, at pH 7 and 9, respectively. Similar values were observed in this work using ionic liquid as a solvent at the same pH conditions (see table 3.4). At room temperature solubility of acetonitrile in water/ NaCl-rich phase is approximately 0.23 in mole fraction [37] which is much higher than the solubility of $[C_4mpyr][NTf_2]$ in water-rich phase (0.0003 mole fraction – see table 3.3), indicating that much higher quantity of acetonitrile would be lost in extraction process.

Figure 3.11 presents yield of the high-pressure extraction of erythromycin from $[C_4mpyr][NTf_2]$ as a function of pressure (figure 3.11a) and temperature (figure 3.11b), where the yield of the erythromycin extract (g extracted erythromycin/ g erythromycin in initial feed) is plotted versus the solvent to feed ratio through the cell, Q (mol CO_2/ mol erythromycin in initial feed). Figure 3.11a shows that, at a constant temperature of 313.2 K, the extraction yield increases markedly with increasing pressure. In figure 3.11b, results obtained at three temperatures (298.2 K, 313.2 K and 323.2 K) and at a constant pressure of 20 MPa are plotted. Yields increase from 298.2 K to 313.2 K and then decrease to 323.2 K.

Burgos-Solorzano et al. [23] measured the solubility of erythromycin in CO_2 at 313.2 K and 333.2 K and at pressure up to 30 MPa. They have shown that the solubility is exceptionally high for a high molar mass substance. It also displays a steep increase from 313.2 K to 333.2 K, at all pressures studied. This behaviour is usually interpreted as an indication that the increase of the vapour pressure of the solute with temperature is the dominant factor controlling solubility, surpassing the effect of the decrease of solvent's density. At 313.2 K, solubilities changed from below their detection limit (app. 1×10^{-4} mol fraction) at 10 MPa to 8.8×10^{-4} mol fraction at 20 MPa, which might explain result of figure 3.11a. However, the peculiar behaviour of the yields represented in figure 3.11b cannot be explained on the bases of solubility in CO_2 alone. As pointed out, for instance, by Machida et al. [41], high pressure carbon dioxide dissolves in large amounts in many ionic liquids, decreasing their solvent power. The experimental data for the solubility of high pressure carbon dioxide in $[C_4mpyr][NTf_2]$ [42, 43] showed that it decreases markedly with an increase in temperature, as normally happens with gases dissolved in liquids. Additionally, the nature of interactions between erythromycin and ionic liquid, which is also dependent on temperature, can influence the extraction yield of erythromycin as well. The difference in extraction yield obtained at 298.2 K and 313.2 K is most likely consequence of these interactions. The attraction forces between like-molecules are weak at 298.2 K, while they are significantly superior at 313.2 K, improving the extraction yield. Although, high extraction

yield of erythromycin was expected at 333.2 K due to the nature of interactions between erythromycin and ionic liquid (γ = 2.41), we believe that notably lower solubility of CO_2 in [C$_4$mpyr][NTf$_2$] determined the inferior extraction yield of erythromycin, as it is presented in figure 3.11b.
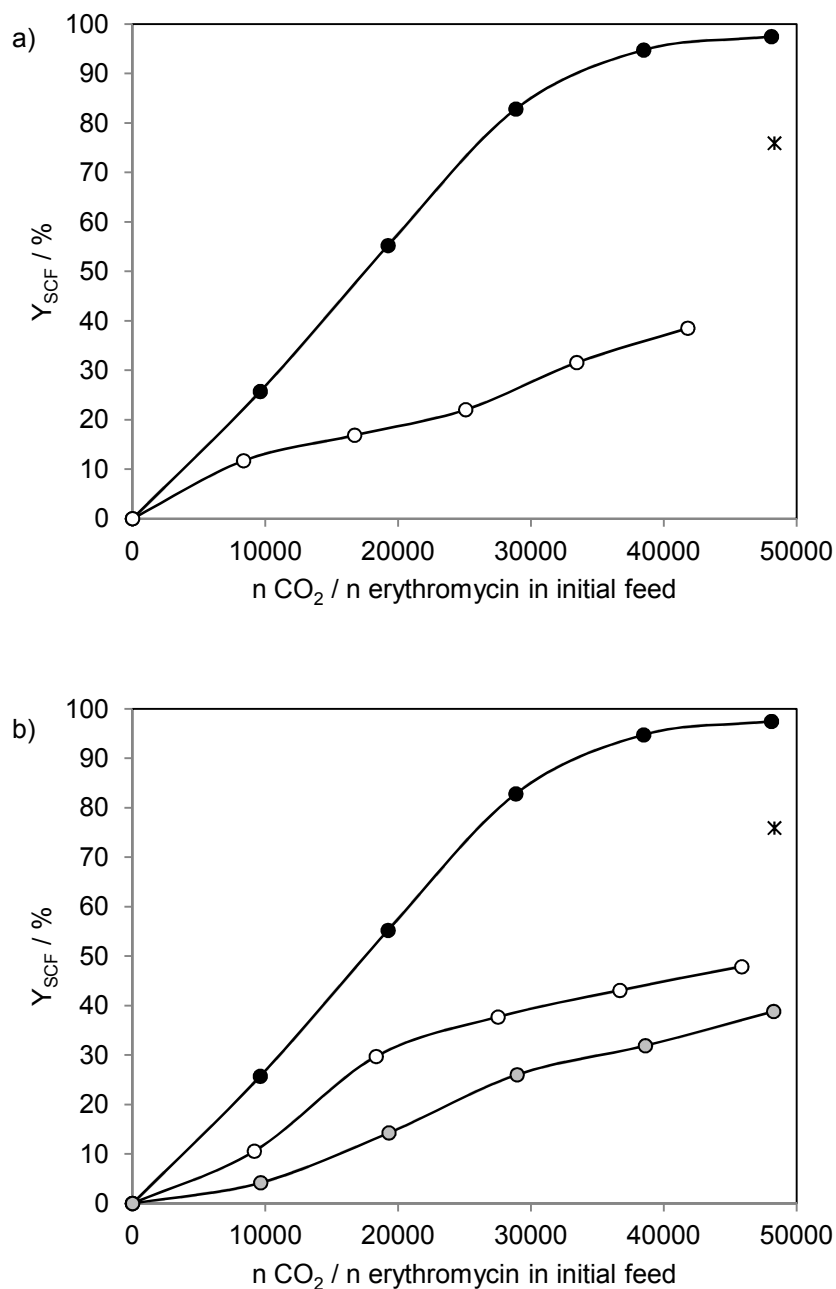
Figure 3.11 Dependence of the extraction yield on the specific amount of solvent (Q). (a) The effect of pressure at 313.2 K where empty and filled circles stand for 10 MPa and 20 MPa, respectively. (b) The effect of temperature at 20 MPa where empty, filled and grey circles stand for 298.2 K, 313.2 K and 333.2 K, respectively. The star data point corresponds to supercritical extraction of erythromycin from water saturated ionic liquid at 20 MPa and at 313 K.

High yield of supercritical extraction (97.4 %) was observed at 20 MPa and 313.2 K (see figure 3.11a). It is known, however, that presence of water in ionic liquid may influence extraction yield. In order to evaluate possibility of integration of erythromycin extraction from aqueous solution using hydrophobic ionic liquid and recovery of erythromycin from ionic liquid using high-pressure CO_2, the extract of the multistage liquid extraction (pH 7.2) was treated with supercritical CO_2 under aforementioned optimized conditions (20 MPa and 313.2 K). Thus, the initial concentration of erythromycin in water saturated ionic liquid was 9001 µgmL^{-1} (i = 10 in table 3.6). An extraction yield of 75.9 % was achieved with a solvent to feed ratio of 48,311 (mol CO_2/ mol erythromycin), as shown in figure 3.11 (the data point labelled as a "star"). The decrease of the high-pressure CO_2 extraction yield, when compared to extraction yields obtained from the dehydrated ionic liquid can be attributed to the presence of water in the saturated ionic liquid solution. In fact, it was shown that 1 % of water decreases the solubility of CO_2 in an ionic liquid for approximately 10 % [41].

The concentration of ionic liquid in collected extracts at 20 MPa and at 298.2 K, 313.2 K and 333.2 K was determined. ^{19}F NMR chemical shift at -79 ppm (see figure 3.7), which corresponds to CF_3-group from ionic liquid's anion clearly showed the presence of the ionic liquid in all extracts. The standard CHNS elemental analysis revealed that after the high-pressure CO_2 extraction at 20 MPa, 1.45 mass % and 1.05 mass % [C$_4$mpyr][NTf$_2$] was present in the extract obtained from dry [C$_4$mpyr][NTf$_2$] at 333.2 K, and from water saturated [C$_4$mpyr][NTf$_2$] at 313.2 K , respectively, while no ionic liquid was detected when extraction was carried out from dry [C$_4$mpyr][NTf$_2$], at both 298.2 K and 313.2 K. The discrepancy of IL content obtained from ^{19}F NMR and CHNS elemental analysis is not clear yet.
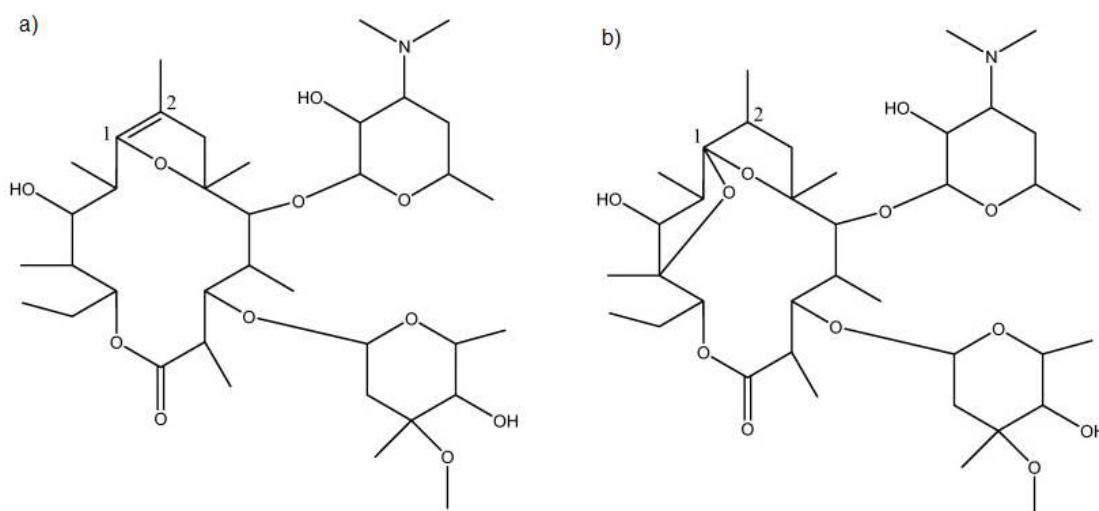
Figure 3.12 Chemical structures of erythromycin's degradation products: (a) erythromycin enol ether and (b) anhydroerythromycin A.

As it has been mentioned before, several studies have shown that erythromycin A is unstable in strong acidic and alkaline solutions [40], undergoing dehydration reaction and forming products that are antibacterially inactive. The study of erythromycin degradation is more important in acidic media since the best extraction yields are achieved for both organic solvents and ionic liquid (this work). Figure 3.12 shows chemical structure of erythromycin degradation products in acidic medium, anhydroerythromycin A and erythromycin enol ether. Chemically, keto-group at position 1 of cyclotetradecane (see figure 3.1) converts to either enol ether group (figure 3.12a) or two ether groups (figure 3.12b). According to the study on kinetics for the degradation of erythromycin A in acidic aqueous solution [42], the main degradation product is anhydroerythromycin A.
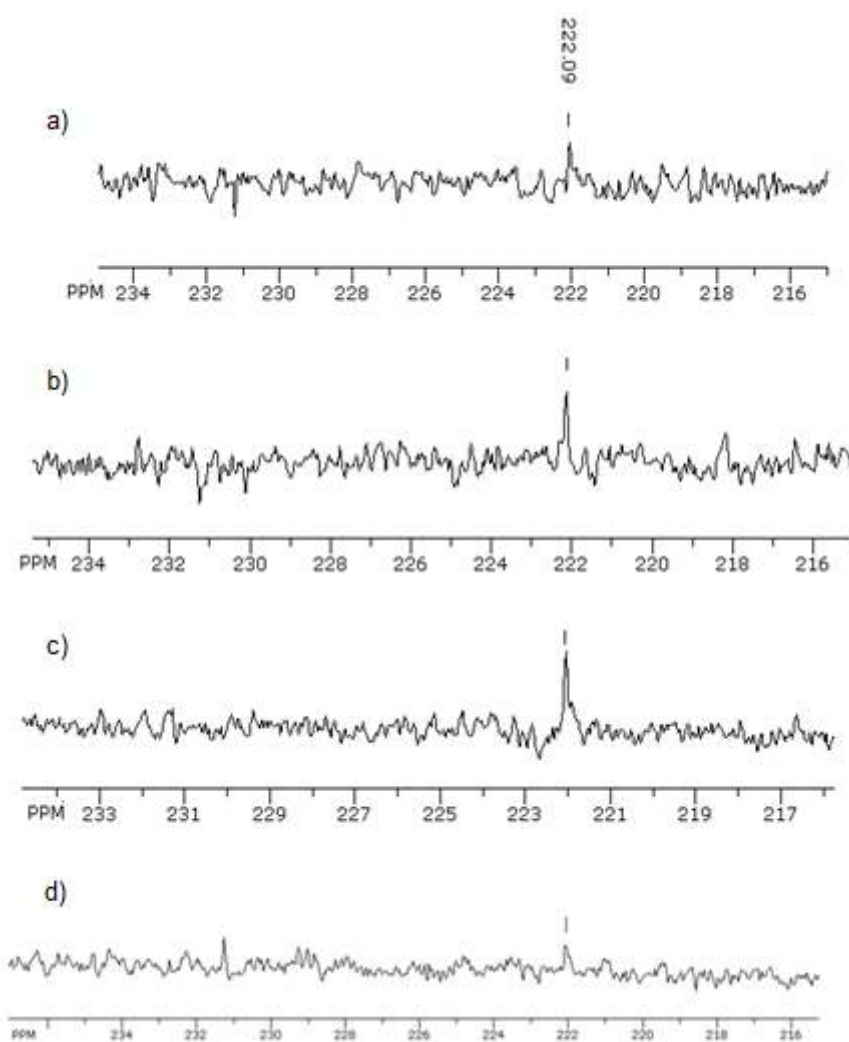
Figure 3.13 ^{13}C NMR - Chemical shift at 222 pm assigned to two ether groups existing in anhydroerythromycin A for: (a) neat erythromycin, (b) extracted sample at 298 K and 20 MPa from water free ionic liquid, (c) extracted sample at 333 K and 20 MPa from water free ionic liquid, and (c) extracted sample at 313 K and 20 MPa from water-saturated ionic liquid.

For that reason, we performed ^{13}C NMR of following samples (see fig. 3.13): neat erythromycin; the extracts after high-pressure CO_2 extraction carried out at 20 MPa, from water-free ionic liquid at two temperatures, 298.2 K and 333.2 K; as well as the extract obtained after integrated liquid-liquid and high-pressure CO_2 extraction which involved aqueous buffer solution. All these samples were left for 14 days in refrigerator prior to scCO$_2$ extraction. The spectrum of extracts obtained from all samples revealed no significant presence of the main degradation product, anhydroerythromycin A, corresponding to chemical shift at 222 ppm [42]. This confirms chemical stability of erythromycin in [C$_4$mpyr][NTf$_2$] ionic liquid even in water-saturated samples after 14 days.

Conclusions

The solubilities of erythromycin in [C$_4$mim][NTf$_2$], [C$_{10}$mim][NTf$_2$], [P$_{6\ 6\ 6\ 14}$][Cl], [N$_{4\ 1\ 1\ 1}$][NTf$_2$], [N$_{1\ 8\ 8\ 8}$][NTf$_2$] and [C$_4$mpyr][NTf$_2$] as a function of temperature were reported. The solubilities in all selected ionic liquids were slightly enhanced by increase of temperature. (Liquid + liquid) and (solid + liquid) equilibria were observed for (erythromycin + [N$_{1\ 8\ 8\ 8}$][NTf$_2$]), while for all other (erythromycin + ionic liquid) systems only (solid + liquid) equilibria were detected. Based on solubility data, the activity coefficients of erythromycin in ionic liquids were calculated and comparisons with ideal solutions made. The semi-empirical Grant equation was used to correlate the solubility data, with relative standard deviation within ± 0.12 %.

The supercritical carbon dioxide extraction of erythromycin from aforementioned ionic liquids was performed at temperature of 313.2 K and under pressure of 20 MPa. The extraction yield of erythromycin was affected by the nature of interactions between erythromycin and ionic liquids, which decreased as the attraction forces between unlike-molecules increased. The highest extraction yield of erythromycin (97.4 %) was achieved from [C$_4$mpyr][NTf$_2$]. On the other hand, visible amount of ionic liquid was detected in erythromycin extract when extraction was carried out from [P$_{6\ 6\ 6\ 14}$][Cl] and [N$_{1\ 8\ 8\ 8}$][NTf$_2$]. ^{19}F NMR and elemental analysis confirmed the presence of corresponding ionic liquid in all collected extracts. The ionic liquid [C$_4$mpyr][NTf$_2$] was chosen as the best candidate for liquid-liquid extraction of erythromycin from aqueous solution, followed by high-pressure CO_2 recovery of erythromycin from the ionic liquid.

Data on mutual solubility of [C$_4$mpyr][NTf$_2$] hydrophobic ionic liquid and water system are generated, where slight influence of temperature on solubility was observed. Results of liquid extraction of erythromycin from aqueous solutions by [C$_4$mpyr][NTf$_2$] as a function of pH and feed to IL volume ratio are reported along with results of high-pressure CO_2 extraction of erythromycin from ionic liquid as a function of pressure, temperature and presence of water. As pH values decreased partition coefficient of erythromycin between IL and aqueous phase rapidly increased. The same trend was observed for the yield of liquid extraction. Partition coefficient slightly decreased from 43 to 38.2 and consequently extraction yield diminished from 97.7 % to 90.5 % as the volume ratio of IL to antibiotic aqueous solution changed from 1 to 0.25

at fixed pH 9. Ten-stage liquid extraction gave satisfactory results: the overall yield of 84 % using in total forty times higher volume of aqueous solution then ionic liquid. It should be noted that other important factor such as interfering species, ionic strength and temperature may influence the extraction yield.

At the constant temperature of 313.2 K the high-pressure CO_2 extraction rate increases with increasing pressure. At the constant pressure of 20 MPa the temperature effect was influenced by two different factors: the nature of interactions between erythromycin and [C$_4$mpyr][NTf$_2$], and the solubility of CO_2 in IL. At conditions where CO_2 is in the supercritical region, the temperature increase resulted in the decrease of the extraction rate due to lower solubility of CO_2 in IL. At 298 K, the extraction rate was manly limited by the strong attractive forces between erythromycin and [C$_4$mpyr][NTf$_2$]. The high-pressure CO_2 extraction of erythromycin from the ionic liquid containing aqueous buffer solution exhibited lower extraction yield. It was verified that erythromycin extract contain 1.05 mass % of the ionic liquid.

No significant presence of main degradation product, anhydroerythromycin A, was observed. This confirms chemical stability of erythromycin in [C$_4$mpyr][NTf$_2$] ionic liquid even in water-saturated sample after 14 days.

References

[1] L. Tessier, P. Bouchard, M. Rahni, Separation and purification of benzylpenicillin produced by fermentation using coupled ultrafiltration and nanofiltration technologies, Journal of Biotechnology, 116 (2005) 79-89.

[2] K. Schügerl, J. Hubbuch, Integrated bioprocesses, Current Opinion in Microbiology, 8 (2005) 294-300.

[3] S. Charles A, A review of the environmental fate and aquatic effects of a series of C4 and C8 oxo-process chemicals, Chemosphere, 45 (2001) 339-346.

[4] J. McFarlane, W.B. Ridenour, H. Luo, R.D. Hunt, D.W. DePaoli, R.X. Ren, Room temperature ionic liquids for separating organics from produced water, Separation Science and Technology, 40 (2005) 1245-1265.

[5] J.D. Holbrey, I. Lopez-Martin, G. Rothenberg, K.R. Seddon, G. Silvero, X. Zheng, Desulfurisation of oils using ionic liquids: selection of cationic and anionic components to enhance extraction efficiency, Green Chemistry, 10 (2008) 87-92.

[6] A. Arce, A. Pobudkowska, O. Rodríguez, A. Soto, Citrus essential oil terpenless by extraction using 1-ethyl-3-methylimidazolium ethylsulfate ionic liquid: Effect of the temperature, Chemical Engineering Journal, 133 (2007) 213-218.

[7] A. Arce, H. Rodríguez, A. Soto, Purification of ethyl tert-butyl ether from its mixtures with ethanol by using an ionic liquid, Chemical Engineering Journal, 115 (2006) 219-223.

[8] D. Gorri, A. Ruiz, A. Ortiz, I. Ortiz, The use of ionic liquids as efficient extraction medium in the reactive separation of cycloolefins from cyclohexane, Chemical Engineering Journal, 154 (2009) 241-245.

[9] C.L.S. Louros, A.F.M. Cláudio, C.M.S.S. Neves, M.G. Freire, I.M. Marrucho, J. Pauly, J.A.P. Coutinho, Extraction of biomolecules using phosphonium-based ionic liquids + K3PO4 aqueous biphasic systems, International Journal of Molecular Sciences, 11 (2010) 1777-1791.

[10] Z. Du, Y.-L. Yu, J.-H. Wang, Extraction of proteins from biological fluids by use of an ionic liquid/aqueous two-phase system, Chemistry – A European Journal, 13 (2007) 2130-2137.

[11] J. Wang, Y. Pei, Y. Zhao, Z. Hu, Recovery of amino acids by imidazolium based ionic liquids from aqueous media, Green Chemistry, 7 (2005) 196-202.

[12] H. Zhao, S. Xia, P. Ma, Use of ionic liquids as 'green' solvents for extractions, Journal of Chemical Technology & Biotechnology, 80 (2005) 1089-1096.

[13] S.G. Cull, J.D. Holbrey, V. Vargas-Mora, K.R. Seddon, G.J. Lye, Room-temperature ionic liquids as replacements for organic solvents in multiphase bioprocess operations, Biotechnology and Bioengineering, 69 (2000) 227-233.

[14] A. Soto, A. Arce, M.K. Khoshkbarchi, Partitioning of antibiotics in a two-liquid phase system formed by water and a room temperature ionic liquid, Separation and Purification Technology, 44 (2005) 242-246.

[15] C.-H. Ma, L. Wang, Y.-S. Yan, G.-B. Che, Y.-S. Yin, R.-Z. Wang, D.-Y. Li, Extraction of tetracycline via ionic liquid two-phase system, Chemical Research in Chinese Universities, 25 (2009) 832-835.

[16] Y. Jiang, H. Xia, J. Yu, C. Guo, H. Liu, Hydrophobic ionic liquids-assisted polymer recovery during penicillin extraction in aqueous two-phase system, Chemical Engineering Journal, 147 (2009) 22-26.

[17] L.A. Blanchard, D. Hancu, E.J. Beckman, J.F. Brennecke, Green processing using ionic liquids and CO2, Nature, 399 (1999) 28-29.

[18] A.M. Scurto, S.N.V.K. Aki, J.F. Brennecke, CO2 as a separation switch for ionic liquid/organic mixtures, Journal of the American Chemical Society, 124 (2002) 10276-10277.

[19] V. Najdanovic-Visak, A. Serbanovic, J.M.S.S. Esperança, H.J.R. Guedes, L.P.N. Rebelo, M. Nunes da Ponte, Supercritical carbon dioxide-induced phase changes in (ionic liquid, water and ethanol mixture) solutions: Application to biphasic catalysis, ChemPhysChem, 4 (2003) 520-522.

[20] M.C. Kroon, J. van Spronsen, C.J. Peters, R.A. Sheldon, G.-J. Witkamp, Recovery of pure products from ionic liquids using supercritical carbon dioxide as a co-solvent in extractions or as an anti-solvent in precipitations, Green Chemistry, 8 (2006) 246-249.

[21] E.M. Saurer, S.N.V.K. Aki, J.F. Brennecke, Removal of ammonium bromide, ammonium chloride, and zinc acetate from ionic liquid/organic mixtures using carbon dioxide, Green Chemistry, 8 (2006) 141-143.

[22] J. Liu, X. Sun, D. Fu, S. Zhao, Phase equilibria for separation of high boiling point organics from ionic liquids by supercritical CO2 or C3H8, Chemical Engineering Journal, 147 (2009) 63-70.

[23] G.I. Burgos-Solórzano, J.F. Brennecke, M.A. Stadtherr, Solubility measurements and modeling of molecules of biological and pharmaceutical interest with supercritical CO2, Fluid Phase Equilibria, 220 (2004) 55-67.

[24] U. Domańska, E. Bogel-Łukasik, Solid–liquid equilibria for systems containing 1-butyl-3-methylimidazolium chloride, Fluid Phase Equilibria, 218 (2004) 123-129.

[25] U. Domańska, M. Królikowski, K. Paduszyński, Phase equilibria study of the binary systems (N-butyl-3-methylpyridinium tosylate ionic liquid + an alcohol), The Journal of Chemical Thermodynamics, 41 (2009) 932-938.

[26] S.M. Lai, M.Y. Yuen, L.K.S. Siu, K.M. Ng, C. Wibowo, Experimental determination of solid-liquid-liquid equilibrium phase diagrams, AIChE Journal, 53 (2007) 1608-1619.

[27] J.M. Prausnitz, R.N. Lichtenthaler, E.G. Azevedo, Molecular thermodynamics of fluid-phase equilibria, Pearson Education, 1998.

[28] D.J.W. Grant, M. Mehdizadeh, A.H.L. Chow, J.E. Fairbrother, Non-linear van't Hoff solubility-temperature plots and their pharmaceutical interpretation, International Journal of Pharmaceutics, 18 (1984) 25-38.

[29] Z. Wang, J. Wang, M. Zhang, L. Dang, Solubility of erythromycin A dihydrate in different pure solvents and acetone + water binary mixtures between 293 K and 323 K, Journal of Chemical & Engineering Data, 51 (2006) 1062-1065.

[30] I. Miroshnyk, L. Khriachtchev, S. Mirza, J. Rantanen, J. Heinämäki, J. Yliruusi, Insight into thermally induced phase transformations of erythromycin A dihydrate, Crystal Growth & Design, 6 (2005) 369-374.

[31] J.W. Hutchings, K.L. Fuller, M.P. Heitz, M.M. Hoffmann, Surprisingly high solubility of the ionic liquid trihexyltetradecylphosphonium chloride in dense carbon dioxide, Green Chemistry, 7 (2005) 475-478.

[32] W. Wu, J. Zhang, B. Han, J. Chen, Z. Liu, T. Jiang, J. He, W. Li, Solubility of room-temperature ionic liquid in supercritical CO2 with and without organic compounds, Chemical Communications, (2003) 1412-1413.

[33] J.H. Ford, G.C. Prescott, J.W. Hinman, E.L. Caron, Colorimetric determination of erythromycin, Analytical Chemistry, 25 (1953) 1195-1197.

[34] M.G. Freire, C.M.S.S. Neves, P.J. Carvalho, R.L. Gardas, A.M. Fernandes, I.M. Marrucho, L.M.N.B.F. Santos, J.A.P. Coutinho, Mutual solubilities of water and hydrophobic ionic liquids, The Journal of Physical Chemistry B, 111 (2007) 13082-13089.

[35] Z. Alfassi, R. Huie, B. Milman, P. Neta, Electrospray ionization mass spectrometry of ionic liquids and determination of their solubility in water, Analytical and Bioanalytical Chemistry, 377 (2003) 159-164.

[36] Z. Li, F. Qin, H. Bao, X. Gu, Study on new solvent extraction systems for erythromycin, Journal of Chemical Technology & Biotechnology, 80 (2005) 772-781.

[37] Q. Le, L. Shong, Y. Shi, Extraction of erythromycin from fermentation broth using salt-induced phase separation processes, Separation and Purification Technology, 24 (2001) 85-91.

[38] T. Gu, L. Zhang, Partition coefficient of some antibiotics, peptides and amino acids in liquid-liquid partitioning of the acetonitrile-water system at subzero temperatures, Chemical Engineering Communications, 194 (2007) 828-834.

[39] G.J. Lye, D.C. Stuckey, Extraction of erythromycin-A using colloidal liquid aphrons: I. Equilibrium partitioning, Journal of Chemical Technology & Biotechnology, 75 (2000) 339-347.

[40] Y.-H. Kim, T.M. Heinze, R. Beger, J.V. Pothuluri, C.E. Cerniglia, A kinetic study on the degradation of erythromycin A in aqueous solution, International Journal of Pharmaceutics, 271 (2004) 63-76.

[41] D. Fu, X. Sun, J. Pu, S. Zhao, Effect of water content on the solubility of CO2 in the ionic liquid [bmim][PF6], Journal of Chemical & Engineering Data, 51 (2006) 371-375.

[42] A. Hassanzadeh, J. Barber, G.A. Morris, P.A. Gorry, Mechanism for the degradation of erythromycin A and erythromycin A 2'-ethyl succinate in acidic aqueous solution, The Journal of Physical Chemistry A, 111 (2007) 10098-10104.

Chapter IV

Solubility of supercritical carbon dioxide in ionic liquids: Measurements and modelling

Introduction

The biphasic IL-CO_2 systems have gained significant importance in many technological processes due to characteristic gas-liquid phase behaviour [1] and therefore potential widespread applications. Various applications were proposed in the literature, including recovery of diverse solute without any cross-contamination [2-6]; homogenous catalysis [7, 8]; continuous reaction design where CO_2 might be used as a solvent or reagent/product carrier [7]; melting point depression transforming ionic salts to ionic liquids [9-11]; improving solubility of poorly soluble reaction gases in ILs [8, 12]; and supported ionic liquid phase (SILP) concept for gas separation [13], as well as for CO_2 capture [14]. The most of the published work on IL applications has been related to ionic liquids based on imidazolium cation due to their well-known thermophysical properties (more than 80 % of experimental data presented in the ILThermo database [15] are related to imidazolium based ionic liquids).

Although phosphonium based ionic liquids (PILs) have previously received scant attention, they show some advantages over imidazolium based ionic liquids such as higher thermal stability, faster kinetic of salt formation, the absence of acidic proton and thus stable to nucleophilic and basic conditions, lower density which provides potential benefits for some application and potential to became less expensive due to their bulk production (Cytec) [16]. Therefore, there is significant interest in developing industrial processes employing phosphonium based ionic liquids [17]. Institut Français du Pétrole (IFP) developed catalysis for the dimerization, codimerization and oligomerization of olefins using PILs. Eastman Chemical Company commercialized the process of epoxidation of butadiene to 3,4-epoxybut-1-ene and its isomerisation to 2,5-dihydrofuran using trioctyl(octadecyl)phosphonium iodide. Central Glass Company transformed Sonogashira coupling reaction, initially performed in organic solvents such as toluene or tetrahydrofuran to much more efficient, using PILs instead.

It is clear that the research on thermophysical properties and physical behaviour of phosphonium based ionic liquids are required. Several works concerning thermophysical properties [18-22], phase behaviour of CO_2 + PILs [23-26] and potential applications of CO_2 + PILs systems have been published recently [27-31]. Novel amino-functionalized phosphonium ionic liquids have been used for CO_2 capture which occurs due to chemical absorption, leading to the higher efficiency of the process [27, 28]. Smuts et al. [29] have studied different ionic liquids as a stationary phase in supercritical fluid chromatography showing that phosphonium based stationary phase performed better than others. The carboxilation of an amine to 1,3-subsituted urea by CO_2 was significantly improved in the presence of the ionic liquid catalysts such as tetra-n-butylphosphonium bromide and 1-ethyl-3-methylimidazolium chloride [30]. Livi et al. [31] have modified lamellar silicate by using supercritical CO_2 and phosphonium based ionic liquid improving the thermal stability and intercalation between the layers of organoclays.

Therefore, the study of the solubility of high-pressure CO_2 in ionic liquids recently received increased attention, as essential for the design of any separation and reaction processes. In this context, the most studied ionic liquids are the ones based on the immidazolium cations. Several studies were reported in order to study the influence on the solubility of the anion, as well as of changing the length of the alkyl chain and branching.

In 2000, Kazarian et al. [32] reported a direct indication of the effect of an anion in the weak Lewis acid–base interactions with CO_2 molecules using in situ infra-red spectroscopy. Cadena et al. [33] combined both experimental and molecular simulation approaches and concluded that the major factor controlling CO_2 solubility is the nature of the anion while the cation plays a secondary role, which is in agreement with the spectroscopic studies. The authors observed also that the presence of the acidic hydrogen is responsible for the direct association of anions with the C2 carbon of the imidazolium ring.

It was shown that ionic liquids based on anions with fluoroalkyl groups are capable to dissolve higher amounts of CO_2 compared with non-fluorinated anions such as dicyanamide, nitrate and ethylsulfate ($[DCA]^-$, $[NO_3]^-$, $[EtSO_4]^-$). The same effect – higher solubility was observed by adding fluorinated groups into the alkyl chain of cation [34].

When it comes to ionic liquids based on different than immidazolium cations, data on solubility of CO_2 are either scarce or even absent. Scovazzo's group has studied the solubility of CO_2 in various ammonium, pyrrolidinium and phosphonium ionic liquids at 303 K and at atmospheric pressure [35-37]. The influence of temperature on the solubility of CO_2 in trimethylbutylammonium and 1-butyl-1-methylpyrrolidinium bis(trifluoromethylsulfonyl)imide was studied at atmospheric pressure by Costa Gomes and co-workers [38, 39]. Yim et al. [40] recently published the solubility of CO_2 in 1-butyl-1-methylpyrrolidinium bis(trifluoromethylsulfonyl)imide up to 45 MPa. The solubility of the same systems was studied by Brennecke at al. [41] in addition to the CO_2-triisobutylmethylphosphonium p-toluenesulfonate mixture. Solubilities of CO_2 in two ionic liquids, trihexyl(tetradecyl)phosphonium bis(trifluoromethylsulfonyl)imide and trihexyl(tetradecyl)phosphonium chloride in the wide range of pressures (up to 37 MPa) were reported by Carvalho et al [25]. and Song et al [26].

In this work, we present the experimental solubility of CO_2 in eight different ionic liquids at 313.2 K and 323.2 K and pressures up to 22 MPa. To investigate the influence of the cation, six of the ILs studied have the bis(trifluoromethylsulfonyl)imide anion ($[NTf_2]^-$) coupled with either trihexyl(tetradecyl)phosphonium ($[P_{6\ 6\ 6\ 14}]^+$), 1-butyl-3-methylimidazolium ($[C_4mim]^+$), 1-decyl-3-methylimidazolium ($[C_{10}mim]^+$), 1-butyl-1-methylpyrrolidinium ($[C_4mpyr]^+$), butyltrimethylammonium ($[N_{4\ 1\ 1\ 1}]^+$), or methyltrioctylammonium ($[N_{1\ 8\ 8\ 8}]^{+)}$ as the cation. Additionally we also considered the trihexyl(tetradecyl)phosphonium chloride ($[P_{6\ 6\ 6\ 14}][Cl]$) and trihexyl(tetradecyl)phosphonium bromide ($[P_{6\ 6\ 6\ 14}][Br]$) ionic liquids to check the effect of replacing the anion.

Although experimental data on solubility are essential to provide information about a system and help to understand its behaviour, due to the abundance of ionic liquids, correlation and prediction models are required. The IL-CO_2 systems have been described by several models, such as the Peng–Robinson equation of state (PR EoS) [42-44], Soft Statistical Associating Fluid Theory (soft-SAFT) [45], Perturbed-Chain Statistical Associating Fluid Theory (PC-SAFT) [46] and Quantum chemistry calculations of solvation thermodynamics (COSMOtherm) [47].

In this work we applied either the Peng-Robinson (PR) or Soave-Redlich-Kwong (SRK) equation of state, additionally incorporating association – Cubic Plus Association equation of state (CPA EoS), in order to describe the physical interactions and the intermolecular specific association interactions in IL-CO_2 systems.

The experimental density and surface tension data, presented in this work, were required to calculate the critical temperature of $[P_{6\ 6\ 6\ 14}][Br]$ using the Eötvos equation [48]. The experimental densities were compared with both the experimental data published recently [22, 49] and the densities calculated by Gardas and Coutinho model [50].

Materials

All ionic liquids studied in this work are presented in table 4.1, along with their full names, abbreviations, chemical structures, purities and the water content after drying. In order to decrease the water content and volatile compounds to negligible values, all ionic liquids were dried in vacuum (0.1 Pa), while stirring at moderate temperature (up to 70 ºC) for at least 72 h. The water contents after the vacuum procedure, determined by Karl Fischer coulometric titration (Metrohm 831 KF coulometer) were no higher than 155 ppm in all studied cases, as can be observed from table 4.1. Carbon dioxide (99.98 % purity) was supplied by Air Liquide and was used without further purification.

Experimental procedure

The experimental technique used in this work was based on the saturation isochoric method. As presented in figure 4.1, the apparatus is based on a high-pressure sapphire cell which has an internal volume of approximately 30 cm^3 and allows sampling of both vapour (top) and liquid (bottom) phase. The bottom and the top of the cell are connected to sample loops, which are linked to an expansion zone through a pair of cold traps. The whole system is placed in a thermo-stated air bath, apart from the cold traps which are kept at low temperature in order to separate CO_2 dissolved in IL.

Table 4.1 Ionic liquids used in this study
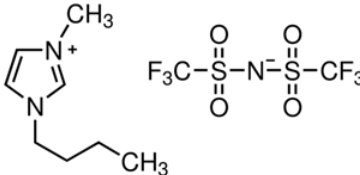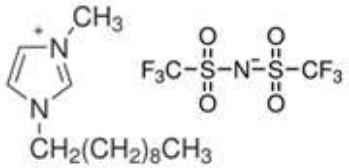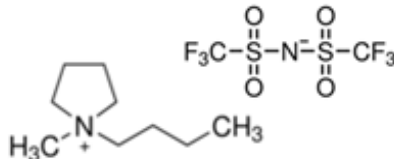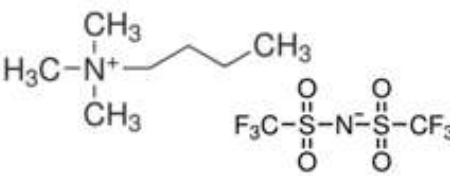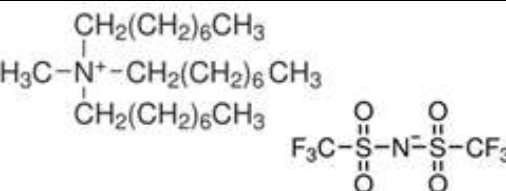
Chemical Name	Abbreviation	Structure	Purity / mass %	Water content after drying/ ppm
1-butyl-3-methylimidazolium bis(trifluoromethylsulfonyl)imide	[C$_4$mim][NTf$_2$]		> 98 %	60
1-decyl-3-methylimidazolium bis(trifluoromethylsulfonyl)imide	[C$_{10}$mim][NTf$_2$]		> 98 %	95
1-butyl-1-methylpyrrolidinium bis(trifluoromethylsulfonyl)imide	[C$_4$mpyr][NTf$_2$]		> 99 %	175
Butyltrimethylammonium bis(trifluoromethylsulfonyl)imide	[N$_{4\,1\,1\,1}$][NTf$_2$]		> 99 %	155
Methyltrioctylammonium bis(trifluoromethylsulfonyl)imide	[N$_{1\,8\,8\,8}$][NTf$_2$]		> 99 %	100

Table 4.1 Continuation

Chemical Name	Abbreviation	Structure	Purity / mass %	Water content after drying/ ppm
Trihexyl(tetradecyl)phophonium bis(trifluoromethylsulfonyl)imide	[P$_{6\,6\,6\,14}$][NTf$_2$]		> 98 %	112
Trihexyl(tetradecyl)phophonium chloride	[P$_{6\,6\,6\,14}$][Cl]		> 95 %	120
Trihexyl(tetradecyl)phophonium bromide	[P$_{6\,6\,6\,14}$][Br]		> 95 %	112

Figure 4.1 Scheme of the apparatus used for high-pressure phase equilibrium determination: (1) high-pressure sapphire cell, (2) magnetic stirrer, (3) sampling loop, (4) air bath, (5) heating controller, (6) cold trap, and (7) expansion volume.

In order to calculate the mass of CO_2 dissolved in the IL, a calibration of the expansion volume was achieved previously by adding a high purity nitrogen gas to the system at controlled temperature. An exact amount of gas was released into the expansion volume and the pressure was recorded. Using this data the density of nitrogen was obtained from the NIST database [51] and the expansion volumes were determined (V_{bottom} = 704.97 cm^3 and V_{top} = 702.14 cm^3).

The temperature control of the air bath was made by using a Hart Scientific temperature controller (model 2100), with a stability of ± 0.005 ºC to ± 0.02 ºC. This controller uses a RTD probe from the same supplier (model 2622) as well as a heater. In order to ensure a uniform bath temperature, a high-power ventilator was used. The pressure in the system was measured by a Setra pressure transducer (model Model 204/C204). The transducer was calibrated against a Bourdon tube pressure gauge (Heise model CMM). The calibration of the temperature and pressure sensors was initially checked by measuring values of the vapour pressure of pure carbon dioxide. The estimated precision of the pressure determination is ± 0.07 bar, while the estimated temperature uncertainty is ± 0.1 K. The expansion pressure was measured by a Keller high-accuracy low-pressure sensor (model Leo) with a precision of 0.003 bar.

The solubility measurements were performed at two different temperatures, 313.2 K and 323.2 K and high pressure up to 22 MPa. Before testing any particular system, air was removed from the cell and tubing system which were kept under vacuum during the night. The required temperature was settled and ionic liquid (approximately 7 mL) was loaded to the cell. The pressure of CO_2 was slowly increased by using a manually driven screw-injector connected to

the bottom of the cell, until the required pressure was reached. In the same time, CO_2 removed the residual amount of IL from the tubing line before the cell, guaranteeing that all IL was in contact with CO_2 during the 2 h stirring period. The system was left resting the next 2 h to enable the complete separation of the two phases. Before commencing the work, the time taken to reach equilibrium was estimated by sampling the liquid phase in regular intervals until few consecutive samples showed essentially the same concentration (mole fraction) of CO_2. Even though 1 h stirring time was sufficient, we fixed it at 2 h in order to guarantee the equilibrium. Sampling of the bottom IL-rich phase was performed, followed by an expansion of the loop into the calibrated volume. Low temperature in cold trap provoked precipitation of IL while dissolved CO_2 was released to the expansion volume. The expansion pressure of CO_2 was recorded. The quantity of IL in the sample was measured using Kern 770 balance with the accuracy of ±0.0001 g, while the amount of CO_2 was calculated using the expansion pressure, temperature of the system, the expansion volume (V_{bottom}) and density of CO_2 which was obtained from the NIST database [51], according to the measured values. This allowed the calculation of the mole fraction solubility of CO_2 in the liquid phase.

All experiments were performed at least twice and the average result was taken into account. The reproducibility was ± 0.01 mole fraction of CO_2.

4.1 High-pressure solubility of carbon dioxide in ionic liquids based on bis(trifluoromethylsulfonyl)imide and chloride

Modelling

In this work we have evaluated two cubic equations of state, Peng-Robinson (PR) and Soave-Redlich-Kwong (SRK), as well as an associative equation of state, the Cubic-Plus-Association (CPA) to describe the high pressure solubilities of carbon dioxide in ionic liquids.

The modelling of gas solubilities in ionic liquids has been the subject of many recent publications [43-47]. Different models, from the most simple to the most complex have been suggested, and it is not yet clear whether ionic liquids should or not be considered as associating components. In order to clarify this issue, we compare here cubic equations of state (PR and SRK) with an associative equation of state (CPA). The difference between both classes of equations of state is whether or not explicit association contributions are considered, as is the case in the CPA equation of state.

All these equations of state can be written using the same expression for the Helmholtz energy:

$$A = A^{cubic} + A^{Assoc} \tag{4.1}$$

where A^{cubic} and A^{Assoc} are the cubic and association term of the Helmholtz energy given by equations 4.2 and 4.3, respectively.

$$A^{cubic} = \frac{an}{b(\delta_2 - \delta_1)} ln\left(\frac{1 + b\rho\delta_1}{1 + b\rho\delta_2}\right) - nRT\, ln(1 - b\rho) \tag{4.2}$$

where a, b and ρ are the energy parameter, co-volume parameter and the molar density, respectively.

$$A^{assoc} = RT \sum_i n_i \sum_{A_i} \left[ln\left(X_{A_i}\right) - \frac{X_{A_i}}{2} + \frac{1}{2}\right] \tag{4.3}$$

where X_{Ai} stands from the fraction of molecule i not bonded at the site A.

For the SRK EoS δ_1 equals to 1 and δ_2 equals to 0. For the PR EoS: $\delta_1 = 1 + \sqrt{2}$ and $\delta_2 = 1 - \sqrt{2}$. The CPA EoS can use either the SRK or the PR cubic term. For the SRK and PR EoS A^{assoc} is zero and therefore $A = A^{cubic}$.

The cubic-plus-association equation of state (CPA EoS) is thus a combination of a simple cubic equation of state for the description of the physical interactions with the Wertheim association term, which takes into account the specific associating interactions.

In the SRK and PR EoS the pure component a and b parameters are usually obtained from the pure component critical properties (T_c and P_c) and acentric factors, while for CPA they are regressed from pure component vapour pressure and liquid density data. The expressions for the a parameter of the three equations of state, as well as the expressions for obtaining b for the SRK and PR EoS are different, and can be found in the literature [52].

In the associative contribution, X_{Ai} is related to the association strength Δ^{AiBj} between sites A and B belonging to two different molecules (i, j) and is calculated solving simultaneously the following set of equations:

$$X_{A_i} = \frac{1}{1 + \rho \sum_j x_j \sum_{B_j} X_{B_j} \Delta^{A_i B_j}} \tag{4.4}$$

where the association strength is calculated from:

$$\Delta^{A_i B_j} = g(\rho) \left[exp\left(\frac{\varepsilon^{A_i B_j}}{RT}\right) - 1 \right] b_{ij} \beta^{A_i B_j} \tag{4.5}$$

$$g(\rho) = \frac{1}{1 - 1.9\eta} \tag{4.6}$$

$$\eta = \frac{1}{4} b\rho \tag{4.7}$$

and $g(\rho)$ is a simplified hard-sphere radial distribution function.

Thus, the CPA EoS has five pure compound parameters (a_0, c_1, b, ε, β) for associating components, but only three (a_0, c_1, b) are required for non-associating compounds. All these

parameters are generally obtained by fitting experimental pure component liquid density (ρ) and vapour pressure data (p), taking into account the association scheme that provides the number and type of association sites for each associating compound [53]. The objective function commonly used to fit the CPA pure component parameters is:

$$OF = \sum_i^{NP} \left(\frac{P_i^{exp.} - P_i^{calc.}}{P_i^{exp.}} \right)^2 + \sum_i^{NP} \left(\frac{\rho_i^{exp.} - \rho_i^{calc.}}{\rho_i^{exp.}} \right)^2 \qquad (4.8)$$

where the same weight is given to the description of vapour pressures and liquid densities. For ionic liquids, as there is a much larger uncertainty in vapour pressures than in liquid densities, we have used a weighting factor to consider the best description of liquid densities, while still providing a qualitative description of IL vapour pressures. For that, we have multiplied the pressure sum in eq. 4.8 by 0.1 and the density sum by 0.9.

When these equations of state are applied to mixtures, the energy and co-volume parameters in the cubic contribution are calculated using van der Waals one-fluid mixing rules. A single adjustable binary interaction parameter for the cross-energy term (k_{ij}) is the only parameter regressed from binary data:

$$a = \sum_i \sum_j x_i x_j a_{ij} \qquad (4.9)$$

$$a_{ij} = \sqrt{a_i a_j}\left(1 - k_{ij}\right) \qquad (4.10)$$

$$b = \sum_i x_i b_i \qquad (4.11)$$

Results and discussion

Table 4.2 presents the solubility of carbon dioxide in several ionic liquids at two temperatures (313.2 K and 323.2 K) and at different pressures. As expected, solubility of CO_2 in ionic liquids was enhanced by pressure increase. For all systems studied the solubility was higher at lower temperature. No experimental data on the solubility of CO_2 in ionic liquids $[N_{4\ 1\ 1\ 1}][NTf_2]$ and $[N_{1\ 8\ 8\ 8}][NTf_2]$ have been reported in the temperature and pressure range of our work, and therefore no comparisons could be made. A graphical comparison of our solubility results with data published in literature for $[C_4mim][NTf_2]$, $[C_{10}mim][NTf_2]$, $[C_4mpyr][NTf_2]$, $[P_{6\ 6\ 6\ 14}][NTf_2]$, and $[P_{6\ 6\ 6\ 14}][Cl]$ is presented in figure 4.2. We have increased the pressure range of the data for most systems and the experimental data reported here is generally in good agreement with those available in the literature. For the system CO_2 + $[C_4mim][NTf_2]$ a very good agreement (average deviation of 1.4 %) is observed with the data published by Aki et al. [54] which are available only at 313 K. A good agreement is also obtained with the data reported by Carvalho et al. [43] in the lower pressure region while small deviations are noticed at the higher pressures.

Table 4.2 Experimental data on solubility of carbon dioxide in ionic liquids [a]

Ionic Liquid	T / K	p / MPa	x_{CO_2}	T / K	p / MPa	x_{CO_2}
[C$_4$mim][NTf$_2$]	313.2	8.08	0.698	323.2	8.22	0.673
		10.01	0.737		10.07	0.716
		14.95	0.770		15.06	0.757
		20.10	0.779		19.94	0.765
[C$_{10}$mim][NTf$_2$]	313.2	8.07	0.769	323.2	8.13	0.758
		10.07	0.826		10.10	0.790
		14.96	0.870		15.16	0.829
		20.13	0.878		20.15	0.849
[C$_4$mpyr][NTf$_2$]	313.2	8.06	0.666	323.2	9.01	0.650
		10.62	0.765		10.36	0.732
		15.51	0.819		15.14	0.795
		20.38	0.853		20.06	0.817
[N$_{4\,1\,1\,1}$][NTf$_2$]	313.2	8.58	0.769	323.2	9.18	0.744
		10.59	0.813		10.57	0.778
		15.26	0.871		15.35	0.828
		20.37	0.879		19.63	0.854
[N$_{1\,8\,8\,8}$][NTf$_2$]	313.2	8.09	0.825	323.2	8.08	0.789
		10.06	0.848		10.06	0.822
		15.24	0.906		15.19	0.864
		20.24	0.907		20.56	0.879
[P$_{6\,6\,6\,14}$][NTf$_2$]	313.2	8.09	0.815	323.2	8.83	0.761
		10.15	0.820		10.18	0.802
		15.23	0.845		15.34	0.829
		19.93	0.848		20.17	0.833
[P$_{6\,6\,6\,14}$][Cl]	313.2	8.21	0.767	323.2	8.80	0.714
		9.96	0.787		10.37	0.749
		14.99	0.808		14.35	0.784
		20.44	0.824		20.71	0.802

[a] Standard uncertainties u are u(T) = 0.1 K, u(p) = 0.07 MPa, u(x_{CO_2}) = 0.01.

The data reported by Shin et al. [42] show a deviation of 3.5 % and 4 % for the solubility at 313 K and 323 K, respectively. In the case of the solubility of CO_2 in [C$_{10}$mim][NTf$_2$] at 323.2 K, remarkable good agreement with the data reported by Ren et al. [44] , with a deviation less than 1 %. Unfortunately, solubility data at 313.2 K are not available for this system in the literature. Our data for the system CO_2 + [P$_{6\,6\,6\,14}$][NTf$_2$] are in a very good agreement with that reported by Carvalho et al. [25] at both temperatures: deviation of 0.3 % at 313.2 K and 1.3 % at 323.2 K. The solubility at approximately 10 MPa for both temperatures is in good agreement with the data published by Song et al. [26]. On the other hand, at lower pressure these data showed deviations in comparison with both our data and data reported by Carvalho et al. [25]. Somewhat higher discrepancies were noticed in the case of [P$_{6\,6\,6\,14}$][Cl] + CO_2 system between our and data by Carvalho et al. [25] at lower pressures, while at higher pressure good

agreement was observed. The solubilities for the system CO_2 + [C$_4$mpyr][NTf$_2$] at 8 MPa for both temperatures show relatively good agreement with the ones presented by Yim et al. [40]. However, much higher discrepancies were observed as pressure increases, approximately 15 %.
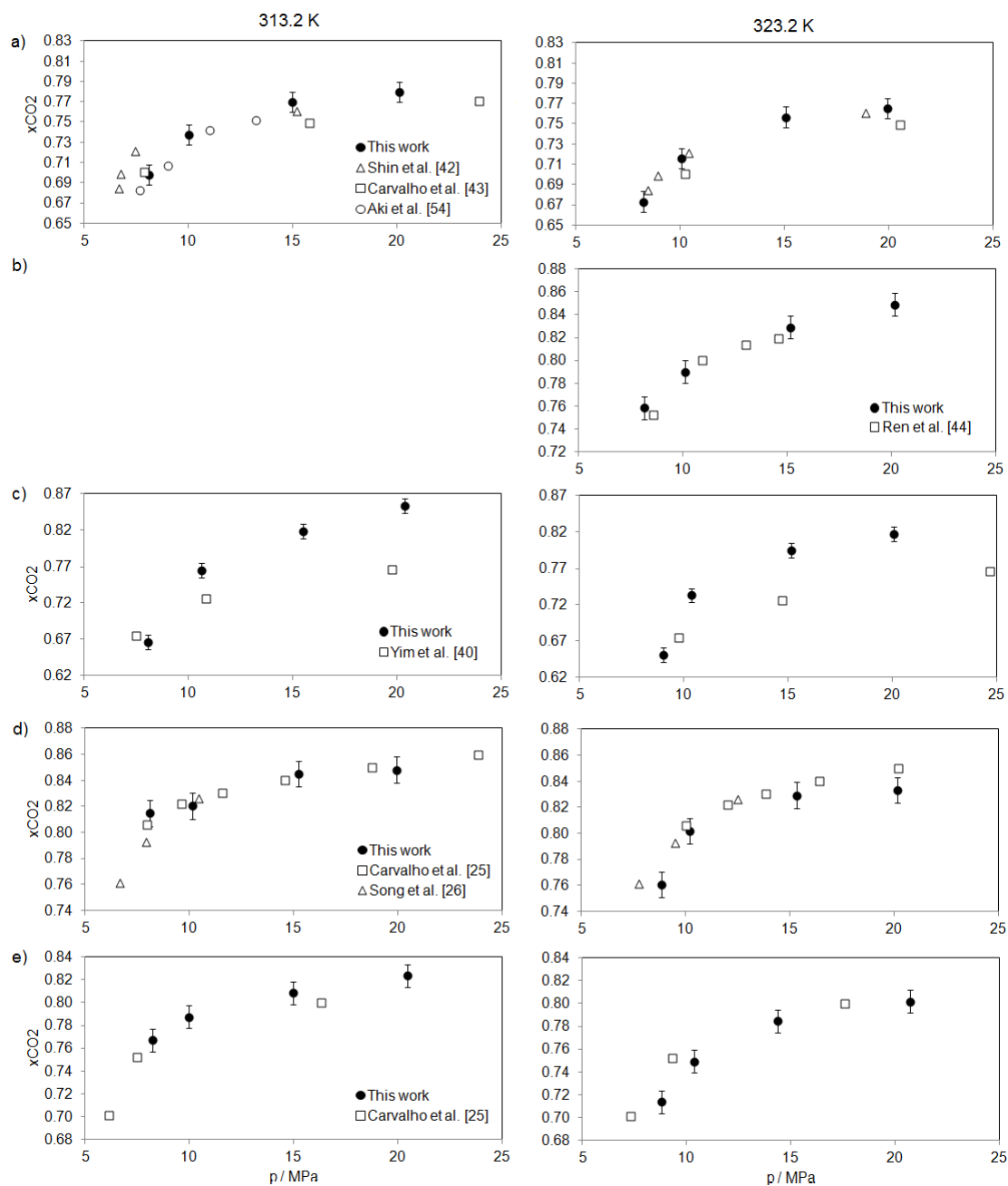
Figure 4.2 Data comparison of solubility of CO_2 in ionic liquids at 313.2 K and 323.2 K: a) [C$_4$mim][NTf$_2$], b) [C$_{10}$mim][NTf$_2$], c) [C$_4$mim][NTf$_2$], d) [P$_{6,6,6,14}$][NTf$_2$], and e) [P$_{6,6,6,14}$][Cl].
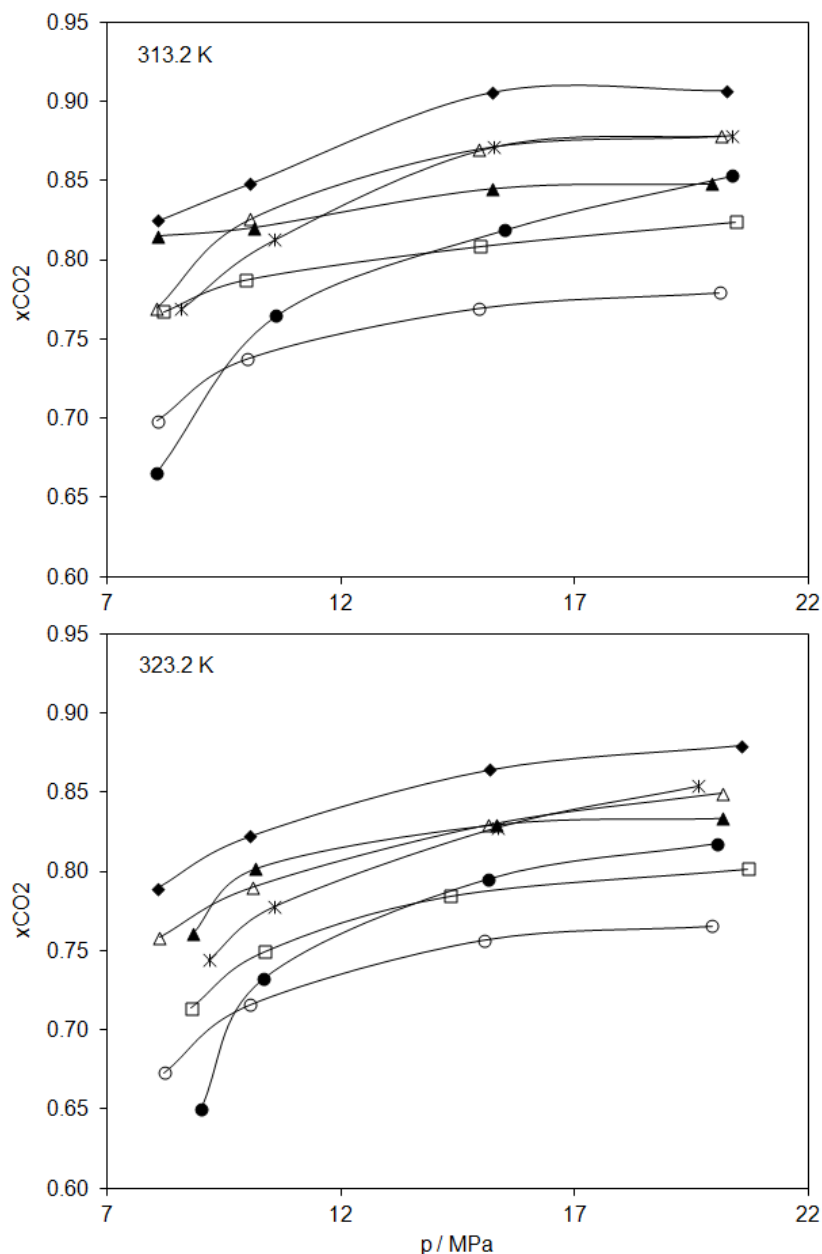
Figure 4.3 Composition-pressure diagrams for CO_2 + ionic liquids at 313.2 K (above) and at 323.2 K (below): [C_4mim][NTf_2] (empty circles), [C_{10}mim][NTf_2] (empty triangles), [Pyrr$_{4,1}$][NTf_2] (filled circles), [$N_{4,1,1,1}$][NTf_2] (asterisk), [$N_{1,8,8,8}$][NTf_2] (filled rhomboid), [$P_{6,6,6,14}$][NTf_2] (filled triangles) and [$P_{6,6,6,14}$][Cl] (empty squares).

Figure 4.3 presents the solubility data for all studied systems at 313.2 K (figure 4.3 a)) and at 323.2 K (figure 4.3 b)). The highest solubility of carbon dioxide was observed in [$N_{1\ 8\ 8\ 8}$][NTf_2]. This ionic liquid dissolves as much as 0.91 mole fraction of CO_2 at 20 MPa and 313.2 K. It is clear that the order of solubility of CO_2 in the various ionic liquids do not varies with both pressure and temperature changes. Even though solubility curves for different ionic liquids cross each other, it can be noted that they have similar shape for alike cations. Thus, solubility

curves for $[C_4mim][NTf_2]$ and $[C_{10}mim][NTf_2]$ are quasi-parallel for both temperatures. The same is valid for $[P_{6\,6\,6\,14}][NTf_2]$ and $[P_{6\,6\,6\,14}][Cl]$, as well as for $[N_{4\,1\,1\,1}][NTf_2]$ and $[N_{1\,8\,8\,8}][NTf_2]$.

At the highest pressure, the solubility of CO_2 in the studied ionic liquids at 313.2 K increases in the following order: $[C_4mim][NTf_2]$ < $[P_{6\,6\,6\,14}][Cl]$ < $[P_{6\,6\,6\,14}][NTf_2]$ ~ $[C_4mpyr][NTf_2]$ < $[C_{10}mim][NTf_2]$ ~ $[N_{4\,1\,1\,1}][NTf_2]$ < $[N_{1\,8\,8\,8}][NTf_2]$. On the other hand, at 323.2 K the order of increasing CO_2 solubility changed to: $[C_4mim][NTf_2]$ < $[P_{6\,6\,6\,14}][Cl]$ < $[C_4mpyr][NTf_2]$ ~ $[P_{6\,6\,6\,14}][NTf_2]$ < $[C_{10}mim][NTf_2]$ ~ $[N_{4\,1\,1\,1}][NTf_2]$ < $[N_{1\,8\,8\,8}][NTf_2]$.

In general, the CO_2 solubility increases with an increase in the alkyl chain length of cation [54], which is already well known for imidazolium ionic liquids. Our results allow verifying the alkyl chain length influence of ammonium based ionic liquids. For instance, at an average pressure of 20.3 MPa, the solubility increased from 0.88 mole fraction for $[N_{4\,1\,1\,1}][NTf_2]$ to 0.91 mole for $[N_{1\,8\,8\,8}][NTf_2]$, verifying the same trend as shown for imidazolium ionic liquid.

For modelling, the critical properties, as well as the vapour pressures and liquid densities of CO_2 were obtained from the DIPPR database [55]. The critical temperatures for imidazolium based ILs were taken from Rebelo's work with the Eötvos equation [56], while for the other ILs they were predicted from the available surface tension and liquid density data, using the same methodology. The critical pressures and the acentric factors were obtained from Valderrama et al. [57]. All these values are presented in table 4.3 and were used for the PR and SRK calculations. Additionally, the critical temperatures were also used in the CPA EoS. It shall be noted here that as ionic liquids are very low volatile species, their critical properties cannot be accurately determined, and so there is an additional source of uncertainty for any thermodynamic model requiring such data.

Table 4.3 Critical properties of CO_2 and ionic liquids

Compound	T_c / K	p_c / MPa	ω
CO_2	304.2[a]	7.380[a]	0.2236[a]
$[C_4mim][NTf_2]$	1077.0[c]	2.765[b]	0.3004[b]
$[C_{10}mim][NTf_2]$	800.0[c]	1.867[b]	0.5741[b]
$[C_4mpyr][NTf_2]$	1093.1[b]	2.425[b]	0.3467[b]
$[N_{4\,1\,1\,1}][NTf_2]$	1079.6[d]	2.588[b]	0.3334[b]
$[N_{1\,8\,8\,8}][NTf_2]$	750.6[d]	1.064[b]	0.9962[b]
$[P_{6\,6\,6\,14}][NTf_2]$	805.5[d]	0.795[b]	0.7947[b]
$[P_{6\,6\,6\,14}][Cl]$	803.9[d]	0.851[b]	0.8915[b]

[a] DIPPR database [55]

[b] Valderrama et al. [57]

[c] Rebelo et al. [56]

[d] predicted by Eötvos equation using experimental data for the surface tension (γ) and molar volume (V_m) [15].

Table 4.4 Ionic liquid vapour pressure and liquid density data from the literature

ILs	p / Pa	T_{range} / K	Refs.	ρ^{liq} / gcm^{-3}	T_{range} / K	Refs.
[C$_4$mim][NTf$_2$]	0.0062-0.1091	437.8-484.2	[58]	1.4422-1.3285	293.5-414.9	[59]
	0.0122-0.4660	457.7-517.4	[60]	1.4561-1.4079	278.2-328.2	[61]
				1.4606-1.3756	273.2-363.2	[62]
				1.4370-1.4083	298.2-328.2	[63]
[C$_{10}$mim][NTf$_2$]	-			1.2824-1.1918	293.2-393.2	[64]
[C$_4$mpyr][NTf$_2$]	-			1.4123-1.3554	278.2-343.2	[65]
				1.3980-1.2939	293.5-414.9	[66]
				1.3940-1.3660	298.2-348.2	[67]
				1.4091-1.3152	293.2-393.2	[68]
[N$_{4\,1\,1\,1}$][NTf$_2$]	-			1.3963-1.2886	293.5-414.9	[67]
				1.4123-1.3673	278.2-328.2	[62]
				1.3747-1.3439	293.2-333.2	[20]
[N$_{1\,8\,8\,8}$][NTf$_2$]	-			1.1198-1.0821	278.2-328.2	[62]
				1.0823-1.0611	293.2-333.2	[19]
[P$_{6\,6\,6\,14}$][NTf$_2$]	-			1.0501-1.0296	293.2-333.2	[19]
				1.0666-1.0412	298.2-333.4	[19]
[P$_{6\,6\,6\,14}$][Cl]	-			0.8826-0.8644	293.2-333.2	[19]
				0.8916-0.8709	298.1 -333.1	[69]

To obtain the CPA pure component parameters, liquid density data for the ionic liquids were obtained from the literature, as well as vapour pressure data for $[C_4mim][NTf_2]$ (table 4.4). For the other studied ILs no vapour pressure data were found in the literature. The available data were correlated as a function of temperature to generate estimates of both liquid densities and vapour pressures at the same temperatures using the following equations:

$$d = \frac{A}{B^{\left(1+\left(1-\frac{T}{C}\right)\right)^D}}$$
(4.12)

$$\ln(p) = A + \frac{B}{T+C}$$
(4.13)

In the case of vapour pressures, as mentioned before, a weighting factor was used in the objective function to be minimized (eq. 4.8) to provide a qualitative description of ionic liquid vapour pressures. For ionic liquids with no measured vapour pressure, it was assumed that in the reduced temperature range between 0.40 and 0.60 used to estimate the parameters, the vapour pressures could be described by the following equation where the *A* and *B* parameters were regressed considering a vapour pressure of 10^{-6} Pa at 273.15 K and the critical pressure given at table 4.3:

$$\ln P = A - \frac{B}{T}$$
(4.14)

These vapour pressure equations are expectedly unreliable, but they were used to generate vapour pressure data for our qualitative fitting of the CPA EoS parameters for ionic liquids. Other authors have fitted parameters for other EoS solely to liquid densities, but in that case one may obtain higher vapour pressures for pure ionic liquids that those resulting from our approach. Additionally to the modelling results using SRK and PR, different association schemes proposed in the literature [53] were tested in order to achieve the best description of the experimental data using the CPA EoS. In this work we have considered one site (1A), two-site (2B) and four associating sites (4C) in the ionic liquids and we considered CO_2 as a non-associating component.

Initially, the estimation of the pure compound parameters was performed by a simultaneous regression of vapour pressure and liquid density data, considering CO_2 and ionic liquids as non-associating compounds. Thus, only a_0, c_1 and b were estimated and their values are given in tables 4.5 and 4.6, where we also compare the density estimates obtained with SRK and PR.

The global average deviations (AAD) were calculated by the following equation, where X can be the vapour pressure, the liquid density or the CO_2 solubility as will be used later:

$$AAD = \frac{1}{NP}\sum_{i=1}^{NP} ABS\left[\frac{X_{calc,i}-X_{exp,i}}{X_{exp,i}}\right] * 100$$
(4.15)

where *NP* is number of experimental data points.

Table 4.5 Non-associating CPA EoS (SRK cubic term) IL pure compound parameters and comparison of the modelling results for pure ILs with the SRK EoS

Compound	a_0	c_1	$b \cdot 10^4$	AAD			
				CPA (SRK)		SRK	
	$(Pa\ m^6\ mol^{-2})$		$(m^3\ mol^{-1})$	P^σ	$\rho^{liq.}$	P^σ	$\rho^{liq.}$
[C$_4$mim][NTf$_2$]	27.850	0.622	3.220	3.22	2.02	[b]	6.67
[C$_{10}$mim][NTf$_2$]	19.100	1.206	3.914	-	1.17	[b]	21.5
[C$_4$mpyr][NTf$_2$]	18.120	0.840	3.197	-	1.29	[b]	4.13
[N$_{4\,1\,1\,1}$][NTf$_2$]	16.920	0.860	3.012	-	1.32	[b]	2.72
[N$_{1\,8\,8\,8}$][NTf$_2$]	28.220	1.228	5.786	-	0.98	[b]	11.4
[P$_{6\,6\,6\,14}$][NTf$_2$]	35.960	1.111	7.141	-	1.04	[b]	4.58
[P$_{6\,6\,6\,14}$][Cl]	29.910	1.080	5.798	-	1.01	[b]	16.5
Global AAD				[a]	1.26		9.64

[a] the deviation to the control vapour pressure data generated from eq. 4.15 did not exceed 3.2 %.

[b] deviation higher than 100 %.

Table 4.6 Non-associating CPA EoS (PR cubic term) pure compound parameters and comparison of the modelling results for pure ILs with the PR EoS

Compound	a_0	c_1	$b \cdot 10^4$	AAD			
				CPA (PR)		PR	
	$(Pa\ m^6\ mol^{-2})$		$(m^3\ mol^{-1})$	P^σ	$\rho^{liq.}$	P^σ	$\rho^{liq.}$
[C$_4$mim][NTf$_2$]	31.457	0.613	3.240	3.62	2.07	[b]	20.1
[C$_{10}$mim][NTf$_2$]	21.721	1.187	3.942	-	1.24	[b]	11.0
[C$_4$mpyr][NTf$_2$]	20.637	0.822	3.224	-	1.35	[b]	36.5
[N$_{4\,1\,1\,1}$][NTf$_2$]	19.290	0.840	3.038	-	1.38	[b]	9.50
[N$_{1\,8\,8\,8}$][NTf$_2$]	31.998	1.210	5.824	-	1.04	[b]	24.7
[P$_{6\,6\,6\,14}$][NTf$_2$]	40.822	1.092	7.192	-	1.11	[b]	6.99
[P$_{6\,6\,6\,14}$][Cl]	33.944	1.062	5.839	-	1.07	[b]	6.47
Global AAD				[a]	1.32		16.5

[a] the deviation to the control vapour pressure data generated from eq. 4.15 did not exceed 3.6 %.

[b] deviation higher than 100 %.

As can be observed, the flexibility given by fitting the EoS parameters to liquid densities provides much better density estimates as those obtained from cubic equations of state using critical properties. Additionally, as critical properties for ionic liquids cannot be experimentally determined, this approach, based on the fitting pure component data provides a more reasonable and accurate approach for modelling IL systems. Also, while using the CPA EoS in the non-associating version, there seems to be no advantage in using the PR term instead of the more simpler SRK term. For this reason we have adopted the SRK cubic term in CPA for the following results.

Table 4.7 Associating 1A CPA EoS (SRK cubic term) pure compound parameters for ILs

Compound	a_0 (Pa m^6 mol^{-2})	c_1	$b \cdot 10^4$ (m^3 mol^{-1})	$\varepsilon \cdot 10^{-4}$ (J.mol^{-1})	$\beta \cdot 10^4$	AAD P^σ	AAD $\rho^{liq.}$
[C$_4$mim][NTf$_2$]	27.784	0.623	3.220	0.854	62.66	3.636	2.02
[C$_{10}$mim][NTf$_2$]	19.310	1.186	3.920	1.526	1.693	-	1.17
[C$_4$mpyr][NTf$_2$]	18.165	0.834	3.197	1.795	1.005	-	1.29
[N$_{4\,1\,1\,1}$][NTf$_2$]	17.067	0.841	3.013	2.272	1.000	-	1.33
[N$_{1\,8\,8\,8}$][NTf$_2$]	27.685	1.258	5.746	0.392	3.109	-	1.12
[P$_{6\,6\,6\,14}$][NTf$_2$]	35.901	1.112	7.132	0.025	6.686	-	1.05
[P$_{6\,6\,6\,14}$][Cl]	29.512	1.111	5.800	0.467	3.060	-	0.99
Global AAD						a	1.28

[a] the deviation to the control vapour pressure data generated from eq. 4.15 did not exceed 3.6 %.

Table 4.8 Associating 2B CPA EoS (SRK cubic term) pure compound parameters for ILs

Compound	a_0 (Pa m^6 mol^{-2})	c_1	$b \cdot 10^4$ (m^3 mol^{-1})	$\varepsilon \cdot 10^{-4}$ (J.mol^{-1})	$\beta \cdot 10^4$	AAD P^σ	AAD $\rho^{liq.}$
[C$_4$mim][NTf$_2$]	27.859	0.616	3.220	1.199	0.193	3.66	2.02
[C$_{10}$mim][NTf$_2$]	18.817	1.176	3.903	1.275	1.000	-	1.25
[C$_4$mpyr][NTf$_2$]	18.119	0.840	3.197	0.530	0.028	-	1.29
[N$_{4\,1\,1\,1}$][NTf$_2$]	17.187	0.831	3.017	0.020	0.861	-	1.34
[N$_{1\,8\,8\,8}$][NTf$_2$]	27.937	1.172	5.752	1.251	1.000	-	1.17
[P$_{6\,6\,6\,14}$][NTf$_2$]	35.139	1.086	7.110	1.322	1.000	-	1.18
[P$_{6\,6\,6\,14}$][Cl]	28.899	1.081	5.760	1.294	1.000	-	1.22
Global AAD						a	1.4

[a] the deviation to the control vapour pressure data generated from eq. 4.15 did not exceed 3.7 %.

Table 4.9 Associating 4C CPA EoS (SRK cubic term) pure compound parameters for ILs

Compound	a_0 (Pa m^6 mol^{-2})	c_1	$b \cdot 10^4$ (m^3 mol^{-1})	$\varepsilon \cdot 10^{-4}$ (J mol^{-1})	$\beta \cdot 10^4$	AAD P^σ	AAD $\rho^{liq.}$
[C$_4$mim][NTf$_2$]	27.809	0.595	3.224	1.067	0.491	3.83	2.03
[C$_{10}$mim][NTf$_2$]	19.484	1.113	3.923	1.187	0.227	-	1.19
[C$_4$mpyr][NTf$_2$]	18.103	0.841	3.197	0.101	0.494	-	1.29
[N$_{4\,1\,1\,1}$][NTf$_2$]	16.957	0.855	3.012	0.934	0.010	-	1.33
[N$_{1\,8\,8\,8}$][NTf$_2$]	28.590	1.094	5.800	1.187	0.461	-	1.03
[P$_{6\,6\,6\,14}$][NTf$_2$]	36.380	1.024	7.159	1.107	0.364	-	1.07
[P$_{6\,6\,6\,14}$][Cl]	29.803	0.897	5.823	1.314	0.928	-	1.10
Global AAD						a	1.29

[a] the deviation to the control vapour pressure data generated from eq. 4.15 did not exceed 3.8 %.

When using association in the CPA EoS, the cubic term parameters and deviations with respect to density are very similar either between the different association schemes (1A, 2B and 4C)

(see tables 4.7, 4.8 and 4.9) and also with the parameters from the non-associating version of CPA. Additionally, the association energy, a measure of the association strength, is typically smaller than that found for alcohols [70] or acids [71], thus it can be concluded that for pure component properties there is no clear advantage in using any of the investigated association schemes for ionic liquids.

Table 4.10 CO_2 solubility data used in modelling work

IL	T / K	P_{range} / MPa	Refs.
[C$_4$mim][NTf$_2$]	313	8.08 - 20.10	a
	323	8.22 - 19.94	
	314	1.29 - 28.07	[42]
	324	1.55 - 33.35	
	313	1.05 - 44.74	[43]
	323	1.30 - 49.99	
	313	1.61 - 13.24	[54]
	313	0.42 - 5.48	[69]
	323	0.49 - 6.59	
	314	0.87 - 18.95	[72]
	324	1.01 - 23.71	
[C$_{10}$mim][NTf$_2$]	313	8.07 - 20.13	a
	323	8.13 - 20.15	
	323	1.44 - 14.59	[44]
[C$_4$mpyr][NTf$_2$]	313	8.06 - 20.38	a
	323	9.01 - 20.06	
	313	0.99 - 39.34	[40]
	323	1.23 - 44.54	
[N$_{4\,1\,1\,1}$][NTf$_2$]	313	8.58 - 20.37	a
	323	9.18 - 19.63	
	338	0.10 - 8.09	[34]
[N$_{1\,8\,8\,8}$][NTf$_2$]	313	8.09 - 20.24	a
	323	8.08 - 20.56	
[P$_{6\,6\,6\,14}$][NTf2]	313	8.09 - 19.93	a
	323	8.83 - 20.17	
	313	0.36 - 39.54	[25]
	323	0.47 - 36.28	
	313	0.72 - 10.45	[26]
	323	0.79 - 12.47	
[P$_{6\,6\,6\,14}$][Cl]	313	8.21 - 20.44	a
	323	8.80 - 20.71	
	313	0.17 - 16.31	[25]
	323	0.27 - 17.59	

[a] this study

Correlation of the CO_2 solubilities in ionic liquids was carried out using the estimated pure component parameters and the different EoS first, without k_{ij} binary interaction parameters (prediction) and latter using a single, temperature independent k_{ij} (correlation).

The data used to check the accuracy of the different equations of state included those presented in this work, as well as other collected from the literature for a broad pressure range (table 4.10).

Indeed, the modelling of higher pressure solubilities (above the CO_2 critical pressure and up to 447 bar) is a stringent test for any thermodynamic model, as the high pressure region of these solubilities is almost flat in a long pressure range.

To regress the k_{ij} values we have employed equation 4.8 where for x we used the CO_2 solubility in the ionic liquid.
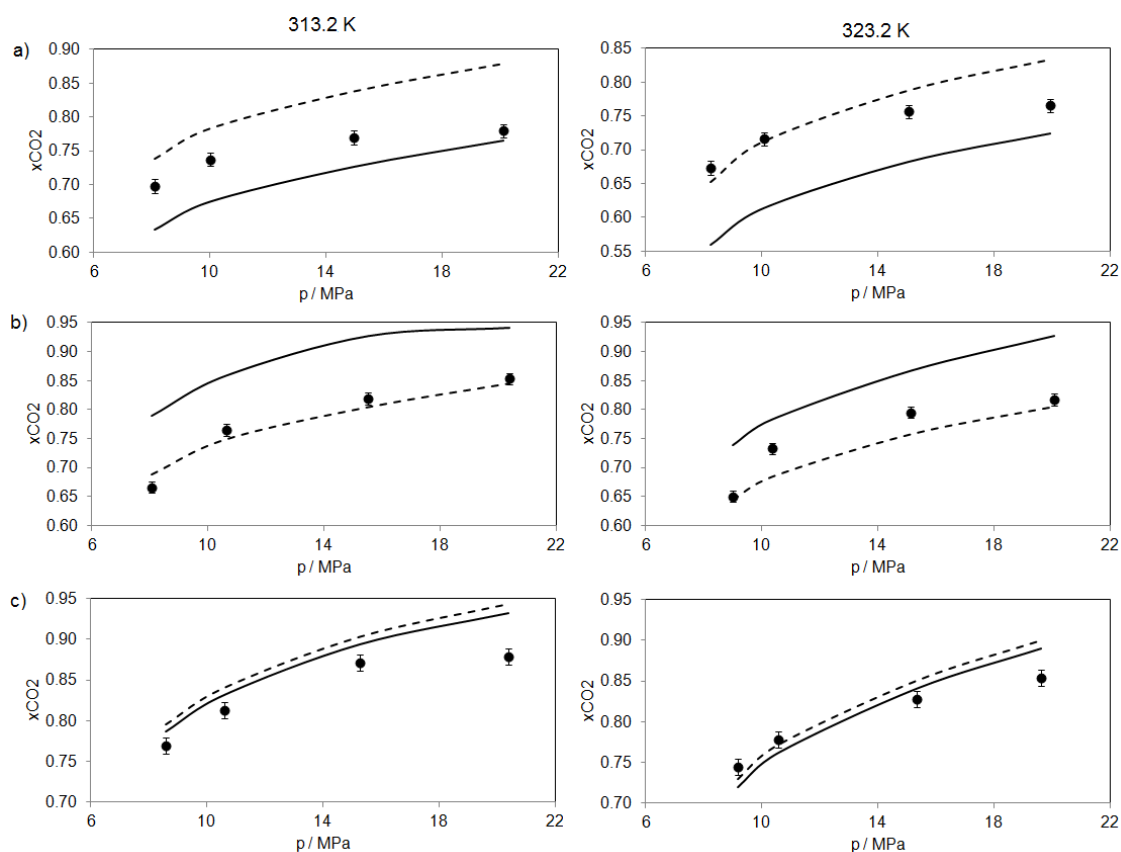
Figure 4.4 Solubilities of CO_2 in: a) [C$_4$mim][NTf$_2$], b) [C$_4$mpyr][NTf$_2$] and c) [N$_{4\,1\,1\,1}$][NTf$_2$] at 313.2 K and 323.2 K. Filled circles stand for experimental solubilities, straight line stands for solubilities predicted (k_{ij} = 0) by CPA EoS with no association included and dashed line stands for solubilities correlated (k_{ij} ≠ 0) by CPA EoS with no association included.

Table 4.11 AAD when k_{ij} is equal to zero (prediction) and binary interaction parameters and AAD when using a fitted k_{ij} (correlation). AAD stands for global average deviation of the mole fraction solubility of CO_2 in ionic liquids, between experimental and modelling results.

		[C$_4$mim][NTf$_2$]	[C$_{10}$mim][NTf$_2$]	[C$_4$mpyr][NTf$_2$]	[N$_{4\,1\,1\,1}$][NTf$_2$]	[N$_{1\,8\,8\,8}$][NTf$_2$]	[P$_{6\,6\,6\,14}$][NTf$_2$]	[P$_{6\,6\,6\,14}$][Cl]
		k_{ij} is equal to zero (prediction)						
PR		13.80	11.84	16.91	6.93	7.58	17.85	25.39
SRK		13.92	12.19	17.03	6.74	a	a	a
CPA(0)	AAD / %	22.83	11.53	14.64	5.53	a	a	a
CPA(1A)		23.02	11.53	14.61	5.87	a	a	a
CPA(2B)		24.31	11.40	14.64	5.41	6.77	17.88	25.20
CPA(4C)		28.83	11.68	14.63	5.63	6.05	18.25	25.53
		fitted k_{ij} (correlation)						
PR	k_{ij}	0.0493	0.0056	0.00526	-0.0006	-0.0008	-0.0032	0.0912
	AAD / %	19.76	11.86	13.54	7.09	7.60	17.60	24.90
SRK	k_{ij}	0.0512	0.0625	0.0568	-0.0018	0.0147	0.0488	0.1111
	AAD / %	20.12	13.84	13.90	7.20	7.39	19.82	24.77
CPA(0)	k_{ij}	-0.03	-0.0001	0.0316	0.0031	0.0041	0.0332	0.0002
	AAD / %	13.66	11.53	13.50	5.11	4.33	19.57	26.37

[a] two-phase equilibria could not be obtained at pressures higher than 9 MPa.

The global average deviations (AAD) between the experimental data and the modelling results are presented for both, k_{ij} equal to zero and adjusted k_{ij} in table 4.11. For all studied systems AAD is lower than 25 %. For the studied IL systems it was found that the use of a fitted k_{ij} value is not so important for describing quantitatively the solubilities, as can be observed from table 4.11, but can make a significant difference to obtain two-phase equilibria at the highest pressures. For some systems $[N_{1\ 8\ 8\ 8}][NTf_2]$-CO_2, $[P_{6\ 6\ 6\ 14}][NTf_2]$-CO_2 and $[P_{6\ 6\ 6\ 14}][Cl]$-CO_2 the use of a fitted k_{ij} is fundamental to extend the two-phase equilibria up to the higher pressure limits, and it was not possible to obtain prediction. For other studied systems ($[C_4mim][NTf_2]$-CO_2, $[C_4mpyr][NTf_2]$-CO_2 and $[N_{4\ 1\ 1\ 1}][NTf_2]$-CO_2), both prediction and correlation were performed as presented in figure 4.4.

In the case of correlation (with fitted k_{ij}), the CPA is better than SRK for all IL-CO_2 studied systems. The SRK gave better results than the CPA for $[C_4mim][NTf_2]$-CO_2 system when k_{ij} equals to zero (prediction). Generaly, phase equilibria is described better by SRK when pressure is lower than critical. In the case of $[C_4mim][NTf_2]$ exist almost 90 experimental solubility results (which is not case for the other ILs) and therefore the final AAD for SRK become lower than one obtained for CPA.

4.2 Trihexyl(tetradecyl)phosphonium bromide: Liquid density, surface tension and solubility of carbon dioxide

Experimental procedure

Density was measured using an Anton Paar vibrating tube densimeter (model DMA 4500M) in the temperature range between 293.2 K and 343.2 K, operating at atmospheric pressure. The apparatus was calibrated by measuring the density of atmospheric air and bi-distillate water at only one temperature, according to the manual instruction. The oscillating U-tube sensor was filled very carefully with 1 mL of the ionic liquid in order to avoid forming of the air bubbles inside the tube. It was excited electronically and kept oscillating continuously at the characteristic frequency which is inversely proportional to the density. The density was determined with corrected viscosity influence and extreme accuracy. The accuracy and reproducibility in the experimental measurements were $5 \cdot 10^{-5}$ g·cm^{-3} and $1 \cdot 10^{-5}$ g·cm^{-3} for density and 0.03 K and 0.01 K for temperature.

Surface tension was measured using a drop shape analysis technique (Data physics, Contact Angle System OCA) operating in the pendent drop mode in the temperature range between 293.2 K and 343.2 K. The temperature control chamber provided an insignificant deviation in temperature (± 0.1 K). The apparatus was calibrated in the temperature range of interest, using few solvents of known surface tension values (water and n-hexane). The dosing system in combination with an electronic syringe unit allows the comfortable and reproducible dosing of

liquids. Each drop was left to equilibrate close to the rapture point when several pictures of the drop were taken and surface tension was recorded. Ten consecutive measurements of surface tension were performed at each temperature and the average values were taken into account. The reproducibility was ± 0.02 mNm^{-1}.

Modelling

The Peng-Robinson equation of state (PR EoS) [73], which was selected to predict and correlate the phase equilibria data, is given by:

$$P = \frac{RT}{V-b} - \frac{a(T)}{V(V+b)+b(V-b)} \qquad (4.16)$$

where P is the pressure, T is the temperature, V is the molar volume, R is the universal gas constant, a is the energy parameter and b is the co-volume parameter.

When the equation of state is applied to mixtures, the energy and co-volume parameters are usually calculated using van der Waals one-fluid mixing rules. A single adjustable binary interaction parameter for the cross-energy term (k_{ij}) is the only parameter regressed from mixture data:

$$a = \sum_i \sum_j x_i x_j a_{ij} \qquad (4.17)$$

$$a_{ij} = \sqrt{a_i a_j}\left(1 - k_{ij}\right) \qquad (4.18)$$

$$b = \sum_i x_i b_i \qquad (4.19)$$

when:

$$a_i = \frac{0.45724R^2 T_{ci}^2}{P_{ci}}\left[1 + \left(0.37464 + 1.54226\omega_i - 0.26992\omega_i^2\right)\left(1 - \sqrt{\frac{T}{T_{ci}}}\right)\right]^2 \qquad (4.20)$$

$$b_i = \frac{0.07780RT_{ci}}{P_{ci}} \qquad (4.21)$$

where a_i and b_i are the pure component parameters.

Results and discussion

Table 4.12 presents the solubility of carbon dioxide in trihexyl(tetradecyl)phophonium bromide ([P$_{6\ 6\ 6\ 14}$][Br]) at two temperatures (313.2 K and 323.2 K) and at different pressures. The solubility of CO_2 in ionic liquid was enhanced by increasing the pressure and decreasing the temperature. There are no published data on solubility of CO_2 in [P$_{6\ 6\ 14}$][Br] in the temperature and pressure range studied in our work, and therefore no comparisons could be made. The

solubility of carbon dioxide in $[P_{6\,6\,6\,14}][Br]$ was compared with CO_2 solubility in ($[P_{6\,6\,6\,14}][Cl]$ and $[P_{6\,6\,6\,14}][NTf_2]$), giving an opportunity to discuss the influence of the anion on solubility as presented in figure 4.5. The CO_2 solubility in ionic liquids containing $[Br]^-$ or $[Cl]^-$ anion are quite similar, although the solubility of CO_2 in $[P_{6\,6\,6\,14}][Cl]$seems to be slightly higher. The highest solubility of carbon dioxide was observed in $[P_{6\,6\,6\,14}][NTf_2]$. This ionic liquid dissolves as much as 0.8450 mole fraction of CO_2 at 152.3 bar and at 313.2 K. The substitution of halogen anion by $[NTf_2]^-$ increases CO_2 solubility for approximately 0.035 mole fraction. This may be due to favourable interactions between CO_2 and the fluoroalkyl substituents on the anion, as already discussed in literature [34]. It is clear that the order of CO_2 solubility in various ionic liquids show similar trends with respect to CO_2 solubility, indicating that the enthalpies and entropies of dissolution are quite similar for the different ionic liquids.

Table 4.12 Experimental data on solubility of carbon dioxide in $[P_{6\,6\,6\,14}][Br]$ [a]

p / MPa	x_{CO2}	p / MPa	x_{CO2}
313.2 K		323.2 K	
8.16	0.762	8.83	0.717
10.54	0.788	10.40	0.741
15.04	0.812	14.94	0.786
20.87	0.818	21.23	0.790

[a] Standard uncertainties u are $u(T)$ = 0.1 K, $u(p)$ = 0.07 MPa, $u(x_{CO2})$ = 0.010.

The density of $[P_{6\,6\,6\,14}][Br]$ was determined as a function of temperature (293.2 K to 343.2 K) at atmospheric pressure. Experimental data are given in table 4.13 along with data predicted by Gardas and Coutinho model [50]:

$$\rho = \frac{Mw}{N_A V(a + bT + cp)} \tag{4.22}$$

where ρ, Mw, N_A, V, T and p are the density in $kg \cdot m^{-3}$, ionic liquid molecular weight in $kg \cdot mol^{-1}$, Avogadro constant, ionic liquid volume in m^3, temperature in K and pressure in MPa, respectively. The values of coefficients a, b and c, adopted from Gardas and Coutinho work [50] are 0.8005 ± 0.0002, (6.652 ± 0.007)$\cdot 10^{-4}$ K^{-1} and (-5.919 ± 0.024)$\cdot 10^{-4}$ MPa^{-1} respectively. The ionic liquid volume (1011 $Å^3$) was calculated using the volume parameters of groups and fragments proposed by Ye and Shreeve [74]. The typical average error in the estimated volume of a cation and anion is 10-20 $Å^3$, which explains the systematic deviation between the experimental and the modelling results of the density data. The calculated densities are lower than the experimental values achieved in this work showing absolute average deviation (AAD) of 3.3 %.
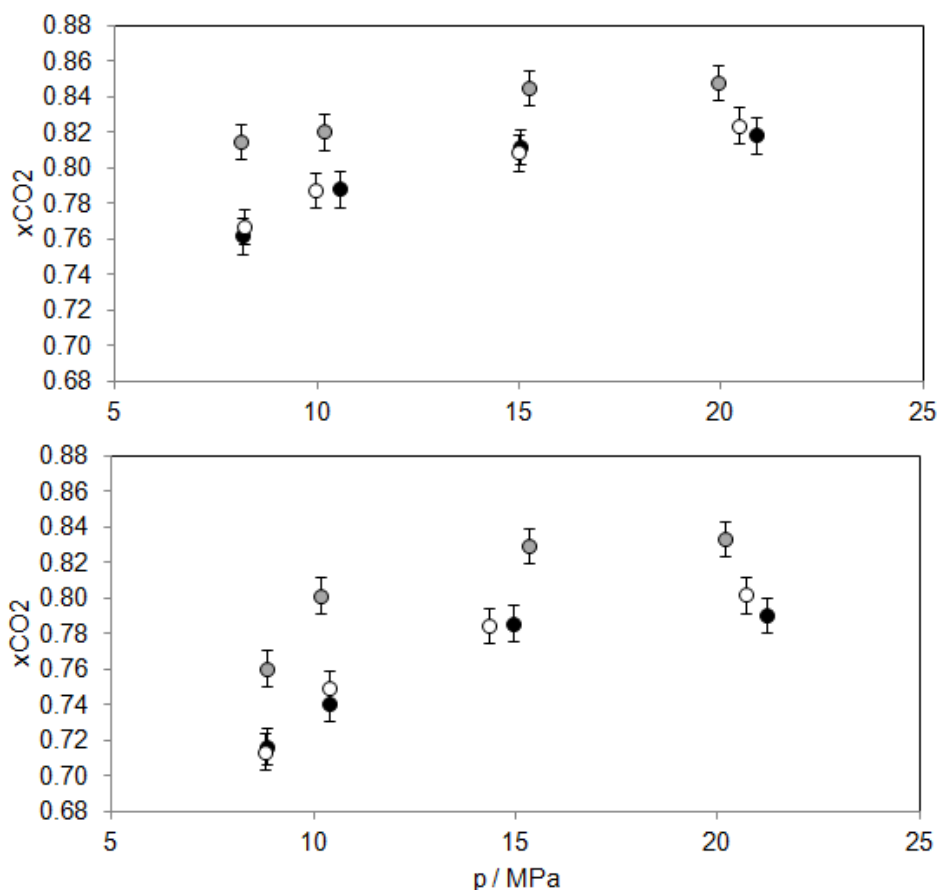
Figure 4.5 Solubility of CO_2 in phosphonium based ionic liquids at 313.2 K (above) and at 323.2 K (below): $[P_{6\,6\,6\,14}][Br]$ (filled circles), $[P_{6\,6\,6\,14}][Cl]$ (empty circles) and $[P_{6\,6\,6\,14}][NTf_2]$ (grey-filled circles).

The densities are plotted as a function of temperature at isobaric conditions as represented in figure 4.6. The experimental density data reported in this work demonstrate AAD up to 0.55 % when compared to the literature data [22, 49]. These small deviations might be outcome of diverse experimental setup used by researchers, as well as a different purity of the samples and water content in ionic liquid.

The experimental surface tension data of $[P_{6\,6\,6\,14}][Br]$ are presented in table 4.14, along with their standard deviations. As expected, surface tension decreases with increasing temperature in the observed temperature range. There are no experimental data on surface tension of $([P_{6\,6\,6\,14}][Br]$ reported in the literature to compare with. Data on surface tension available in the IL Thermo database [15] are mostly related with imidazolium, pyridinium and pyrrolidinium based ionic liquids, while only few data are available for phosphonium based ionic liquids. Kilaru et al. [20] have measured surface tension of ionic liquids based on various cations.

Table 4.13 Experimental and predicted (Gardas and Coutinho model [50]) densities of [P$_{6\,6\,6\,14}$][Br] as a function of temperature at atmospheric pressure [a]

T / K	$\rho^{\,exp}$ / g.cm^{-3}	$\rho^{\,calc}$ / g.cm^{-3}	$(|\rho^{\,calc}-\rho^{\,exp}|/\rho^{\,exp})\cdot 100$ / %
293.15	0.9617	0.9302	3.28
297.15	0.9592	0.9277	3.28
298.15	0.9586	0.9271	3.29
301.15	0.9567	0.9253	3.29
303.15	0.9555	0.9240	3.30
305.15	0.9543	0.9228	3.30
308.15	0.9524	0.9210	3.30
309.15	0.9518	0.9204	3.30
313.15	0.9493	0.9179	3.31
317.15	0.9469	0.9155	3.31
318.15	0.9462	0.9149	3.31
321.15	0.9444	0.9131	3.31
323.15	0.9431	0.9119	3.31
325.15	0.9419	0.9107	3.31
328.15	0.9401	0.9089	3.31
329.15	0.9394	0.9083	3.31
333.15	0.9370	0.9060	3.31
337.15	0.9346	0.9036	3.31
338.15	0.9340	0.9030	3.31
341.15	0.9321	0.9013	3.31
343.15	0.9309	0.9001	3.31
345.15	0.9297	0.8990	3.30
AAD / %			3.30

It has been shown that surface tension decreases with increasing alkyl part in either the cation or anion of ionic liquid. Thus, the long alkyl chains in the cation of [P$_{6\,6\,6\,14}$][Br] lead to the low value of surface tension (29.3 mNm^{-1} at 298.15 K and the atmospheric pressure) due to the fact that the bulky alkyl part is orientated to the surface keeping the charged parts inside the massive phase. Figure 4.7 presents surface tension as a function of temperature. The experimental data were fitted by quantitative structure-property relationship (QSPR) correlation [75] which gave AAD of approximately 28 %.

To calculate the parameters of PR EoS, critical temperatures (Tc), critical pressures (Pc) and acentric factors (ω) of both, carbon dioxide and ionic liquids were required.
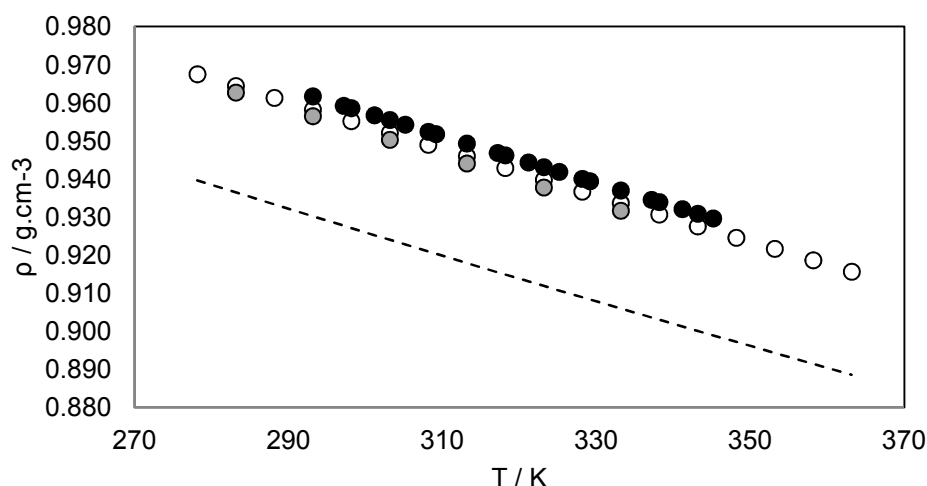
Figure 4.6 Liquid density of [P$_{6 6 6 14}$][Br] as a function of temperature, at atmospheric pressure: the experimental densities achieved in this work (filled circles), the experimental densities presented by Neves et al. [49] (empty circles), the experimental densities presented by Tomé et al. [22] (grey-field circles) and the densities predicted by Gardas and Coutinho model (table 4.13) (dashed line).

Table 4.14 Experimental surface tension, γ, of [P$_{6 6 6 14}$][Br] as a function of temperature at atmospheric pressure [a]

T / K	γ / mN.m^{-1}
293.15	29.97 ± 0.04
298.15	29.32 ± 0.02
303.15	28.94 ± 0.01
308.15	28.53 ± 0.01
313.15	28.15 ± 0.01
318.15	27.81 ± 0.01
323.15	27.46 ± 0.01
328.15	27.12 ± 0.01
333.15	26.78 ± 0.01
338.15	26.57 ± 0.02
343.15	26.24 ± 0.01

[a] Standard uncertainties u are u(T) = 0.1 K, u(γ) = 0.02 mN.m^{-1}.

The experimental data on density and surface tension were necessary to estimate the critical temperature of the ionic liquid, using the Eötvos equation [48]. The empirical methodology is based on the temperature dependence of the liquid density and surface tension. The estimated critical temperature is 783.3 K. The critical pressure and acentric factor of [P$_{6 6 6 14}$][Br] were obtained from Valderrama et al. [57]. The critical properties of carbon dioxide were taken from

the DIPPR database [55]. These data of pure carbon dioxide and [P$_{6\,6\,6\,14}$][Br] are presented in table 4.15, along with the critical properties of [P$_{6\,6\,6\,14}$][Cl] and [P$_{6\,6\,6\,14}$][NTf$_2$].
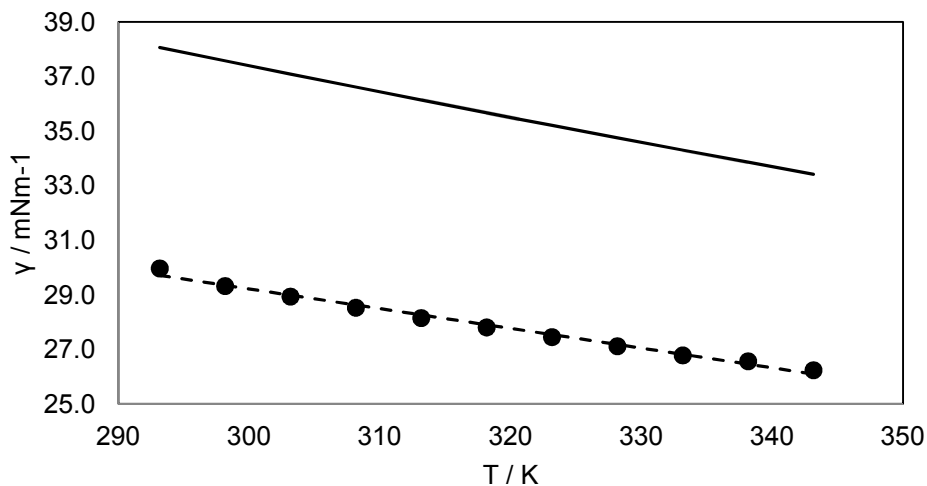
Figure 4.7 Surface tension of [P$_{6\,6\,6\,14}$][Br] as a function of temperature, at atmospheric pressure: experimental data (filled circles), QSPR correlation [75] (straight line) and linear fit (dashed line).

The Peng-Robinson equation of state with van der Waals one-fluid mixing rules was applied for all (carbon dioxide - phosphonium based ionic liquid) systems discussed above. The absolute average deviations (AAD) were calculated by the following equation:

$$AAD = \frac{1}{NP} \sum_{i=1}^{NP} \left| \frac{x_{calc,i} - x_{exp,i}}{x_{exp,i}} \right| * 100 \qquad (4.23)$$

where x_i is the CO$_2$ solubility in an ionic liquid and NP is the number of experimental data points.

Table 4.15 Critical properties of CO$_2$ and ionic liquids.

Compound	T_c / K	P_c / MPa	ω
CO$_2$	304.2[a]	7.380[a]	0.2236[a]
[P$_{6\,6\,6\,14}$][Br]	783.3[b]	0.820[c]	0.8311[c]
[P$_{6\,6\,6\,14}$][Cl]	803.8[d]	0.851[c]	0.8915[c]
[P$_{6\,6\,6\,14}$][NTf$_2$]	805.5[d]	0.795[c]	0.7947[c]

[a] DIPPR database [55]

[b] Predicted by Eötvos equation using experimental data presented in this work

[c] Valderrama et al. [57]

[d] Manic et al. [76].

The absolute average deviations (AAD) between the experimental and calculated mole fractions are presented for both k_{ij} equal to zero and adjusted k_{ij} as presented in table 4.16. The AAD between the experimental and the calculated solubility which correspond to model prediction (k_{ij} equals to zero) are 19.1 % for [P$_{6\,6\,6\,14}$][Br], 18.6 % for [P$_{6\,6\,6\,14}$][Cl] and 13.1 % for ([P$_{6\,6\,6\,14}$][NTf$_2$]. The difference in prediction results may be explained by low volatility nature of ionic liquids. Their critical properties cannot be accurately determined, and so there is an additional source of uncertainty for any thermodynamic model requiring critical parameters.

The temperature dependent binary interaction parameters were determined from experimental data and are presented in table 4.16 along with AAD between the experimental and correlated data. AAD are slightly higher at 313.2 K but not over 1.84 %, as is shown in table 4.16. Peng-Robinson equation of state successfully correlates the solubility data at pressure and temperature studied in this work.

Table 4.16 Binary interaction parameters and absolute average deviations (AAD) when using a fitted k_{ij} (correlation) and AAD for k_{ij} equal to zero (prediction). AAD stands for global average deviation of the mole fraction solubility of CO_2 in ionic liquids, between experimental data and modelling results

	Fitted temperature-dependent k_{ij} (correlation)				k_{ij} is equal to zero (prediction)
	T = 313.2 K		T = 323.2 K		
IL	k_{ij}	AAD / %	k_{ij}	AAD / %	AAD / %
[P$_{6\,6\,6\,14}$][Br]	0.085	1.84	0.097	1.04	19.1
[P$_{6\,6\,6\,14}$][Cl]	0.080	1.17	0.091	0.74	18.6
[P$_{6\,6\,6\,14}$][NTf$_2$]	0.071	1.68	0.080	0.44	13.1

Conclusions

This work reports data on solubility of carbon dioxide in eight different ionic liquids: [C$_4$mim][NTf$_2$], [C$_{10}$mim][NTf$_2$], [C$_4$mpyr][NTf$_2$], [N$_{4\,1\,1\,1}$][NTf$_2$], [N$_{1\,8\,8\,8}$][NTf$_2$], [P$_{6\,6\,6\,14}$][NTf$_2$], [P$_{6\,6\,6\,14}$][Cl] and [P$_{6\,6\,6\,14}$][Br]. A static sampling technique using a high-pressure sapphire cell was employed to measure the solubility at 313.2 K and 323.2 K, in the pressure range of 8-20 MPa. Our data are generally in good agreement with those available in literature for [C$_4$mim][NTf$_2$], [C$_{10}$mim][NTf$_2$], [C$_4$mpyr][NTf$_2$], [P$_{6\,6\,6\,14}$][NTf$_2$] and [P$_{6\,6\,6\,14}$][Cl]. On the other hand, data on solubility of carbon dioxide in [N$_{4\,1\,1\,1}$][NTf$_2$], [N$_{1\,8\,8\,8}$][NTf$_2$] and [P$_{6\,6\,6\,14}$][Br] are published for the first time. For some other systems we have increased the pressure range of the available data. The results indicate that solubility of CO_2 in ILs might be improved either by enhancing the pressure, increasing alkyl chain length in the cation, or by decreasing the temperature.

Additionally, phosphonium based ionic liquids gave an opportunity to discuss influence of the anion on CO_2 solubility in ILs. The substitution of halogen anion by $[NTf_2]^-$ increases CO_2 solubility due to favourable interactions between CO_2 and the fluoroalkyl substituents on the anion.

Prediction (without k_{ij} binary interaction parameters) and correlation (using a temperature independent k_{ij}) of the CO_2 solubilities in ionic liquids was carried out using the PR, SRK and the CPA EoS. According to the results, we conclude that there is no clear advantage in considering association in the ionic liquids for describing either their pure component properties or the CO_2 solubilities in the presented (IL + CO_2) systems. It was found that the use of a fitted k_{ij} value does not have a significant influence on relating quantitatively the solubilities, but may be important to obtain two-phase equilibria at the highest pressures.

Therefore, in the case of phosphonium ILs, the phase behaviour of (PILs-CO_2) system was described by PR EoS, while the temperature-dependent binary interaction parameter was applied. The absolute average deviation was around 20 % when PR EoS was used as a predictive tool. Introducing the temperature-dependent binary interaction parameter in to the equation decreases AAD significantly. The absolute average deviation is somewhat higher at lower temperature in all cases.

The experimental density and surface tension data of $[P_{6\ 6\ 6\ 14}][Br]$ in the temperature range between 293.15 K and 343.15 K and at atmospheric pressure were provided. The measured densities are in a good agreement with the data presented in the literature, as well as with the density values predicted by Gardas and Coutinho method.

References

[1] L.A. Blanchard, D. Hancu, E.J. Beckman, J.F. Brennecke, Green processing using ionic liquids and CO2, Nature, 399 (1999) 28-29.

[2] L.A. Blanchard, J.F. Brennecke, Recovery of organic products from ionic liquids using supercritical carbon dioxide, Industrial and Engineering Chemistry Research, 40 (2001) 287-292.

[3] M.C. Kroon, J. van Spronsen, C.J. Peters, R.A. Sheldon, G.-J. Witkamp, Recovery of pure products from ionic liquids using supercritical carbon dioxide as a co-solvent in extractions or as an anti-solvent in precipitations, Green Chemistry, 8 (2006) 246-249.

[4] E.M. Saurer, S.N.V.K. Aki, J.F. Brennecke, Removal of ammonium bromide, ammonium chloride, and zinc acetate from ionic liquid/organic mixtures using carbon dioxide, Green Chemistry, 8 (2006) 141-143.

[5] V. Najdanovic-Visak, A. Serbanovic, J.M.S.S. Esperança, H.J.R. Guedes, L.P.N. Rebelo, M. Nunes da Ponte, Supercritical carbon dioxide-induced phase changes in (ionic liquid, water and ethanol mixture) solutions: Application to biphasic catalysis, ChemPhysChem, 4 (2003) 520-522.

[6] M.S. Manic, M.N. da Ponte, V. Najdanovic-Visak, Recovery of erythromycin from aqueous solutions with an ionic liquid and high-pressure carbon dioxide, Chemical Engineering Journal, 171 (2011) 904-911.

[7] P.B. Webb, T.E. Kunene, D.J. Cole-Hamilton, Continuous flow homogeneous hydroformylation of alkenes using supercritical fluids, Green Chemistry, 7 (2005) 373-379.

[8] M. Solinas, A. Pfaltz, P.G. Cozzi, W. Leitner, Enantioselective hydrogenation of imines in ionic liquid/carbon dioxide media, Journal of the American Chemical Society, 126 (2004) 16142-16147.

[9] A.M. Scurto, W. Leitner, Expanding the useful range of ionic liquids: melting point depression of organic salts with carbon dioxide for biphasic catalytic reactions, Chemical Communications, (2006) 3681-3683.

[10] A.M. Scurto, E. Newton, R.R. Weikel, L. Draucker, J. Hallett, C.L. Liotta, W. Leitner, C.A. Eckert, Melting point depression of ionic liquids with CO2: Phase equilibria, Industrial & Engineering Chemistry Research, 47 (2007) 493-501.

[11] A. Serbanovic, Ž. Petrovski, M. Manic, C.S. Marques, G.V.S.M. Carrera, L.C. Branco, C.A.M. Afonso, M.N. da Ponte, Melting behaviour of ionic salts in the presence of high pressure CO2, Fluid Phase Equilibria, 294 (2010) 121-130.

[12] Z.K. Lopez-Castillo, S.N.V.K. Aki, M.A. Stadtherr, J.F. Brennecke, Enhanced solubility of hydrogen in CO2-expanded liquids, Industrial & Engineering Chemistry Research, 47 (2007) 570-576.

[13] F. Kohler, D. Roth, E. Kuhlmann, P. Wasserscheid, M. Haumann, Continuous gas-phase desulfurisation using supported ionic liquid phase (SILP) materials, Green Chemistry, 12 (2010) 979-984.

[14] J.E. Bara, T.K. Carlisle, C.J. Gabriel, D. Camper, A. Finotello, D.L. Gin, R.D. Noble, Guide to CO2 separations in imidazolium-based room-temperature ionic liquids, Industrial & Engineering Chemistry Research, 48 (2009) 2739-2751.

[15] Ionic Liquids Database, ILThermo, http://ilthermo.boulder.nist.gov/ILThermo/mainmenu.uix.

[16] C.J. Bradaric, A. Downard, C. Kennedy, A.J. Robertson, Y. Zhou, Industrial preparation of phosphonium ionic liquids, Green Chemistry, 5 (2003) 143-152.

[17] N.V. Plechkova, K.R. Seddon, Applications of ionic liquids in the chemical industry, Chemical Society Reviews, 37 (2008) 123-150.

[18] R.E. Del Sesto, C. Corley, A. Robertson, J.S. Wilkes, Tetraalkylphosphonium-based ionic liquids, Journal of Organometallic Chemistry, 690 (2005) 2536-2542.

[19] J.M.S.S. Esperança, H.J.R. Guedes, M. Blesic, L.P.N. Rebelo, Densities and derived thermodynamic properties of ionic liquids. 3. Phosphonium-based ionic liquids over an extended pressure Range, Journal of Chemical & Engineering Data, 51 (2005) 237-242.

[20] P. Kilaru, G.A. Baker, P. Scovazzo, Density and surface tension measurements of imidazolium-, quaternary phosphonium-, and ammonium-based room-temperature ionic liquids: Data and correlations, Journal of Chemical & Engineering Data, 52 (2007) 2306-2314.

[21] P.J. Carvalho, C.M.S.S. Neves, J.o.A.P. Coutinho, Surface tensions of bis(trifluoromethylsulfonyl)imide anion-based ionic liquids, Journal of Chemical & Engineering Data, 55 (2010) 3807-3812.

[22] L.I.N. Tomé, R.L. Gardas, P.J. Carvalho, M.J. Pastoriza-Gallego, M.M. Piñeiro, J.o.A.P. Coutinho, Measurements and correlation of high-pressure densities of phosphonium based ionic liquids, Journal of Chemical & Engineering Data, 56 (2011) 2205-2217.

[23] J.W. Hutchings, K.L. Fuller, M.P. Heitz, M.M. Hoffmann, Surprisingly high solubility of the ionic liquid trihexyltetradecylphosphonium chloride in dense carbon dioxide, Green Chemistry, 7 (2005) 475-478.

[24] S.P.M. Ventura, J. Pauly, J.L. Daridon, J.A. Lopes da Silva, I.M. Marrucho, A.M.A. Dias, J.A.P. Coutinho, High pressure solubility data of carbon dioxide in (tri-iso-butyl(methyl)phosphonium tosylate + water) systems, The Journal of Chemical Thermodynamics, 40 (2008) 1187-1192.

[25] P.J. Carvalho, V.H. Álvarez, I.M. Marrucho, M. Aznar, J.A.P. Coutinho, High carbon dioxide solubilities in trihexyltetradecylphosphonium-based ionic liquids, The Journal of Supercritical Fluids, 52 (2010) 258-265.

[26] H.N. Song, B.-C. Lee, J.S. Lim, Measurement of CO_2 solubility in ionic liquids: [BMP][TfO] and [P14,6,6,6][Tf2N] by measuring bubble-point pressure, Journal of Chemical & Engineering Data, 55 (2009) 891-896.

[27] Y. Zhang, S. Zhang, X. Lu, Q. Zhou, W. Fan, X. Zhang, Dual amino-functionalised phosphonium ionic liquids for CO_2 capture, Chemistry – A European Journal, 15 (2009) 3003-3011.

[28] B.F. Goodrich, J.C. de la Fuente, B.E. Gurkan, Z.K. Lopez, E.A. Price, Y. Huang, J.F. Brennecke, Effect of water and temperature on absorption of CO_2 by amine-functionalized anion-tethered ionic liquids, The Journal of Physical Chemistry B, 115 (2011) 9140-9150.

[29] J. Smuts, E. Wanigasekara, D. Armstrong, Comparison of stationary phases for packed column supercritical fluid chromatography based upon ionic liquid motifs: a study of cation and anion effects, Analytical and Bioanalytical Chemistry, 400 (2011) 435-447.

[30] Y.N. Shim, J.K. Lee, J.K. Im, D.K. Mukherjee, D.Q. Nguyen, M. Cheong, H.S. Kim, Ionic liquid-assisted carboxylation of amines by CO_2: a mechanistic consideration, Physical Chemistry Chemical Physics, 13 (2011) 6197-6204.

[31] S. Livi, J. Duchet-Rumeau, J.-F. Gérard, Supercritical CO_2–ionic liquid mixtures for modification of organoclays, Journal of Colloid and Interface Science, 353 (2011) 225-230.

[32] S.G. Kazarian, B.J. Briscoe, T. Welton, Combining ionic liquids and supercritical fluids: ATR-IR study of CO dissolved in two ionic liquids at high pressures, Chemical Communications, (2000) 2047-2048.

[33] C. Cadena, J.L. Anthony, J.K. Shah, T.I. Morrow, J.F. Brennecke, E.J. Maginn, Why is CO_2 so soluble in imidazolium-based ionic liquids?, Journal of the American Chemical Society, 126 (2004) 5300-5308.

[34] M.J. Muldoon, S.N.V.K. Aki, J.L. Anderson, J.K. Dixon, J.F. Brennecke, Improving carbon dioxide solubility in ionic liquids, The Journal of Physical Chemistry B, 111 (2007) 9001-9009.

[35] L. Ferguson, P. Scovazzo, Solubility, diffusivity, and permeability of gases in phosphonium-based room temperature ionic liquids: Data and correlations, Industrial & Engineering Chemistry Research, 46 (2007) 1369-1374.

[36] P.K. Kilaru, R.A. Condemarin, P. Scovazzo, Correlations of low-pressure carbon dioxide and hydrocarbon solubilities in imidazolium-, phosphonium-, and ammonium-based room-temperature ionic liquids. Part 1. Using surface tension, Industrial & Engineering Chemistry Research, 47 (2007) 900-909.

[37] P. Scovazzo, D. Camper, J. Kieft, J. Poshusta, C. Koval, R. Noble, Regular solution theory and CO_2 gas solubility in room-temperature ionic liquids, Industrial & Engineering Chemistry Research, 43 (2004) 6855-6860.

[38] J. Jacquemin, P. Husson, V. Majer, M. Costa Gomes, Influence of the cation on the solubility of CO_2 and H_2 in ionic liquids based on the bis(trifluoromethylsulfonyl)imide anion, Journal of Solution Chemistry, 36 (2007) 967-979.

[39] G. Hong, J. Jacquemin, M. Deetlefs, C. Hardacre, P. Husson, M.F. Costa Gomes, Solubility of carbon dioxide and ethane in three ionic liquids based on the bis{(trifluoromethyl)sulfonyl}imide anion, Fluid Phase Equilibria, 257 (2007) 27-34.

[40] J.-H. Yim, H.N. Song, K.-P. Yoo, J.S. Lim, Measurement of CO_2 solubility in ionic liquids: [BMP][Tf2N] and [BMP][MeSO4] by measuring bubble-point pressure, Journal of Chemical & Engineering Data, 56 (2011) 1197-1203.

[41] J.L. Anthony, J.L. Anderson, E.J. Maginn, J.F. Brennecke, Anion effects on gas solubility in ionic liquids, The Journal of Physical Chemistry B, 109 (2005) 6366-6374.

[42] E.-K. Shin, B.-C. Lee, J.S. Lim, High-pressure solubilities of carbon dioxide in ionic liquids: 1-Alkyl-3-methylimidazolium bis(trifluoromethylsulfonyl)imide, The Journal of Supercritical Fluids, 45 (2008) 282-292.

[43] P.J. Carvalho, V.H. Álvarez, I.M. Marrucho, M. Aznar, J.A.P. Coutinho, High pressure phase behavior of carbon dioxide in 1-butyl-3-methylimidazolium bis(trifluoromethylsulfonyl)imide and 1-butyl-3-methylimidazolium dicyanamide ionic liquids, The Journal of Supercritical Fluids, 50 (2009) 105-111.

[44] W. Ren, B. Sensenich, A.M. Scurto, High-pressure phase equilibria of {carbon dioxide (CO2) + n-alkyl-imidazolium bis(trifluoromethylsulfonyl)amide} ionic liquids, The Journal of Chemical Thermodynamics, 42 (2010) 305-311.

[45] J.S. Andreu, L.F. Vega, Modeling the solubility behavior of CO2, H2, and Xe in [Cn-mim][Tf2N] ionic liquids, The Journal of Physical Chemistry B, 112 (2008) 15398-15406.

[46] M.C. Kroon, E.K. Karakatsani, I.G. Economou, G.-J. Witkamp, C.J. Peters, Modeling of the carbon dioxide solubility in imidazolium-based ionic liquids with the tPC-PSAFT equation of state, The Journal of Physical Chemistry B, 110 (2006) 9262-9269.

[47] N.A. Manan, C. Hardacre, J. Jacquemin, D.W. Rooney, T.G.A. Youngs, Evaluation of gas solubility prediction in ionic liquids using COSMOthermX, Journal of Chemical & Engineering Data, 54 (2009) 2005-2022.

[48] J.L. Shereshefsky, Surface tension of saturated vapors and the equation of Eötvös, The Journal of Physical Chemistry, 35 (1930) 1712-1720.

[49] C.M.S.S. Neves, P.J. Carvalho, M.G. Freire, J.A.P. Coutinho, Thermophysical properties of pure and water-saturated tetradecyltrihexylphosphonium-based ionic liquids, The Journal of Chemical Thermodynamics, 43 (2011) 948-957.

[50] R.L. Gardas, J.A.P. Coutinho, Extension of the Ye and Shreeve group contribution method for density estimation of ionic liquids in a wide range of temperatures and pressures, Fluid Phase Equilibria, 263 (2008) 26-32.

[51] NIST Chemistry WebBook, http://webbook.nist.gov/chemistry/.

[52] G.M. Kontogeorgis, G.K. Folas, Thermodynamic models for industrial applications: From classical and advanced mixing rules to association theories, John Wiley & Sons, Chichester (UK), 2010.

[53] S.H. Huang, M. Radosz, Equation of state for small, large, polydisperse, and associating molecules, Industrial & Engineering Chemistry Research, 29 (1990) 2284-2294.

[54] S.N.V.K. Aki, B.R. Mellein, E.M. Saurer, J.F. Brennecke, High-pressure phase behavior of carbon dioxide with imidazolium-based ionic liquids, The Journal of Physical Chemistry B, 108 (2004) 20355-20365.

[55] W.V.W. R.L. Rowley, J.L. Oscarson, Y. Yang, N.F. Giles, DIPPR data compilation of pure chemical properties, in, Design Institute for Physical Properties, AIChE, New York, 2010.

[56] L.P.N. Rebelo, J.N. Canongia Lopes, J.M.S.S. Esperança, E. Filipe, On the critical temperature, normal boiling point, and vapor pressure of ionic liquids, The Journal of Physical Chemistry B, 109 (2005) 6040-6043.

[57] J.O. Valderrama, R.E. Rojas, Critical properties of ionic liquids. Revisited, Industrial & Engineering Chemistry Research, 48 (2009) 6890-6900.

[58] D.H. Zaitsau, G.J. Kabo, A.A. Strechan, Y.U. Paulechka, A. Tschersich, S.P. Verevkin, A. Heintz, Experimental vapor pressures of 1-alkyl-3-methylimidazolium bis(trifluoromethylsulfonyl)imides and a correlation scheme for estimation of vaporization enthalpies of ionic liquids, The Journal of Physical Chemistry A, 110 (2006) 7303-7306.

[59] J. Jacquemin, P. Husson, V. Mayer, I. Cibulka, High-pressure volumetric properties of imidazolium-based ionic liquids: Effect of the anion, Journal of Chemical & Engineering Data, 52 (2007) 2204-2211.

[60] Y.U. Paulechka, D.H. Zaitsau, G.J. Kabo, A.A. Strechan, Vapor pressure and thermal stability of ionic liquid 1-butyl-3-methylimidazolium Bis(trifluoromethylsulfonyl)amide, Thermochimica Acta, 439 (2005) 158-160.

[61] A. Wandschneider, J.K. Lehmann, A. Heintz, Surface tension and density of pure ionic liquids and some binary mixtures with 1-propanol and 1-butanol, Journal of Chemical & Engineering Data, 53 (2008) 596-599.

[62] K.R. Harris, M. Kanakubo, L.A. Woolf, Temperature and pressure dependence of the viscosity of the ionic liquids 1-hexyl-3-methylimidazolium hexafluorophosphate and 1-butyl-3-methylimidazolium bis(trifluoromethylsulfonyl)imide, Journal of Chemical & Engineering Data, 52 (2007) 1080-1085.

[63] R. Gomes de Azevedo, J.M.S.S. Esperança, J. Szydlowski, Z.P. Visak, P.F. Pires, H.J.R. Guedes, L.P.N. Rebelo, Thermophysical and thermodynamic properties of ionic liquids over an extended pressure range: [bmim][NTf2] and [hmim][NTf2], The Journal of Chemical Thermodynamics, 37 (2005) 888-899.

[64] L.I.N. Tomé, P.J. Carvalho, M.G. Freire, I.M. Marrucho, I.M.A. Fonseca, A.G.M. Ferreira, J.o.A.P. Coutinho, R.L. Gardas, Measurements and correlation of high-pressure densities of imidazolium-based ionic liquids, Journal of Chemical & Engineering Data, 53 (2008) 1914-1921.

[65] A.B. Pereiro, H.I.M. Veiga, J.M.S.S. Esperança, A. Rodríguez, Effect of temperature on the physical properties of two ionic liquids, The Journal of Chemical Thermodynamics, 41 (2009) 1419-1423.

[66] J. Jacquemin, P. Nancarrow, D.W. Rooney, M.F. Costa Gomes, P. Husson, V. Majer, A.A.H. Pádua, C. Hardacre, Prediction of ionic liquid properties. II. Volumetric properties as a function of temperature and pressure, Journal of Chemical & Engineering Data, 53 (2008) 2133-2143.

[67] R. Kato, J. Gmehling, Systems with ionic liquids: Measurement of VLE and γ∞ data and prediction of their thermodynamic behavior using original UNIFAC, mod. UNIFAC(Do) and COSMO-RS(Ol), The Journal of Chemical Thermodynamics, 37 (2005) 603-619.

[68] R.L. Gardas, H.F. Costa, M.G. Freire, P.J. Carvalho, I.M. Marrucho, I.M.A. Fonseca, A.G.M. Ferreira, J.A.P. Coutinho, Densities and derived thermodynamic properties of imidazolium-, pyridinium-, pyrrolidinium-, and piperidinium-based ionic liquids, Journal of Chemical & Engineering Data, 53 (2008) 805-811.

[69] S. Raeissi, C.J. Peters, Carbon dioxide solubility in the homologous 1-alkyl-3-methylimidazolium bis(trifluoromethylsulfonyl)imide family, Journal of Chemical & Engineering Data, 54 (2008) 382-386.

[70] M.B. Oliveira, I.M. Marrucho, J.A.P. Coutinho, A.J. Queimada, Surface tension of chain molecules through a combination of the gradient theory with the CPA EoS, Fluid Phase Equilibria, 267 (2008) 83-91.

[71] M.B. Oliveira, M.J. Pratas, I.M. Marrucho, A.J. Queimada, J.A.P. Coutinho, Description of the mutual solubilities of fatty acids and water with the CPA EoS, AIChE Journal, 55 (2009) 1604-1613.

[72] D.-J. Oh, B.-C. Lee, High-pressure phase behavior of carbon dioxide in ionic liquid 1-butyl-3-methylimidazolium bis(trifluoromethylsulfonyl)imide, Korean Journal of Chemical Engineering, 23 (2006) 800-805.

[73] D.-Y. Peng, D.B. Robinson, A new two-constant equation of state, Industrial & Engineering Chemistry Fundamentals, 15 (1976) 59-64.

[74] C. Ye, J.n.M. Shreeve, Rapid and accurate estimation of densities of room-temperature ionic liquids and salts, The Journal of Physical Chemistry A, 111 (2007) 1456-1461.

[75] R.L. Gardas, J.A.P. Coutinho, Applying a QSPR correlation to the prediction of surface tensions of ionic liquids, Fluid Phase Equilibria, 265 (2008) 57-65.

[76] M.S. Manic, A.J. Queimada, E.A. Macedo, V. Najdanovic-Visak, High-pressure solubilities of carbon dioxide in ionic liquids based on bis(trifluoromethylsulfonyl)imide and chloride, The Journal of Supercritical Fluids, 65 (2012) 1-10.

Chapter V

Extraction of high-value products from vegetable materials using ethyl lactate

Introduction

High-value compounds derived from natural sources are of industrial importance due to the increased perception of their health benefits associated with their antioxidant and antimicrobial activities. Some of the examples are derivatives of hydroxycinnamic acid, such as ferulic and caffeic acids, which are the most abundant phenolic acids found in seeds of many plants: cereals, coffee, fruits and vegetables. Studies have shown their potential in the prevention of chronic illnesses such as cardiovascular diseases and cancer [1]. Free ferulic and caffeic acids presented great antioxidant activities with high scavenging effect towards hydrogen peroxide, superoxide, hydroxyl radical and nitrogen dioxide free radicals [2]. This ability has an important role associated to the anti-cancer effect of these compounds. Kaul end Khanduja [3] reported that topical application containing caffeic and ferulic acids resulted in significant protection against anthracene-induced skin tumors while Guerriero et al. [4] showed anti-cancer activity of both acids on hepatocellular carcinoma. Ferulic acid significantly reduced the growth of oral cancer [5] as well as colon and rectal cancer [6].

Another example of phenolic compounds with high biological activity is vanillic acid which belongs to the hydroxybenzoic acid group. Recent bioactivity studies of hydroxy- and polyhydroxybenzoic acids were reviewed by Khadem and Marles [7]. Vanillic acid occurs in many plants and it is known for its anti-sickling and anthelmintic activities. It reduced hepatic fibrosis in chronic liver injury [8], inhibited snake venom 5'-nucleotidase [9] and showed the protective effects in isoproterenol induced cardiotoxic rats [10].

Thymol, a compound characteristic of essential oils, has been identified as an effective antibacterial with relatively low inhibitory concentrations in vitro and somewhat higher concentration in foods [11]. In the recent study [12], thymol demonstrated dose dependent cytotoxic effects on acute promyelotic leukaemia cells after 24 h of exposure.

Furthermore, one of the most widely consumed and studied natural product in history is caffeine. Although research results are controversial, it is believed that low to moderate caffeine intake is generally associated with improvements in alertness, learning capacity, exercise performance, and possibly even in mood [13]. It is also used as an additive in pain medications. Although coffee beans are the most important source of caffeine, it can be obtain from other sources such as green and black tea leaves, guaraná seeds, cocoa beans, *ect*. Coffee beans, beside caffeine and trivial compounds (lipids, proteins and sucrose), contain other active principles such as: purine alkaloid trigonelline which has been recognized as main source of anti-adhesive activity of coffee, since it is very effective inhibitor of *Streptococcus mutans* adsorption [14]; chlorogenic acids as major antioxidant active compounds [15] and their important role during coffee roasting when chlorogenic acids transform into key compounds of coffee flavour and aroma [16]; and coffee oil which is of particular interest to the cosmetic and pharmaceutical industries.

Most of high-value compounds derived from natural sources are obtained by energetically intensive vacuum distillation including several additional steps associated with the use of abundant amounts of organic solvents. Benzene, chloroform, trichloroethylene and dichloromethane have been employed over the years, since information on their harmful effect on human health and environment was unknown. Even though efficient extraction can be achieved using the organic solvents, their use is not suitable due to potential adverse effect which they can have on human health. As an alternative, supercritical fluid technology has been applied to extract various high-value components from natural materials [17]. In the 1980s, supercritical CO_2 extraction technology was recognized as a clean and environmental friendly technology for the removal of caffeine from coffee beans, replacing dichloromethane which might be carcinogenic. Nevertheless, despite good performances, large-scale supercritical applications are burdened with bulky equipment requirements. Consequently, the search for other new alternatives – those that would be less costly, more similar by structure to the classical solvents and yet ambient friendly – continues.

For example, decaffeination of coffee beans has been done by either water or ethyl acetate. Since water is not selective for caffeine, many other compounds which contribute to the coffee flavour are removed from the beans. The essential flavours and aromas are lost as additional treatments are required. Ethyl acetate is much more selective for caffeine and thus, extraction can be accomplished in one-step process. Since it is present in several fruits and vegetables, decaffeination of coffee beans using ethyl acetate is often called "natural decaffeination", despite the fact that the solvent employed in the decaffeination process is obtained from synthetic and not from natural sources.

Since ethyl lactate can be produced from renewable feedstock [18], it is a green and economically viable alternative to traditional solvents: it is fully biodegradable, non-corrosive, non-carcinogenic and non-ozone depleting. Ethyl lactate is approved by the U.S. Food and Drug Administration (FDA) as pharmaceutical and food additive and has been generally recognized as a safe (GRAS) solvent. The molecular structure of ethyl lactate possesses a specific topology of hydrogen bonds present as well in other lactate alpha-hydroxyesters [19]. This allows the formation of intra- and intermolecular associations with ethyl lactate, as either proton donor or proton acceptor [20]. On the other hand, ethyl lactate is soluble in paraffin oils, which fact imposes the formation of some van der Waals interactions [21]. Thus, this ester offers diverse solvent properties that may cover a large number of solutes. Consequently, there are several attempts in the literature to use ethyl lactate as an extraction solvent. For example, Ishida and Chapman [22] reported the potential application of ethyl lactate to extract carotenoids from different sources, such as tomatoes, carrots and corn; Strati and Oreopoulou [23] studied the effect of different extraction parameters on the carotenoid recovery from tomato waste; A bioactive bicyclic diterpene, namely sclareol, was selectively extracted using ethyl lactate and recovered from the liquid solution by a CO_2 gas anti-solvent procedure [24]; Hernández et al. [25] studied the potential application of ethyl lactate to recover squalene from

olive oil deodorizer distillates. Our group also reported the utilization of ethyl lactate for selective separation of α-tocopherol from triglycerides [26].

The solvent selection is one of the essential parameters to envisage any extraction process. Therefore, the knowledge of the solubility of a target component in different solvents is required. In this work, the solubility of caffeine, vanillic acid, ferulic acid, caffeic acid and thymol, in liquid ethyl lactate were measured in the temperature range of 293.2-343.2 K. Although experimental data on solubility are essential to provide information about a system and help to understand its behaviour, correlations and prediction models are also required for the correct design of separation processes.

Since binary systems containing ethyl lactate have been described by some models, such as UNIQUAC [25, 26], UNIFAC activity coefficient models coupled with the Peng–Robinson equation of state (PR–EOS) and the perturbed chain-statistical associating fluid theory (PC-SAFT) [27], the experimental solubilities of caffeine, vanillic acid, ferulic acid, caffeic acid and thymol in ethyl lactate were represented using the UNIQUAC model, as well as the modified (Dortmund) UNIFAC method. Moreover, a simple Cubic Equation of State incorporating association, known as the CPA EoS was applied for the description of the intermolecular physical interactions that include specific association in ethyl lactate containing systems. The CPA EoS was already successfully applied for binary mixtures water + phenolic compounds as reported by Mota et al. [28, 29] and Queimada et al. [30]

Additionally, the potential use of ethyl lactate as an environmentally friendly solvent to extract caffeine from green coffee beans is presented for the first time. Decaffeination of green coffee beans was accomplished by accelerated solvent extraction (ASE) using ethyl lactate and two more environmentally friendly solvents, namely ethanol and ethyl acetate, giving an opportunity to evaluate potential of ethyl lactate as a solvent in decaffeination process. The extraction was performed from both entire coffee beans and crushed coffee beans in order to discuss particle size influence on the extraction yield of caffeine. Moreover, the extraction yield of caffeine vs temperature will be presented since all experiments were performed at three different temperatures (373 K, 423 K and 473 K). Global yield and caffeine recovery obtained for the different extracts were quantified and compared. The undesirable extraction of active principles, such as coffee oil and phenolic compounds, was further analysed.
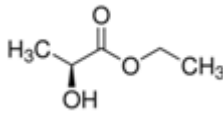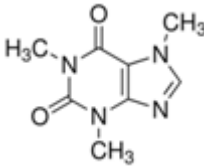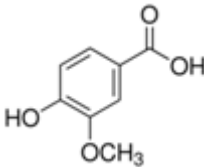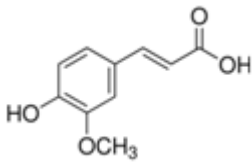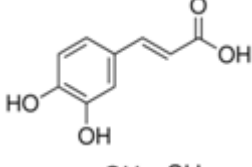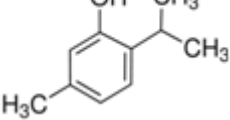
5.1 Solubilities of high-value compounds in ethyl lactate

Materials

Caffeine (99 mass % purity), vanillic acid (97 mass % purity), ferulic acid (99 mass % purity), caffeic acid (≥ 98 mass % purity), thymol (≥ 99.5 mas % purity) and ethyl lactate (98 mass %

purity) were supplied by Sigma-Aldrich as presented in table 5.1, along with their molecular structure. All solutes were used without further purification. We studied solubility of solutes in: a) water-saturated ethyl lactate as received and without any further treatment, and b) dried ethyl lactate. In the case of latter, vacuum at room temperature was applied to ethyl lactate for several days in order to reduce its water content. Karl-Fischer coulometric titration (Metrohm 870 KF Titrino Plus coulometer) was employed to determine the water content before and after the vacuum procedure.

Table 5.1 Chemicals used in this work

Compound	Structure	Supplier	Purity, mass %
Ethyl lactate		Aldrich	98
Caffeine		Sigma-Aldrich	≥ 99
Vanillic acid		Fluka	≥ 97
Ferulic acid		Aldrich	99
Caffeic acid		Sigma	≥ 98
Thymol		Sigma	≥ 99.5

Experimental procedure

Differential scanning calorimetry (DSC) (Netzsch, model DSC 200 F3 Maia) was used in order to obtain the melting point (T_m), enthalpy of fusion (ΔH_{fus}) and differences in heat capacities (ΔC_p) of caffeine, vanillic acid, ferulic acid, caffeic acid and thymol required for modelling the

(solid + liquid) equilibrium. An aluminium crucible with 5 to 7 mg of sample was sealed hermetically and placed in the measuring cell of the calorimeter together with an empty crucible to be used as a reference. The sample was heated under a nitrogen stream over a large temperature range using a 3 Kmin^{-1} heating rate. The measurements for each compound were repeated four times and average melting temperatures, enthalpies of fusion and differences in heat capacities were obtained.

For all the studied solutions, except the one with thymol, (solid + liquid) equilibrium measurements were carried out using the gravimetric method. Ethyl lactate and a solute (caffeine or vanilic acid or ferulic acid or caffeic acid) in excess were placed into a glass vessel with a stirrer. The vessels were put inside a water bath and a stirring plate was used to agitate the samples during 48 h under fixed temperature, controlled by a thermocouple (Julabo ED). The temperature was monitored by a calibrated mercury thermometer, having an accuracy of 0.1 K. After equilibrium had been reached, stirring was stopped and vessels were left stilled for more 48 h to allow a complete phase separation. Samples of clear saturated liquid solution (1 cm^3) were taken by a micropipette and placed into glass vials, while both the mass of the empty vial and the mass of the sample were registered using an AAA 250L balance with the precision of ±0.0001 g. The samples were then placed in a vacuum oven (Precision Scientific 5831) equipped with a vacuum pump (Edwards E2M1.5) for a couple of hours till constant mass of the dry samples were achieved. In order to evaporate all ethyl lactate from the samples, moderate temperature (338 K) and low pressure (1 Pa) were applied. The vials containing dry samples were weighted and the mole fraction solubilities were finally calculated.

In the case of (ethyl lactate + thymol) solutions a visual dynamic method was used to measure the solubility of thymol. Solutions were prepared gravimetrically in the glass cell using an AAA 250L balance, with the precision of ±0.0001 g. After vigorous mixing, the cell was placed in the glass thermostat bath and the sample was heated very slowly (less than 0.5 Kh^{-1} near the equilibrium temperature) with continuous stirring. The temperature at which the last crystal disappeared was taken as that of (solid + liquid) equilibrium.

For both methods, triplicates of each measurement were performed in order to obtain reliable solubility data. The average reproducibility in solid-liquid equilibrium temperature and compositions (mole fractions of solutes in ethyl lactate) was ± 0.3 K and 0.0007, respectively.

Modelling

The solubility of a solute *i* in a liquid phase can be calculated by the following equation [31]:

$$\ln\left[\frac{f_i^{\text{liq}}(T,P)}{f_i^{\text{sol}}(T,P)}\right] = \sum_{\text{tr}} \frac{\Delta_{\text{tr}}H}{R}\left(\frac{1}{T} - \frac{1}{T_{\text{tr}}}\right) - \frac{\Delta C_p}{R}\left[\frac{T_{\text{m}}}{T} - \ln\left(\frac{T_{\text{m}}}{T}\right) - 1\right]$$ (5.1)

where $\Delta_{tr}H$, R, T and ΔC_p are the enthalpy of transition at the transition temperature (T_{tr}), the ideal gas constant, absolute temperature of (solid + liquid) equilibria, and difference of the liquid and solid molar heat capacities, respectively. $\Sigma\Delta_{tr}H$ integrates enthalpies of different solid–solid and fusion phase transitions of the solute.

In this work the experimental solubility data were described by the UNIQUAC model [31] and by the modified UNIFAC (Dortmund) method [32], as well as by the cubic plus association equation of state (CPA EoS) [33, 34].

The UNIQUAC equation [31] (an activity coefficient model) can be used to represent the solubility data and equation 5.1 then becomes:

$$x_{\mathrm{i}} = \frac{1}{\gamma_i} \exp\left[-\sum_{\mathrm{tr}} \frac{\Delta trH}{R}\left(\frac{1}{T} - \frac{1}{T_{\mathrm{tr}}} \right) + \frac{\Delta C_p}{R}\left[\frac{T_{\mathrm{m}}}{T} - \ln\left(\frac{T_{\mathrm{m}}}{T} \right) - 1 \right] \right]$$ (5.2)

where x_i and γ_i are the mole fraction of solute i in the liquid phase and the solute i activity coefficient.

The surface area and volume fraction used in UNIQUAC were based on the volume and area parameters which were calculated using the corresponding group contribution values [35, 36]. The temperature-independent binary interaction parameters were obtained from the correlation of the SLE experimental data.

Equation 5.2 was also applied using the modified UNIFAC model [32] to calculate the solute activity coefficient in the liquid phase. The ACOH – COOH interaction parameters (both groups are present in the chemical structure of the phenolic acids studied) were estimated in this work using the SLE experimental data.

The cubic plus association equation of state (CPA EoS) is a combination of the simple cubic equation of state (SC EoS) and the Wertheim association term. The SC EoS term presents the description of the physical interactions, while the Wertheim association term takes into account the specific association interactions between molecules. The CPA EoS can be expressed in terms of the compressibility factor, where the pure component energy parameter (a) is given by a Soave-type temperature dependence:

$$Z = Z^{phys.} + Z^{assoc.} = \frac{1}{1-b\rho} - \frac{a\rho}{RT(1+b\rho)} - \frac{1}{2}\left(1 + \rho\frac{\partial lng}{\partial\rho} \right)\sum_i x_i \sum_{A_i}\left(1 - X_{A_i} \right)$$ (5.3)

$$a(T) = a_0\left[1 + c_1\left(1 - \sqrt{T_r} \right) \right]^2$$ (5.4)

where ρ and T_r are the molar density and reduced temperature.

The X_{A_i} is related to the association strength Δ^{AiBj} between sites A and B belonging to two different molecules (i, j). Since self- and cross-association are present in the studied systems, X_{A_i} is calculating through the following set of equations:

$$X_{A_i} = \frac{1}{1 + \rho \sum_j x_j \sum_{B_j} X_{B_j} \Delta^{A_i B_j}}$$ (5.5)

$$\Delta^{A_i B_j} = g(\rho) \left[exp\left(\frac{\varepsilon^{A_i B_j}}{RT}\right) - 1 \right] b_{ij} \beta^{A_i B_j}$$ (5.6)

$$\Delta^{A_i B_j} = \sqrt{\Delta^{A_i B_i} \Delta^{A_j B_j}}$$ (5.7)

$$g(\rho) = \frac{1}{1 - 1.9\eta}$$ (5.8)

$$\eta = \frac{1}{4} b\rho$$ (5.9)

Equation 5.6 is used for self-associating molecules where ε^{AiBi} and β^{AiBi} are the association energy and association volume, respectively. The Elliot combining rule (equation 5.7) is used for cross-associating molecules.

The CPA EoS has been recently adopted for complex molecules in order to apply the explicit association energies and volumes for the different associating groups [28-30]. The CPA EoS has five pure component parameters (a_0, c_1, b, ε, β) for associating compounds, which are obtained by the simultaneous correlation of experimental liquid density and vapour pressure data, taking into account the number and type of associating groups. However, these experimental data were only available for ethyl lactate and thymol and they were collected from DIPPR Database [37]. Otherwise, the pure component parameters were calculated using the following equations proposed before for phenolics [28]:

$$a_0 = 0.2267 + 24.38 \frac{T_c^2}{P_c}$$ (5.10)

$$c_1 = -3.557 + (6.289 \times 10^{-3})T_c$$ (5.11)

$$b = -2.328 \times 10^{-5} + 1.884 V_w$$ (5.12)

where T_c, p_c and V_W are the critical temperature (in K), critical pressure (in Pa) and the van der Waals volume (in $m^3 mol^{-1}$), respectively.

The association energies and association volumes of ethyl lactate and thymol were as well determined using the pure component vapour pressure and liquid density data. The methodology described by Mota et al. [28] was used to obtain association energies and volumes for ferulic acid, vanillic acid and caffeic acid, since in these cases the vapour pressure and liquid density data were not available.

Finally, the solubilities of the studied solutes in ethyl lactate were obtained from the following equation:

$$x_i = \frac{\varphi_i^{liq0}}{\varphi_i^{liq}} \exp\left[-\sum_{tr} \frac{\Delta_{tr} H}{R} \left(\frac{1}{T} - \frac{1}{T_{tr}}\right) + \frac{\Delta C_p}{R} \left[\frac{T_m}{T} - \ln\left(\frac{T_m}{T}\right) - 1\right] \right]$$ (5.13)

in which the CPA EoS was used to calculate the fugacity coefficients. As mentioned before, the melting temperatures, enthalpies of fusion and differences in heat capacities were measured by DSC.

The experimental and modelling results were compared in terms of the absolute average deviations (AAD) of the solubility:

$$AAD(\%) = \frac{1}{NP} \sum_i \frac{\left|x_i^{calc} - x_i^{exp}\right|}{x_i^{exp}} \times 100 \tag{5.14}$$

where x_i^{calc} and x_i^{exp} are the calculated and experimental mole fraction solubilities respectively, and NP is the number of available solubility points.

Results and discussion

Measured enthalpies of fusion and melting temperatures along with differences in heat capacities for the studied solutes (caffeine, vanillic acid, ferulic acid, caffeic acid and thymol) are given in table 5.2.

Table 5.2 Average melting points (T_m), enthalpies of fusion (ΔH_{fus}) and differences in heat capacities (ΔC_p) of the compounds studied [*]

compound	T_m / K	ΔH_{fus} / kJmol^{-1}	ΔC_p / Jmol^{-1}K^{-1}
Caffeine	405.8 ± 0.4 [a]	2.6 ± 0.2 [a]	
	505.4 ± 0.0	17.9 ± 0.1	12.0 ± 1.8
Vanillic acid	480.7 ± 0.2	29.1 ± 0.6	64.4 ± 2.5
Ferulic acid	444.9 ± 0.4	31.9 ± 0.9	73.7 ± 9.0
Caffeic acid	464.1 [b]	39.85 [b]	162.7 [c]
Thymol	322.0 ± 0.1	17.4 ± 0.6	66.6 ± 4.7

[*] Maximal standard uncertainties u are $u(Tm) = 0.28$ K, $u(\Delta H_{fus}) = 0.6$, $u(\Delta C_p) = 6.4$.

[a] Solid-solid transition of caffeine.

[b] Calculated using a group contribution method as described elsewhere [28].

[c] Calculated using a group contribution method for the estimation of the heat capacities of liquids [38] and the power-law method to estimate heat capacities of organic solids [39].

A linear base line and a symmetric peak were observed for all the studied compounds, except for caffeine and caffeic acid. In the case of caffeine two phase transformations, solid-solid and solid-liquid, were detected upon heating while it was observed that caffeic acid decomposes before melting. Therefore, the melting point of caffeic acid adopted in this work was the one presented by Mota et al. [28] obtained by a third-order group-contribution method proposed by Marrero and Gani [40]. The difference in heat capacity of caffeic acid was acquired as a

difference of the estimated liquid and solid heat capacities. The heat capacity of the liquid as a function of temperature was estimated by the third-order group-contribution method given by Kolska et al. [38]. The temperature dependence of the group contribution was expressed as an empirical polynomial equation which applies the group contribution parameters determined by both a non-hierarchic and a hierarchic approach. As the non-hierarchic approach showed to be slightly superior, it was used to calculate the heat capacity of liquid caffeic acid. The heat capacity of solid caffeic acid was calculated using the power-law method which has fixed temperature functionality but applies the two-group contribution method to obtain the compound-specific constant employed in the predictive equation [39].

The observed melting point of thymol was in a good agreement with the data reported in literature [41], showing a deviation of 0.7 %. A substantially higher deviation was observed for its fusion enthalpy (20.9 %). Similarly to what was observed by Dong et al. [42], caffeine showed two phase transitions, solid-solid and solid-liquid. In the case of the fusion of caffeine, our data deviated 0.7 % and 9.9 % for melting temperature and enthalpy of fusion, respectively. The properties of the solid-solid transition of caffeine also agreed reasonably with the literature data (1.8 % and 22 % deviations for melting point and fusion enthalpy, respectively). As for thymol and caffeine, the DSC thermograms of ferulic acid showed one endothermic peak and therefore correspond to the one of two polymorphic forms reported by Sohn and Oh. [43]. Measured melting temperature was smaller for 0.7 % while the fusion enthalpy was higher for 22 %.

Table 5.3 and figure 5.1 present the solubility data of caffeine, vanillic acid, ferulic acid, caffeic acid and thymol in ethyl lactate as a function of temperature. Since ethyl lactate is a hygroscopic compound, the solubility in both water-saturated (1.4 mass %) and dried (0.03 mass %) ethyl lactate was determined, thus permitting the understanding of the effect of water on solubility. To the best of our knowledge, there are no published data of the solubility of such given solutes in ethyl lactate with which to compare. The relative affinity of the studied solutes to ethyl lactate follows the order: thymol>>ferulic acid >vanillic acid > caffeine >caffeic acid. As expected, the solubility of all studied solutes in ethyl lactate was moderately enhanced by temperature rise. It was observed that thymol is extremely soluble in ethyl lactate, reaching mole fraction of 0.8985 at 317.8 K which can be explained by its relatively low melting point of 322.0 K and low enthalpy of fusion of 17.4 kJmol^{-1} (see table 5.2). Although the chemical structures of ferulic and caffeic acids (table 5.1) are relatively similar, their solubility in ethyl lactate were quite unlike – 0.0614 and 0.0171 in mole fraction at 333.3 K for ferulic and caffeic acid, respectively. The substitution of one hydroxyl group of caffeic acid by a methyl ether group enhanced the solubility significantly. The solubility of 0.0545 and 0.0614 in mole fraction at 333.3 K were observed for vanillic and ferulic acids, respectively. Thus, comparing these data it can be concluded that the presence of a longer acid alkyl chain increased the solubility only slightly.

Table 5.3 Experimental solubilities of thymol, caffeine, vanillic acid, caffeic acid and ferulic acid in ethyl lactate containing 1.40 mass % of water and dried ethyl lactate containing less than 0.03 mass %.[a] *x* stands for solute mole fraction

T / K	*x*	*T* / K	*x*
1.40 mass % water in ethyl lactate		< 0.03 mass % water in ethyl lactate	
Caffeine			
298.2	0.0192	296.2	0.0144
313.2	0.0305	303.1	0.0198
328.2	0.0418	312.7	0.0253
343.2	0.0508	323.0	0.0319
		333.3	0.0414
Vanillic acid			
298.2	0.0270	296.2	0.0279
313.2	0.0355	303.1	0.0321
328.2	0.0482	312.7	0.0379
343.2	0.0584	323.0	0.0444
		333.3	0.0545
Ferulic acid			
298.2	0.0803	296.2	0.0277
313.2	0.0939	303.1	0.0349
328.2	0.1061	312.7	0.0428
343.2	0.1177	323.0	0.0526
		333.3	0.0614
Caffeic acid			
298.2	0.0129	296.2	0.0089
313.2	0.0165	303.1	0.0103
328.2	0.0203	312.7	0.0119
343.2	0.0230	323.0	0.0142
		333.3	0.0171
Thymol			
301.4	0.6975	301.0	0.6978
304.3	0.7281	303.5	0.7207
307.5	0.7653	307.5	0.7638
307.8	0.7671	308.4	0.7784
308.3	0.7717	309.3	0.7928
316.5	0.8893	311.0	0.8085
318.6	0.9137	313.3	0.8421
		317.8	0.8985

[a] Standard uncertainties *u* are *u*(*T*) = 0.15 K, *u*(*x*) for caffeine, vanillic acid, ferulic acid, caffeic acid equals to 0.0005, while for thymol equals to 0.0007.

It is interesting to note that the solubility of solutes was differently influenced by the presence of water in ethyl lactate solvent (figure 5.1). For example, the solubility of thymol was not changed by water while that of vanillic acid and caffeine was only slightly influenced. On the other hand, a significant increase of the solubility of ferulic and caffeic acids was observed when water was

present in ethyl lactate. Taking into account a low solubility of ferulic and caffeic acids in ethyl lactate, this solubility enhancement suggests a co-solvent effect which may have implications in potential extraction processes.
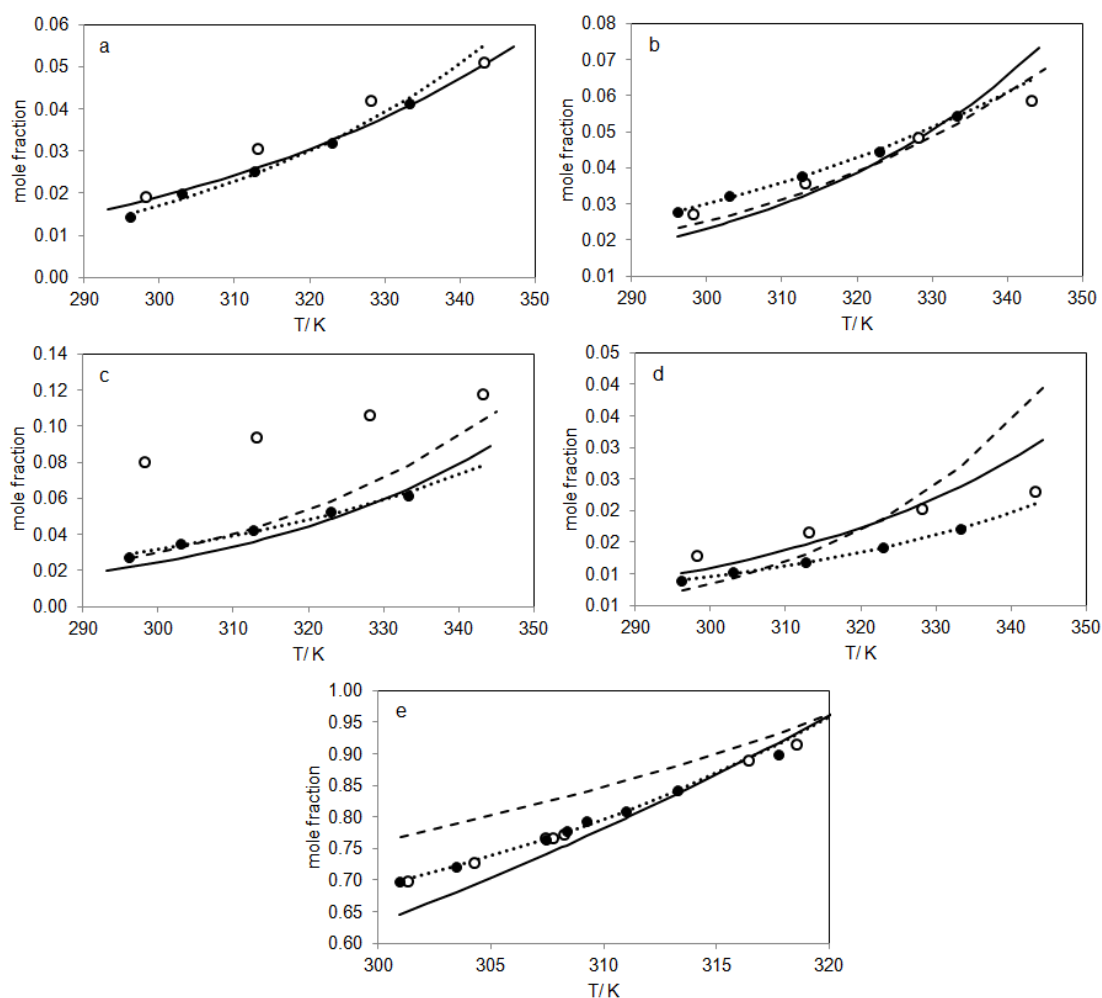
Figure 5.1 Plot of mole fraction against temperature to show the solubility of caffeine (a), vanillic acid (b), ferulic acid (c), caffeic acid (d) and thymol (e) in ethyl lactate: experimental results (empty circle stand for (solute + ethyl lactate) containing 1.40 mass % of water; filled circle stand for (solute + dried ethyl lactate system)). Lines present estimation by the UNIQUAC (round dot line), CPA (straight line) and UNIFAC (dashed line).

According to equation 5.2, the calculation of the ideal solubility of a solute in a solvent at a given temperature is straightforward from the thermophysical property data (melting points, enthalpies of fusion and differences in heat capacities) of the compounds studied and presented in table 5.2. The ideal solubility corresponds to having an activity coefficient equal to one, meaning that the attractive forces between like-molecules (solvent-solvent and solute-solute) are the same as

between unlike-molecules (solvent-solute). For the comparison of the deviation from ideal solution behaviour, it is convenient to present measured (real) solubility as a function of ideal solubility (figure 5.2).
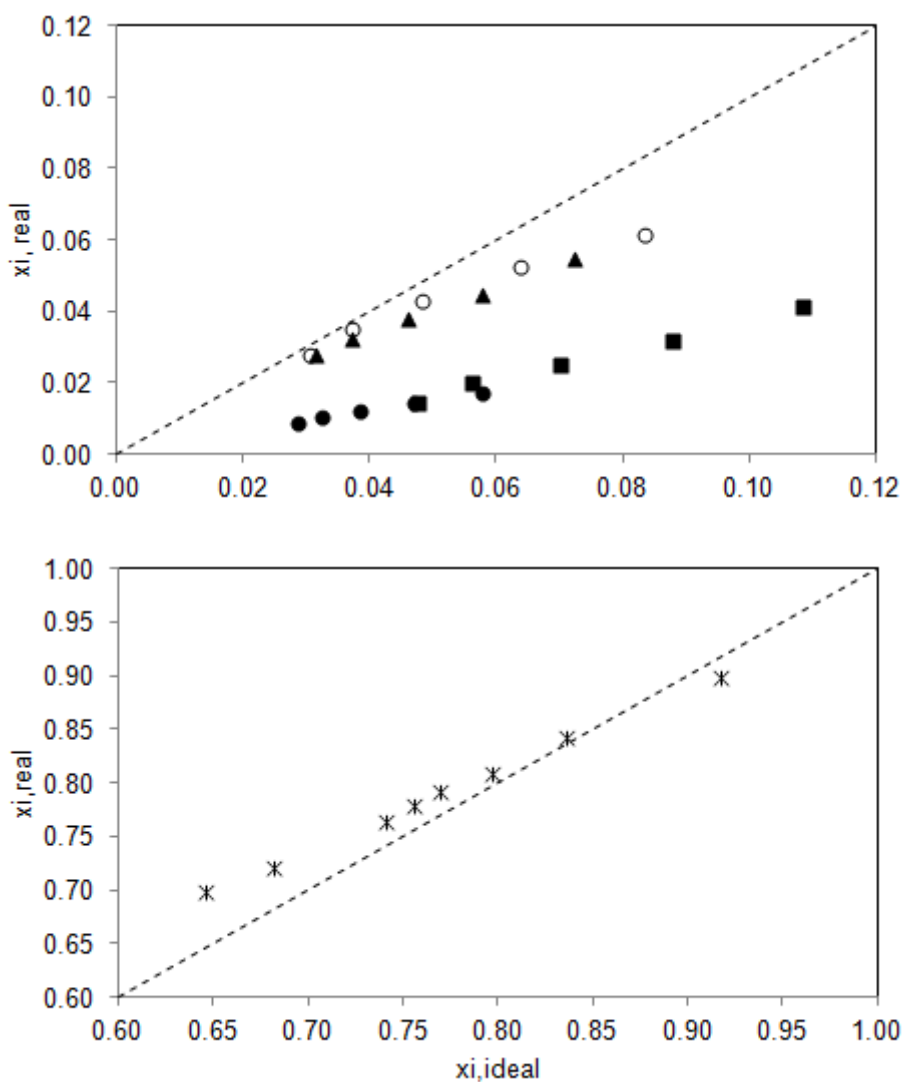
Figure 5.2 Plot of measured mole fraction against ideal mole fraction. The filled squares, filled triangles, empty circles, filled circles and asterisk stand for caffeine, vanillic acid, ferulic acid, caffeic acid and thymol, respectively. The straight dashed line corresponds to the ideal solution (activity coefficient γ = 1) calculated from equation 5.2, while areas above and below this line present region of $\gamma < 1$ and $\gamma > 1$, respectively.

A straight dashed line corresponds to the ideal solution – activity coefficient γ_i = 1. On the other hand, the area above this relates to the solubility higher than ideal, indicating a tendency toward ordering between the two unlike-molecule components ($\gamma_i < 1$). Conversely, the area below the

dashed line indicates a tendency toward phase separation or clustering in the solution, meaning that the attractive forces between like-molecules are superior to those of unlike-molecules (γ_i >1). For all the studied solutes except thymol, the activity coefficients were larger than unity, suggesting the presence of repulsive solute-solvent interactions. On the other hand, there are specific attraction forces between thymol and ethyl lactate, reflected in an activity coefficient lower than unity. Ferulic and vanillic acids showed a close to ideal behaviour at lower temperatures. As the temperature rises, solute-solvent interactions get weaker and are dominated by solute-solute and solvent-solvent cluster formations.

Calculated volume and area parameters of the UNIQUAC model (r_i and q_i) are included in table 5.4 along with the temperature-independent binary interaction parameters (a_{ij} and a_{ji}) obtained from fitting the experimental solubility data. The volume and area parameters are proportional to van der Waals volume (V_w) and van der Waals area (A_w) which are presented in table 5.5. As can be seen in figure 5.1, the UNIQUAC equation demonstrated an excellent description of the experimental data. The absolute average deviations comparing experimental and calculated solubilities were 3.9 % for caffeine, 0.98 % for vanillic acid, 3.6 % for ferulic acid, 0.97 % for caffeic acid and 0.47 % for thymol.

Table 5.4 Interaction (a_{ij}, a_{ji}) and structural (r_i, q_i) parameters for the UNIQUAC model

i	a_{ij} / K	a_{ji} / K	r_i	q_i
Ethyl lactate			4.441	3.928
Caffeine	409.11	-222.00	7.0534	5.6400
Vanillic acid	15.564	51.572	6.6638	5.6000
Ferulic acid	384.41	-207.61	5.8266	5.0040
Caffeic acid	380.93	-147.59	6.2624	5.1600
Thymol	459.35	-306.35	6.4931	4.8640

Table 5.5 Critical temperatures (T_c), critical pressures (p_c), van der Waals volumes (V_W) and van der Waals surface areas (A_W) used

compound	T_c / K	p_c / MPa	$V_w \cdot 10^5$ / $m^3 mol^{-1}$	$A_w \cdot 10^{-6}$ / $m^2 mol^{-1}$
Ethyl lactate [37]	607.0	3.74	6.74	0.98
Caffeine [44]	855.6	4.15	10.11 [37]	1.40 [37]
Vanillic acid [45]	905.2	3.45	8.84 [a]	1.25 [a]
Ferulic acid [28]	854.6	3.64	10.70	1.41 [a]
Caffeic acid [28]	876.2	5.11	9.50	1.29 [a]
Thymol [37]	698.3	3.41	9.85	1.22

[a] Calculated using the group-contribution approach proposed by Bondi [35].

Table 5.6 shows the group composition of the substances studied in the case of applying the modified (Dortmund) UNIFAC model. The volume parameter (R_k) for the CHCOO group (present in ethyl lactate) was considered to be 1.2700, as is for the rest of groups comprising main group 11 (ester) given by Gmehling et al. [32]. The corresponding surface area parameter (Q_k) was calculated to be 0.9901, according to Bondi [46]. The rest of group R_k and Q_k parameters together with the temperature-dependent interaction parameters (a_{ij}, a_{ji}, b_{ij}, b_{ji}, c_{ij}, c_{ji}) were obtained from the literature.

Table 5.6 Group composition adopted to represent the chemical structure of solutes and ethyl lactate for UNIFAC method

	ethyl lactate	vanillic acid	ferulic acid	caffeic acid	thymol
CH3	2				2
CH2	1				
CH					1
CH=CH			1	1	
AC		2	2	1	1
ACH		3	3	3	3
ACCH3					1
ACOH		1	1	2	1
OH(s)	1				
CHCOO	1				
OCH3		1	1		
COOH		1	1	1	

In the case of thymol, the calculated values of solubility correspond to model predictions and give an absolute average deviation (AAD) between the experimental and calculated mole fractions of 6.9 %. As mentioned before, the ACOH-COOH group interaction was estimated in this work, including non-zero *bij* and *bji* parameters, in order to represent the phenolic acid solubilities. The values obtained are given in table 5.7 along with a comparison with those reported in literature.

Table 5.7 Modified UNIFAC interaction parameters between the ACOH and COOH groups: comparison between parameters regressed in this work and those reported in the literature

i	j	a_{ij}	b_{ij}	c_{ij}	Refs.
ACOH	COOH	401.88	0.0	0.0	[32]
		415.72	-1.97	0.0	this work
COOH	ACOH	281.08	0.0	0.0	[32]
		120.50	-2.37	0.0	this work

Table 5.8 Pure component parameters used in the CPA EoS

Compound	a_0 / Pam^6mol^{-2}	c_1	$b \cdot 10^4$ / m^3mol^{-1}	OH		COOH		AAD / %	
				$\varepsilon \cdot 10^{-4}$ / $Jmol^{-1}$	$\beta \cdot 10^2$	$\varepsilon \cdot 10^{-4}$ / $Jmol^{-1}$	$\beta \cdot 10^3$	p	ρ
Ethyl lactate	1.994	1.030	1.030	1.875	4.046			0.513	0.062
Caffeine	4.532	1.824	1.672						
Vanillic acid	6.017	2.136	1.432	1.837	1.185	3.201	0.010		
Ferulic acid	5.118	1.818	1.783	1.871	1.345	2.756	3.698		
Caffeic acid	3.890	1.953	1.557	1.134	6.255	2.756	3.698		
Thymol	3.113	1.140	1.418	2.242	3.796			0.396	0.019

The AAD obtained between the experimental and calculated mole fractions were 11.4 % for vanillic acid, 9.6 % for ferulic acid and 24.7 % for caffeic acid. Caffeine solubility could not be calculated due to the lack of parameter for cycl-CO group. Figure 5.1 shows a comparison between the solubility calculations attained with the modified UNIFAC model and those obtained with the other models applied in this work.

The CPA pure component parameters for the solutes were calculated from available experimental values according to equations 5.10-12. The van der Waals volume for vanillic acid was calculated using a group contribution approach proposed in literature. All calculated and adopted data are presented in table 5.8.

The CPA EoS showed initially absolute average deviations (AAD) up to 72 % when the pure component parameters were calculated according to equations 5.10-12. A small temperature-independent binary interaction parameter (k_{ij}) was thus necessary to decrease the AAD. The CPA modelling results thus obtained are presented in figure 5.1. The absolute average deviation for caffeine, vanillic acid, ferulic acid and caffeic acid are 6.05 % (k_{ij} = - 0.043), 13.71 % (k_{ij} = - 0.213), 14.97 % (k_{ij} = - 0.022) and 24.21 % (k_{ij} = - 0.018), respectively. The mixture of ethyl lactate and caffeic acid showed the highest AAD. The correlated k_{ij}'s are negative which means that the interactions between the molecules are stronger than expected by the CPA EoS. The ether group in vanillic acid was not taken into account for associative interactions which leads to the highest k_{ij} value. For the mixture of ethyl lactate and thymol, the CPA EoS gave a very small absolute average deviation (AAD = 3.17 %) without adjusting the binary interaction parameter. This result leads to a conclusion that the CPA EoS is a good predictive tool for systems with self- and cross-association whenever binary interaction parameters cannot be obtained. It was also confirmed that the CPA EoS can still give satisfactory results if the pure component parameters of the solutes are obtained only from their molecular structure, whereas a small k_{ij} is the only parameter to be determined from experimental data.

5.2 Accelerated solvent extraction of caffeine from green coffee beans using ethyl lactate

Materials

Green coffee beans (*Coffea Arabica* variety) were purchased from the Spanish market (Cafés la Mexicana). Ethyl lactate (≥ 98 mass % purity) and ethyl acetate (≥ 99.7 mass % purity) were obtained from Sigma-Aldrich (St. Louis, MO, USA) while ethanol (99.5 % (v/v) purity) was supplied by Panreac (Castellar del Vallés, Barcelona, Spain). Caffeine standard (≥ 99.0 mass % purity) was obtained from Fluka (Höchstädtan der Donau, Germany). Water content of 11.2 mass % in green coffee beans was determined gravimetrically when green coffee beans were

dried in an oven (Jouan EU: 55.Thermo Fisher Scientific Inc. Waltham, MA, USA) at 85 °C during 24 hours until the constant mass reached.

The green coffee beans were ground in a ceramic mortar using liquid nitrogen which facilitated their crushing. Different size particles were separated using CISA sieves (CISA Cedacería Industrial S.L., Barcelona, Spain), applying manual agitation. Three different sizes of particles were employed in the experiments: the entire green beans (SP1) and ground green beans – particles size of 500-1500 μm (SP2) were utilized in accelerated solvent extraction; while ground green beans – particles size of 250-500 μm were used for determination of total caffeine content in green coffee beans.

Experimental procedure

Total caffeine content in green coffee beans was determined by liquid extraction of caffeine from solid matrix at 333 K, using Stuart Orbital S150 shaker apparatus (Bibby Scientific Limited, Stone, UK). 3 g of ground green coffee – particles size of 250-500 μm were soaked with ethanol and agitated at 333 K during 80 h. Additionally, the solvent was replaced by fresh ethanol in different intervals of time, until the caffeine extracted in the latter portion of ethanol was around 2 mass % of total caffeine extracted.

The accelerated solvent extraction (ASE) of caffeine from green coffee beans was carried out in an ASE 350 system (Dionex Corporation, Sunnyvale, CA, USA) equipped with a solvent controller unit. A scheme of the equipment is shown in figure 5.3.
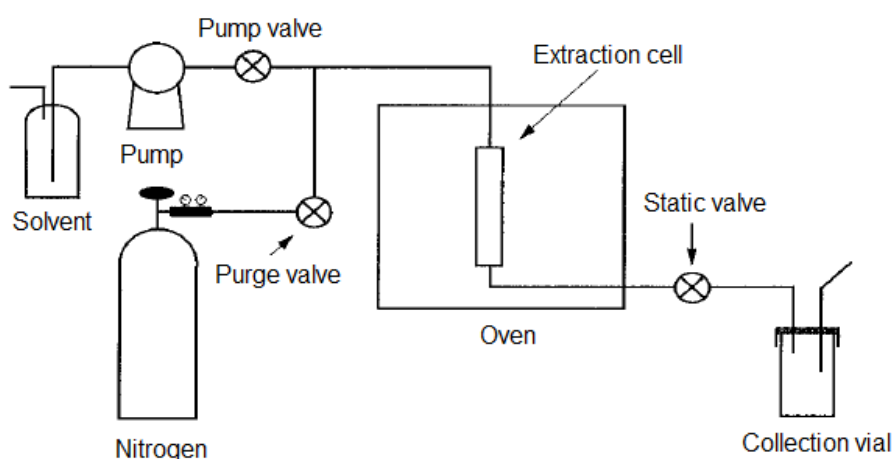

Figure 5.3 Scheme of ASE device employed in the extraction of caffeine from green coffee beans.

Decaffeination of green coffee beans (entire coffee beans – SP1 and ground coffee beans – SP2) was accomplished using ethyl lactate and two more solvents, namely ethanol and ethyl acetate at three different temperatures (373 K, 423 K and 473 K). The operating pressure of 10 MPa ensures the liquid state of the solvents employed at the temperatures studied.

Approximately 3 g of solid sample was loaded into the stainless steel extraction cell (10 mL) which was closed and placed on the ASE system carousel. The cell was filled with a solvent, placed into the oven and heated-up to the desired temperature. During the heat-up period the cell pressure increases due to solvent expansion. Therefore, a static valve pulses open and closed automatically when the cell pressure exceeds the set point in order to prevent over-pressurization of the cell. During this venting, the solvent that escaped was collected in the vial, while the fresh solvent was added into the cell to maintain pressure. A 10 min static period followed when the cell was equilibrated at desired temperature. After the static period, fresh solvent added to flush the lines and cell was forced out of the cell using pressurized nitrogen. The extract was collected in the vial. All experiments were carried out by duplicate. The extracts were placed in glass vials and stored in fridge until solvent elimination process which was achieved by Rotavapor R-210 (Büchi Labortechnik AG, Flawil, Switzerland). The dried samples were kept in fridge (approximately 4 ^{o}C) until further analyses.

Quantification of caffeine in obtained extracts was performed using Varian ProStar Analytical HPLC (Agilent Technologies. Santa Clara, California, USA) equipped by ternary pump, thermostatic controlled column oven, 410 auto-sampler with a 20 μL sample loop and diode array detector. All the modules were controlled by PC with interface and HPLC Varian Star system control software. Separation was achieved on Microsorb-MV100 C-18 column (250 x 4.6 mm; 5 μm particle size) fitted with suitable pre-column. Based on the method of Sharma et al. [47], the solvent system used was a combination of gradient and isocratic elution of acetonitrile (A) and 0.1% (w/v) ortho-phosphoric acid in water (B), as following: 0 min 10% A, 15 min 30% A, 20 min 35% A, 22min 20% A, 25 min 10% A, with a flow rate of 0.8 mL/min and column compartment temperature of 35ºC. Presence of caffeine in the different samples was identified by comparing its retention time and UV-Vis spectra at 210 nm with a previously compiled caffeine spectrum, while its amount was calculated from a calibration curve of caffeine standard, determined by linear regression. HPLC analysis was carried out by duplicate.

In order to estimate the yield of extracted oils, the total oil content of the green coffee beans was obtained gravimetrically after hexane extraction. Fatty acid profile was determined after base catalyzed methanolysis of the extract, based on the Torres et al. method [48]. To prepare fatty acid methyl esters (FAMEs), 1 mL of 0.5 M sodium methoxide was added to 0.5 mL of the sample and the mixture was resting for 30 min at 333 K. After addition of 200 μl water, the FAMEs were extracted with hexane. Analysis of the obtained FAMEs was performed by gas-liquid chromatography (Agilent 7890A GC System, Agilent Technologies, Santa Clara, CA, USA) onto a HP-5ms fused silica capillary column (30 m × 0.25 mm; 0.25 μm phase thickness) coated with (5%-phenyl)-methylpolysiloxane, from Agilent Technologies. Based on the method

reported by Tzu-Li et al. [49], the column temperature program started at 60 ^{o}C for 1 minute and went up to 140 ^{o}C, with the heating rate of 25 ^{o}C/min, increasing up to 200 ^{o}C, with the heating rate of 5 ^{o}C/min, reaching finally 300 ^{o}C, with the heating rate of 10 ^{o}C/min. Sample of 1 µL was injected in split mode (1:20). The carrier gas, helium, was delivered at 1.4 bar. The injector temperature was 250 ^{o}C, while mass spectrometer ion source and interface temperatures were 230 ^{o}C and 280 ^{o}C, respectively. Mass spectrometer was used in total ion current mode. The main FAMEs present in the sample were identified by comparison with standard mass spectra from library (Wiley 229). Retention times in minutes were: methyl myristate 13.39; methyl palmitate 17.24; methyl linoleate 19.80; methyl oleate 19.87; methyl stearate 20.20; methyl arachidate 22.49; and methyl behenate 24.40.

The presence of phenolic-type antioxidants was determined using the Folin-Ciocalteau (FC) reagent by the Singleton et al. method [50]. The results were expressed as GAE (mg of gallic acid/ g of sample). 3 mL of distilled water was mixed with 50 µL of either sample or gallic acid calibration standard. Then, 250 µL of FC reagent was added and the content of the tube was swirled to mix and incubated 3 min at room temperature. Furthermore, 0.75 mL of sodium carbonate solution (20 % w/v) was added to the mixture, followed by addition of 0.95 mL of distilled water. The mixture was resting for 2 h at room temperature. The absorbance was measured at 765 nm in GENESYS 10UV Scanning spectrophotometer (Thermo Fisher Scientific Inc. Waltham, MA, USA). The samples of gallic acid calibration standard was used to create calibration curve which is further utilized to determined corresponding gallic acid concentration of the samples.

Results and discussion

Figure 5.4 shows the kinetic behaviour of caffeine extraction from the ground green coffee beans – particles size of 250-500 µm which was carried out in a Stuart Orbital S150 shaker apparatus using ethanol as a solvent. Total caffeine extraction was accomplished in 80 h at 333 K. The total caffeine content in the green coffee beans was determined to be 9.3 mg of caffeine/ g of green coffee beans (0.93 mass %), which is in agreement with the values reported for *Coffea Arabica* variety in literature [51] (caffeine content in coffee beans is approximately 1 mass %).

Results obtained after accelerated solvent extraction of the caffeine from entire (SP1) and ground (SP2) green coffee beans, using the three different solvents at 373 K, 423 K and 473 K are presented in table 5.9, along with their absolute deviations. The global yields (g of extract/ g of green coffee beans x 100) correspond to the average value since each experiment was carried out by duplicate, showing the average absolute relative deviation (AARD) of 9.4 %. As expected, despite the solvent employed, extraction yield increased significantly with increasing temperature. The major increase of the global extraction yield with temperature was observed in

the case when using ethyl lactate as extraction solvent (see table 5.9 and figure 5.5). Moreover, higher extraction yields were obtained when extraction was carried out from the ground beans (SP2) employing either ethyl lactate, ethanol or ethyl acetate. Although the behaviour observed was opposite in the case of ethyl lactate at 473 K, difference was not noteworthy.
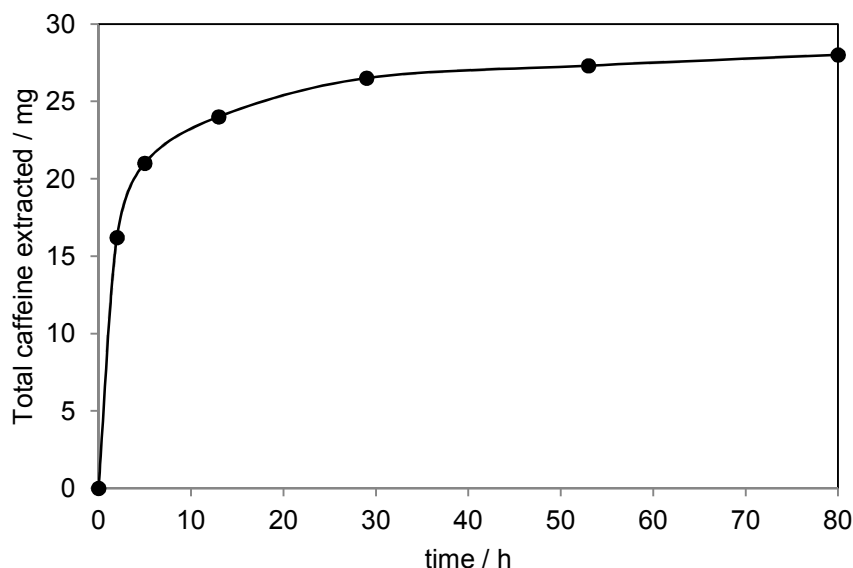
Figure 5.4 The kinetic behaviour of caffeine extraction from the ground green coffee beans carried out in a Stuart Orbital S150 shaker apparatus using ethanol as a solvent.

Table 5.9 Extraction yield (g of extract / g of green coffee beans x 100) obtained in the ASE of green coffee beans using ethyl lactate, ethanol and ethyl acetate. SP1 – entire beans; SP2 – ground beans

Extraction solvent	Particle size	T / K		
		373	423	473
Ethyl lactate	SP1	0.31 ± 0.06	1.48 ± 0.02	12.60 ± 2.69
	SP2	1.79 ± 0.03	2.75 ± 0.05	10.08 ± 0.11
Ethanol	SP1	0.44 ± 0.19	1.41 ± 0.04	5.65 ± 0.62
	SP2	2.44 ± 0.11	3.55 ± 0.14	8.68 ± 0.34
Ethyl acetate	SP1	0.23 ± 0.03	0.38 ± 0.07	3.25 ± 0.26
	SP2	1.57 ± 0.08	1.97 ± 0.07	4.47 ± 0.20

Caffeine content in the collected extracts was determined by HPLC analyses which were run in duplicates, showing an absolute deviation between measurements lower than 6.7 % in all

cases. Figure 5.6 shows a typical chromatogram of the extracts obtained after accelerated solvent extraction at 473 K using ethyl lactate (a), ethanol (b) and ethyl acetate (c).

Figure 5.5 Overall extract yields after ASE of entire green coffee beans (SP1) using ethyl lactate (filled squers), ethanol (filled triangles) and ethyl acetate (filled circles) as a function of temperature.

Figure 5.6 HPLC chromatogram of the extractc of green coffee beans (SP1) obtained at 473 K when using ethyl lactate (a), ethanol (b) and ethyl acetate (c).

The results presented in table 5.10 indicate that the higher caffeine concentrations (mass % of caffeine in the extract) were obtained at 423 K, despite the solvent employed. Although a narrow range of temperatures was explored, 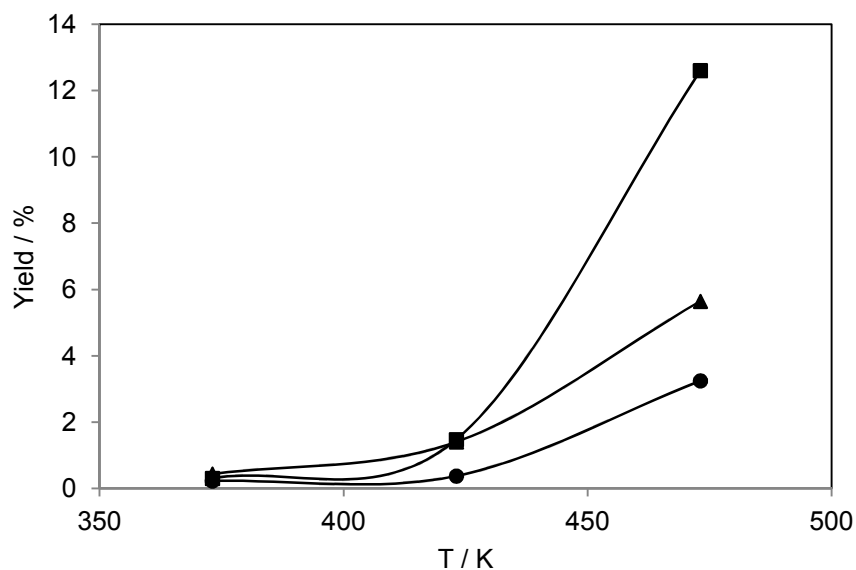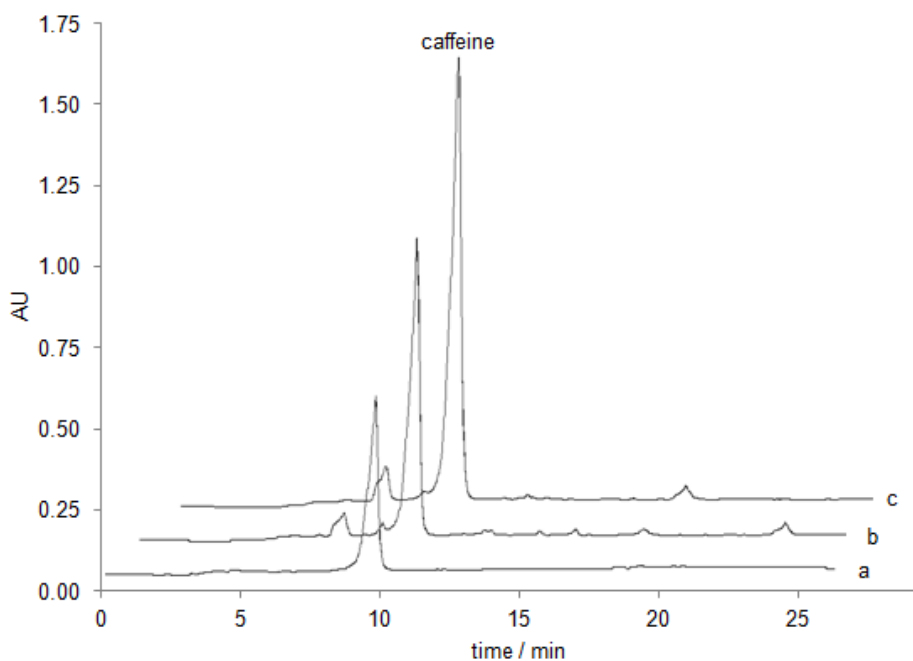it gives the impression that the selectivity towards the extraction of caffeine reaches a maximum at certain temperature, after which decreases. Such behaviour was observed for all extraction solvents studied. Certainly, the highest concentrations of caffeine in the extracts were obtained when ethyl acetate was utilized as an extraction solvent, followed by ethanol and ethyl lactate (see figure 5.6). Among the solvents employed, ethyl acetate is definitely the most selective for caffeine extraction from green coffee beans.

Table 5.10 Caffeine content (g caffeine / g extract x 100) obtained by the ASE from green coffee beans using ethyl lactate, ethanol and ethyl acetate. SP1 – entire beans; SP2 – ground beans

Extraction solvent	Particle size	T / K		
		373	423	473
Ethyl lactate	SP1	2.63	5.28	4.25
	SP2	3.86	6.20	5.82
Ethanol	SP1	4.79	7.53	7.79
	SP2	4.77	7.29	6.83
Ethyl acetate	SP1	6.79	15.52	11.80
	SP2	5.99	10.25	10.15

Table 5.11 Caffeine recovery (g of caffeine in the extract / g of caffeine in green coffee beans sample x 100) obtained by the ASE from green coffee beans using ethyl lactate, ethanol and ethyl acetate. SP1 – entire beans; SP2 – ground beans

Extraction solvent	Particle size	T / K		
		373	423	473
Ethyl lactate	SP1	0.89	8.41	57.13
	SP2	7.41	18.33	63.08
Ethanol	SP1	2.07	11.38	47.20
	SP2	12.51	27.82	63.80
Ethyl acetate	SP1	1.68	6.49	41.29
	SP2	10.13	21.76	48.71

Considering the total caffeine content determined for the green coffee beans employed in this study (0.93 mass %), the recovery of caffeine (mg caffeine in the extract / mg caffeine in green coffee beans sample) was calculated for all experimental assays and presented in table 5.11. At 373 K and 423 K, the major amount of caffeine was recovered by ethanol, while ethyl acetate and ethyl lactate express slightly lower recovery potential. Significant caffeine recovery (57-63 %) was obtained after accelerated solvent extraction from either entire (SP1) or ground (SP2) green coffee beans using ethyl lactate at 473 K. It should be pointed out that the elevated

caffeine recovery was obtained in just 10 min, while commercial decaffeination process using dichloromethane takes approximately 10 h to achieve caffeine recovery of 97% [52]. Accelerated solvent extraction (ASE) permits the use of organic solvents at high pressure and temperature above their boiling points. The elevated extraction temperature, among the solute-matrix interactions disruption, leads to lower viscosity and thus, faster diffusion rates occur, facilitating the solvent penetration into the solid matrix and enhancing extraction [53]. Consequently, considerably shorter extraction times leads to a prominent solute recovery. Therefore, ethyl lactate is a feasible benign alternative to traditional liquid solvents for the recovery of caffeine from green coffee beans.

Coffee beans, beside the most important alkaloid – caffeine, contain phenolics which are valuable components due to their antioxidant activity. The main phenolic components which could be found in the green coffee beans are phenolic acids, particularly chlorogenic acids. According to their specific characteristics discussed previously, reduction of their removal from the green coffee beans during decaffeination is required. Therefore, the co-extraction of phenolics was studied in terms of the total phenolic compounds (TPC) content in the samples studied. Considering the mass % of the TPC determined in all extracts collected (table 5.12) together with the extraction yields presented in table 5.9, it can be concluded that low amounts of phenolic compounds have been removed from the green coffee beans in all cases studied.; The amount of phenolics extracted per gram of processed green coffee beans was always lower than 1.3 mass %, despite the solvent or temperature applied. Additionally, taking into account the mean content of chlorogenic acids present in *Arabica* coffee (6.5 mass %), less than 20 mass % of total chlorogenic acids was removed from the green coffee beans.

Table 5.12 Total phenolic acids content measured using the Folin & Ciocalteau reagent (g gallic acid equivalents / g extract x 100). SP1 – entire beans; SP2 – ground beans

Extraction solvent	Particle size	T / K		
		373	423	473
Ethyl lactate	SP1	2.51	5.31	8.67
	SP2	10.64	11.77	12.67
Ethanol	SP1	5.84	5.87	13.94
	SP2	8.97	9.84	13.91
Ethyl acetate	SP1	5.32	8.94	17.44
	SP2	3.07	5.71	15.74

Since lipids contribute to coffee sensory quality, it is desirable to reduce the removal of lipids from green coffee beans during decaffeination process. Thus, the amount of coffee oils removed during the accelerated solvent extraction of caffeine from the green coffee beans was determined and reported in table 5.13. As expected, considerably higher amount of oils was recovered when extraction was carried out from the ground green coffee beans (SP2). Both

ethanol and ethyl acetate demonstrated higher affinity to the coffee oils than ethyl lactate when extraction was performed at 473 K. The results obtained for ethyl lactate and ethanol at lower temperatures were quite similar, while in the case of ethyl acetate recovery of coffee oils was relatively high. Further, the content of oils in the extracts collected decreased as temperature increased. The main FAMEs identified in the samples were methyl palmitate, methyl linoleate and methyl stearate which is in agreement with data available in the literature [54].

Table 5.13 Lipid content (g of oil / g of extract x 100) obtained by the ASE from green coffee beans using ethyl lactate, ethanol and ethyl acetate. SP1 – entire beans; SP2 – ground beans

Extraction solvent	Particle size	T / K		
		373	423	473
Ethyl lactate	SP1	12.9	3.2	4.7
	SP2	48.4	36.9	10.4
Ethanol	SP1	17.4	8.8	6.6
	SP2	41.8	31.2	25.6
Ethyl acetate	SP1	16.0	17.9	13.6
	SP2	79.7	60.6	29.0

Conclusions

In this work, the solubility of caffeine, vanillic acid, ferulic acid, caffeic acid and thymol in both dry and water saturated ethyl lactate was measured as a function of temperature, at atmospheric pressure. All values of the solubility were found to increase with temperature. Thermophysical properties of the studied solutes, namely, enthalpies of fusion and melting temperatures along with differences in heat capacities were obtained by DSC. From the thermophysical and solubility data, activity coefficients were calculated. It was found that for all the studied solutes except thymol, the activity coefficients were larger than unity, suggesting the presence of repulsive solute-solvent interactions. On the other hand, there are specific attractive forces between thymol and ethyl lactate, reflecting in activity coefficients lower than unity.

The obtained solubility data were represented using UNIQUAC and UNIFAC as well as using the cubic plus asssociation (CPA) equation of state. The UNIQUAC model provided an excellent description of the solubility data, with the absolute average deviations (AAD) of 3.9 % for caffeine, 0.98 % for vanillic acid, 3.6 % for ferulic acid, 0.97 % for caffeic acid and 0.47 % for thymol,. The UNIFAC-based model showed reasonable predictive capabilities for the mixtures studied. Good agreement between the experimental and calculated mole fractions were obtained for vanillic acid (AAD of 11.4 %), ferulic acid (AAD of 9.6 %), and thymol (AAD of 6.9 %) while somewhat inferior agreement was observed for caffeic acid (AAD of 24.7 %).

The CPA EoS represented very well the (solid + liquid) equilibrium data of the solutes studied, namely caffeine, vanillic acid, ferulic acid, caffeic acid and thymol in ethyl lactate, but only when a small binary interaction parameter was regressed from the experimental solubility data. The CPA modelling results for such complex molecules are surprisingly good, given the higher predictive character of the CPA EoS when compared with the activity coefficient models. It also clearly shows the importance of including associative effects in the model.

Additionally, the ethyl lactate potential to recover caffeine from green coffee beans was presented. Accelerated solvent extraction of caffeine when entire green coffee beans were processed at 473 K during 10 min, provided high caffeine recovery (~ 60 %), while small quantities of phenolic acids and coffee oils were achieved. Thus, ethyl lactate is a promising agrochemical solvent that might be utilized for the recovery of caffeine from green coffee beans, coffee wastes or even other natural sources of caffeine.

References

[1] Z. Zhao, M. Moghadasian, Bioavailability of hydroxycinnamates: a brief review of in vivo and in vitro studies, Phytochemistry Reviews, 9 (2010) 133-145.

[2] S. Ou, K.-C. Kwok, Ferulic acid: pharmaceutical functions, preparation and applications in foods, Journal of the Science of Food and Agriculture, 84 (2004) 1261-1269.

[3] A. Kaul, L. Khanduja, Polyphenols inhibit promotional phase of tumorigenesis: Relevance of superoxide radicals, Nutrition and Cancer, 32 (1998) 81-85.

[4] E. Guerriero, A. Sorice, F. Capone, S. Costantini, P. Palladino, M. D'ischia, G. Castello, Effects of lipoic acid, caffeic acid and a synthesized lipoyl-caffeic conjugate on human hepatoma cell lines, Molecules, 16 (2011) 6365-6377.

[5] H. Mori, K. Kawabata, N. Yoshimi, T. Tanaka, T. Murakami, T. Okada, H. Murai, Chemopreventive effects of ferulic acid on oral and rice germ on large bowel carcinogenesis, Anticancer Research, 19 (1999) 3775-3778.

[6] K. Kawabata, T. Yamamoto, A. Hara, M. Shimizu, Y. Yamada, K. Matsunaga, T. Tanaka, H. Mori, Modifying effects of ferulic acid on azoxymethane-induced colon carcinogenesis in F344 rats, Cancer Letters, 157 (2000) 15-21.

[7] S. Khadem, R.J. Marles, Monocyclic phenolic acids; hydroxy- and polyhydroxybenzoic acids: Occurrence and recent bioactivity studies, Molecules, 15 (2010) 7985-8005.

[8] A. Itoh, K. Isoda, M. Kondoh, M. Kawase, M. Kobayashi, M. Tamesada, K. Yagi, Hepatoprotective effect of syringic acid and vanillic acid on concanavalin A-induced liver injury, Biological & Pharmaceutical Bulletin, 32 (2009) 1215-1219.

[9] B. Dhananjaya, A. Nataraju, C. Raghavendra Gowda, B. Sharath, C. D'souza, Vanillic acid as a novel specific inhibitor of snake venom 5′-nucleotidase: A pharmacological tool in evaluating the role of the enzyme in snake envenomation, Biochemistry (Moscow), 74 (2009) 1315-1319.

[10] P. Stanely Mainzen Prince, S. Rajakumar, K. Dhanasekar, Protective effects of vanillic acid on electrocardiogram, lipid peroxidation, antioxidants, proinflammatory markers and histopathology in isoproterenol induced cardiotoxic rats, European Journal of Pharmacology, 668 (2011) 233-240.

[11] P.C. Braga, M. Dal Sasso, M. Culici, T. Bianchi, L. Bordoni, L. Marabini, Anti-inflammatory activity of thymol: Inhibitory effect on the release of human neutrophil elastase, Pharmacology, 77 (2006) 130-136.

[12] D.D. Deb, G. Parimala, S. Saravana Devi, T. Chakraborty, Effect of thymol on peripheral blood mononuclear cell PBMC and acute promyelotic cancer cell line HL-60, Chemico-Biological Interactions, 193 (2011) 97-106.

[13] V. Kumar, G.A. Ravishankar, Current trends in producing low levels of caffeine in coffee berry and processed coffee powder, Food Reviews International, 25 (2009) 175-197.

[14] M. Daglia, R. Tarsi, A. Papetti, P. Grisoli, C. Dacarro, C. Pruzzo, G. Gazzani, Antiadhesive Effect of Green and Roasted Coffee on Streptococcus mutans' Adhesive Properties on Saliva-Coated Hydroxyapatite Beads, Journal of Agricultural and Food Chemistry, 50 (2002) 1225-1229.

[15] C. Rice-Evans, N. Miller, G. Paganga, Antioxidant properties of phenolic compounds, Trends in Plant Science, 2 (1997) 152-159.

[16] A. Farah, M.C. Monteiro, V. Calado, A.S. Franca, L.C. Trugo, Correlation between cup quality and chemical attributes of Brazilian coffee, Food Chemistry, 98 (2006) 373-380.

[17] M. Herrero, J.A. Mendiola, A. Cifuentes, E. Ibáñez, Supercritical fluid extraction: Recent advances and applications, Journal of Chromatography A, 1217 (2010) 2495-2511.

[18] C.S.M. Pereira, V.M.T.M. Silva, A.E. Rodrigues, Ethyl lactate as a solvent: Properties, applications and production processes - a review, Green Chemistry, 13 (2011) 2658-2671.

[19] S. Aparicio, R. Alcalde, Insights into the ethyl lactate + water mixed solvent, The Journal of Physical Chemistry B, 113 (2009) 14257-14269.

[20] S. Aparicio, S. Halajian, R. Alcalde, B. García, J.M. Leal, Liquid structure of ethyl lactate, pure and water mixed, as seen by dielectric spectroscopy, solvatochromic and thermophysical studies, Chemical Physics Letters, 454 (2008) 49-55.

[21] J. Drapeau, M. Verdier, D. Touraud, U. Kröckel, M. Geier, A. Rose, W. Kunz, Effective insect repellent formulation in both surfactantless and classical microemulsions with a long-lasting protection for human beings, Chemistry & Biodiversity, 6 (2009) 934-947.

[22] B.K. Ishida, M.H. Chapman, Carotenoid extraction from plants using a novel, environmentally friendly solvent, Journal of Agricultural and Food Chemistry, 57 (2009) 1051-1059.

[23] I.F. Strati, V. Oreopoulou, Effect of extraction parameters on the carotenoid recovery from tomato waste, International Journal of Food Science & Technology, 46 (2011) 23-29.

[24] X.C. Tombokan, R.M. Aguda, D.A. Danehower, P.K. Kilpatrick, R.G. Carbonell, Three-component phase behavior of the sclareol–ethyl lactate–carbon dioxide system for GAS applications, The Journal of Supercritical Fluids, 45 (2008) 146-155.

[25] E.J. Hernández, P. Luna, R.P. Stateva, V. Najdanovic-Visak, G. Reglero, T. Fornari, Liquid−liquid phase transition of mixtures comprising squalene, olive oil, and ethyl lactate: Application to recover squalene from oil deodorizer distillates, Journal of Chemical & Engineering Data, 56 (2011) 2148-2152.

[26] G. Vicente, A. Paiva, T. Fornari, V. Najdanovic-Visak, Liquid–liquid equilibria for separation of tocopherol from olive oil using ethyl lactate, Chemical Engineering Journal, 172 (2011) 879-884.

[27] R. Ferreira, N. Pedrosa, I.M. Marrucho, L.P.N. Rebelo, Biodegradable polymer-phase behavior: Liquid–liquid equilibrium of ethyl lactate and poly(lactic acid), Journal of Chemical & Engineering Data, 53 (2007) 588-590.

[28] F.t.L. Mota, A.n.J. Queimada, S.o.P. Pinho, E.n.A. Macedo, Aqueous solubility of some natural phenolic compounds, Industrial & Engineering Chemistry Research, 47 (2008) 5182-5189.

[29] F.L. Mota, A.J. Queimada, S.P. Pinho, E.A. Macedo, Solubility of drug-like molecules in pure organic solvents with the CPA EoS, Fluid Phase Equilibria, 303 (2011) 62-70.

[30] A.n.J. Queimada, F.t.L. Mota, S.o.P. Pinho, E.n.A. Macedo, Solubilities of biologically active phenolic compounds: Measurements and modeling, The Journal of Physical Chemistry B, 113 (2009) 3469-3476.

[31] J.M. Prausnitz, R.N. Lichtenthaler, E.G. Azevedo, Molecular thermodynamics of fluid-phase equilibria, Pearson Education, 1998.

[32] J. Gmehling, J. Li, M. Schiller, A modified UNIFAC model. 2. Present parameter matrix and results for different thermodynamic properties, Industrial & Engineering Chemistry Research, 32 (1993) 178-193.

[33] G.M. Kontogeorgis, M.L. Michelsen, G.K. Folas, S. Derawi, N. von Solms, E.H. Stenby, Ten years with the CPA (Cubic-Plus-Association) equation of state. Part 1. Pure compounds and self-associating systems, Industrial & Engineering Chemistry Research, 45 (2006) 4855-4868.

[34] G.M. Kontogeorgis, M.L. Michelsen, G.K. Folas, S. Derawi, N. von Solms, E.H. Stenby, Ten years with the CPA (Cubic-Plus-Association) equation of state. Part 2. Cross-associating and multicomponent systems, Industrial & Engineering Chemistry Research, 45 (2006) 4869-4878.

[35] A. Bondi, Van der Waals volumes and radii, The Journal of Physical Chemistry, 68 (1964) 441-451.

[36] G.M. Kontogeorgis, G.K. Folas, Thermodynamic models for industrial applications: From classical and advanced mixing rules to association theories, John Wiley & Sons, Chichester (UK), 2010.

[37] W.V.W. R.L. Rowley, J.L. Oscarson, Y. Yang, N.F. Giles, DIPPR data compilation of pure chemical properties, in, Design Institute for Physical Properties, AIChE, New York, 2010.

[38] Z. Kolska, J. Kukal, M. Zabransky, V. Růzička, Estimation of the heat capacity of organic liquids as a function of temperature by a three-level group contribution method, Industrial & Engineering Chemistry Research, 47 (2008) 2075-2085.

[39] B.T. Goodman, W.V. Wilding, J.L. Oscarson, R.L. Rowley, Use of the DIPPR Database for development of quantitative structure−property relationship correlations: Heat capacity of solid organic compounds, Journal of Chemical & Engineering Data, 49 (2003) 24-31.

[40] J. Marrero, R. Gani, Group-contribution based estimation of pure component properties, Fluid Phase Equilibria, 183–184 (2001) 183-208.

[41] J.S. Chickos, C.M. Braton, D.G. Hesse, J.F. Liebman, Estimating entropies and enthalpies of fusion of organic compounds, The Journal of Organic Chemistry, 56 (1991) 927-938.

[42] J.-X. Dong, Q. Li, Z.-C. Tan, Z.-H. Zhang, Y. Liu, The standard molar enthalpy of formation, molar heat capacities, and thermal stability of anhydrous caffeine, The Journal of Chemical Thermodynamics, 39 (2007) 108-114.

[43] Y. Sohn, J. Oh, Characterization of physicochemical properties of ferulic acid, Archives of Pharmacal Research, 26 (2003) 1002-1008.

[44] G. Xu, A.M. Scurto, M. Castier, J.F. Brennecke, M.A. Stadtherr, Reliable computation of high-pressure solid−fluid equilibrium, Industrial & Engineering Chemistry Research, 39 (2000) 1624-1636.

[45] A. Stassi, R. Bettini, A. Gazzaniga, F. Giordano, A. Schiraldi, Assessment of solubility of ketoprofen and vanillic acid in supercritical CO_2 under dynamic conditions, Journal of Chemical & Engineering Data, 45 (2000) 161-165.

[46] A. Bondi, Physical properties of molecular crystals, liquids, and glasses, Wiley, New York, 1968.

[47] V. Sharma, A. Gulati, S.D. Ravindranath, V. Kumar, A simple and convenient method for analysis of tea biochemicals by reverse phase HPLC, Journal of Food Composition and Analysis, 18 (2005) 583-594.

[48] L. Vázquez, T. Fornari, F.J. Señoráns, G. Reglero, C.F. Torres, Supercritical carbon dioxide fractionation of nonesterified alkoxyglycerols obtained from shark liver oil, Journal of Agricultural and Food Chemistry, 56 (2008) 1078-1083.

[49] T.-L. Lu, C.-S. Chen, F.-L. Yang, J.-M. Fung, M.-Y. Chen, S.-S. Tsay, J. Li, W. Zou, S.-H. Wu, Structure of a major glycolipid from Thermus oshimai NTU-063, Carbohydrate Research, 339 (2004) 2593-2598.

[50] V.L. Singleton, R. Orthofer, R.M. Lamuela-Raventós, Analysis of total phenols and other oxidation substrates and antioxidants by means of folin-ciocalteu reagent, in: P. Lester (Ed.) Methods in Enzymology, Academic Press, 1999, pp. 152-178.

[51] H. Ashihara, A. Crozier, Caffeine: a well known but little mentioned compound in plant science, Trends in Plant Science, 6 (2001) 407-413.

[52] R.J. Clarke, Coffee | Decaffeination, in: C. Editor-in-Chief: Benjamin (Ed.) Encyclopedia of Food Sciences and Nutrition (Second Edition), Academic Press, Oxford, 2003, pp. 1506-1511.

[53] B.E. Richter, B.A. Jones, J.L. Ezzell, N.L. Porter, N. Avdalovic, C. Pohl, Accelerated solvent extraction: A technique for sample preparation, Analytical Chemistry, 68 (1996) 1033-1039.

[54] S. Dussert, A. Laffargue, A.d. Kochko, T. Joët, Effectiveness of the fatty acid and sterol composition of seeds for the chemotaxonomy of Coffea subgenus Coffea, Phytochemistry, 69 (2008) 2950-2960.

Chapter VI

Final discussion

The research performed in this thesis was focused on separation processes where conventional techniques which employ volatile organic solvents were modified using alternative solvents instead, in order to achieve sustainability requirements which became the main society concerns. Although simply replacing of conventional solvent with a more environmentally benign one is a crucial issue, economical sustainability is of significant importance as well. Therefore, achieving further improvements such as process intensification, facile product recovery, and higher extraction rates are beneficial.

Each chapter of the thesis includes a comprehensive discussion of the presented results. Thus, the potential improvements that could be introduced into the studied processes will be discussed herein.

The deacidification process is one of the few stages in refining of the crude oil, which has the maximum economic impact on oil production, since it determines the quality of the final product. The commercially used methods for deacidification are chemical and physical refining, while miscella deasidification is exclusively used for the refining of cottonseed oil. For oils with high acidity, chemical deacidification causes an excessive lost of neutral oil (up to 25 %) due to hydrolysis and thereby production of low commercial value soap stock. Although suitable for high acidity oils treatment, physical deacidification requires high temperature and moderated pressures and often forms by-products such as polymers and *trans* isomers. As can be seen, conventional methods present various limitations which can be overcome by new approaches and their combination with current technologies. Liquid-liquid extraction can be carried out at ambient temperature and pressure with minimal losses of natural components, reducing the energy consumption. Short-chain alcohols are usually used as extraction solvents, achieving low acidity oil as a final product with a significant decrease of the neutral oil loss. For example, Meirelles and co-workers [1-4] have been studied solvent extraction of free fatty acids from various vegetable oils using mixture (ethanol + water) as an extraction solvent. Generally, partition coefficients of FFAs between oil-rich and solvent-rich phases were around 1, selectivity was quite low (it was raised up to 200 in the best cases), while the neutral oil loss was around 5. Therefore, the deacidification of soybean oil was performed using either PEGs or ILs as alternative to short-chain alcohols. Since different PEGs (PEG200, PEG400, PEG2000, and PEG4000) and two ILs, namely [C$_4$mim][NTf$_2$] and AMMOENG100 exhibited complete miscibility with free fatty (linoleic) acid and a very low solubility in soybean oil, they appeared as promising media for the deacidification, causing lower losses of neutral oil. In the case of the higher molar mass PEGs and [C$_4$mim][NTf$_2$], distribution coefficients of linoleic acid between oil-rich and solvent-rich phases were around 1 which is comparable with short-chain alcohols. Nevertheless, considerably high distribution coefficients of linoleic acid between oil-rich and solvent-rich phases were obtain for AMMOENG100, ranking from approximately 5 to 8, since the Cocos alkyl chain in AMMOENG100 is a mixture, having approximately 50 mass % of lauric acid alkyl chain. To the best of our knowledge, these present the highest values ever reported in literature in the case of deacidification of oils by solvent extraction. The separation factors

achieved for low acidity oil were between 250 and 400 for all studied cases except for AMMOENG100, when it reached value of approximately 600. These values were reduced as initial acid content of oil increased. Furthermore, PEGs and ILs showed favourable values of neutral oil loss (*NOL*) which present another important parameter for the extraction process design, having the highest value of 3.54 % when AMMOENG100 was employed as extraction solvent at 323.2 K. Utilization of these solvents might be seen as a disadvantage due to their high boiling points which would caused energetically intensive and costly separation of FFAs from the solvents. Nonetheless, the additional separation step is not necessary since biodiesel production has been successfully carried out using ionic liquids either as reaction medium or catalysts [5, 6]. The valuable product, biodiesel, can be easily separated from ionic liquid due to formation of another phase, giving an opportunity for reusing ionic liquid.

Antibiotics are usually produced by fermentation, yielding low concentrations aqueous solutions which further separation and purification affect significantly their final manufacturing cost. Various separation methods such as solvent extraction, adsorption, ion-exchange chromatography, crystallization, membrane based techniques, or their combinations have been used for antibiotics recovery. However, solvent extraction is commonly used method due to its effectiveness and economical advantages achieved by using volatile organic solvents. Chloroform, dichloromethane, ethyl/butyl acetate and methanol-acetone mixture have been regularly used for extraction of erythromycin. Although butyl acetate is considered as the most suitable solvent due to its biodegradability and low toxicity, its high boiling point makes the process energetically costly. The highest partition coefficient of erythromycin between various organic and water phases have been achieved in alkaline environment [7, 8], where erythromycin undergoes degradation forming products that are antibacterial inactive [9]. Therefore, liquid-liquid partitioning should be carried out under neutral condition where erythromycin is the most stable, providing relevant results. Since erythromycin exists mostly in cationic form for pH equal to 7, ionic liquids could be suitable solvents for its purification.

In order to design environmentally benign purification of erythromycin, hydrophobic ionic liquids were employed for liquid-liquid partitioning, while erythromycin recovery from ILs was performed by high-pressure carbon dioxide. In this case, the high quality product might be achieved due to particular phase behaviour of IL + CO_2 mixtures, while ILs and CO_2 can be easily reused. As solubility of erythromycin in ILs plays a crucial role in designing the purification process properly, it was studied as a function of temperature. Comparing with volatile organic solvents, the lowest solubility of erythromycin obtained in [C_4mpyr][NTf_2] is similar with those attained in VOCs [10] (around 0.02 in mole fraction, in the case of ethanol and acetone) while other ILs studied demonstrated considerably higher dissolving strength (up to 0.097 in mole fraction). [C_4mpyr][NTf_2] was chosen for two-step recovery of erythromycin, achieving excellent extraction yields. Liquid-liquid partitioning was controlled by pH, while recovery of pure erythromycin was possible by controlling operational conditions (pressure and temperature). It should be noticed that 80 mL of the initial erythromycin solution was treated with solely 2 mL of the ionic liquid

solvent when multistage extraction was performed, resulting in the overall yield of 84 %. This suggests that, on the contrary to the traditional extraction, where abundant quantities of organic solvents are employed, the process with ionic liquid used significantly less amount of solvent. The sample obtained from the multistage extraction was treated by supercritical CO_2 under optimized conditions. The extraction yield of erythromycin decreased from 97.4 % to 75.9 % as the ionic liquid was saturated with water, while the final product was contaminated by the ionic liquid.

High-value compounds derived from vegetable sources are usually obtained by energetically intensive vacuum distillation including several additional steps associated with the use of abundant amounts of organic solvents. As an alternative, supercritical fluid technology has been applied in order to avoid utilization of volatile organic solvents which use became limited due to potential adverse effect which they can have on human health. Despite good performances, large-scale supercritical processes require massive equipment which additionally augments cost of the process. Accelerated solvent extraction (ASE) has been recognized as an alternative to common separation and supercritical fluid extraction processes, since ASE employs less quantities of extraction solvent and reduces extraction time. Additionally, in order to meet environmental sustainability, organic solvents regularly used in ASE might be replaced by biodegradable solvent ethyl lactate, produced from renewable feedstocks.

Decaffeination of green coffee beans was performed by ASE using ethyl lactate, ethanol and ethyl acetate, giving an opportunity to compare ethyl lactate with commonly used organic solvents. Solubility of caffeine in ethyl lactate was determined as a function of temperature. Solubility of 3.2 mass % at 303 K is over those reported for ethanol or ethyl acetate (around 1 mass %). Accelerated solvent extraction of caffeine when entire green coffee beans were processed at 473 K during 10 min, provided high caffeine recovery (~ 60 %), while small quantities of phenolic acids and coffee oils were extracted when ethyl lactate was employed. In the case of ethanol and ethyl acetate lower extraction yields of caffeine were achieved, while elevated quantities of phenolic acid and coffee oils were removed from the coffee beans. Thus, ethyl lactate is a promising environmentally benign solvent that might be utilized for the recovery of caffeine from green coffee beans, without extracting components which are responsible for roasted coffee flavour.

The results herein presented demonstrate that ionic liquids have been successfully utilized for deacidification process, while their combination with high-pressure CO_2 allows recovery of erythromycin from aqueous solution, achieving high extraction yields. Ethyl lactate, as an extraction solvent performed better than ethanol or ethyl acetate when employed for accelerated solvent extraction of caffeine from green coffee beans. It is important to emphasize that the separation processes studied might be efficiently performed, replacing volatile organic solvents by environmentally benign alternatives.

References

[1] C.E.C. Rodrigues, R. Antoniassi, A.J.A. Meirelles, Equilibrium data for the system rice bran oil + fatty acids + ethanol + water at 298.2 K, Journal of Chemical & Engineering Data, 48 (2003) 367-373.

[2] C.E.C. Rodrigues, A. Filipini, A.J.A. Meirelles, Phase equilibrium for systems composed by high unsaturated vegetable oils + linoleic acid + ethanol + water at 298.2 K, Journal of Chemical & Engineering Data, 51 (2005) 15-21.

[3] C.E.C. Rodrigues, E.C.D. Peixoto, A.J.A. Meirelles, Phase equilibrium for systems composed by refined soybean oil + commercial linoleic acid + ethanol + water, at 323.2 K, Fluid Phase Equilibria, 261 (2007) 122-128.

[4] C.B. Gonçalves, A.J.A. Meirelles, Liquid–liquid equilibrium data for the system palm oil + fatty acids + ethanol + water at 318.2K, Fluid Phase Equilibria, 221 (2004) 139-150.

[5] T. De Diego, A. Manjon, P. Lozano, M. Vaultier, J.L. Iborra, An efficient activity ionic liquid-enzyme system for biodiesel production, Green Chemistry, 13 (2011) 444-451.

[6] D. Fang, J. Yang, C. Jiao, Dicationic Ionic Liquids as Environmentally Benign Catalysts for Biodiesel Synthesis, ACS Catalysis, 1 (2010) 42-47.

[7] Z. Li, F. Qin, H. Bao, X. Gu, Study on new solvent extraction systems for erythromycin, Journal of Chemical Technology & Biotechnology, 80 (2005) 772-781.

[8] Q. Le, L. Shong, Y. Shi, Extraction of erythromycin from fermentation broth using salt-induced phase separation processes, Separation and Purification Technology, 24 (2001) 85-91.

[9] Y.-H. Kim, T.M. Heinze, R. Beger, J.V. Pothuluri, C.E. Cerniglia, A kinetic study on the degradation of erythromycin A in aqueous solution, International Journal of Pharmaceutics, 271 (2004) 63-76.

[10] Z. Wang, J. Wang, M. Zhang, L. Dang, Solubility of erythromycin A dihydrate in different pure solvents and acetone + water binary mixtures between 293 K and 323 K, Journal of Chemical & Engineering Data, 51 (2006) 1062-1065.